BLASTING BRIDGES AND CULVERTS: WATER OVERPRESSURE AND VIBRATION EFFECTS ON FISH AND HABITAT

By

Kristen N. Dunlap

RECOMMENDED:

Dr. Terrance Quinn II

Dr. John Kelley

Ms. Jackie Timothy

Dr. William Smoker, Advisory Committee Chair

Dr. William Smoker, Director, Fisheries Division

APPROVED:

Dr. Denis Wiesenburg
Dean, School of Fisheries and Ocean Sciences

Dr. Lawrence Duffy, Dean of the Graduate School

July 28, 2009
Date

BLASTING BRIDGES AND CULVERTS: WATER OVERPRESSURE AND VIBRATION EFFECTS ON FISH AND HABITAT

A

THESIS

Presented to the Faculty

of the University of Alaska Fairbanks

in Partial Fulfillment of the Requirements

for the Degree of

MASTER OF SCIENCE

By

Kristen N. Dunlap, B.S.

Fairbanks, Alaska

August 2009

ABSTRACT

Water overpressures and ground vibrations from blasting may injure or kill salmonid fish in streams and embryos in streambeds. Explosives are used to remove failing structures in remote areas of the Tongass National Forest that impair watershed function. The State of Alaska Department of Fish and Game standards limit blast induced water overpressures to 2.7 lb/in^2 (18.6 kPa) and streambed vibrations to 0.5 in/s (13 mm/s) when embryos are present. Researchers, however, have reported salmonid mortality from pressures only as low as 12.3 and 19.3 lbs/in^2 (85 and 133 kPa) and embryo mortality from vibrations as low as 5.75 in/s (146 mm/s). I recorded in-stream overpressures and streambed vibrations with hydrophones and geophones at various distances from log bridge, log culvert, and metal culvert blasts. Peak water pressures (lb/in^2) were directly related to cube-root scaled distances with an attenuation rate of -1.51. Peak particle velocities in gravel were directly related to square-root scaled distances (SRSD, ft/lb$^{1/2}$) with an attenuation rate of -0.75. Water pressures were less than 7.1 lb/in^2 (49.0 kPa) in all but one blast, and streambed vibrations did not exceed 5.5 in/s in gravel streambeds. State standards should be revised to reflect reported mortality and these observations of blasts in streams.

TABLE OF CONTENTS

Page

SIGNATURE PAGE i
TITLE PAGE ii
ABSTRACT iii
TABLE OF CONTENTS iv
LIST OF FIGURES vi
LIST OF TABLES vi
LIST OF APPENDICES vii
PREFACE AND ACKNOWLEDGMENTS viii
CHAPTER 1 GENERAL INTRODUCTION 1
Background 1
Literature Review 2
Explosive Mechanics 2
Explosives and explosions 2
Shock and sound waves 3
Vibrations 4
Water Overpressures 5
Effects on fish 6
Swim bladder 6
Hemorrhaging 7
Other injuries 8
Levels that cause harm 10
Factors affecting injury 12
Vibration effects on embryos 13
Indirect effects 15
Predicting effects on fish 16

Peak Pressure 17
Impulse 17
Energy Flux 18
Bladder Oscillation Parameter 19
Others 19
CHAPTER 2 BLASTING BRIDGES AND CULVERTS IN FISH STREAMS IN ALASKA 25
Abstract 25
Background 25
Methods 27
Site Descriptions 27
Blasting Operations 28
Instrumentation Field Methods 29
Challenges 30
Data Analysis 30
Results 31
Discussion 32
Stream overpressures 32
Streambed vibrations 32
Summary 33
References 34
CHAPTER 3 GENERAL CONCLUSIONS 49
Literature Review 49
Stream overpressures and streambed vibrations 50
References 54

LIST OF FIGURES

Page

Figure 1.1. Pressure-time history attenuation. 21
Figure 1.2. Shock front and rarefaction 21
Figure.1.3. Water pressure-time history and corresponding bubble pulse 22
Figure.1.4. Diagram of internal organs 23
Figure.1.5. Otolith motion in response to sound 23
Figure.1.6. Diagram of fish inner ear 24
Figure 2.1 Map of study area 41
Figure 2.2. Before and after pictures of a blast site 42
Figure 2.3. Charge placement diagrams 43
Figure 2.4. Hydrophone and geophone placement 43
Figure 2.5. Water overpressures versus cube-root-scaled distance 45
Figure 2.6. Water overpressure time-histories 46
Figure 2.7. Ground vibrations versus scaled distance for different substrate types 47
Figure 2.8. Vertical component vibration waveforms in different substrate types 48
Figure A1.1 Site specification data sheet 69
Figure A1.2 Shot and sensor setup data sheet 71
Figure A1.3 Log stringer bridge explosive design 72
Figure A1.4 Box log culvert explosive design 73
Figure A1.5 Metal culvert explosive design 74

LIST OF TABLES

Table A1.1 Site and structure specifications 70
Table A1.2 Shot and sensor setup summary 72
Table A1.3 Hydrophone and geophone results summary for all shots 75

LIST OF APPENDICES

Page

APPENDIX 1 MATERIALS AND METHODS 61
APPENDIX 2 SITE D2-1 LOG CULVERT 82
APPENDIX 3 SITE D2-2 LOG CULVERT 88
APPENDIX 4 SITE D4 WATER BAR 93
APPENDIX 5 SITE D8 LOG BRIDGE 99
APPENDIX 6 SITE D11 LOG CULVERT 105
APPENDIX 7 SITE D12 LOG CULVERT 110
APPENDIX 8 SITE D15 LOG CULVERT 116
APPENDIX 9 SITE D16 LOG CULVERT 122
APPENDIX 10 SITE D17 LOG CULVERT 126
APPENDIX 11 SITE D19 LOG CULVERT 131
APPENDIX 12 SITE D20 LOG CULVERT 136
APPENDIX 13 SITE D21 LOG CULVERT 141
APPENDIX 14 SITE D22-1 LOG BRIDGE 143
APPENDIX 15 SITE D22-2 LOG BRIDGE 146
APPENDIX 16 SITE F13 LOG BRIDGE 150
APPENDIX 17 SITE F14 LOG BRIDGE 156
APPENDIX 18 SITE F16 CORRUGATED METAL PIPE 162
APPENDIX 19 SITE F19 CORRUGATED METAL PIPE 168
APPENDIX 20 SITE F21 CORRUGATED METAL PIPE 174

PREFACE AND ACKNOWLEDGMENTS

In order to examine pressure and vibration attenuation rates from blasting in and near shallow streams I accompanied the U.S.D.A. Forest Service, Sitka Ranger District during blasting operations in the summer of 2007. We used explosives to remove several log structures on northern Baranof Island in small streams of low to moderate gradient. I monitored pressure values in streams with hydrophones and vibrations in streambeds with geophones during 19 blasts. The results of this study were prepared for an engineering publication[1] requiring English units. Units in this paper are reported in English units with SI units following in parenthesis.

The purpose of this research is to provide biologists within the Alaska Department of Fish and Game a better understanding of blasting in and around sensitive salmon streams and to provide information for updating the Department's blasting standard. This thesis is presented in manuscript format. Appropriate permissions were obtained for all previously published figures. Chapter 2 is published in the Journal of Explosives Engineering and was presented at the 35th Annual Conference on Explosives and Blasting Technique in Denver, CO in February 2009.

This research would not have been possible without the help of Aimone-Martin Associates[2]. Funding for this project was provided by the State of Alaska Department of Natural Resources and Department of Fish and Game. I would like to thank the hard working blasters and the Forest Service Sitka Ranger District for allowing me to conduct research during for project. I am grateful for Tess Quinn who worked by my side in the field and made data collection possible. I am forever indebted to Cathy Aimone-Martin of Aimone-Martin and Associates for helping me sort through my raw data and teaching me about blast vibrations. I also express thanks to the International Society of Explosives Engineers (ISEE) for their support and encouragement and the Black Hills and Northern

[1] Published as Dunlap, K. N. 2009. Blasting bridges and culverts in fish streams in Alaska. Journal of Explosives Engineering 26:16-23.

[2] Aimone-Martin Associates, LLC, New Mexico Corporate Office, 1005 Bullock Ave., Socorro, NM 87801

Plains Chapters of the ISEE for making it financially possible for me to present and share my research with the blasting community. I would also like to thank my committee members: Bill Smoker for accepting and supporting this unorthodox fisheries research, Terry Quinn for patiently answering all of my statistics and study design questions, John Kelley for invaluable technical support during field work planning, and Jackie Timothy, who encouraged me to undertake this research and supported me throughout the process. Finally, I owe an enormous thanks to Christian Kolden who is my first editor, my technical support, my shoulder to cry on, my motivation, and hopefully someday my husband.

CHAPTER 1 GENERAL INTRODUCTION

Background

Fish are adapted to an environment full of sound and vibration. Water is an excellent medium for mechanical wave transmission. Sound travels in water at a speed of 4,921 ft/s to 5,053 ft/s (1,500 to 1,540 m/s) and can propagate long distances with little attenuation in comparison to air (Dahl et al. 2007). Natural sound originates from several sources including wave action, currents, rain, wind, and other organisms. Sound can also originate from boat traffic, shipping, dredging, sonar, and construction activities in or near water. Sudden releases of large energy from events like pile driving, seismic exploration, and explosions create fast moving high energy sound waves in water. Explosives are used in or near water for harbor deepening, excavation, resource development, road construction, and demolition.

In southeast Alaska, Pacific salmon (*Oncorhynchus sp.*) are abundant and it is common for blasting to occur near spawning and rearing habitat. In the Tongass National Forest explosives are used for removing abandoned stream crossing structures left in place from logging operations before 1978, when best management practices began mandating their removal. Today, many log structures are collapsing and impairing watershed function and blocking fish access to miles of upstream rearing and spawning habitat. Conventional removal methods requiring heavy equipment are not feasible due to forest re-growth and remote locations of these structures. Blasting is a feasible removal method.

The levels of blast induced water overpressures and streambed vibrations that cause salmonid mortality are not known. The rate of shock wave attenuation in shallow stream environments is also unknown. The State of Alaska Department of Fish and Game (ADF&G) regulates blasting in and near streams that provide important habitat for anadromous fish. The regulation standard states that 'Without prior written approval from the Department of Fish and Game, no person may discharge an explosive that produces or is likely to produce and instantaneous pressure change greater than 2.7 lb/in^2

in the swim bladder of a fish or produces or is likely to produce a peak particle velocity greater than 0.5 in/s in a spawning bed during the early stage of egg incubation' (ADF&G 1991). The standard was based on a review of available literature and the levels selected represented levels below those known to be harmful to fish.

The goals of this study were to review and summarize available literature on explosive effects on fish to assist resource managers in updating the ADF&G blasting standard; and to examine pressure and vibration attenuation rates from blasting in and near shallow streams. The following section is meant to familiarize the reader with the rudiments of explosive and shock wave physics and to provide a summary of literature related to explosive effects on fish.

Literature Review

Explosive Mechanics

Explosives and explosions

Explosives can be separated into categories based on their detonation velocities, i.e. high and low explosives. High explosives are initiated by any one of or a combination of heat, shock, impact, or friction, and release supersonic shock waves into surrounding materials (ISEE 1998). Low explosives that burn rather than detonate include pyrotechnics, propellants, and black powder (Cooper and Kurowski 1996). High explosives were used during this study.

It is important to understand what happens during an explosion to determine how it will affect nearby fish. In general, explosions are chemical reactions that produce heat, light, and gas. An explosion is defined by Cooper (1996) as "a large-scale, noisy, rapid expansion of matter into a volume much greater than its original volume." The rapid expansion of gas applies strong forces in the form of shock waves to surrounding materials resulting in fragmentation, displacement, air blast, vibration, and pressure waves in water (ISEE 1998).

Shock and sound waves

Blast energy travels through materials as shock or sound waves. A shock wave is a very quick moving high-pressure disturbance. Shock waves can permanently deform a material by stressing it beyond elastic limits so it cannot return to its original state. In contrast, sound waves move at lower pressures than shock waves. They do not produce enough stress to permanently deform a material and their distortion is completely reversible (Cooper and Kurowski 1996). Stress applied by shock and sound waves is defined as force per unit area and is what causes materials to distort or change shape. This amount of distortion or change in shape is called strain. The range of stress where strain (distortion) is completely reversible is called elastic range. Hooke's Law applies within this range and states that stress/strain = constant. There are three constants that describe the movement or behavior of a material. First, shear strain changes the shape, not the volume of an object. Second, pure dilation changes the volume, not the shape of an object. The third constant is tensile or pulling stress, which only changes the length of a material (Cooper and Kurowski 1996).

All waves travel through media, or material, as either body or surface waves. Body waves are classified as compressive or shear waves. Compressive waves are also called primary or P-waves and have particle motion along the direction of propagation, called the longitudinal or radial direction. Shear waves are also called secondary or S-waves and have a particle motion that is perpendicular (transverse direction) to the direction of propagation. Liquids and gases don't have shear properties so can only support compressive waves (Siskind 2000).

Surface waves are typically lower frequency than body waves and Rayleigh waves are the most common type when assessing blast vibrations. Particles in a Rayleigh wave move in elliptical motions that Siskind (2000) compares to ocean waves impacting a beach. Rayleigh waves are common in layers of soil above bedrock and can be particularly destructive.

Body and surface waves are subject to internal friction among particles which decreases pressure as distance increases. Higher frequency sound waves create more friction and thus attenuate, or dissipate, faster than lower frequencies. Fast moving, high pressure shock waves lose energy and pressure through an additional mechanism as they are overtaken by a rarefaction wave as shown in Figure 1.1 (Cooper and Kurowski 1996). A typical explosive shock wave has a steep front caused by the rapid expansion of gas. This steep front moves quickly through materials compressing them as it passes. The rarefaction wave as shown in Figure 1.2, travelling immediately behind the shock front, moves through compressed material that has greater density than the material the shock front is moving through, thus giving the rarefaction wave greater velocity than the shock front. Over time and distance it will overtake and decrease the front's peak pressure and eventually transform into a sound wave (Cooper 1996).

Vibrations

Blast energy traveling through solid media, such as ground or streambeds, moves as vibrations that propagate via particle motion. That motion is often measured as velocity (in/s, mm/s), displacement (in, mm), or acceleration (in/s^2, mm/s^2). Velocity, most commonly measured as peak particle velocity (PPV), is defined by Siskind (2000) as the "highest particle velocity of any of the three components of motion without respect to plus or minus sign." The motion of a particle can be approximated by a sine wave. Peak velocity (V), displacement (D), acceleration (A), and frequency (f) are related by:

$$V = 2\pi fD = A/2\pi f$$

$$A = 2\pi fV = 4\pi^2 f^2 D$$

$$D = v/2\pi f = A/4\pi^2 f^2$$

Particle motion is most commonly recorded and reported as velocity. This has become standard practice in seismograph use and damage assessment because particle velocity is less sensitive to changes in geologic conditions than acceleration or displacement. Other factors that can influence vibration intensity are charge weight per 8 millisecond delay, spatial distribution of explosives, vibration duration, explosive confinement and coupling, and the distance that waves must travel (ISEE 1998).

Water Overpressures

When an explosion occurs underwater, a high amount of energy moves away from the blast center in the form of a shock front and spreads in all directions (Simmonds and MacLennan 2005). In most cases, underwater explosions and their subsequent shocks are described for point explosions in free-field conditions. These conditions describe a large open body of water with only surface and bottom boundaries from which pressure waves reflect (Simmonds and MacLennan 2005).

An underwater explosion creates a rapidly expanding bubble of gas that sharply increases pressure at the bubble's surface. Eventually inertia of the surrounding water and elastic properties of gas cause the bubble to contract, and pressure at the bubble's surface becomes less than ambient pressure. The bubble's size continues oscillating up to 10 or more times in ideal conditions creating a pulse between positive and negative pressures (Cole 1948). The pressure-time signature recorded from an explosion can be separated into two parts. The first contains a near instantaneous rise to a maximum peak pressure caused by detonation followed by an exponential decay to a minimum pressure. The second part of part of the wave is caused by the more slowly occurring chemical reaction of the explosion. The entire process takes place in milliseconds (Figure 1.3).

Boundary reflections affect pressure waves when the observation distance from the explosion (along the line of propagation) is more than the charge depth below the surface or height above the bottom (shallow water). The shock front travels much faster than reflections and is unaffected by reflections (Simmonds and MacLennan 2005). Surface reflections essentially invert a wave. When a positive pressure wave reaches the surface, there is not enough atmospheric pressure to resist it. A resulting negative pressure is formed at the surface and reflected as a near opposite of the direct wave (Cole 1948). The reflected surface wave can cause large rarefactions (high negative pressures) when it interacts with the rarefaction portion of the direct wave. However, pressures are difficult to predict because most water cannot withstand high tension, probably less than one atmosphere (14.7 lb/in^2, 101 kPa) (Cole 1948). Waves reflected from the bottom have positive pressure fronts and travel slower than surface reflected waves. If these are the only two boundaries present, the resultant pressure is the sum of the surface, bottom, and direct wave. Waves become increasingly more complicated when more boundaries exist (Simmonds and MacLennan 2005). Physical factors such as temperature and density can affect a wave that has been reduced to normal acoustic intensity (Cole 1948).

Effects on fish

Fish are adapted to sense sonic vibrations and have receptors in their tissue to transform these signals into nerve impulses used for locomotor and behavioral responses for activities like detecting and capturing prey, avoiding predators, and communication.

Few researchers have examined the effects of explosions on fish, and fewer have examined the effects of blast induced vibrations on embryos. The following is a discussion of literature related to the effects of blast induced water overpressures on fish and vibration effects on embryos in gravel.

Swim bladder

The swim bladder is the most commonly damaged organ in fish subjected to shock waves from blasting. Fish tissue has a density similar to that of water. A pressure wave travelling through water will pass relatively undisturbed through tissue until it contacts the swim bladder, a gas filled organ used to regulate buoyancy and detect sound in some fishes. Goertner et al. (1994) showed that the presence of a gas-filled swim bladder is the cause of most pressure injuries in fish. In his study, fish without swim bladders were injected in the coelom with air prior to exposure. Their viscera were completely destroyed after explosions and they had injuries similar to those suffered by fish with swim bladders. Yelverton et al. (1975) examined explosive effects in physostomous (open-pneumatic-duct) and physoclistous (closed or absent duct) fish and determined that the method of gas secretion and resorption had no effect on injuries because the initial pressure wave moved too quickly through the fish to allow gas to leave or enter the gas bladder.

When a shock wave reaches the air/tissue interface at the swim bladder wall, some of the pressure wave is reflected, creating a negative pressure. This is similar to the rarefaction process at the air/water interface discussed earlier. When the rarefaction following the first positive peak contacts the swim bladder wall it is subject to the negative pressure from the direct rarefaction in addition to that of the reflected wave. As incoming pressures change from positive to negative the swim bladder contracts under compression and expands under tension. Since tissues are more resistant to compressive forces than to tensile forces, the swim bladder wall can be more readily damaged by extreme negative pressures (Simmonds and MacLennan 2005).

This is supported by observations from several studies in which fish autopsied after explosions suffered outwardly burst swim bladders (Hubbs and Rechnitzer 1952; Kearns and Boyd 1965; Yelverton et al. 1975). Other studies noted patches of missing scales on either side of the body in the area of the swim bladder, evisceration of the fish through the mouth or anus, and distention of the abdomen, all of which indicate an outwardly burst swim bladder (Coker and Hollis 1950; Christian 1973).

Hemorrhaging

Hemorrhage has been commonly reported as an injury during post blast autopsies and used in assessing damage levels. Baxter (1971) observed hemorrhage in gill capillaries, liver, kidney, and gonads. Houghton and Munday (1987) collected wild fish after blasting and noted hemorrhaging in the kidneys, stomach, liver, and heart of gadids. They also noted epidermal hemorrhages in the anal fins of walleye pollock (*Theragra chalcogramma*) and in the pelvic fins of herring (*Clupea sp.*) along with severe kidney bleeding.

Hubbs and Rechnitzer (1952) and Goertner et al. (1994) suggested that extreme rarefactions can form bubbles in body fluids and liberate dissolved gases enough to rupture the walls of unprotected blood vessels. It is possible that accumulation of such gases as nitrogen in the circulatory system can result in embolisms, and can expand gas bubbles large enough to cause physiological harm on the vessel walls. Goertner et al. (1994) reported that fish without swim bladders exposed to blasts died from loss of blood as a result of hemorrhage at the gills attributed to violent radial oscillation of gas microbubbles. Others died from hemorrhage in the cranium or brain damage secondary to differential shearing of the otoliths.

Other injuries

Other commonly damaged organs were in the vicinity of the swim bladder (Figure 1.4) and included the kidney, liver, and spleen (Yelverton et al. 1975). Ogawa et al. (1977) reported that the liver was damaged by less pressure than were the swim bladder, and kidneys, and that the heart and bones had the greatest resistance. Torn ribs, ruptured body walls, intestines, and peritoneum damage occurred in extreme cases (Houghton and Munday 1987).

Sverdrup et al. (1994) studied the effects of sub-lethal explosions on stress hormones in Atlantic salmon. They found that among primary stress hormones plasma cortisol declined for about 6 hours followed by a gradual rise about 48 hours after shock exposure. Plasma A and NA did not change significantly throughout the post shock period. As for secondary stress hormones, the atrial content of A (albumin) and NA (sodium) were significantly lower after 24 to 48 hours. There was no significant change in plasma chloride. Elevated levels of plasma CA (calcium) and plasma cortisol indicate primary responses to stress; in fish this includes bursts of jumping and rapid swimming. Fish exposed to non-lethal underwater blasts may not be able to express the alarm reaction by an intermediate release of primary stress hormones because of temporary endothelial impairment that could prohibit the coeliaco mesenteric artery from contracting in response to potassium (K^+), acetylcholine (Ach), and A (Sverdrup et al. 1994). Behavioral changes such as the inability to express the alarm reaction may make fish more susceptible to predation. Teleki and Chamberlain (1978) observed gulls preying on stunned fish after blasts.

Damage to the octavolateralis system could also present as behavioral changes. The octavolateralis system describes the mechanosensory function in fishes and is composed of the auditory, equilibrium, lateral line, and electrosensory systems. All of these systems use tiny hair cell receptors. The following discussion on the octavolateral system is based on text from fish biology (Barton 2007) and physiology texts (Evans 1998).

The auditory system in fish is responsible for hearing. Underwater sound is composed of compression waves and particle displacement. The lower portion of a fish's inner ear (fish only have inner ears) is responsible for hearing. Fish can be grouped into hearing specialists that perceive sound through direct and indirect stimulation, and generalists that are only equipped to process direct stimulation. Direct stimulation occurs when fluid particles are displaced in the inner ear. This happens when the otolith, which is supported by ciliary bundles of sensory hair cells, moves (Figure 1.5). As a pressure wave reaches a fish, the fish moves with the pressure wave because it is of similar density to water. The heavier and denser otolith lags in movement bending and stimulating the ciliary hair cells in the macula, which send sound signals to the brain. Indirect stimulation is when compression waves are transferred from the swimbladder to the inner ear. This functional connection between the swimbladder and inner ear is called an otophysic connection and allows movement in the swimbladder imparted by compression waves to be transferred to the inner ear, where the maculae are stimulated. Hearing specialists have higher sensitivity and respond to a wider range of frequencies than generalists.

Of about 25,000 extant species of fish, hearing and sensitivity range studies have been conducted on fewer than 100 (Mann et al. 2007). Hearing specialists with connections to the inner ear (otophysic connections) had higher hearing sensitivity than fish with swimbladders and no inner ear connection in a study conducted by Mann et al. (2007). Hastings and Popper (2005) suggest that although limited data exists, intense sounds may potentially damage sensory receptors in the inner ear under specific conditions. Others suggest that sounds of less intensity, or less duration, may result in temporary hearing loss or hearing threshold shift (Popper et al. 2005).

Equilibrium and the lateral line systems assist with balance and movement. There are two types of equilibrium, static and dynamic. Static equilibrium orients a fish when still, and dynamic equilibrium deals with movement in a direction. The upper part of the fish's inner ear regulates static equilibrium with otoliths and sensory hairs that function similarly to those in the lower inner ear. Dynamic equilibrium is regulated by neuromasts within the lateral line. Each neuromast consists of clusters of hair cells that detect water movement and displacement. The lateral line system plays an important role in detecting predators and prey, locating wave sources, orientation and locomotion, schooling, and obstacle avoidance. The sagitta, lapillus, and asteriscus otoliths in the inner ear are associated with equilibrium and hearing (Figure 1.6). Goertner et al. (1994) observed erratic swimming and bleeding around the otoliths in hogchokers exposed to underwater explosions. Ogawa et al. (1976) also observed erratic swimming in carp (*Cyprinus sp*.) and an unspecified type of sea bream after blast exposure. Ten carp reportedly had mild spasms for about two months and returned to normal while sea bream recovered in one week.

Electonsensory systems vary between species, but in general, there are two types of electroreceptors located in the skin. Ampullary receptors consist of hair cells surrounded by a conductive gel, they respond to prolonged low frequency (0.1 to 50 Hz) electrical stimuli. Tuberous receptors are not exterior, are not sensitive to direct current, become insensitive to prolonged stimiuli, and respond to frequencies up to 2,000 Hz. There have been no studies to date that examine the effect of in-water overpressures on the electrosensory system of a fish.

Levels that cause harm

Several researchers have caged fish and exposed them to blasts in an attempt to determine injury and mortality thresholds. They have reported a large range of results due to high variability in equipment sensitivity, experimental conditions, and species examined. The most widely referenced level was reported by Hubbs and Rechnitzer (1952) as 40-70 lbs/in^2 (276-482 kPa or 229-234 dB re 1 micropascal) for several species of fish exposed to dynamite explosions. In 1960, Hubbs et al. (1960) exposed fish to deep water blasts and found that most survived blast overpressures higher than 70 lbs/in^2 (483 kPa). However, they observed severe damage in anchovy (*Engraulis mordax*) at peak pressures of 171 lbs/in^2 (1179 kPa). The corresponding rarefaction was -23 lbs/in^2 (-156 kPa). For comparison, Fernet (1982) reported lethal rarefaction pressures for rainbow trout between -70 and -115 lbs/in^2 (-483 to -793 kPa). Teleki and Chamberlain (1978) exposed several caged freshwater species to underwater blasting and found lethal levels between 1 and 21.8 lbs/in^2 (7 and 150 kPa). Interestingly, of the 13 caged species in this study, carp (n = 2) incurred lethal injuries at the lowest and highest levels reported. Yelverton et al. (1975) reported 0% mortality for carp at levels between 128 and 1309 lbs/in^2 (883 and 9025 kPa).

Acute internal injury occurred between 4.4 and 21.7 lb/in^2 (30 and 150 kPa) in Lake Erie fish, including yellow perch (*Perca flavescens fluviatalis*) that were caged and exposed to well confined underwater blasts (McAnuff and Booren 1989). Teleki and Chamberlain (1978) reported 10 to 20% mortality in yellow perch at 21.7 lb/in^2 (40 kPa).

Other researchers have correlated pressure impulse with fish mortality (Yelverton et al. 1973; Gaspin 1975; Fernet 1982; Munday et al. 1986; Houghton and Munday 1987).

For Alaskan species that could have been present during this study, lethal levels have been reported for coho and chum salmon (*Oncorhynchus kisutch* and *O. keta*), rainbow trout (*Oncorhynchus mykiss*), and Dolly Varden char (*Salvelinus namaycush*). The State of Alaska Blasting Standards for the Protection of Fish (ADF&G 1991) are based on a field monitoring study in which juvenile wild and hatchery salmonids were exposed to blast overpressures from rock blasting near a stream. Coho and chum salmon and Dolly Varden char showed no sign of injury at 2.7 lbs/in^2 (18.6 kPa) (Bird and Roberson 1984). Houghton and Munday (1987) reported 50% mortality at 21 and 19.3

lb/in^2 (145 and 133 kPa) for chum and coho smolts respectively. Fernet (1982) caged rainbow trout and exposed them to construction blasts in the Bowe River in Alberta, Canada. Peak pressures between 33 and 290 lbs/in^2 (228 and 1996 kPa) caused no mortality. Lower mortalities for rainbow trout were reported by Teleki and Chamberlain (1978). They found 10-20% mortality at 12.3 lbs/in^2 (85 kPa) and 95% mortality at 14.5 lbs/in^2 (100 kPa).

Factors affecting injury

The physiological make-up of fish present can help determine the type and degree of injury they may sustain if exposed to a blast. Fish with swim bladders are more vulnerable to blast injury than those without. Species with thick-walled swim bladders are more resistant to shock (Fitch and Young 1948; Gaspin et al. 1976). Body shape and construction can also determine how much shock a fish can withstand. Species with laterally compressed bodies have more surface area to receive a shock wave making them more susceptible. Rigid body wall construction increases likelihood of injury because it limits flexing during swim bladder oscillation. These fish exhibit more internal bleeding and kidney bruising than fish with flimsy bodies (Gaspin et al. 1976). Smaller fish sustain swim bladder injury from less pressure than do larger fish (Yelverton et al. 1975) making juveniles and early life stages more susceptible to injury than adults. Blast exposure can rupture gonads and disturb eggs in mature fish in some cases (Baxter 1971). Orientation to blast can also influence the degree and type of damage. Fish receiving a pressure wave on the abdominal or lateral side are more likely to sustain damage to kidney, liver, and swim bladder than fish receiving a wave on the head or caudal side (Ogawa et al. 1977).

Environmental factors can influence the magnitude and propagation of a pressure wave before it contacts a fish. Houghton and Munday (1987) recorded blast overpressures in water and noted that surface and bottom reflection and the distance from the source to the target influenced the resulting pressure wave. Other factors such as the water temperature, salinity, turbidity, and depth of fish can all influence the pressure wave and its impact on fish. If a shot is detonated near a water body, the media through which the shock waves has to travel and the interface it must cross to enter the water can also affect its strength.

Shot design and charge type can affect shock wave origination. For instance, the higher the weight of explosive per delay, the larger the shock wave will be (Cooper 1996). End-fired line charges or continuous lengths of explosives can produce smaller and less focused shock waves than point charges weighing the same amount (Simmonds and MacLennan 2005). Other important shot design elements to consider are explosive confinement and stemming type, the material a charge is coupled to and how well it is coupled, and the depth of charge in water. Explosives shot in open water produce higher amplitude and frequency shock waves than do contained detonations (Cole 1948). Hempen et al. (2007) recorded blast-induced water pressures from confined and unconfined shots and found that confined shots produced lower pressures than do much smaller shots in open water.

Vibration effects on embryos

Incubating embryos can be damaged by mechanical agitation. Sensitivity to shock was examined as early as the 1950's to maximize hatchery success. Embryos were most sensitive to shock before the blastopore closed (Smirnov 1954; Smirnov 1959). Smirnov (1954) showed that excessive physical shock can tear the perivitelline membrane and cause the yolk to leak into the perivitelline space and cause death.

Kostyuchenko (1973) exposed eggs from 16 species of saltwater fish to mechanical shock from an air gun, electric pulse generator, and TNT. Upon examination, some of the eggs showed signs of deformation and displacement in the embryo, membrane, and yolk deformation. Eggs were injured by all sources of shock and those exposed to TNT were injured at a greater radius.

Post et al. (1974) compared incubating rainbow trout eggs exposed to physical shock to eggs not subject to physical shock and found no significant difference. The authors report that their study exposed eggs to accelerations up to 322 ft/s^2 (98.1 m/s^2)

and that their results explained earlier reports of Dolly Varden trout eggs incubating in natural circumstances surviving nuclear seismic shock levels of about 100 ft/s^2 (30.4 m/s^2) recorded on Amchitka Island. The accelerations recorded in Post et al. (1974) were later compared to accelerations in Faulkner et al. (2006) who found that lake trout (*Salvelinus namaycush*) exposed to blasts from an open pit mine suffered no detrimental effects at velocities of 1.12 in/s (28.5 mm/s) and accelerations of about 6.8 ft/s^2 (2.1 m/s^2), suggesting that accelerations in the rainbow trout study were much higher (Faulkner et al. 2006).

Faulkner et al. (2006) were the first to attempt to correlate peak particle velocity (PPV) and embryo mortality. Their selection of PPV as a descriptor of blast intensity was largely based on the *Guidelines for the Use of Explosives In or Near Canadian Fisheries Waters* (Wright and Hopky 1998) which limits blast induced vibrations in salmon spawning beds to PPVs no greater than 0.5 in/s (13 mm/s). The Alaska Department of Fish and Game has a similar standard with the same PPV limit and is largely the basis for this study.

Faulkner et al. (2008) exposed rainbow trout embryos at various stages of development to blast simulations in a laboratory. Shock was induced by the historical drop height method and a newly created drop apparatus designed to more accurately simulate a blast shock wave. Lab simulations had higher frequencies and were shorter in vibration than real blasts. To compensate for shorter duration, the authors repeated shock exposure to eggs. This did not result in increased mortality which indicates that PPV is the most important factor in predicting egg mortality due to blasting. The highest PPV tested was 9.66 in/s (245.4 mm/s) which was significantly greater than procedural control mortality. Peak particle velocities of 5.21 in/s (132.3 mm/s) and lower produced no mortality. Eggs exposed to shock in spawning gravels showed higher mortality than those free in water and was highest for both cases during epiboly, when the mesodermal sheath replaces the vitelline membrane around the yolk (Faulkner et al. 2008).

The lethal limits of PPV used in this study are supported by Jensen's (2003) report in which results from a previous study were converted from units of energy (ergs) to velocity (PPV). The previous study (Jensen and Alderdice 1989) examined the sensitivity of five species of Pacific salmon (*Oncorhynchus sp.*) and steelhead trout (*Salmo gairdneri*) to mechanical shock by the drop height method at discrete developmental stages. This study reported that all six species tested were sensitive to mechanical shock and Chinook salmon (*Oncorhynchus tshawytscha*) were the most sensitive. All species showed increasing sensitivity from pre-activation to epiboly. Sensitivity declined rapidly during organogenesis and until around 150 degree days coinciding with the completion of epiboly (Jensen and Alderdice 1989). The peak particle velocity corresponding to the energy (estimated from drop height tests) that causes 10% egg mortality in Chinook embryos is 5.75 in/s (146 mm/s); for chum 16.38 in/s (416 mm/s), for coho 9.09 in/s (231 mm/s), for pink 24.53 in/s (623 mm/s); for sockeye 32.99 in/s (838 mm/s); and for steelhead embryos is 13.07 in/s (332 mm/s).

These studies relate PPV to embryo mortality during various developmental stages. It is important to remember that development is greatly affected by water temperature which could in turn affect shock sensitivity. Temperature can alter the physical properties of an egg by changing the permeability of the vitelline membrane or changing the fatty acid composition of cell membrane lipids (Jensen and Alderdice 1989). Sensitivity may also vary with other species, or between stocks of the same species (Fitzsimons 1994).

Indirect effects

Indirect effects are other effects caused by a blast that can indirectly affect fish. These indirect or secondary effects could be caused by increased sediment, turbidity, toxicity, and other changes in the physical environment that may increase predation or change the structure of the marine community by changing habitat, selectively removing food sources, etc. "This secondary process may involve changes in the physical and/or vegetative structure of a region which may reduce an organism's chance of survival" (Simenstad 1974 in Lewis 1996). Turbidity clouds are therefore most likely over silt or where the percentage of silt and clay exceeds 50% (Athearn 1968 in Lewis 1996).

Sediment particles greater than 1mm in diameter settle rapidly and are less likely to remain suspended in the water column.

Predicting effects on fish

Since the 1950's, there have been many attempts to model and predict fish kill resulting from underwater explosions. Study designs have ranged from observing dead floating fish after an underwater explosion (Coker and Hollis 1950; Hubbs and Rechnitzer 1952) and counting those that sank during dive surveys (Kearns and Boyd 1965; Houghton and Munday 1987) to exposing caged fish to blasts at selected distances and orientations (Yelverton et al. 1975; Teleki and Chamberlain 1978; Wiley et al. 1981; McAnuff and Booren 1989). Most studies reported results as a range in which a proportion of mortality occurred (i.e. the radius within which 50% of fish are expected to die).

Mortality observations and blast parameters have been used to create several prediction models. Keevin and Hempen (1997), Lewis (1996), and Simmonds and MacLennan (2005) summarize and discuss available prediction methods. According to Keevin and Hempen (1997), the exact pressure waveform measurement responsible for fish mortality is unknown.

The following discussion of prediction methods assumes free-field conditions and focuses on prediction methods for the parameters peak pressure, impulse, and energy flux. When an explosion occurs in a free-field, the resulting pressure wave propagates far without boundary effects. In this case, empirical equations can be applied to predict several parameters in the pressure-time waveform (Cole 1948). Free-field equations cannot be used to predict energy flux or impulse when boundary reflections are present (Simmonds and MacLennan 2005).

Peak Pressure

Peak pressure describes the highest amplitude in the pressure time history and is commonly reported in units of pounds per square inch (lb/in^2), kilopascals (kPa), or atmospheres (atm). Teleki and Chamberlain (1978) exposed several species of caged fish to 201 blasts and found a direct correlation between charge size and blast overpressures in water. They found that pressures between 4.3 and 12.3 lb/in^2 (30 and 85 kPa) caused significant tissue damage, and pressures in the range of 10.0 to 21.8 lb/in^2 (69 to 150 kPa) caused injury to greater than 95% of fish. Other authors found high variability in peak pressure values between similar shots and no correlation between mortality and peak pressure (Hubbs and Rechnitzer 1952; Christian 1973; Yelverton et al. 1975).

Nevertheless, this is the easiest prediction method to understand and is very easy to monitor, thus is used in regulations in North America (Wright 1982; ADF&G 1991; Wright and Hopky 1998). However, most regulations do not distinguish between positive and negative pressures which is problematic because fish are more resilient to higher pressures (compression), than to negative pressures (rarefaction). Typically, the rarefaction in an explosive pressure-signature is lower than the positive peak. The minimum pressure can be calculated if certain constants are known for explosive type.

Impulse

Impulse is the integral of the pressure-time waveform. Perhaps the most commonly used impulse model was developed by Yelverton et al. (1975). The authors investigated the effects of explosives on 13 body-weight groups of eight species of swimbladder fish caged in an artificial pond. Their study reported a strong correlation between mortality and impulse. In order to use the model, one must know fish weight, target depth, detonation depth, and charge weight.

Since its development, several researchers have tested the Yelverton model. Gaspin et al. (1976) found that impulse predicted mortality when the charge and target were less than 3 meters deep. Munday et al. (1986) found that caged coho survived greater impulses than previously predicted and that impulse was not a good predictor of damage when charges were buried. Hill (1978) found that the impulse model roughly predicted the results of some early observational studies. Wright (1982) suggested that ranges predicted by impulse should be doubled for shallow charges or when detonation occurs under ice to compensate for rarefaction effects. Other authors have tested the impulse model and found similar results and limitations (Hempen and Keevin 1995; Keevin 1995).

Yelverton et al. (1975) tested fish close to the surface in an area where the rarefaction is large. The impulse model is a good predictor in depths less than around 10 m (32.8 ft) but it can greatly underestimate mortality (Simmonds and MacLennan 2005). Houghton and Munday (1987) reported that impulse models fall short of ideal because they only consider the positive portion of the wave and exclude the rarefaction which may cause the swim bladder to rupture Most later researchers agree that the impulse model developed by Yelverton et al. (1975) is a good predictor for ranges of fish mortality when charges and fish are less than a few meters from the surface (Gaspin 1975, (Hill 1978; Lewis 1996; Keevin et al. 1999; Simmonds and MacLennan 2005).

In summary, impulse models are desirable because they incorporate bottom reflected waves, but fall short of ideal because they only consider the positive portion of the wave, excluding the negative side which may cause the swim bladder to rupture (Houghton and Munday 1987).

Energy Flux

Energy flux is the rate of energy flow through a unit area of surface (Wright 1982). The physiological effects on fish of this parameter were first explored by Ogawa in a series of studies designed to determine a method to predict the effects (Ogawa 1976; Sakaguchi et al. 1976; Ogawa 1977; Ogawa et al. 1977; Ogawa 1978; Ogawa et al. 1978; Ogawa et al. 1979). Other studies support the use of energy flux as a predictor in deeper water (Lewis 1996; Keevin and Hempen 1997). Baxter et al. (1982) proposed an easily used energy flux model that took fish weight and depth into account. The energy flux calculation in Baxter et al. (1982) should only be used to predict mortality at depth because it doesn’t account for surface pressure release (Simmonds and MacLennan 2005).

Bladder Oscillation Parameter

Another mortality prediction method relies on theoretical predictions of oscillations of the swim bladder (Goertner 1978; Wiley et al. 1981; Goertner 1982; O'Keefe 1984; Goertner et al. 1994). The bladder oscillation parameter is a theoretical constant that is calculated based on the expected radius of a sphere that represents the swim bladder for a given species. Simmonds and MacLennan (2005) suggest that the model developed by Goertner (1978) is the most realistic to date although it is complicated and difficult to apply in practice. To complete the calculations of the Goertner model one must have the pressure-time signature, the fish swim bladder model with specific ratios for each species, and the interaction between the two. O’Keefe (1984) created several contour plots from the Goertner (1978) model of kill probability for various weights and depths of charges and fish. This is a complicated set of calculations for which the user needs to know the charge weight, depth of burst, location and size of fish to use the contour plots in (O'Keefe 1984). The predictions apply to horizontal distances only.

Others

The theory of bulk cavitation has also been proposed as a prediction method. This method predicts the region where water is “torn apart” by a surface reflected shock wave, or defined otherwise as the place where a reflected rarefaction interacts with the rarefaction portion of the direct wave and the resulting negative pressure is greater than that which water can support, so it is “torn apart” into many tiny bubbles (Christian 1973). Gaspin et al. (1976) found no correlation between bulk cavitation and mortality; however, O’Keefe and Young (1984) suggested that bulk cavitation would be a good predictor of mortality for fish without swim bladders because all fish should be susceptible to tissue damage from cavitation.

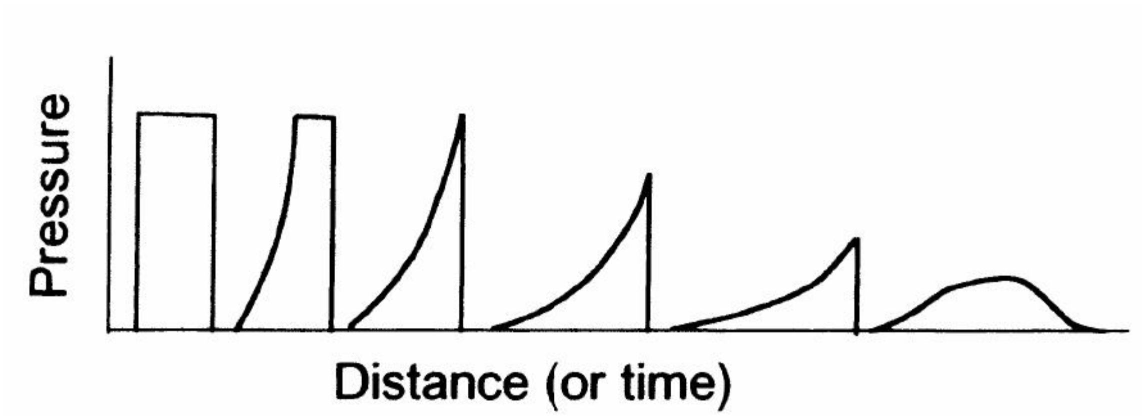

Figure 1.1. Pressure-time history attenuation. Typical attenuation of a square shock wave (by permission from Cooper 1996).

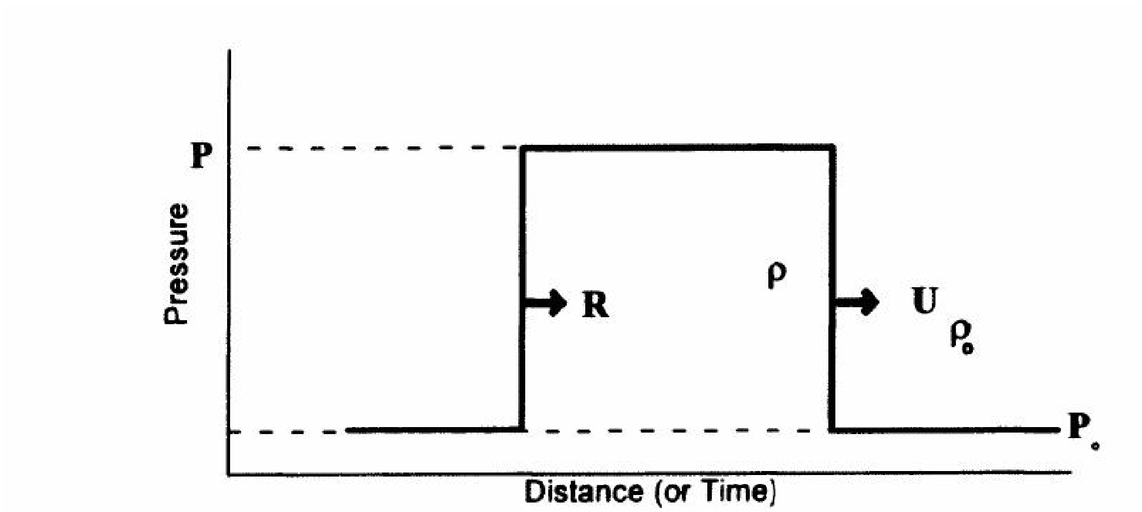

Figure 1.2. Shock front and rarefaction. Square wave shock pulse with positive pressure front and subsequent rarefaction (by permission from Cooper 1996).

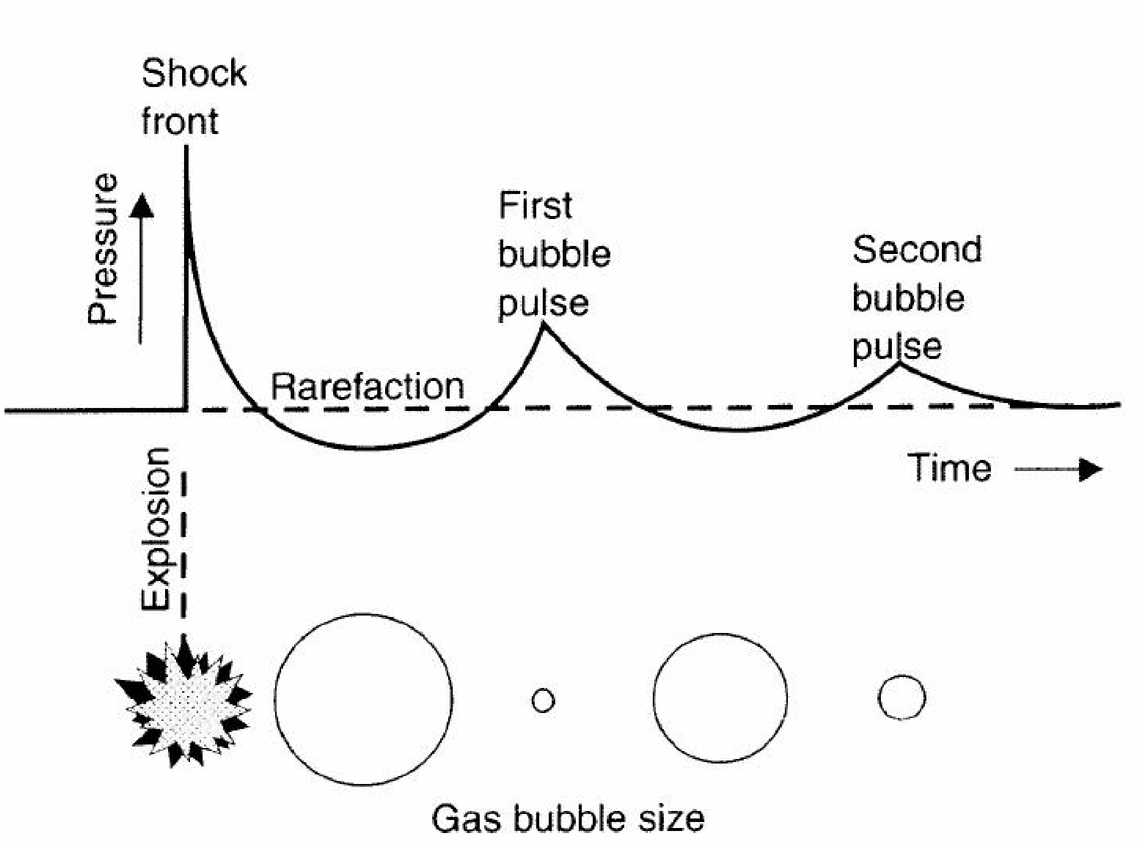

Figure 1.3. Water pressure-time history and corresponding bubble pulse. Example of an explosion induced underwater pressure wave at an observation point. The dashed line represents ambient water pressure. In free-field conditions as shown, gas bubble oscillations create corresponding positive and negative pressures (by permission from Simmonds and MacLennan 2005).

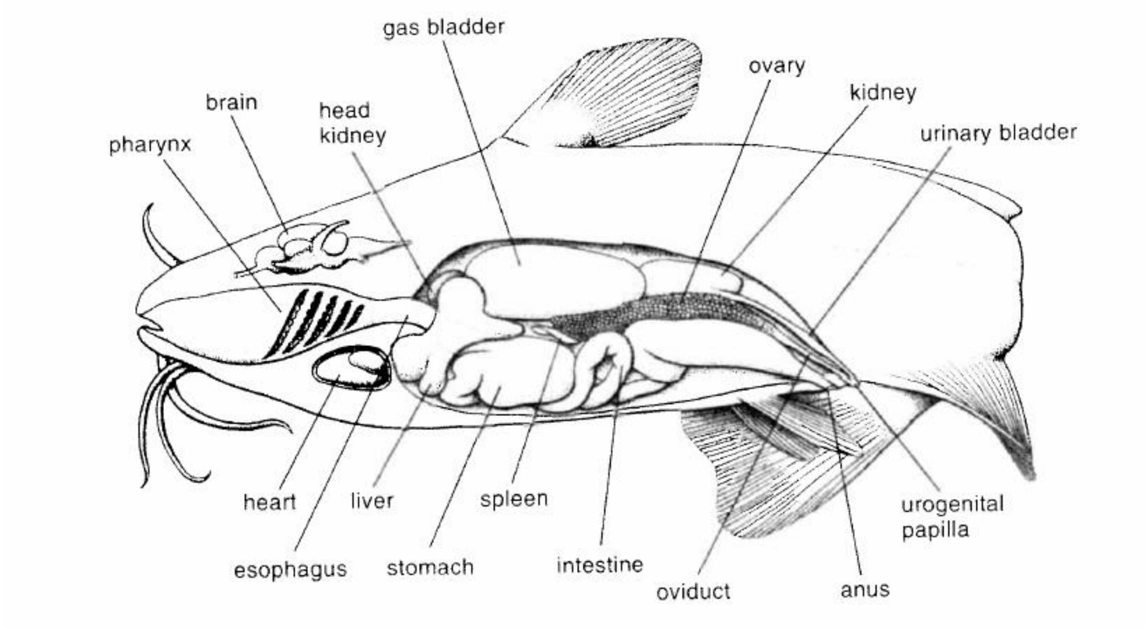

Figure 1.4. Diagram of internal organs. (by permission from Barton 2007).

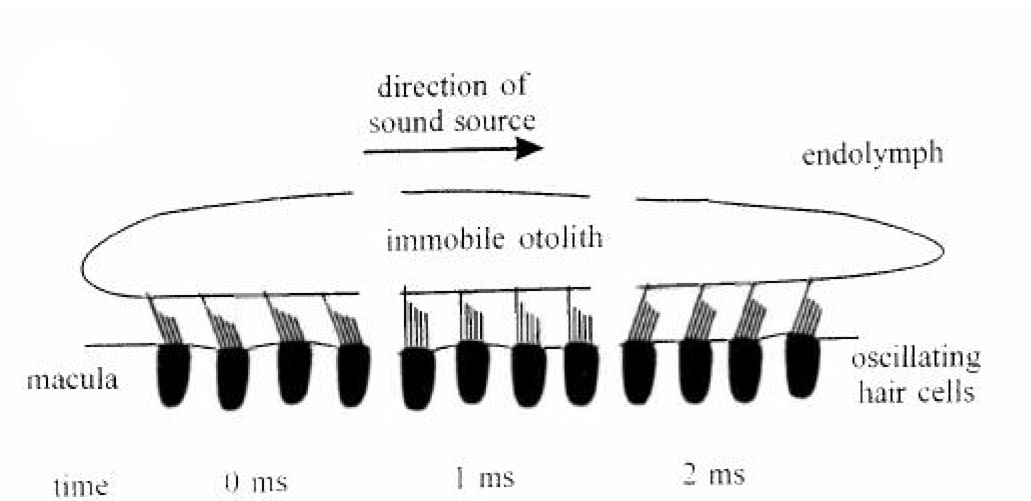

Figure 1.5. Otolith motion in response to sound. Passing sound waves cause motion of hair cell bundles supporting the otolith (by permission from Evans 1998).

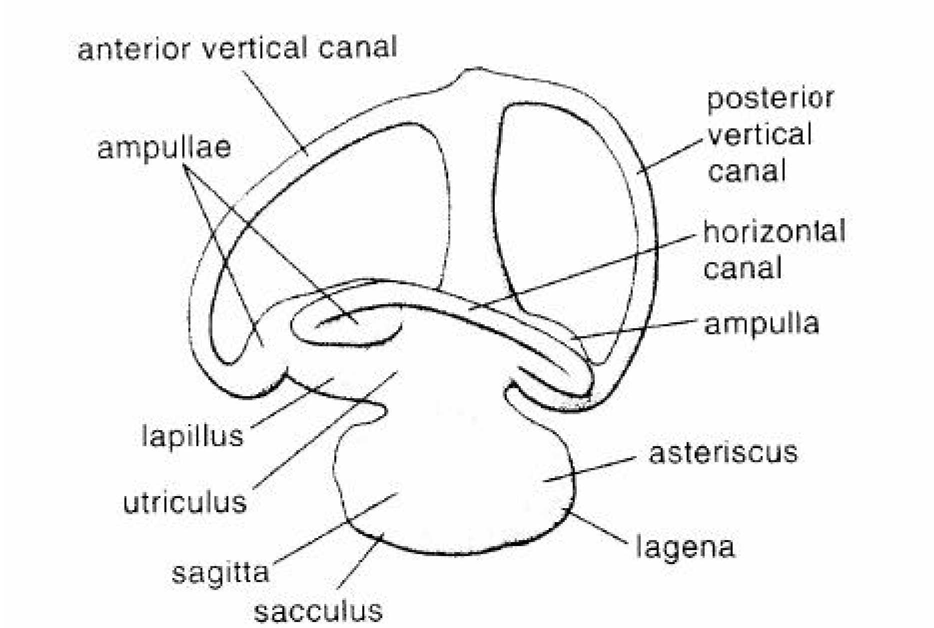

Figure 1.6. Diagram of fish inner ear. The upper and lower inner ear of a cutthroat trout (*Oncorhynchus clarkii*). (by permission from Barton 2007).

CHAPTER 2 BLASTING BRIDGES AND CULVERTS IN FISH STREAMS IN ALASKA[3,4]

Abstract

There are several thousand remote stream crossing structures in the Tongass National Forest in Alaska in need of removal. In 2007 thirty-three collapsing log bridges, log culverts, and metal culverts no longer in use were removed with explosives. Species of salmon, trout, char, and sculpin are present in the project area. Blasting overpressures may injure or kill fish in streams and ground vibrations can damage salmonid embryos in streambeds. Regulatory agencies offer guidelines with limits for blasting induced overpressures and vibrations. However, there has been no quantification of blast overpressures in shallow streams. Methods used to predict lethal levels for various blasting applications have not been completely validated. This research provides guidance for analyzing ground vibrations and water overpressures during blasting activities in or around fish streams.

Overpressures and vibrations were recorded during 19 shots. Three hydrophones and four geophones were placed within streams at various distances from blasted structures. Peak water pressures were found to have a significant relationship with cube-root scaled distances when plotted on a log-log plot. Peak particle velocity data were evaluated against square-root scaled distances and grouped by stream substrate type (e.g. gravel, organics, bedrock) taking into consideration source coupling. Regression analysis provided a significant attenuation model with moderate data scatter.

Background

During the summer of 2007 geophones and hydrophones were deployed in streams to monitor blasting activities on northern Baranof Island in Southeast Alaska

---

[3] Text in this chapter has been modified from the published version.
[4] Published as Dunlap, K. N. 2009. Blasting bridges and culverts in fish streams in Alaska. Journal of Explosives Engineering 26:16-23.

shown in Figure 2.1. Hydrophones were suspended in streams near geophones coupled to the streambed. Blasting was part of a U.S. Forest Service watershed improvement project to remove abandoned stream crossing structures shown in Figure 2.2 left in place from logging activities in the 1960's. The log culverts shown are collapsing, blocking fish passage, and impairing watershed function. I worked on this project as a graduate student for the University of Alaska Fairbanks, School of Fisheries and Ocean Sciences, and as a Habitat Biologist for Alaska Department of Natural Resources and Department of Fish and Game.

Explosives were placed on bridge decks, within the road bed, and inside culverts positioning them in or adjacent to streams. This study characterized explosive ground vibrations and water pressures in streams in an effort to provide a better understanding of propagation and attenuation properties in an environment suitable for fish. Water overpressures can be particularly harmful to fish with swimbladders such as the salmonids in these streams (Yelverton et al. 1975). Ground vibrations traveling through streambeds can jostle and damage incubating embryos that may be present in the streambed.

When water pressure changes are slow (minutes to hours) juvenile fish with swimbladders can withstand extreme pressure changes up to 73.5 lbs/in^2 (Bishai 1961). Fish subject to rapid pressure changes from blasting sustain substantially more injury and mortality (Ogawa et al. 1976). Extreme negative pressures, or rarefactions, can outwardly rupture the swimbladder (Wiley et al. 1981). Surrounding organs such as kidneys, liver, and spleen can be damaged by excessive changes in swimbladder size and shape (Keevin and Hempen 1997). Exceedingly high water overpressures can damage scales and injure the heart or spine. Several factors including age, developmental stage, orientation to blast, and body shape may affect the degree of injury. Fish present in the study area ranged from 1 to 7 inches long. Exact overpressure levels that injure and kill fish are unknown. Several regions require permits for blasting in water but few provide guidance on permissible pressure levels for fish. The State of Alaska Department of Fish and Game (ADF&G) Rationale for Blasting Standards states that explosive use cannot create a pressure change greater than 2.7 lb/in^2 in the swimbladder of a fish (ADF&G 1991). The Guidelines for the Use of Explosives In or Near Canadian Fisheries Waters reference a higher level of 14.5 lb/in^2 (Wright and Hopky 1998).

Incubating embryos are extremely sensitive to mechanical shock (Quinn 2005). Exposure to blast vibration can cause egg mortality and premature hatching and recent studies have attempted to examine what those levels are (Faulkner et al. 2008). Regulatory guidelines limit peak particle velocities to 0.5 in/sec in spawning beds to protect incubating eggs near blasting activities (ADF&G 1991; Wright and Hopky 1998).

This study was conducted to provide a better understanding of best practices for blasting activities in or near streams with rearing fish and incubating eggs. Previous research was performed on unconfined shots in controlled settings using a wide variety of experimental designs and equipment (Keevin et al. 1999). However, there is no accepted standard experimental design for collecting water pressure and vibration data in the field. Limited resources are available to establish realistic guidelines. Data presented in this paper are formatted so that blasters can use the design charge weights in conjunction with distance to critical habitat to meet safe criteria established by regulatory agencies. Furthermore, this information can be used by agencies to improve or clarify regulations involving blasting near sensitive fish habitat.

Methods

Site Descriptions

Figure 2.3 shows a typical blasting site consisting of the remnants of an old logging road and stream crossing. The streams monitored were typically between mountain slopes and floodplains with low to moderate gradients (<5%). These channels are part of the alluvial fan process group of channels which are affected by sediment movement and accretion, and change course frequently. Steeper streams in the study area were more incised and belonged to the moderate gradient mixed control process group where sediment deposition processes are limited. Lower gradient flood plain channels highly influenced by sediment deposition were also within the study area (Paustian

1992). Most of the streams in this study flow directly to or are tributaries of larger channels that empty into the ocean.

Dolly Varden char, cutthroat and rainbow trout, and coho, pink, and chum salmon use these streams (Johnson and Weiss 2006). Generally, adult salmon and char migrate upriver to spawn in gravel substrate during the summer and fall, and cutthroat trout in late spring. Salmon and char eggs hatch mid to late winter and trout eggs in mid summer. Newly emerged alevins reside in gravel substrate for a period of development. Shortly after young pink and chum salmon swim up through the gravel, they migrate to sea. Coho salmon spend 1 to 2 years rearing in freshwater before migrating to sea. Dolly Varden, cutthroat, rainbow, and coho juveniles typically reside in tributaries to larger channels and are present in stream systems year round (Quinn 2005).

Blasting Operations

Two types of water resistant explosive products were used during this project: an ammonium nitrate/fuel oil (ANFO) blasting agent (Austinite WR 300); and a packaged emulsion (Emulex 917). Dual-delay detonators (25/350ms) and 150 gr/ft detonating cord were used to prime shots. Initiating systems included an electrical pulse initiator, a powder punch, and a remote detonating system. Total TNT equivalent charge weights for all blasts ranged from 47 to762 lbs.

Shot configurations as shown in Figure 2.3 varied from site to site depending on size and condition of the crossing-structure as well as the geology and hydrology of the stream. Crossing structures included log stringer bridges, box log culverts, and corrugated metal pipe (CMP) culverts. Log stringer bridges were 26 to 45 ft long with 1 to 2 ft of surface decking. Two or more sill logs (1.5 to 4.5 ft diameter) on either side of the stream support stringer logs that span the channel. These structures were usually loaded with several hundred pounds of emulsion coupled to the sill logs, underneath the bridge's surface. Box log culverts are similar in design to stringer bridges, but have more fill (2 to 12 ft). ANFO was the main blasting agent for removing these structures and was buried in the roadbed or placed underneath the culvert if accessible. CMP culverts ranged in length from 24 to 30 ft, in diameter from 1 to 2 ft, and were covered with 0 to 24 inches of fill. Strings of emulsion were placed inside and along the bottom of these culverts.

Instrumentation Field Methods

Figure 2.4 shows a typical layout of sensors with respect to a blast. Sensors were connected to four and eight channel Instantel Minimate Plus™ vibration monitors. Three piezoelectric hydrophones (47 lb/in^2) and four triaxial geophones were placed in streams for each shot. Distances ranged from 15 to 507 ft from the shot to the sensor and were measured in a straight line and in the stream channel for geophones and hydrophones respectively. Hydrophones were used to record overpressures (lb/in^2) in the stream as fish would experience and geophones recorded vibrations (PPV) in the streambed as incubating embryos would experience.

Hydrophones sampled pressures 65,536 times per second with an operating frequency range of 8 to 500Hz. They were connected to vibration monitors programmed to record for one second after trigger levels exceeded set levels. Trigger levels were set 0.4 lb/in^2 higher than the ambient stream pressure and ranged between 0.2 and 1.5 lb/in^2. Hydrophones were suspended in the water column by a tripod or other available suspension system such as low branches or logs. Water depths ranged from 0.5 to 5 ft and sensors were suspended 4 to 12 inches from the surface.

Standard triaxial geophones sealed with epoxy sampled vibrations up to 10 in/sec and frequencies between 2 to 250 Hz. Seismographs were programmed to record for two seconds after vibrations exceeded 0.5 in/sec. Streambed placement depended on the substrate present at each site. Geophones with long spikes were buried 4 to 6 inches in suitable substrates and 10 to 12 lb sandbags were placed on top. When large cobbles or woody debris prevailed it was impossible to bury geophones deeply or use spikes. Under these circumstances geophones were buried as deeply as possible with small or no spikes and then covered with a sandbag.

Challenges

A few challenges encountered during this study should be noted as they affected the study's design. Blasting in rugged remote areas prohibited the use of large vehicles to transport supplies, limiting the amount of sampling equipment. Rain and high humidity complicated the use of electronics. All electronic equipment was charged on a portable generator nightly and dried in a tent. Challenges encountered while placing geophones included difficulties digging small holes in stream bottoms and achieving adequate coupling in variable substrates. Hydrophone placement was affected by water depth which made distances variable. Fluctuating water levels affected trigger level and location selections. Varied structures and streams complicated selecting placements that would get reliable, reproducible, representative data.

Data Analysis

Peak water overpressures and cube-root scaled distances were log transformed and analyzed using linear regression methods. Residual analysis and remedial measures were applied to analyze outliers and remove data points influenced by energy transfer from ground to water.

Peak particle velocities and scaled distances from 60 waveforms were also log transformed for analysis. Overall attenuation was first examined using simple linear regression methods. Residual analysis and graphical methods suggested separating PPVs into substrate types. Categories included gravel (0.08 to 2.5 inches diameter, n=47), organics (<0.08 inches, n=3), bedrock (> 13 ft, n=3), and a source coupling issue originating from the point of detonation (n=7). PPVs were separated by substrate type and compared to scaled distances using regression methods to determine each groups initial PPVs and attenuation. Four different combinations of intercept and slope parameters for all groups were compared through an analysis of covariance (ANCOVA) to determine the best model.

A more in-depth explanation of field and analytical methods is given in Appendix 1.

Results

Peak pressure frequencies ranged from 19 to 1818 Hz. Four waveforms exhibited negative peaks and 23 were positive. Negative peak pressures ranged from -6.6 to -0.2 lb/in^2 and positive peak pressures from 0.2 to 88.5 lb/in^2. Simple linear regression methods provided a good fitting model shown in Figure 2.5 relating water overpressure to CRSD ($R^2 = 0.83$). Statistical testing showed the model *water overpressure* = $146CRSD^{-1.51}$ to be statistically ($p<0.001$, SE = 0.05).

Typical waveforms recorded in this study had positive peaks followed by a quick drop to a comparable negative peak. Figure 2.6 shows water overpressure waveforms from two hydrophones that recorded the same shot. The closer hydrophone was placed at 78 ft (5.6 $ft/lb^{1/3}$) and shows an initial high frequency wave from detonation. The second waveform was recorded at 230 ft (16.5 $ft/lb^{1/3}$). High frequency pressures from detonation attenuated quickly and did not exceed trigger levels at farther distances.

PPVs for combined scaled distances ranged from 0.5 to 7.4 in/sec and peak frequencies ranged from 4.4 to 172.4 Hz. Although data scatter was high ($R^2 = 0.38$) the model $PPV = 6.2SRSD^{-0.81}$ was statistically significant ($p < 0.001$, SE = 0.14).

For gravel substrate PPVs were 0.6 to 5.5 in/sec with peak frequencies between 4.6 to 172.4 Hz. Organic substrate PPVs had the highest range between 4.6 and 7.4 in/sec with peak frequencies ranging from 4.4 to 64.1 Hz. Bedrock substrate displayed the lowest and least variable PPVs between 0.5 and 0.7 in/sec and peak frequencies ranged from 24.4 to 46.7 Hz. Peak particle velocities from the shot with a source coupling issue were 0.5 to 1.4 in/sec and peak frequencies between 0.5 to 102.4 Hz. When individually regressed attenuation rates were -0.75 for gravel, -0.82 for organics, -0.12 for bedrock, and -0.63 for source coupling issues. Initial values, or y-intercepts, were 6.09 in/sec for gravel, 18.46 in/sec for organics, 0.71 in/sec for bedrock, and 2.43 in/sec for source coupling issues. The best model to describe this data included different initial values and a similar slope ($p < 0.001$, SE = 0.09). PPV attenuation by substrate type is shown in Figure 2.7.

Figure 2.8 shows attenuation differences in waveforms recorded from geophones placed at similar scaled distances in organic, gravel, and bedrock substrates. Geophones coupled in organic substrates recorded the highest initial PPVs and degree of coupling, followed by gravel, and then bedrock. Close-ups of waveforms in Figure 2.8 show higher frequencies in organics than both other groups. Gravel substrate and the source coupling issue group had near identical attenuation rates but different initial values. Sensors for both groups were placed in gravel substrate explaining similarities in attenuation.

Discussion

Stream overpressures

The results of this study show that absolute peak pressures are related to cube-root scaled distance. At a 1 ft cube-root scaled distance, peak overpressures were predicted to be 146 lb/in^2 and have an exponential attenuation rate of -1.51. Seventy-nine percent of overpressure peaks obtained in this study were below the safe level of 14.5 lbs/in^2 suggested by the Canadian Department of Fisheries and Oceans (DFO) (Wright and Hopky 1998). Four values recorded by hydrophones closer than 8 ft/lb$^{1/3}$ were above the safe limit. The Alaska Department of Fish and Game (ADF&G 1991) suggests a more conservative safe limit of 2.7 lbs/in^2. Sixty-six percent of peak overpressures were within these limits (Figure 2.5). Half of those were recorded above the corresponding safe CRSD of 26 ft/lb$^{1/3}$ and the other half below. Thirty-three percent of values were above 2.7 lb/in^2. Safe levels from both agencies are shown in Figure 2.5.

Streambed vibrations

When compared overall, peak particle velocities and scaled distances had a significant relationship. However, the relationships improved when PPVs were stratified by substrate type (Figure 2.8). Partial detonation and different initial values suggest that energy was decoupled at the point of detonation in the source coupling group. Three waveforms from different distances were recorded for both the organic and bedrock substrate groups. Further data should be collected to make additional assumptions on their attenuation rates.

Gravel substrates where incubating eggs can be found are the focus of regulations limiting blasting vibrations to 0.5 in/sec. Figure 2.7 shows the regulatory limit of 0.5 in/sec and a 100-percentile line encompassing all of the values for gravel substrate. All of the recorded values are above regulatory levels. The corresponding scaled distance for safe levels is 63 ft/lb$^{1/2}$. Only one data point appears within the safe limit of 0.5 in/sec in the figure. The peak particle velocity for this point is 0.47 in/sec and was recorded during a shot with source coupling issues. This value was obtained after filtering the data to reduce high frequency noise affecting the waveform's peak. All trigger levels were set at 0.5 in/sec and it is likely that if they were set lower there would be ample data below the safe limit.

Summary

There is a need for more data collection and further analysis of pressure and vibration attenuation. Specifically, data should be collected for blasting in streams with various depths, sinuosity, water velocities, temperatures, and substrate types. Additional data should also be collected and compared for different explosive coupling methods and various methods of sensor placement at lower trigger levels. Due to technological advances in monitoring equipment, the relationship between peak pressures and injury and mortality thresholds should be re-examined for various species and life stages so that regulatory levels can be as accurate as possible. Results discussed in this study are representative of pressure and vibration attenuation for blasting stream crossing structures in shallow alluvial process and floodplain streams. The information presented in this paper is shown in a format (Figure 2.5 and Figure 2.7) that can be used for planning this type of activity.

References

ADF&G (Alaska Department of Fish and Game). 1991. Blasting standards for the protection of fish. Alaska Department of Fish and Game, Division of Habitat, Juneau.

Barton, M. 2007. Bond's biology of fishes. Thomson Brooks/Cole, Belmont, CA.

Baxter, L., E. E. Hayes, G. R. Hampson, and R. H. Backus. 1982. Mortality of fish subjected to explosive shock as applied to oil well severance on George's Bank. Woods Hole Oceanographic Institute, WHOI-82-54 Woods Hole, Massachusetts.

Baxter, R. E. 1971. Effects of explosives detonated in ice on northern pike, Kuskokwim River. Alaska Department of Fish and Game, Divsion of Commercial Fisheries, Informational Leaflet no. 154, Bethel, AK.

Bird, F. H., and K. Roberson. 1984. Keystone Canyon blasting study. Alaska Department of Fish and Game, Commercial Fisheries Division. Glennallen, AK.

Bishai, H. M. 1961. The effect of pressure on the survival and distribution of larval and young fish. Journal du conseil 26(3):292-311.

Christian, E. A. 1973. The effects of underwater explosions on swimbladder fish. Naval Ordnance White Oak Laboratory, NOLTR 73-103, Silver Spring, MD.

Coker, C. M., and E. H. Hollis. 1950. Fish mortality caused by a series of heavy explosions in Chesapeake Bay. Journal of Wildlife Management 14(4):435-445.

Cole, R. H. 1948. Underwater explosions. Princeton University Press, Princeton.

Cooper, P. W. 1996. Explosives engineering. Wiley-VCH, New York.

Cooper, P. W., and S. R. Kurowski 1996. Introduction to the Technology of Explosives. Wiley-VCH, New York.

Dahl, P. H., J. H. Miller, D. H. Cato, and R. K. Andrew. 2007. Underwater ambient noise. Acoustics Today 3(1):23–34.

Dunlap, K. 2009. Blasting bridges and culverts in fish streams: water overpressure and vibration analysis. Thirty-fifth annual conference on explosives and blasting technique. Denver.

Evans, D. H. 1998. The physiology of fishes, 2nd edition. CRC Press, Boca Raton, FL.

Faulkner, S. G., W. M. Tonn, M. Welz, and D. R. Schmitt. 2006. Effects of explosives on incubating lake trout eggs in the Canadian arctic. North American Journal of Fisheries Management 26(4):833-842.

Faulkner, S. G., M. Welz, W. M. Tonn, and D. R. Schmitt. 2008. Effects of simulated blasting on mortality of rainbow trout eggs. Transactions of the American Fisheries Society 137(1):1-12.

Fernet, D. A. 1982. The Effects of underwater detonation of explosives on caged fish in the Bow River, Alberta. Environmental Management Associates, Calgary, Alberta.

Fitch, J. E., and P. H. Young. 1948. Use and effect of explosives in California coastal waters. California Fish and Game 34(2):53-70.

Fitzsimons, J. D. 1994. Survival of lake trout embryos after receiving physical shock. The Progressive Fish Culturist 56(2):149-151.

Gaspin, J. B. 1975. Experimental investigations of the effects of underwater explosions on swimbladder fish (I)1973 Chesapeake Bay tests. Naval Surface Weapons Center, White Oak Laboratory NSWC/WOL/TR 75-58, Silver Spring, MD.

Gaspin, J. B., M. L. Wiley, and G. B. Peters. 1976. Experimental investigations of the effects of underwater explosions on swimbladder fish (II) 1975 Chesapeake Bay tests. Naval Surface Weapons Center, White Oak Laboratory NSWC/WOL/TR 76-58, Silver Spring, MD.

Goertner, J. F. 1978. Dynamic model for explosion injury to fish Naval Surface Weapons Center, Research and Technology Department, Alexandria, VA.

Goertner, J. F. 1982. Prediction of underwater explosion safe ranges for sea mammals. Naval Surface Weapons Center, NSWC TR 82-188, Silver Spring, MD.

Goertner, J. F., M. L. Wiley, G. A. Young, and W. W. McDonald. 1994. Effects of underwater explosions on fish without swimbladders. Naval Surface Warfare Center, White Oak Laboratory, NSWC TR 88-114, Silver Spring, MD.

Hastings, M. C., and A. N. Popper. 2005. Effects of sound on fish. California Department of Transportation, Transportation Contract No. 43A0139, Sacramento.

Hempen, G. L., and T. M. Keevin. 1995. Underwater blasting effects models: a critical evaluation of I-Blast. Twenty-first annual conference on explosives and blasting technique. Nashville, Tennesee. 236-247.

Hempen, G. L., and T. M. Keevin. 1997. Underwater pressure recording: industry standardization. Twenty-third annual conference on explosives and blasting technique. Las Vegas. 237-246.

Hempen, G. L., T. M. Keevin, and T. L. Jordan. 2007. Underwater blast pressures from a confined rock removal during the Miami harbor deepening project. Thirty-third annual conference on explosives and blasting technique. Nashville. 23-35.

Hill, S. H. 1978. A guide to the effects of underwater shock waves on Arctic marine mammals and fish. Institute of Ocean Sciences, Patricia Bay, 78-26, Sidney, BC.

Houghton, J. P., and D. R. Munday. 1987. Effects of linear explosive seismic energy releases on fish in alaska's transition zones. The Alaska Oil and Gas Association, 06793-004-020.

Hubbs, C. L., and A. B. Rechnitzer. 1952. Report on experiments designed to determine effects of underwater explosions on fish life. California Fish and Game 38(3):333-366.

Hubbs, C. L., E. P. Shultz, and R. L. Wisner. 1960. Preliminary report on investigations of the effects on caged fishes of underwater nitro-carbonitrate explosions University of California, Scripps Institute of Oceanography, La Jolla, CA.

ISEE (International Society of Explosives Engineers). 1998. Blasters' handbook™, 17th edition. International Society of Explsoives Engineers, Cleveland, Ohio.

ISEE (International Societ of Explosives Engineers). 1999. Field practice guidelines for blasting seismographs. International Society of Explosives Engineers, Cleveland.

Jensen, J. O. T. 2003. New mechanical shock sensitivity units in support of criteria for protection of salmonid eggs from blasting or seismic disturbance. Fisheries and Oceans Canada, Can. Tech. Rep. Fish. Aquat. Sci. 2452, Nanaimo, British Columbia.

Jensen, J. O. T., and D. F. Alderdice. 1989. Comparison of mechanical shock sensitivity of eggs of five Pacific salmon (*Oncorhynchus*) species and steelhead trout (*Salmo gairdneri*). Aquaculture 78(2):163-181.

Johnson, J., and E. Weiss. 2006. Catalog of waters important for spawning, rearing, or migration of anadromous fishes. Alaska Department of Fish and Game, Special Publication No. 04-06, Anchorage.

Kearns, R. K., and F. C. Boyd. 1965. The effect of a marine seismic exploration on fish populations in British Columbia coastal waters. Canadian Fish Culturist 34:3-26.

Keevin, T. M. 1995. The effects of underwater explosions on fish with techniques to mitigate those impacts. Dissertation. University of Illinois at Urbana-Champaign, Urbana, IL.

Keevin, T. M., J. B. Gaspin, G. R. Gitschlag, G. L. Hempen, T. L. Linton, M. Smith, and D. G. Wright. 1999. Underwater explosions: natural resources concerns, uncertainty of effects, and data needs. Twenty-fifth annual conference on explosives and blasting technique. Nashville. 105-116.

Keevin, T. M., and G. L. Hempen. 1997. The environmental effects of underwater explosions with methods to mitigate impacts. US Army Corps of Engineers, St. Louis.

Kostyuchenko, L. P. 1973. Effect of elastic waves generated in marine seismic prospecting on fish eggs in the Black Sea. Hydrobiological Journal 9(3):45-48.

Lewis, J. A. 1996. Effects of underwater explosions on life in the sea. Department of Defence, Defence Science and Technology Organisation, Aeronautical and Maritime Research Laboratory, DSTO-GD-0080 DSTO-GD-0080, Melbourne, Victoria.

Mann, D. A., P. A. Cott, B. W. Hanna, and A. N. Popper. 2007. Hearing in eight species of northern Canadian freshwater fishes. Journal of Fish Biology 70(1):109-120.

McAnuff, L. A., and R. T. Booren. 1989. Fish mortality study during underwater blasting operations in Lake Erie off Nanticoke, Ontario. International Society of Explosives Engineers 1989G:131-143.

McAnuff, L. A., and A. Curic. 1997. Testing environmental guidelines for subaqueous blasting operations. International Society of Explosives Engineers 1997G:553-564.

Munday, D. R., G. L. Ennis, D. G. Wright, D. C. Jeffries, E. R. McGreer, and J. S. Mathers. 1986. Development and evaluation of a model to predict effects of buried underwater blasting charges on fish populations in shallow water areas. Department of Fisheries and Oceans, Habitat Management Division, Can. Tech. Rep. Fish. Aquat. Sci. 1418, Vancouver.

O'Keefe, D. J. 1984. Guidelines for predicting the effects of underwater explosions on swimbladder fish. Naval Surface Weapons Center, NSWC TR 82-326 AD-A148 870, Silver Spring, MD.

O'Keefe, D. J., and G. A. Young. 1984. Handbook on the environmental effects of underwater explosions. Naval Surface Weapons Center, NSWC TR 83-240 NSWC TR 83-240, Silver Spring, MD.

Ogawa, T., I. Fukuyama, and I. Itoh. 1979. Injuries to fish due to underwater pressure waves IV, dynamic response of internal organs. Journal of the Industrial Explosives Society, Japan 40(2):86-94.

Ogawa, T., I. Fukuyama, and S. Sakaguchi. 1977. A study on injuries to fish due to underwater pressure waves II. Journal of the Industrial Explosives Society, Japan 38(6):349-356.

Ogawa, T., I. Fukuyama, S. Sakaguchi, and T. Narahira. 1978. Injuries to fish due to underwater pressure waves III. Journal of the Industrial Explosives Society 39:196-204.

Ogawa, T., Fukuyama, I., and Ito, I. 1976. Injuries to fish due to underwater pressure waves. Journal of Industrial Explosives Society, Japan 37(6):291-299.

Ogawa, T., Fukuyama, I., and Ito, I. 1978. Injuries to fish due to underwater pressure waves IV, dynamic response of internal organs. Journal of Industrial Explosives Society, Japan 40(2):86-94.

Ogawa, T., Fukuyama, I., and Sakaguchi, S. 1977. Injuries to fish due to underwater pressure waves II, injuries to internal organs. Journal of Industrial Explosives Society, Japan 38(6):349-356.

Paustian, S. J. 1992. A channel type user's guide for the Tongass National Forest, Southeast Alaska. USDA Forest Service R10-TP-26, Alaska Region.

Popper, A. N., M. E. Smith, P. A. Cott, B. W. Hanna, A. O. MacGillivray, M. E. Austin, and D. A. Mann. 2005. Effects of exposure to seismic airgun use on hearing of three fish species. The Journal of the Acoustical Society of America 117(6):13.

Post, G., D. V. Power, and T. M. Kloppel. 1974. Survival of rainbow trout eggs after receiving physical shocks of known magnitude. Transactions of the American Fisheries Society 103(4):711-716.

Quinn, T. P. 2005. The behavior and ecology of Pacific salmon and trout. University of Washington Press, Seattle.

Sakaguchi, S., O. Fukuhara, S. Umezawa, M. Fuhiya, and T. Ogawa. 1976. The influence of underwater explosions on fishes. Nansei Regional Fieheries Research Laboratory.

Simmonds, E. J., and D. N. MacLennan 2005. Fisheries acoustics: theory and practice, 2nd edition. Blackwell Publishing, Iowa.

Siskind, D. E. 2000. Vibrations from blasting, 1st edition. International Society of Explosives Engineers, Cleveland.

Smirnov, A. I. 1954. The effect of mechanical agitation on developing eggs of the pink salmon (Onchorynchus gorbuscha, Salmonidae). Doklady Akademii Nauk SSSR, Translation series, Fisheries Research Board of Canada Series 231 97:365-368.

Smirnov, A. I. 1959. The effect of mechanical agitation in different periods of development on the eggs of autumn chum salmon (Oncorhyncus keta, Salmonidae). Doklady Akademii Nauk SSSR, Translation series, Fisheries Research Board of Canada Series 230 105:873-876.

Sverdrup, A., P. G. Kjellsby, P. G. Krüger, R. Floysand, F. R. Knudsen, P. S. Enger, G. Serck-Hanssen, and K. B. Helle. 1994. Effects of experimental seismic shock on vasoactivity of arteries, integrity of the vascular endothelium and on primary stress hormones of the Atlantic salmon. Journal of Fish Biology 45:973-995.

Teleki, G. C., and A. J. Chamberlain. 1978. Acute effects of underwater construction blasting on fishes in Long Point Bay, Lake Erie. Journal of the Fisheries Research Board of Canada 35:1191-1198.

Wiley, M. L., J. B. Gaspin, and J. F. Goertner. 1981. Effects of underwater explosions on fish with a dynamical model to predict fishkill. Ocean Science and Engineering 6(2):223-284.

Wright, D. G. 1982. A discussion paper on the effects of explosives on fish and marine mammals in the waters of the Northwest Territories. Department of Fisheries and Oceans, Western Region, Can. Tech. Rep. Fish. Aquat. Sci. 1052, Winnepeg, Manitoba.

Wright, D. G., and G. E. Hopky. 1998. Guidelines for the use of explosives in or near canadian fisheries waters. Department of Fisheries and Oceans, Can. Tech. Rep. Fish. Aquat. Sci. 2107.

Yelverton, J. T., D. R. Richmond, E. R. Fletcher, and R. K. Jones. 1973. Safe distance from underwater explosions for mammals and birds. Lovelace Foundation for Medical Education and Research prepared for National Technical Information Service, DNA 3114T, Albequerque.

Yelverton, J. T., D. R. Richmond, W. Hicks, H. Saunders, and E. R. Fletcher. 1975. The relationship between fish size and their response to underwater blast. National Technical Information Service, DNA 3677T DNA 3677T, Albuquerque.

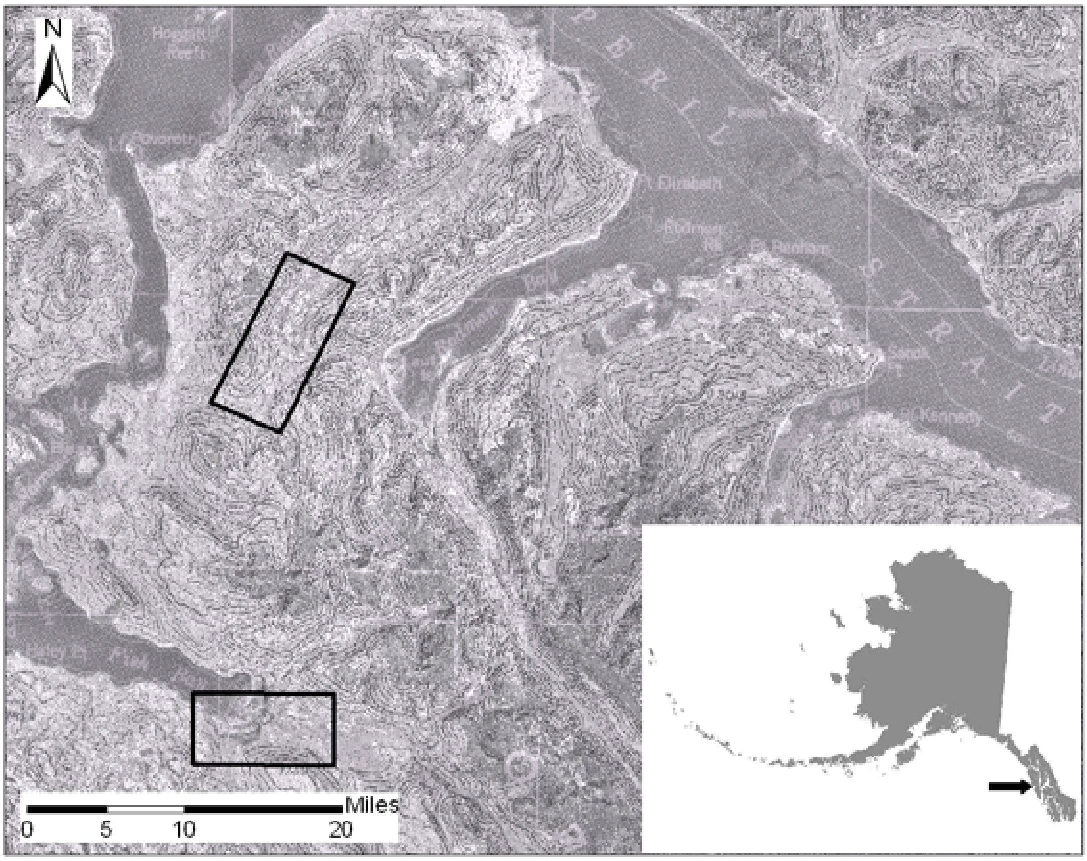

Figure 2.1 Map of study area. Blasts were monitored in two watersheds on northern Baranof Island in Southeast Alaska
.

Figure 2.2. Before and after pictures of a blast site. Photos taken from the same perspective. Left photo shows a failing log culvert. Right photo shows the same location 2 years later.

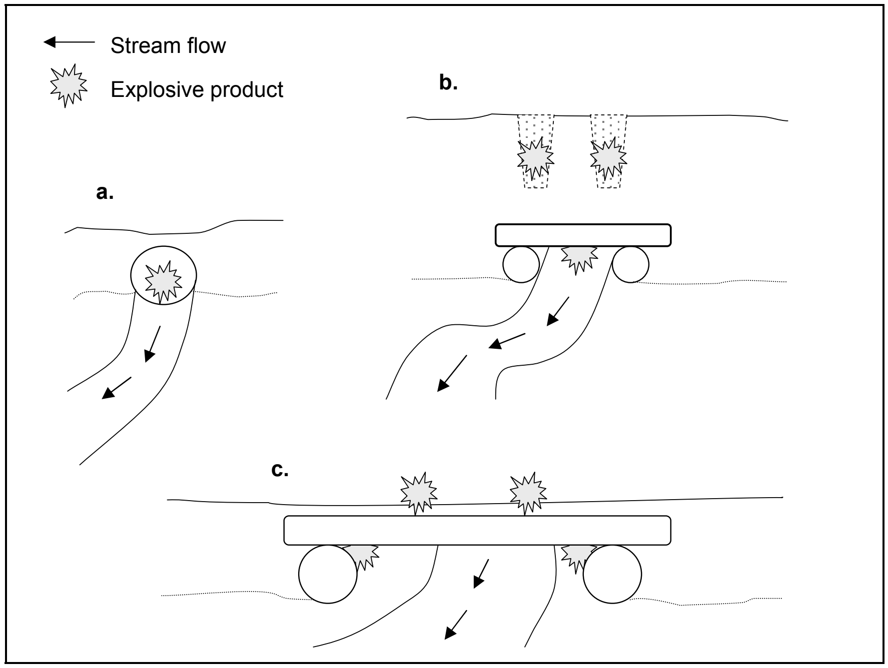

Figure 2.3. Charge placement diagrams. Shown for metal culverts (a), log culverts (b), and stringer bridges (c).

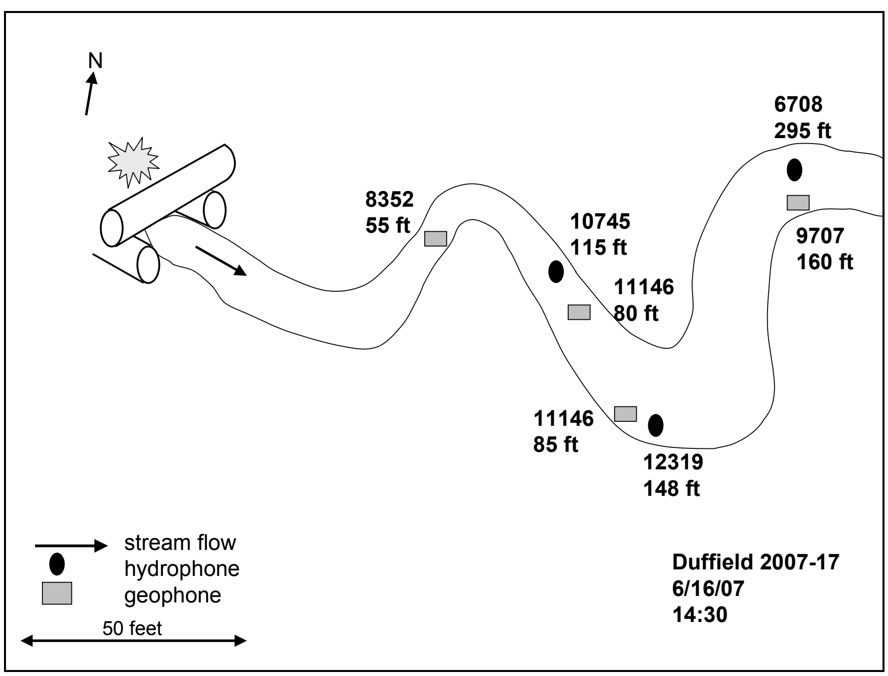

Figure 2.4. Hydrophone and geophone placement. Typical placement relative to detonation point.

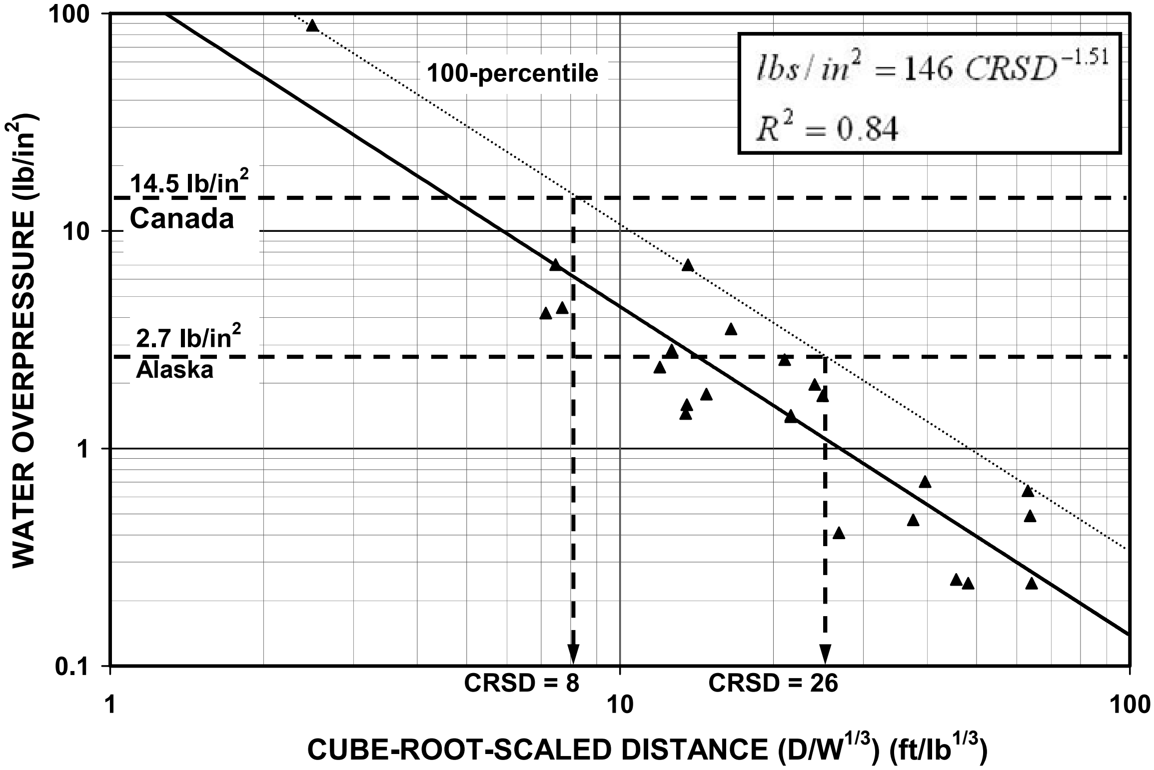

Figure 2.5. Water overpressures versus cube-root-scaled distance. Data recorded in streams during bridge and culvert blasting. ADF&G and Canadian regulatory limits to protect fish are also shown.

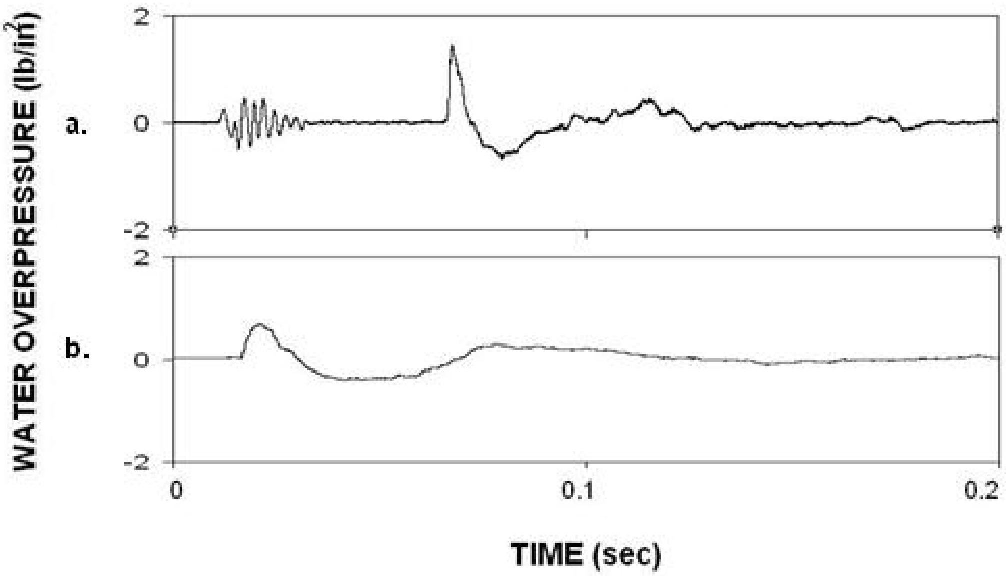

Figure 2.6. Water overpressure time-histories. Waveforms recorded during same shot by hydrophones at 78 ft (5.6 ft/lb$^{1/3}$) (a), and at 230 ft (16.5 ft/lb$^{1/3}$) (b). Time scale begins independently for each hydrophone.

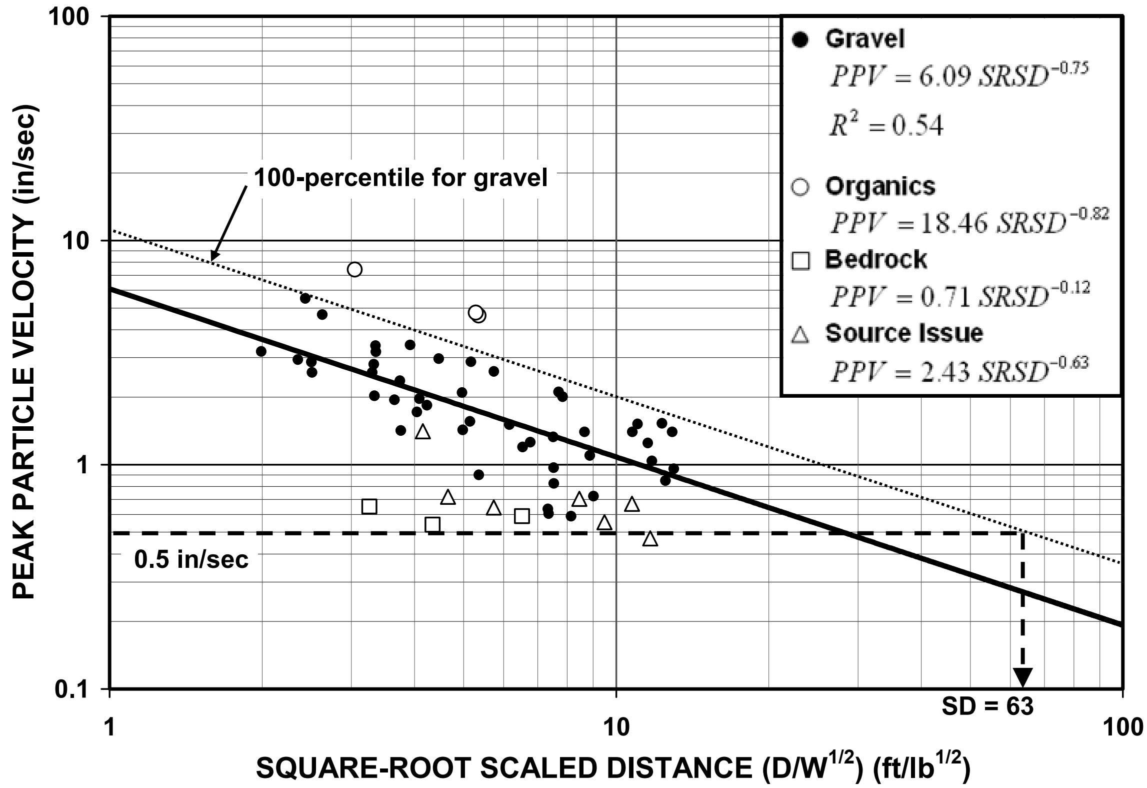

Figure 2.7. Ground vibrations versus scaled distance for different substrate types. Data recorded in streambeds during bridge and culvert blasting. ADF&G regulatory limit to protect embryos incubating in streambeds and 100-percentile line for all of gravel data shown.

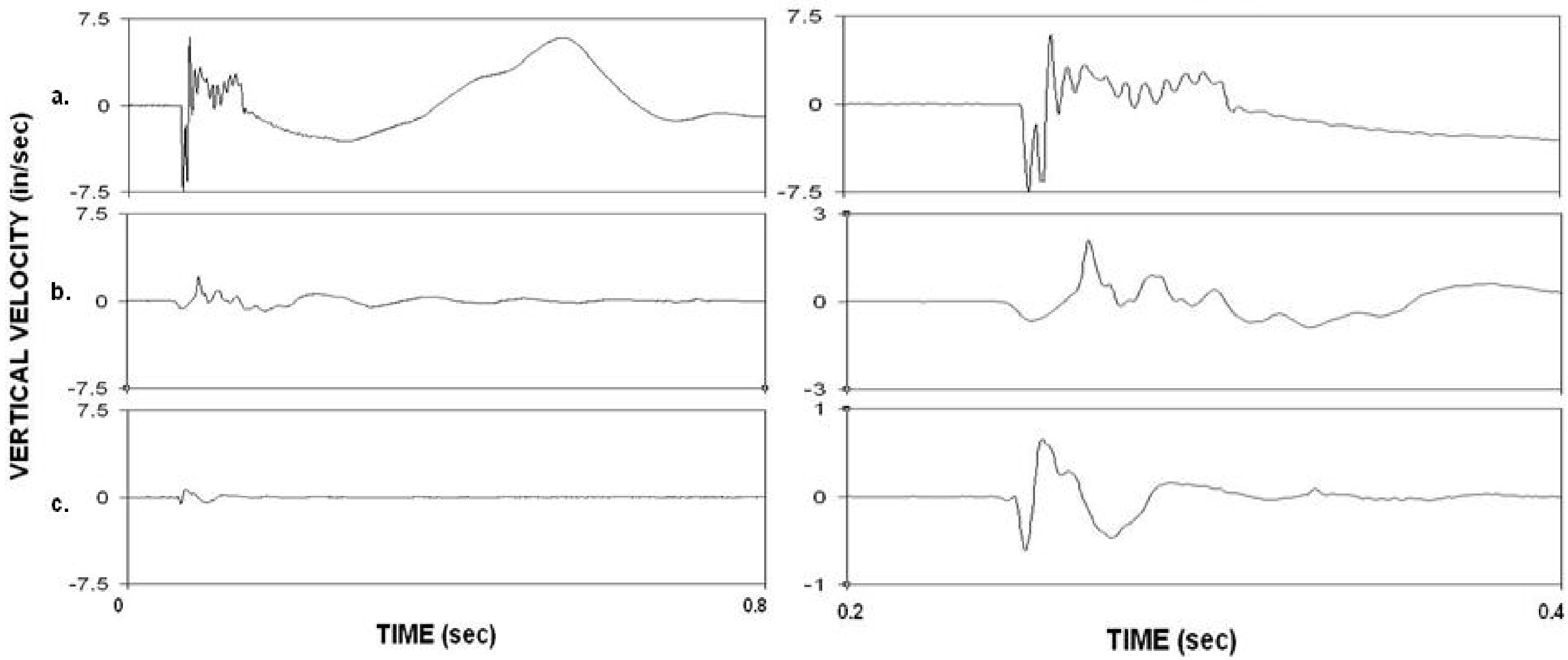

Figure 2.8. Vertical component vibration waveforms in different substrate types. Vibrations in (a) organics recorded at 45 ft (3 ft/lb^2), in (b) gravel at and 52 ft (3.4 ft/lb^2), and (c) bedrock at 75 ft (3.3 ft/lb^2). Waveforms on the right are zoomed in, note the difference in scales.

CHAPTER 3 GENERAL CONCLUSIONS

Literature Review

It is difficult to compare this study with previous studies due to large differences in study designs including experimental settings, shock wave parameters measured, species tested, sensing equipment, and interpretation of data. Few studies aside from laboratory experiments have been conducted under similar settings. Most studies conducted in lab settings involve unconfined, open water shots as opposed to confined shots used for construction and demolition projects. Hempen et al. (2007) confirmed that explosives shot in open water produce higher amplitude and frequency shock waves than confined detonations. This is problematic because mortality prediction models and regulations that are based on them were created for construction and demolition blasting activities. Several authors have noted the need for more data collection in the field to test existing models or develop more accurate ones (Lewis 1996; Hempen and Keevin 1997; Keevin et al. 1999).

Monitoring equipment has improved radically over time, further complicating comparisons between results and mortality observed by early laboratory research and mortality expected in the field. Hempen and Keevin (1997) review previous studies and offer thoughtful suggestions for standardizing underwater pressure recording technology. They point out that several different sensors and recording systems have been used from copper-ball crusher gauges to commercially available hydrophones. They found that the recording equipment used by Yelverton et al. (1975) could not accurately record the first positive peak pressure from blasting so they had to back-extrapolate the curve to estimate impulse (area under the curve). Several early studies were limited by similar problems explaining why impulse was selected as a more accurate predictor of damage and mortality than peak pressure.

Methods for underwater overpressure monitoring and prediction are not as developed as those for monitoring peak particle velocities from blasting. Measurements of shock waves in water require more sensitive equipment than do measurements in solids because shock waves move at much higher velocities in water than solids. The required sensitivity is debated. Hempen and Keevin (1997) suggest equipment and calibration standards for monitoring blasts and recommend using a transducer configuration and oscilloscope with a digitizing interval of 0.1 microseconds up to 0.5 microseconds. While this equipment is ideal, it may be difficult to employ in field situations where more data is needed, due to its size, durability, and cost.

There is a growing need for more precise information on the effects of shock waves on fish and other sensitive species. Keevin and Hempen (1997) point out several study priorities including the collection of more pressure waveform/mortality data in many different field situations, testing of more species at various life stages, and further investigations on how shot designs affect pressure waves. In addition to existing study needs, I propose field testing of available equipment to compare accuracy and feasibility; incorporation of bioacoustic knowledge and sensory thresholds into assessments of the effects of blasting on fish; investigation of peak negative pressure as a mortality predictor; and the inclusion of simultaneously recorded air overpressures, water overpressures, and ground vibrations.

Stream overpressures and streambed vibrations

Peak water overpressures recorded in this study were below 7.1 lb/in^2 (49.0 kPa) in all but one instance and 71.4 % of all pressure recordings were below the ADF&G regulatory level of 2.7 lb/in^2 (19 kPa). The largest negative peak pressure recorded was -6.6 lb/in^2 (-46 kPa). When compared to observed mortality for species that could be present in this area (salmonids, rainbow trout, Dolly Varden char) in other studies, the levels recorded in this study are consistently lower. The lowest reported mortality for salmonids was for coho salmon smolts where 50% of test fish died at 19.3 lbs/in^2 (133 kPa) (Houghton and Munday 1987). Rainbow trout are physiologically similar to salmonids and char as all three are in the family Salmonidae. The lowest reported mortality level for rainbow trout was 12.3 lb/in^2 (85 kPa) and killed 10-20% of 3.9 to 15.7 in (100 to 400 mm) caged fish (Teleki and Chamberlain 1978).

A single overpressure recorded during this study exceeded the upper sensing limit of monitoring equipment. It was roughly estimated to be 88.5 lb/in^2 (610 kPa). Blast induced shock waves originate at high levels and attenuate exponentially. The sensor that recorded this level was placed at a much closer scaled distance (2.5 CRSD) than all subsequent tests (7.1 CRSD or farther). Because the initial rise to peak occurred so fast and exceeded the equipment's sensing range, data transfer from the sensor to the recording unit was interrupted and we were unable to record a corresponding negative pressure.

Peak overpressure and cube-root scaled distances were significantly related with an exponential attenuation rate of -1.51 in shallow streams. There have been no other studies to date that report water overpressure attenuation rates in shallow stream settings. However, attenuation rates have been reported for other water environments and are as follows: -2.6 along the bottom of deep water for buried charges (Hubbs and Rechnitzer 1952); -1.23 for charges confined in rock during harbor deepening (Hempen et al. 2007), and -0.88 for trench blasting in a large river with fast current (McAnuff and Curic 1997).

Peak particle velocities recorded in gravel streambeds did not exceed 5.5 in/s (140 mm/s). The highest overall peak particle velocity recorded was 7.4 in/s (188 mm/s) and occurred in organic substrate not suitable for spawning salmonids. Consequently, this peak particle velocity is not relevant to predictions of embryo mortality. Nearly all PPVs recorded during this study exceeded the regulatory level of 0.5 in/s (13 mm/s). Site conditions and other factors prohibited us from setting trigger levels lower than 0.5 in/s (Appendix 1). This value is less than those that have caused mortality in other studies. No significant mortality was observed in rainbow trout eggs exposed to 5.2 in/s (132 mm/s) during epiboly, their most sensitive stage of development (Faulkner et al. 2008). Ten percent of Chinook eggs exposed to 5.75 in/s (146 mm/s) during epiboly died, while other salmonids species had higher thresholds (Jensen 2003). Although blasting occurred at a time when embryos were not present, the studies reviewed here suggest that if eggs were present at the scaled distances sampled in this study they would not have been harmed.

I observed peak particle velocities, related to square-root scaled distances, to attenuate exponentially at a rate of -0.75. This is less than the typical attenuation of -1.6. Most ground vibrations from blasting have attenuation slopes between -1.0 and -2.0 (ISEE 1998). Attenuations can be less when surface waves are present. Other factors may have increased vibrations and decreased attenuations in this study are site geology and sensor coupling. Areas with deep soil or alluvial deposits are characterized by lower frequencies and larger displacements. Flat topography and high water tables were present in this study and can also increase vibrations. Porous and gravelly materials do not efficiently transmit seismic energy unless water is present to fill the voids between gravel particles improving seismic wave transmission. Although measures were taken to ensure proper sensor coupling in streambeds, the inherent complexity of the streambeds caused less than ideal coupling. Poor coupling most commonly causes exaggerated estimates of ground motion (ISEE 1998).

The attenuation rates reported in this study are the first observed in small forest streams and can be used in future planning for blasting in and near small streams. The results are presented so that blasters can adjust charge weights per delay and distances to limit water overpressures and peak particle velocities to safe levels for salmonid fish in streams and streambeds.

Based on the results of this study and literature review, I propose updating the Alaska Department of Fish and Game's Blasting Standard to reflect the results of the best available literature. The lowest reported mortality for salmonid species was 12.3 lb/in^2 (85 kPa) and killed 10-20% of 3.9 to 15.7 in (100 to 400 mm) caged fish (Teleki and Chamberlain 1978). Recent studies found no mortality in rainbow trout eggs exposed to 5.2 in/s (132 mm/s) and 10% mortality in Chinook eggs exposed to 5.75 in/s (146 mm/s) (Faulkner et al. 2008, Jensen 2003). The simplest method to avoid impacts to fish and embryos is to conduct blasting when species are not present. Life history and timing vary between and within species from site to site. In Southeast Alaska, adults generally migrate upstream to spawn in late summer and early fall. Embryos generally develop in stream gravels through the fall and hatch during winter. Pink, chum, and some sockeye and Chinook salmon migrate to sea during the first late spring or early summer after they hatch. Coho, some sockeye and Chinook salmon, rainbow and cutthroat trout, and Dolly Varden char can spend 1 to 3 years rearing in freshwater before they migrate to sea so they can be present year round. If possible, blasting activities should not occur from the time when adults are migrating upstream to the time embryos have completed epiboly, or during times of outmigration. I recommend changing the limit for blast-induced water overpressures in Alaskan streams from 2.7 to 10.0 lb/in^2 (19 to 69 kPa); and changing the limit for blast-induced vibrations in spawning gravels during sensitive stages of embryonic development from 0.5 to 5.0 in/s (13 to 127 mm/s).

References

ADF&G (Alaska Department of Fish and Game). 1991. Blasting standards for the protection of fish. Alaska Department of Fish and Game, Division of Habitat, Juneau.

Barton, M. 2007. Bond's biology of fishes. Thomson Brooks/Cole, Belmont, CA.

Baxter, L., E. E. Hayes, G. R. Hampson, and R. H. Backus. 1982. Mortality of fish subjected to explosive shock as applied to oil well severance on George's Bank. Woods Hole Oceanographic Institute, WHOI-82-54 Woods Hole, Massachusetts.

Baxter, R. E. 1971. Effects of explosives detonated in ice on northern pike, Kuskokwim River. Alaska Department of Fish and Game, Divsion of Commercial Fisheries, Informational Leaflet no. 154, Bethel, AK.

Bird, F. H., and K. Roberson. 1984. Keystone Canyon blasting study. Alaska Department of Fish and Game, Commercial Fisheries Division. Glennallen, AK.

Bishai, H. M. 1961. The effect of pressure on the survival and distribution of larval and young fish. Journal du conseil 26(3):292-311.

Christian, E. A. 1973. The effects of underwater explosions on swimbladder fish. Naval Ordnance White Oak Laboratory, NOLTR 73-103, Silver Spring, MD.

Coker, C. M., and E. H. Hollis. 1950. Fish mortality caused by a series of heavy explosions in Chesapeake Bay. Journal of Wildlife Management 14(4):435-445.

Cole, R. H. 1948. Underwater explosions. Princeton University Press, Princeton.

Cooper, P. W. 1996. Explosives engineering. Wiley-VCH, New York.

Cooper, P. W., and S. R. Kurowski. 1996. Introduction to the Technology of Explosives. Wiley-VCH, New York.

Dahl, P. H., J. H. Miller, D. H. Cato, and R. K. Andrew. 2007. Underwater ambient noise. Acoustics Today 3(1):23–34.

Dunlap, K. N. 2009. Blasting bridges and culverts in fish streams in Alaska. Journal of Explosives Engineering 26(3):16-23.

Evans, D. H. 1998. The physiology of fishes, 2nd edition. CRC Press, Boca Raton, FL.

Faulkner, S. G., M. Welz, W. M. Tonn, and D. R. Schmitt. 2008. Effects of simulated blasting on mortality of rainbow trout eggs. Transactions of the American Fisheries Society 137(1):1-12.

Faulkner, S. G., W. M. Tonn, M. Welz, and D. R. Schmitt. 2006. Effects of explosives on incubating lake trout eggs in the Canadian arctic. North American Journal of Fisheries Management 26(4):833-842.

Fernet, D. A. 1982. The Effects of underwater detonation of explosives on caged fish in the Bow River, Alberta. Environmental Management Associates, Calgary, Alberta.

Fitch, J. E., and P. H. Young. 1948. Use and effect of explosives in California coastal waters. California Fish and Game 34(2):53-70.

Fitzsimons, J. D. 1994. Survival of lake trout embryos after receiving physical shock. The Progressive Fish Culturist 56(2):149-151.

Gaspin, J. B. 1975. Experimental investigations of the effects of underwater explosions on swimbladder fish (I)1973 Chesapeake Bay tests. Naval Surface Weapons Center, White Oak Laboratory NSWC/WOL/TR 75-58, Silver Spring, MD.

Gaspin, J. B., M. L. Wiley, and G. B. Peters. 1976. Experimental investigations of the effects of underwater explosions on swimbladder fish (II) 1975 Chesapeake Bay tests. Naval Surface Weapons Center, White Oak Laboratory NSWC/WOL/TR 76-58, Silver Spring, MD.

Goertner, J. F. 1978. Dynamic model for explosion injury to fish Naval Surface Weapons Center, Research and Technology Department, Alexandria, VA.

Goertner, J. F. 1982. Prediction of underwater explosion safe ranges for sea mammals. Naval Surface Weapons Center, NSWC TR 82-188, Silver Spring, MD.

Goertner, J. F., M. L. Wiley, G. A. Young, and W. W. McDonald. 1994. Effects of underwater explosions on fish without swimbladders. Naval Surface Warfare Center, White Oak Laboratory, NSWC TR 88-114, Silver Spring, MD.

Grogan, A. 2005. Design and testing of a bubble curtain at Whirl Bay, BC. International Society of Explosives Engineers 2005G:1-11.

Hastings, M. C., and A. N. Popper. 2005. Effects of sound on fish. California Department of Transportation, Transportation Contract No. 43A0139, Sacramento.

Hempen, G. L., and T. M. Keevin. 1995. Underwater blasting effects models: a critical evaluation of I-Blast. Twenty-first annual conference on explosives and blasting technique. Nashville, Tennesee. 236-247.

Hempen, G. L., and T. M. Keevin. 1997. Underwater pressure recording: industry standardization. Twenty-third annual conference on explosives and blasting technique. Las Vegas. 237-246.

Hempen, G. L., T. M. Keevin, and T. L. Jordan. 2007. Underwater blast pressures from a confined rock removal during the Miami harbor deepening project. Thirty-third annual conference on explosives and blasting technique. Nashville. 23-35.

Hill, S. H. 1978. A guide to the effects of underwater shock waves on Arctic marine mammals and fish. Institute of Ocean Sciences, Patricia Bay, 78-26, Sidney, BC.

Houghton, J. P., and D. R. Munday. 1987. Effects of linear explosive seismic energy releases on fish in alaska's transition zones. The Alaska Oil and Gas Association, 06793-004-020.

Hubbs, C. L., and A. B. Rechnitzer. 1952. Report on experiments designed to determine effects of underwater explosions on fish life. California Fish and Game 38(3):333-366.

Hubbs, C. L., E. P. Shultz, and R. L. Wisner. 1960. Preliminary report on investigations of the effects on caged fishes of underwater nitro-carbonitrate explosions University of California, Scripps Institute of Oceanography, La Jolla, CA.

ISEE (International Societ of Explosives Engineers). 1999. Field practice guidelines for blasting seismographs. International Society of Explosives Engineers, Cleveland.

ISEE (International Society of Explosives Engineers). 1998. Blasters' handbook™, 17th edition. International Society of Explsoives Engineers, Cleveland, Ohio.

Jensen, J. O. T. 2003. New mechanical shock sensitivity units in support of criteria for protection of salmonid eggs from blasting or seismic disturbance. Fisheries and

Oceans Canada, Can. Tech. Rep. Fish. Aquat. Sci. 2452, Nanaimo, British Columbia.

Jensen, J. O. T., and D. F. Alderdice. 1989. Comparison of mechanical shock sensitivity of eggs of five Pacific salmon (Oncorhynchus) species and steelhead trout (Salmo gairdneri). Aquaculture 78(2):163-181.

Johnson, J., and E. Weiss. 2006. Catalog of waters important for spawning, rearing, or migration of anadromous fishes. Alaska Department of Fish and Game, Special Publication No. 04-06, Anchorage.

Kearns, R. K., and F. C. Boyd. 1965. The effect of a marine seismic exploration on fish populations in British Columbia coastal waters. Canadian Fish Culturist 34:3-26.

Keevin, T. M. 1995. The effects of underwater explosions on fish with techniques to mitigate those impacts. Dissertation. University of Illinois at Urbana-Champaign, Urbana, IL.

Keevin, T. M., and G. L. Hempen. 1997. The environmental effects of underwater explosions with methods to mitigate impacts. US Army Corps of Engineers, St. Louis.

Keevin, T. M., J. B. Gaspin, G. R. Gitschlag, G. L. Hempen, T. L. Linton, M. Smith, and D. G. Wright. 1999. Underwater explosions: natural resources concerns, uncertainty of effects, and data needs. Twenty-fifth annual conference on explosives and blasting technique. Nashville. 105-116.

Kostyuchenko, L. P. 1973. Effect of elastic waves generated in marine seismic prospecting on fish eggs in the Black Sea. Hydrobiological Journal 9(3):45-48.

Lewis, J. A. 1996. Effects of underwater explosions on life in the sea. Department of Defence, Defence Science and Technology Organisation, Aeronautical and Maritime Research Laboratory, DSTO-GD-0080 DSTO-GD-0080, Melbourne, Victoria.

Mann, D. A., P. A. Cott, B. W. Hanna, and A. N. Popper. 2007. Hearing in eight species of northern Canadian freshwater fishes. Journal of Fish Biology 70(1):109-120.

McAnuff, L. A., and A. Curic. 1997. Testing environmental guidelines for subaqueous blasting operations. International Society of Explosives Engineers 1997G:553-564.

McAnuff, L. A., and R. T. Booren. 1989. Fish mortality study during underwater blasting operations in Lake Erie off Nanticoke, Ontario. International Society of Explosives Engineers 1989G:131-143.

Munday, D. R., G. L. Ennis, D. G. Wright, D. C. Jeffries, E. R. McGreer, and J. S. Mathers. 1986. Development and evaluation of a model to predict effects of buried underwater blasting charges on fish populations in shallow water areas. Department of Fisheries and Oceans, Habitat Management Division, Can. Tech. Rep. Fish. Aquat. Sci. 1418, Vancouver.

Ogawa, T., Fukuyama, I., and Ito, I. 1976. Injuries to fish due to underwater pressure waves. Journal of Industrial Explosives Society, Japan 37(6):291-299.

Ogawa, T., I. Fukuyama, and I. Itoh. 1979. Injuries to fish due to underwater pressure waves IV, dynamic response of internal organs. Journal of the Industrial Explosives Society, Japan 40(2):86-94.

Ogawa, T., I. Fukuyama, and S. Sakaguchi. 1977. A study on injuries to fish due to underwater pressure waves II. Journal of the Industrial Explosives Society, Japan 38(6):349-356.

Ogawa, T., I. Fukuyama, S. Sakaguchi, and T. Narahira. 1978. Injuries to fish due to underwater pressure waves III. Journal of the Industrial Explosives Society 39:196-204.

O'Keefe, D. J. 1984. Guidelines for predicting the effects of underwater explosions on swimbladder fish. Naval Surface Weapons Center, NSWC TR 82-326 AD-A148 870, Silver Spring, MD.

O'Keefe, D. J., and G. A. Young. 1984. Handbook on the environmental effects of underwater explosions. Naval Surface Weapons Center, NSWC TR 83-240 NSWC TR 83-240, Silver Spring, MD.

Paustian, S. J. 1992. A channel type user's guide for the Tongass National Forest, Southeast Alaska. USDA Forest Service R10-TP-26, Alaska Region.

Popper, A. N., M. E. Smith, P. A. Cott, B. W. Hanna, A. O. MacGillivray, M. E. Austin, and D. A. Mann. 2005. Effects of exposure to seismic airgun use on hearing of three fish species. The Journal of the Acoustical Society of America 117(6):13.

Post, G., D. V. Power, and T. M. Kloppel. 1974. Survival of rainbow trout eggs after receiving physical shocks of known magnitude. Transactions of the American Fisheries Society 103(4):711-716.

Quinn, T. P. 2005. The behavior and ecology of Pacific salmon and trout. University of Washington Press, Seattle.

Sakaguchi, S., O. Fukuhara, S. Umezawa, M. Fuhiya, and T. Ogawa. 1976. The influence of underwater explosions on fishes. Nansei Regional Fieheries Research Laboratory.

Simmonds, E. J., and D. N. MacLennan 2005. Fisheries acoustics: theory and practice, 2nd edition. Blackwell Publishing, Iowa.

Siskind, D. E. 2000. Vibrations from blasting, 1st edition. International Society of Explosives Engineers, Cleveland.

Smirnov, A. I. 1954. The effect of mechanical agitation on developing eggs of the pink salmon (Onchorynchus gorbuscha, Salmonidae). Doklady Akademii Nauk SSSR, Translation series, Fisheries Research Board of Canada Series 231 97:365-368.

Smirnov, A. I. 1959. The effect of mechanical agitation in different periods of development on the eggs of autumn chum salmon (Oncorhyncus keta, Salmonidae). Doklady Akademii Nauk SSSR, Translation series, Fisheries Research Board of Canada Series 230 105:873-876.

Sverdrup, A., P. G. Kjellsby, P. G. Krüger, R. Floysand, F. R. Knudsen, P. S. Enger, G. Serck-Hanssen, and K. B. Helle. 1994. Effects of experimental seismic shock on vasoactivity of arteries, integrity of the vascular endothelium and on primary stress hormones of the Atlantic salmon. Journal of Fish Biology 45:973-995.

Teleki, G. C., and A. J. Chamberlain. 1978. Acute effects of underwater construction blasting on fishes in Long Point Bay, Lake Erie. Journal of the Fisheries Research Board of Canada 35:1191-1198.

Wiley, M. L., J. B. Gaspin, and J. F. Goertner. 1981. Effects of underwater explosions on fish with a dynamical model to predict fishkill. Ocean Science and Engineering 6(2):223-284.

Wright, D. G. 1982. A discussion paper on the effects of explosives on fish and marine mammals in the waters of the Northwest Territories. Department of Fisheries and Oceans, Western Region, Can. Tech. Rep. Fish. Aquat. Sci. 1052, Winnepeg, Manitoba.

Wright, D. G., and G. E. Hopky. 1998. Guidelines for the use of explosives in or near canadian fisheries waters. Department of Fisheries and Oceans, Can. Tech. Rep. Fish. Aquat. Sci. 2107.

Yelverton, J. T., D. R. Richmond, E. R. Fletcher, and R. K. Jones. 1973. Safe distance from underwater explosions for mammals and birds. Lovelace Foundation for Medical Education and Research prepared for National Technical Information Service, DNA 3114T, Albuquerque.

Yelverton, J. T., D. R. Richmond, W. Hicks, H. Saunders, and E. R. Fletcher. 1975. The relationship between fish size and their response to underwater blast. National Technical Information Service, DNA 3677T DNA 3677T, Albuquerque.

APPENDIX 1 MATERIALS AND METHODS

I collected data for this project while working for the Alaska Department of Natural Resources (DNR), Office of Habitat Management and Permitting with the assistance of a DNR field tech. We worked together to demolish and monitor stream crossing obstructions with staff from the USDA Forest Service Sitka Ranger District.

Monitoring Equipment

I recorded underwater pressure and vibration data with Instantel Minimate Plus ™ vibration monitors. They were either four channel monitors which recorded data from a single geophone or eight channel units that supported either two geophones or one hydrophone. All monitors were programmed to start recording when a set trigger level was exceeded and retained 0.25 seconds of pre-trigger activity. Monitors were capable of recording up to 65,536 samples per second. I selected these units because of their ability to simultaneously record streambed vibrations and underwater pressure, in addition to their portability and durability.

I sampled underwater pressures with high output pressure sensitive piezoelectric hydrophones (Geo Space ™ MP-24). Hydrophones were able to record pressures in the range of 0 to 47 lb/in^2 (324 kPa), with a sensitivity of 0.034 volts per lb/in^2, and resolution of 0.0237 lb/in^2 (0.16 kPa). The operating frequency was 8 to 500 Hz and natural frequency around 8 Hz. Cables connecting hydrophones to vibration monitors were 200 ft (60m). Hydrophones were manufacturer calibrated prior to use.

Blast vibrations in the streambed were sampled with standard triaxial goephones. Each three-component borehole phone was sealed with epoxy for waterproofing. Sensors were able to record up to 10 in/s (254 mm/s) at 2 to 250 Hz frequencies with a resolution of 0.000625 in/s (0.0159 mm/s). Sensor density was 133 lb/ft^3 (2.13 g/cc) and cable length was 6 ft (1.8m). Geophones were manufacturer calibrated prior to use.

Explosive Products

Three types of explosive products were used for blasting. The first, an ammonium nitrate prill (Austinite WR300) was a free flowing water resistant ammonium nitrate fuel-oil (ANFO) containing 5.7% fuel oil, density of 62.4 lb/ft^3 (0.90 g/cc), and detonation velocity of 14,300 ft/s (4,380 m/s). The second was a continuous length of packaged emulsion cartridges (Emulex 917; 2 ½ x 16 in; 63 x 400 mm) weighing 3.33 lbs (1.51 kg) each with 73.0 lb/ft^3 (1.17 g/cc) density and 17,000 ft/s (5,577 m/s) detonation velocity. The third explosive (Emuline) consisted of a continuous length of smaller emulsion cartridges (7/8 x 16 in; 22 x 400 mm, 0.31 lb/ft, 0.47 kg/m) with an attached line of detonating cord with 65.6 lb/ft^3 (1.05 g/cc) density and 14,000 ft/s (4,270 m/s) detonating velocity.

Nonelectric detonators and detonating cord were used to prime explosives. Nonelectric shock tube detonators had dual delays, one on each end of a length of noiseless shock tube (e.g., 25ms and 350 ms) and 0.03oz (750 mg) of pentaerythritol tetranitrate (PETN) base charge. Detonating cord comprised 150 grains/ft (31.9 gr/m) PETN and detonated at 22,000 ft/s (6,700 m/s).

Site Description

Crossing structures were located in the Fish Bay and Duffield watersheds on northern Baranof Island in Southeast Alaska. We chose to blast sites in the Fish Bay watershed first because less snow made the area more accessible than the Duffield site. The terrain found in these two watersheds was typical of mountain slope and floodplain process groups. Site topography and locations are described in Chapter 1 (Dunlap 2009). All work was conducted out of temporary field camps. Electronic equipment was maintained and charged nightly with portable generators.

Data Collected

Due to the remote location of the blasting sites and time constraints, we collected individual site and structure information three weeks prior to blasting during a reconnaissance visit. We observed structure type, width of road, depth of fill, span/length of log bridges and culverts, average log diameter, distance between sill logs, average sill log diameter, and diameter and length for metal culverts. We also recorded upstream and downstream gradients, and substrate types (e.g., material within the streambed). The data collection form is shown in Figure A1.1. Substrates were grouped into five categories and the most common substrate was recorded for each stream. Categories were described as fines (<0.07 in; <2 mm), gravels (0.07 to 2.5 in; 2 to 64 mm), cobbles (2.5 to 10.0 in; 64-256mm), boulders (>64 in; >256 mm), and rock (>15.7 in; >4 m). For analysis, sites were divided into three groups: fines, gravels, and boulders/bedrock. There were no sites dominated by cobble substrate. The boulder and bedrock categories were combined due to site similarities. Table summarizes data collected during reconnaissance.

We collected additional information on the day of blasting including date, time, weather, crew, photographs, explosive types, shot design, and sensor setup information. The data collection form is shown in Figure A1.2. Table A1.1 summarizes data collected on the day of blasting. Appendices 2 through 20 contain more detailed information on site and shot specifications.

Monitoring Equipment Setup

We deployed three hydrophones and four geophones in the stream for each blast. Terrain and hydrologic variation were factors used to determine where we placed sensors. Hydrophones and geophones were placed near each other in most cases. Straight line (line of sight) and stream distance were measured from the charge to the sensors for each shot. A summary of sensor setup information is shown in Table A1.2.

Hydrophones were suspended 4 to 12 in (10.6 to 30.5 cm) below the water surface from a tripod or other available means such as low hanging branches. We programmed trigger levels at each location to be 0.4 lb/in^2 (2.8 kPa) above ambient stream pressures recorded with each hydrophone. Vibration monitors recorded signals sent from the hydrophones at the maximum sample rate of 65,636 samples per second for one second after trigger levels were exceeded. Sensor depth, water depth, stream width, and substrate type were recorded at each sensor.

Geophones were placed according to manufacturer directions and a field guide published by the International Society of Explosives Engineers (1999). In ideal conditions, we were able to bury geophones 4 to 6 in (10.6 to 15.2 cm) deep with long ground spikes attached. In some cases large rocks and woody debris in the streambed prevented us from burying the geophones at the ideal depths and also prevented the use of the ground spikes. All geophones were covered with a 10 to 12 lb (4.5 to 5.4 kg) sandbags. Trigger levels were set at 0.5 in/s (12.7 mm/s) to avoid false triggers from wildlife and workers. Vibration units recorded at 1,024 samples per second for two seconds after trigger levels were exceeded. For each geophone we recorded a setup description including burial depth, water depth, stream width, and substrate type.

Explosive Methods

Shots were configured according to individual site conditions. For instance, if a structure was collapsing but still had enough space to crawl underneath, we placed explosives beneath the structure. If sufficient working space didn’t exist, we placed explosives in existing surface holes or dug holes where possible. If water was too deep beneath a structure or there was too much gap between the structure’s underside and the explosives, we placed explosives on top of alder logs for elevation. Although site characteristics varied shot setup, some similarities existed for each structure type. Shot designs for each site are described in Appendices 2 through 20.

Log stringer bridges were between 26 and 45 ft (7.9 and 13.7 m) long with 1 to 2 ft (0.3 to 0.6 m) of surface decking and large sill logs (1.5 to 4.5 ft; 0.5 and 1.4 m) lining stream banks. These structures were loaded with several hundred pounds of emulsion well coupled to the sill logs underneath the bridge’s surface, and strategically placed emulsion and ANFO on the bridge decking. A typical bridge shot design is shown in Figure A1.3.

Box log culverts had more road fill (2 to 12 ft; 0.6 to 3.7 m) on top of stringer logs than bridges. Consequently, we placed large amounts of emulsion and ANFO in surface holes and underneath the structure when possible. A typical box log culvert shot design is shown in Figure A1.4.

Corrugated metal culverts were loaded with 2 to 4 strings of emulsion bound together and primed with detonating cord. In all shots emulsion strings rested on the bottom of the culvert. This is shown in Figure A1.5.

Data Processing

Pressure and vibration waveforms were analyzed and evaluated for anomalies prior to statistical analysis. Some were filtered to remove extremely high frequency noise. Events triggered by falling debris or wildlife were removed completely. Water pressure data were treated for negative polarity suggested by consistently negative shock fronts in waves recorded by two hydrophones. This was corrected by applying an inverse scaling factor (-1) to invert the waveforms. The third hydrophone was treated for a resistor mismatch issue. In this instance the vibration unit was calibrated at 0.034 volts per lb/in^2 sensitivity and should have been 0.258 volts per lb/in^2. The treatment was to apply a scaling/correction factor of 0.133 to the waves. In one instance pressure values exceeded the sensor range. Shot F21 on June 3, 2007 exceeded pressure ranges on the hydrophone placed 15 ft (4.6 m) from the shot. The peak was estimated by projecting pressure value lines until they intersected at a peak.

Positive and negative peak water pressures were recorded in addition to the most common frequency in the fast Fourier transform (FFT) analysis. Positive peak particle velocities (PPV), peak frequency, and the most common FFT frequency for transverse, vertical, and longitudinal directions were also recorded. All are shown in Table A1.3 and more detailed results and time-history plots can be found in Appendices 2 through 20.

Peak pressures and vibrations were compared to scaled distances. It is necessary to use a charge-based scaling factor to compare different sized blasts (Siskind 2000). Absolute peak water pressures were regressed against cube-root scaled distances (CRSD) using the stream distance to determine CRSD. CRSD is used for scaling steep-fronted compression waves at a distance and is routinely used for air pressures. It is calculated as

$$\text{CRSD} = \frac{\text{distance}}{\sqrt[3]{\text{charge weight}}}, \frac{\text{ft}}{\text{lb}^{1/3}}.$$

The highest PPV recorded from each triaxial geophone was correlated with square-root scaled distance (SRSD) using the straight line distance from charge to sensors. Ground vibration analyses make use of SRSD as the scaling parameter (Siskind 2000). It is calculated as

$$\text{SRSD} = \frac{\text{distance}}{\sqrt{\text{charge weight}}}, \frac{\text{ft}}{\text{lb}^{1/2}}.$$

Cube and square-root scaled distances are based on the maximum charge weight per 8 millisecond delay. Since this project used different types of explosives, each were converted to their trinitrotoluene (TNT) equivalent charge weight for scaling purposes. TNT equivalence is calculated by multiplying charge weight by a scaling factor determined for that type of explosive. The scaling factor was determined by using the formula

$$\text{TNT equivalency} = \frac{\left(\dfrac{\text{energy of detonation, kJ/cc}}{\text{density g/cc}}\right)}{\left(\dfrac{\text{TNT energy of detonation kJ/cc}}{\text{TNT density g/cc}}\right)}.$$

There are 7,000 grains per pound of PETN. To determine the weight of detonating cord for each shot we multiplied the grains per foot by the length and divided by 7,000 to get the weight in pounds. The following factors were used to determine TNT equivalence: ANFO (0.82), PETN (1.27), and Emulsion (0.62).

Statistical Analysis

Data from 19 shots were analyzed with Microsoft Excel (2003) and SPSS Graduate Student (v.15.0). Predictor (peak water pressures and peak particle velocities) and response (CRSD and SRSD) variables were transformed by natural logarithms (ln) prior to analysis in all cases to linearize relationships and normalize variations that occurred over several orders of magnitude. Residual analysis and remedial measures were applied to analyze outliers and remove data points influenced by falling debris or unwanted energy transfer. Logarithms of 27 peak water overpressures and CRSD were regressed using simple linear regression methods. Logarithms of 60 peak particle velocities and corresponding SRSDs were regressed using the same methodology. High variation and spread suggested separating peak particle velocities into three categories based on their substrate type ("fines", "gravels", "boulders/bedrock"), and a fourth category that represents a shot in which energy was decoupled at the source ("source coupling issue"). Attenuation relationships with SRSD in each category were examined with an Analysis of Covariance (ANCOVA).

References

Dunlap, K. 2009. Blasting Bridges and Culverts in Fish Streams: Water Overpressure and Vibration Analysis. Thirty-Fifth Annual Conference on Explosives and Blasting Technique. International Society of Explosives Engineers, Denver, CO.

ISEE. 1999. ISEE Field Practice Guidelines for Blasting Seismographs. Pages 279-285 *in*. International Society of Explosives Engineers, Inc., Cleveland, OH.

Siskind, D. E. 2000. Vibrations from blasting, 1st edition. International Society of Explosives Engineers, Cleveland, OH.

Preliminary Stream Data

Site #:
milepost:

Date: **Time:**	**Initials:**	**GPS Waypoint:**	**GPS Coordinates:**
Weather:			

Upstream Picture #: Location taken:	**Down Stream Picture #:** Location taken:	**Other Pics / Desc:**

Structure Type (Circle One):

Log Bridge	Log Culvert	Metal Culvert
Width (of road): Depth of Fill: Span (length): Avg. log diameter: Distance between Sill Logs:	Width (of road): Depth of Fill: Span (length): Avg. log diameter: Distance between Sill Logs:	Width (of road): Depth of Fill: Culvert Diameter: Culvert Length:

Stream Gradient:

Eye level of shooter:	Eye level of shooter:
Upstream reading:	Downstream reading:
Distance between:	Distance between:

Density:

Additional Substrate Info:

circle dominant types present:

Fines	<2mm (smaller than ladybug)
Gravels	2-64 (ladybug to tennis ball)
Cobbles	64-256 (tennis ball to basketball)
Boulders	>256mm (larger than basketball)
Rock	>4m (boulders and blocks bigger than 4 m)

Additional Notes:

Site Sketch
indicate direction of flow

Site #:
milepost:

Figure A1.1 Site specification data sheet. Form used to collect site and structure information during reconnaissance trips.

Table A1.1 Site and structure specifications. Recorded during reconnaissance trip.

Site Name	Shot Date and Time	Structure Type	Road Width	Fill Depth	Dnstream Grade	Upstream Grade	Substrate Type	Log Bridges and Box Log Culverts				CMPs	
								Span / Length	Stringer Diameter	Between Sill Logs	Sill Log Diameter	Culvert Diamete	Culvert Length
			(ft)	(ft)	(%)	(%)		(ft)	(ft)	(ft)	(ft)	(ft)	(ft)
D02	6/18/07 12:14	LC	25	2.5	4	5	gravel	4	1.2	4.0	2.8	na	na
D02-2	6/18/07 13:49	LC	25	2.5	4	5	gravel	4	1.2	4.0	2.8	na	na
D04	6/18/07 15:03	WB	24	na	3	4	gravel	na	na	na	na	na	na
D08	6/20/07 11:05	LB	23	1.5	3	4	gravel	28	2.0	16.8	2.8	na	na
D11	6/20/07 16:37	LC	25	1.0	1	2	gravel	36	1.0	4.6	2.0	na	na
D12	6/21/07 11:00	LC	11	2.0	1	2	gravel	25	0.8	2.7	1.7	na	na
D15	6/17/07 9:46	LC	21	1.0	3	3	gravel	28	1.0	3.0	2.0	na	na
D16	6/16/07 16:33	LC	22	11.0	3	4	gravel	35	1.0	5.5	3.3	na	na
D17	6/16/07 14:27	LC	22	5.0	3	5	gravel	12	1.8	3.0	2.0	na	na
D19	6/15/07 13:59	LC	35	12.0	11	9	bedrock	40	1.0	6.5	1.0	na	na
D20	6/14/07 12:33	LB	18	1.5	4	6	gravel	35	3.0	24.5	5.0	na	na
D21	6/13/07 18:31	LB	25	1.5	5	4	gravel	45	4.0	33.0	4.5	na	na
D22	6/13/07 15:16	LB	25	0.0	3	5	gravel	43	2.0	28.0	3.0	na	na
D22-2	6/13/07 12:03	LB	25	0.0	3	5	gravel	43	2.0	28.0	3.0	na	na
F13	6/6/07 10:13	LB	26	1.5	1	1	gravel	33	2.5	10.2	2.8	na	na
F14	6/5/07 15:30	LB	21	0.6	1	1	gravel	26	2.0	23.5	1.7	na	na
F16	6/4/07 17:54	CMP	22	0.0	1	1	gravel	na	na	na	na	2.0	24
F19	6/4/07 11:45	CMP	23	2.0	0	0	gravel	na	na	na	na	1.3	24
F21	6/3/07 13:57	CMP	24	1.9	2	0	fines	na	na	na	na	2.0	30

LC log culvert
WB water bar
LB log bridge
CMP corrugated metal pipe

Blasting Day Data

Site #:
milepost:

Date of shot:		Shot time:		Weather:		Data Crew:		BIC:	
Water Temp:									

Variables:

Charge weight (lbs):	
depth of charge:	
Predicted distance for no injuries (x):	

Distances (from table):

station	divisor	distance
1		
2		
3		
4		

Sensor Data:

	SN	**Straight dist.**	**Wet dist.**	**Sensor depth**	**Stream width**	**Stream depth**	**Substrate present**
geo 1:							
geo 2:							
geo 3:							
geo 4:							
hydro 1							
hydro 2							
hydro 3							

After Pictures and Notes:

upstream:
downstrm:
other:

Additional Notes:

Figure A1.2 Shot and sensor setup data sheet

Table A1.2 Shot and sensor setup summary. Includes shot name, date and time, structure types, explosives setup, product amounts, TNT equivalence, and distances from shot to hydrophones and geophones.

Site Name	Shot Date and Time	Structure Type	Coupling Level	Explosives			Total Charge Weight	TNT Equivalent	Distance Between Shot and Sensor						
									Stream Distance			Straight Distance			
				detcord (150 gr.)	ANFO	Emulsion			Hydro 6708	Hydro 12319	Hydro 10745	Seism 8352	Seism 9707	Seism 11146-1	Siesm 11146-2
				(ft)	(lbs)	(lbs)	(lbs)	(lbs)	(ft)	(ft)	(ft)	(ft)	(ft)	(ft)	(ft)
D02	6/18/07 12:14	LC	C	200	220	15	239	195	230	78	78	58	150	65	80
D02-2	6/18/07 13:49	LC	C	0	55	3	58	47	230	78	78	58	150	65	80
D04	6/18/07 15:03	WB	WC	300	605	40	651	529	na	na	na	77	204	84	93
D08	6/20/07 11:05	LB	C	150	825	45	873	708	335	235	235	180	240	70	100
D11	6/20/07 16:37	LC	C	75	220	15	237	192	420	210	144	120	300	160	180
D12	6/21/07 11:00	LC	DC	125	275	15	293	238	257	441	507	170	193	166	199
D15	6/17/07 9:46	LC	C	200	275	15	294	240	167	84	84	52	114	58	83
D16	6/16/07 16:33	LC	C	170	275	25	304	246	201	134	108	115	150	70	90
D17	6/16/07 14:27	LC	DC	0	165	55	220	169	295	148	115	160	55	80	85
D19	6/15/07 13:59	LC	WC/C	140	220	1140	*1363	*891	440	220	110	150	300	75	100
D20	6/14/07 12:33	LB	C	250	0	1218.6	1224	762	440	220	80	180	110	55	65
D21	6/13/07 18:31	LB	C	290	0	1431	1437	895	440	220	220	290	140	110	150
D22	6/13/07 15:16	LB	DC	0	0	218.6	219	136	330	110	110	270	90	60	95
D22-2	6/13/07 12:03	LB	DC	0	0	231	231	143	330	110	110	270	90	60	95
F13	6/6/07 10:13	LB	C	380	495	190	693	534	174	115	58	115	174	58	77
F14	6/5/07 15:30	LB	C	250	495	200	700	537	178	120	60	115	174	58	77
F16	6/4/07 17:54	CMP	C	240	0	250	255	162	130	90	42	52	98	31	42
F19	6/4/07 11:45	CMP	C	60	0	200	201	126	132	88	60	132	44	58	88
F21	6/3/07 13:57	CMP	C	80	0	350	352	219	76	45	15	18	79	45	78

C coupled
WC well-coupled
DC decoupled

LC log culvert
WB water bar
LB log bridge
CMP corrugated metal pipe

* Total charge weight per 25 millisecond delay was 853 lbs (TNT equivalent 530 lbs).

Figure A1.3 Log stringer bridge explosive design. Top: typical explosive placement for removing a log stringer bridge. Middle: Emulsion is well-coupled to sill and stringer logs. Bottom: ANFO is buried in surface decking and primed with emulsion and detonating cord

Figure A1.4 Box log culvert explosive design. Top: explosive placement for removing a box log culvert. Middle: boxes of emulsion are placed beneath the structure and connected to a detonating cord loop. Bottom: ANFO is buried deeply in the road fill and tied into detonating cord

Figure A1.5 Metal culvert explosive design. Top: typical explosive placement for removing a metal culvert. Middle: lengths of emulsion are bound together and pulled through the culvert. Bottom: assembling lengths of emulsion prior to placement.

Table A1.3 Hydrophone and geophone results summary for all shots. Summary of peak water pressures and frequencies recorded by hydrophones in streams and vibrations recorded by triaxial geophones in streambeds for 19 shots detonated in or near streams.

Site Name	Structure Type/ Coupling Level	Total TNT Equiv per Delay	Sensor Type	S/N	Scaled Distance	Stream Pressures			Streambed Vibrations								
						Peaks			Transverse			Vertical			Longitudinal (radial)		
						Positive	Negative	FFT Freq.	Velocity	Freq.	FFT Freq.	Velocity	Freq.	FFT Freq.	Velocity	Freq.	FFT Freq.
		(lbs)			seism: (ft/lbs$^{1/2}$) hydro: (ft/lbs$^{1/3}$)	(lb/in^2)	(lb/in^2)	(Hz)	(in/s)	(Hz)	(Hz)	(in/s)	(Hz)	(Hz)	(in/s)	(Hz)	(Hz)
D02	LC / coupled	195	Seism	9707	10.7				0.31	7.0	5.0	0.67	21.4	17.3	0.33	9.8	7.0
			Seism	8352	4.2				0.68	9.7	6.5	1.41	102.4	12.8	0.59	14.6	4.8
			Seism	11146-2	5.7				0.42	6.4	5.3	0.65	17.1	21.8	0.41	11.4	5.8
			Seism	11146-1	4.7				0.16	20.5	4.8	0.72	86.2	10.0	0.55	9.7	6.0
			Hydro	6708	13.5	nt											
			Hydro	12319	39.7	0.71	-0.40	10.5									
			Hydro	10745	13.5	1.45	-0.66	18.5									
D02-2	LC / coupled	47	Seism	9707	21.9				nt			nt			nt		
			Seism	8352	8.5				0.44	9.8	10.5	0.71	17.7	13.5	0.52	23.3	15.8
			Seism	11146-2	11.7				0.43	18.9	16.8	0.47	19.7	20.3	0.40	17.6	13.5
			Seism	11146-1	9.5				0.15	32.1	5.0	0.56	19.9	22.0	0.44	19.7	16.5
			Hydro	6708	63.7	0.49	-0.37	14.0									
			Hydro	12319	21.6	1.40	-0.59	23.5									
			Hydro	10745	21.6	1.42	-0.66	23.5									
D04	WB / well-coupled	529	Seism	9707	8.9				0.80	7.6	5.0	1.10	12.2	12.5	0.99	7.3	4.5
			Seism	8352	3.3				1.31	8.7	9.5	3.40	84.7	11.0	0.86	72.5	5.0
			Seism	11146-2	4.0				1.46	36.5	5.3	1.72	19.0	10.8	0.60	19.7	10.8
			Seism	11146-1	3.7				0.79	13.1	4.8	1.95	56.8	7.8	0.84	10.4	2.0
			Hydro	6708		1.79	-1.03	9.5									
			Hydro	12319		3.27	-1.35	16.5									
			Hydro	10745		3.53	-1.64	17.0									

Site Name	Structure Type/ Coupling Level	Total TNT Equiv per Delay	Sensor Type	S/N	Scaled Distance	Stream Pressures			Streambed Vibrations								
						Peaks			Transverse			Vertical			Longitudinal (radial)		
						Positive	Negative	FFT Freq.	Velocity	Freq.	FFT Freq.	Velocity	Freq.	FFT Freq.	Velocity	Freq.	FFT Freq.
		(lbs)			seism: (ft/lbs$^{1/2}$) hydro: (ft/lbs$^{1/3}$)	(lb/in^2)	(lb/in^2)	(Hz)	(in/s)	(Hz)	(Hz)	(in/s)	(Hz)	(Hz)	(in/s)	(Hz)	(Hz)
D08	LB / coupled	708	Seism	9707	9.0				0.16	31.8	6.5	0.73	46.7	5.0	0.44	5.1	4.8
			Seism	8352	6.8				0.50	8.5	5.0	1.26	56.8	5.0	0.17	39.4	3.3
			Seism	11146-1	2.6				2.52	5.6	6.0	4.67	18.3	6.5	0.97	6.2	6.3
			Seism	11146-2	3.8				0.36	22.2	4.8	1.42	10.0	6.5	1.41	6.0	6.3
			Hydro	6708	26.4	nt											
			Hydro	12319	26.4	nt											
			Hydro	10745	37.6	0.47	-0.39	10.0									
D11	LC / coupled	192	Seism	9707	21.7				nt			nt			nt		
			Seism	8352	8.7				0.90	7.4	7.0	0.50	166.7	7.5	1.40	7.3	6.8
			Seism	11146-1	11.5				0.21	10.5	7.0	0.60	103.1	8.5	1.25	6.6	6.5
			Seism	11146-2	11.5				0.80	6.3	6.8	0.84	102.4	8.3	0.96	7.4	6.8
			Hydro	6708	72.8	nt											
			Hydro	12319	36.4	nt											
			Hydro	10745	25.0	0.66	-1.75	286.0									
D12	LC / decoupled	238	Seism	9707	12.5				0.34	51.5	6.0	0.85	51.0	5.8	0.24	5.9	5.8
			Seism	8352	11.0				0.53	7.3	6.0	1.52	102.4	7.3	0.53	7.1	8.5
			Seism	11146-1	10.8				0.38	5.9	6.3	1.40	56.8	7.5	0.20	6.3	4.8
			Seism	11146-2	12.9				0.24	4.8	7.0	1.40	128.2	7.0	0.21	86.2	7.0
			Hydro	6708	41.5	nt											
			Hydro	12319	71.2	nt											
			Hydro	10745	81.8	1.09	-1.02	70.5									

Site Name	Structure Type/ Coupling Level	Total TNT Equiv per Delay	Sensor Type	S/N	Scaled Distance	Stream Pressures: Peaks Positive	Stream Pressures: Peaks Negative	Stream Pressures: FFT Freq.	Streambed Vibrations: Transverse Velocity	Transverse Freq.	Transverse FFT Freq.	Vertical Velocity	Vertical Freq.	Vertical FFT Freq.	Longitudinal (radial) Velocity	Longitudinal (radial) Freq.	Longitudinal (radial) FFT Freq.
		(lbs)			seism: (ft/lbs$^{1/2}$) hydro: (ft/lbs$^{1/3}$)	(lb/in^2)	(lb/in^2)	(Hz)	(in/s)	(Hz)	(Hz)	(in/s)	(Hz)	(Hz)	(in/s)	(Hz)	(Hz)
D15	LC / coupled	240	Seism	9707	7.4				0.61	7.1	6.5	0.56	68.5	43.0	0.46	9.5	6.3
			Seism	8352	3.4				0.89	23.4	9.3	2.11	34.0	10.3	3.19	6.9	9.3
			Seism	11146-2	5.4				0.81	6.3	6.0	0.90	42.7	9.8	0.90	8.4	6.0
			Seism	11146-1	3.7				1.02	8.8	6.3	1.60	18.3	9.3	2.37	8.0	9.5
			Hydro	6708	13.5	nt											
			Hydro	12319	26.9	0.41	-0.19	9.5									
			Hydro	10745	13.5	1.59	-1.49	17.5									
D16	LC / coupled	246	Seism	9707	9.6				nt			nt			nt		
			Seism	8352	7.3				0.31	6.4	4.5	0.64	56.8	4.0	0.31	36.5	1.8
			Seism	11146-1	4.5				1.32	36.5	6.0	1.39	19.7	9.3	2.97	9.5	3.8
			Seism	11146-2	5.7				0.88	4.5	3.5	2.61	30.0	8.3	1.58	5.3	2.5
			Hydro	6708	32.1	nt											
			Hydro	12319	17.2	nt											
			Hydro	10745	21.4	nt											
D17	LC / decoupled	169	Seism	9707	4.2				1.60	73.5	24.8	1.05	42.7	2.3	1.84	39.4	2.3
			Seism	8352	12.3				0.35	9.5	3.3	1.01	5.1	6.3	1.53	4.6	4.0
			Seism	11146-1	6.2				0.65	4.2	4.8	1.51	51.5	6.3	0.64	4.4	4.0
			Seism	11146-2	6.5				0.49	4.9	4.3	1.20	73.5	4.3	0.61	4.3	4.0
			Hydro	6708	53.4	nt											
			Hydro	12319	20.8	nt											
			Hydro	10745	26.8	nt											

Site Name	Structure Type/ Coupling Level	Total TNT Equiv per Delay	Sensor Type	S/N	Scaled Distance	Stream Pressures			Streambed Vibrations								
						Peaks			Transverse			Vertical			Longitudinal (radial)		
						Positive	Negative	FFT Freq.	Velocity	Freq.	FFT Freq.	Velocity	Freq.	FFT Freq.	Velocity	Freq.	FFT Freq.
		(lbs)			seism: $(ft/lbs^{1/2})$ hydro: $(ft/lbs^{1/3})$	(lb/in^2)	(lb/in^2)	(Hz)	(in/s)	(Hz)	(Hz)	(in/s)	(Hz)	(Hz)	(in/s)	(Hz)	(Hz)
D19	LC / well-coupled	530	Seism	9707	13.0				nt								
			Seism	8352	6.5				0.21	46.7	39.8	0.37	42.4	31.5	0.59	24.4	30.0
			Seism	11146-1	3.3				0.40	42.7	45.5	0.65	36.5	27.0	0.30	102.4	1.8
			Seism	11146-2	4.3				0.37	51.0	43.0	0.54	46.7	25.3	0.49	42.7	37.3
			Hydro	6708	54.4	nt											
			Hydro	12319	27.2	nt											
			Hydro	10745	13.6	6.99	-4.31	67.5									
D20	LB / coupled	762	Seism	8352	6.5				nt			nt			nt		
			Seism	9707	4.0				0.47	9.0	10.5	0.85	25.6	22.0	0.17	27.0	25.5
			Seism	11146-1	2.0				1.37	5.3	2.0	3.20	24.4	18.8	1.61	8.4	8.0
			Seism	11146-2	2.4				0.53	19.0	22.0	2.94	46.7	16.5	1.30	15.1	13.3
			Hydro	6708	8.8	nt											
			Hydro	12319	48.2	0.24	0.22	8.5									
			Hydro	10745	24.1	1.97	-1.35	18.0									
D21	LB / coupled	895	Seism	8352	9.7				nt			nt			nt		
			Seism	11146-1	3.7				nt			nt			nt		
			Seism	11146-2	5.0				nt			nt			nt		
			Seism	9707	4.7				nt			nt			nt		
			Hydro	6708	22.8	nt											
			Hydro	12319	22.8	nt											
			Hydro	10745	45.7	0.25	-0.22	8.5									

Site Name	Structure Type/ Coupling Level	Total TNT Equiv per Delay	Sensor Type	S/N	Scaled Distance	Stream Pressures			Streambed Vibrations								
						Peaks			Transverse			Vertical			Longitudinal (radial)		
						Positive	Negative	FFT Freq.	Velocity	Freq.	FFT Freq.	Velocity	Freq.	FFT Freq.	Velocity	Freq.	FFT Freq.
		(lbs)			seism: (ft/lbs$^{1/2}$) hydro: (ft/lbs$^{1/3}$)	(lb/in^2)	(lb/in^2)	(Hz)	(in/s)	(Hz)	(Hz)	(in/s)	(Hz)	(Hz)	(in/s)	(Hz)	(Hz)
			Seism	8352	22.6				nt			nt			nt		
			Seism	11146-1	5.0				nt			nt			nt		
			Seism	11146-2	7.9				nt			nt			nt		
D22	LB / decoupled	143	Seism	9707	7.5				0.18	86.2	55.5	0.77	172.4	99.8	0.97	51.0	40.0
			Hydro	6708	21.0	nt											
			Hydro	12319	63.1	0.64	-0.39	10.5									
			Hydro	10745	21.0	2.56	-1.11	24.5									
			Seism	8352	23.2				nt			nt			nt		
			Seism	9707	7.7				nt			nt			nt		
			Seism	11146-2	8.1				0.38	36.5	29.0	0.55	86.2	32.3	0.59	86.2	29.3
D22-2	LB / decoupled	136	Seism	11146-1	5.1				0.53	39.4	56.0	1.56	46.3	53.3	0.80	51.0	31.0
			Hydro	6708	21.4	nt											
			Hydro	12319	21.4	nt											
			Hydro	10745	64.2	0.24	-0.17	10.0									
			Seism	9707	7.5				0.73	17.1	3.5	0.83	56.8	7.5	0.12	128.2	1.5
			Seism	8352	5.0				1.05	15.1	3.5	1.43	128.2	3.5	0.66	25.6	4.5
			Seism	11146-1	2.5				1.16	24.4	6.8	2.58	16.0	7.0	1.34	7.4	3.3
F13	LB / coupled	534	Seism	11146-2	3.3				0.59	8.4	3.0	2.03	39.4	7.0	1.37	9.7	3.5
			Hydro	6708	21.4	nt											
			Hydro	12319	14.2	nt											
			Hydro	10745	7.1	4.12	-4.19	51.0									

Site Name	Structure Type/ Coupling Level	Total TNT Equiv per Delay	Sensor Type	S/N	Scaled Distance	Stream Pressures			Streambed Vibrations								
						Peaks			Transverse			Vertical			Longitudinal (radial)		
						Positive	Negative	FFT Freq.	Velocity	Freq.	FFT Freq.	Velocity	Freq.	FFT Freq.	Velocity	Freq.	FFT Freq.
		(lbs)			seism: $(ft/lbs^{1/2})$ hydro: $(ft/lbs^{1/3})$	(lb/in^2)	(lb/in^2)	(Hz)	(in/s)	(Hz)	(Hz)	(in/s)	(Hz)	(Hz)	(in/s)	(Hz)	(Hz)
F14	LB / coupled	537	Seism	9707	7.5				0.83	128.2	2.0	1.33	172.4	9.3	1.04	12.8	7.3
			Seism	8352	5.0				0.93	5.3	2.0	2.10	128.2	6.3	1.49	42.3	6.0
			Seism	11146-1	2.5				1.11	9.7	13.0	1.57	36.5	11.5	2.87	5.0	1.8
			Seism	11146-2	3.3				0.78	34.2	13.3	1.20	36.5	11.8	2.81	29.2	2.0
			Hydro	6708	21.9	nt											
			Hydro	12319	7.4	nt											
			Hydro	10745	14.8	1.78	-1.28	13.0									
F16	CMP / coupled	162	Seism	9707	7.7				1.15	4.7	3.0	2.11	51.5	4.0	0.40	4.0	3.0
			Seism	8352	4.1				1.73	4.7	1.8	1.97	51.5	4.0	0.68	4.5	4.0
			Seism	11146-1	2.4				2.60	5.8	3.3	5.52	25.6	22.0	2.58	3.5	3.3
			Seism	11146-2	3.3				1.12	56.8	1.5	2.58	14.6	4.3	2.18	14.4	2.8
			Hydro	6708	23.8	nt											
			Hydro	12319	16.5	2.96	-3.55	16.5									
			Hydro	10745	7.7	4.45	-2.73	27.5									
F19	CMP / coupled	126	Seism	9707	3.9				0.69	51.0	2.5	3.42	64.1	2.5	1.88	8.1	2.5
			Seism	11146-1	5.2				0.44	72.5	5.5	2.88	72.5	7.8	1.83	9.3	7.5
			Seism	11146-2	7.8				1.67	128.2	7.8	2.01	42.3	7.8	1.92	172.4	7.8
			Seism	8352	11.8				0.52	7.5	7.5	0.94	18.5	18.5	1.04	14.0	14.0
			Hydro	6708	26.3	nt											
			Hydro	12319	17.6	nt											
			Hydro	10745	12.0	2.37	-2.25	1490.0									

Site Name	Structure Type/ Coupling Level	Total TNT Equiv per Delay	Sensor Type	S/N	Scaled Distance	Stream Pressures			Streambed Vibrations								
						Peaks			Transverse			Vertical			Longitudinal (radial)		
						Positive	Negative	FFT Freq.	Velocity	Freq.	FFT Freq.	Velocity	Freq.	FFT Freq.	Velocity	Freq.	FFT Freq.
		(lbs)			seism: (ft/lbs$^{1/2}$) hydro: (ft/lbs$^{1/3}$)	(lb/in^2)	(lb/in^2)	(Hz)	(in/s)	(Hz)	(Hz)	(in/s)	(Hz)	(Hz)	(in/s)	(Hz)	(Hz)
F21	CMP / coupled	219	Seism	8352	1.2				nt			nt			nt		
			Seism	9707	5.3				1.67	8.1	7.8	1.27	9.7	10.3	4.63	7.1	4.8
			Seism	11146-1	3.0				4.79	4.4	4.0	7.41	64.1	0.7	5.76	3.0	3.3
			Seism	11146-2	5.3				4.77	4.4	4.3	3.59	11.9	7.8	1.99	26.9	3.0
			Hydro	6708	12.6	2.24	-2.84	9.0									
			Hydro	12319	7.5	7.01	-6.61	26.5									
			Hydro	10745	2.5	88.5*	*	*									

LC log culvert
WB water bar
LB log bridge
CMP corrugated metal pipe

nt sensor not triggered
* positive peak was estimated, unable to determine negative peak and frequencies

APPENDIX 2 SITE D2-1 LOG CULVERT. Site diagram and setup information, hydrophone and geophone time histories

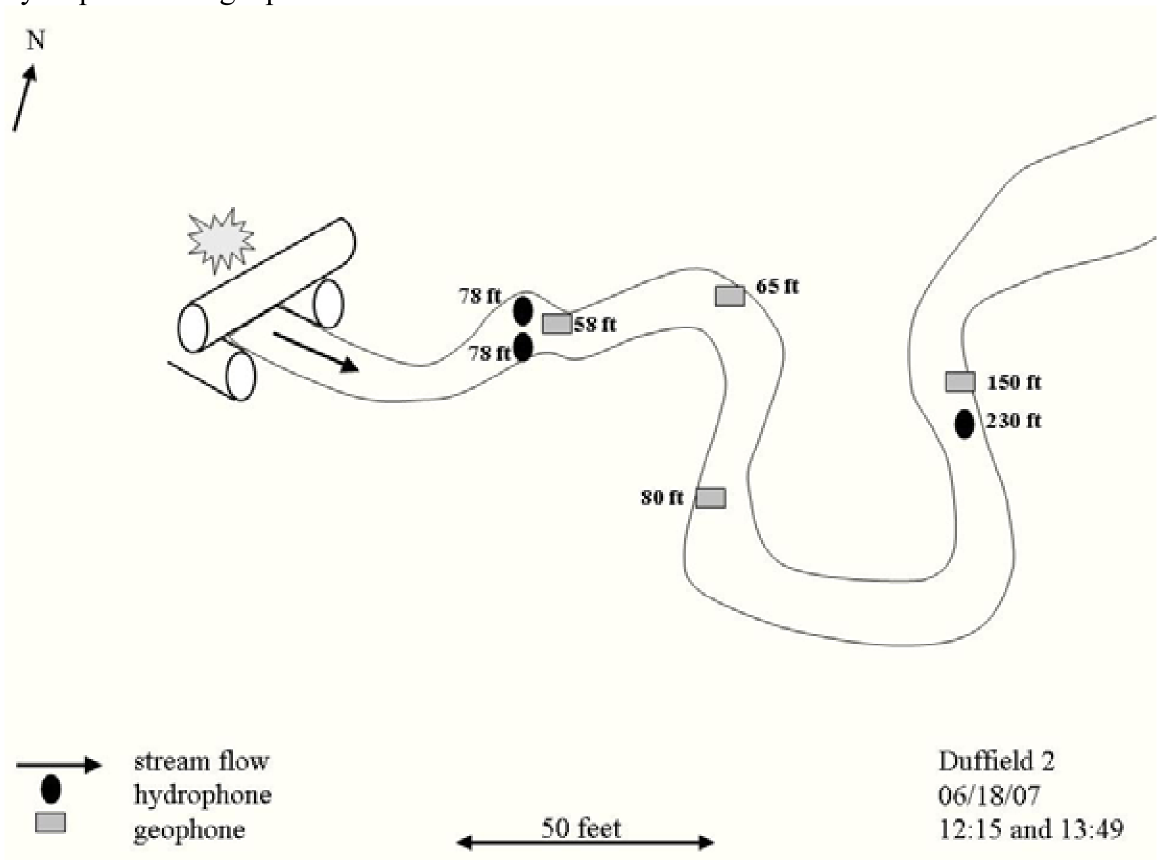

Structure, site, and shot information recorded during shot

Span / Length (ft)	Stringer Diameter (ft)	Between Sill Logs (ft)	Sill Log Diameter (ft)	Road Width (ft)	Fill Depth (ft)	Stream Grade (%)	Substrate Type
4	1.2	4.0	2.8	25	2.5	4-5	gravel

detcord (150 gr.) (ft)	ANFO (lbs)	Emulsion (lbs)	Total # / Delay (lbs)	TNT Equivalent (lbs)	Coupling level
200	220	15	239	195	coupled

(13.5 SD)

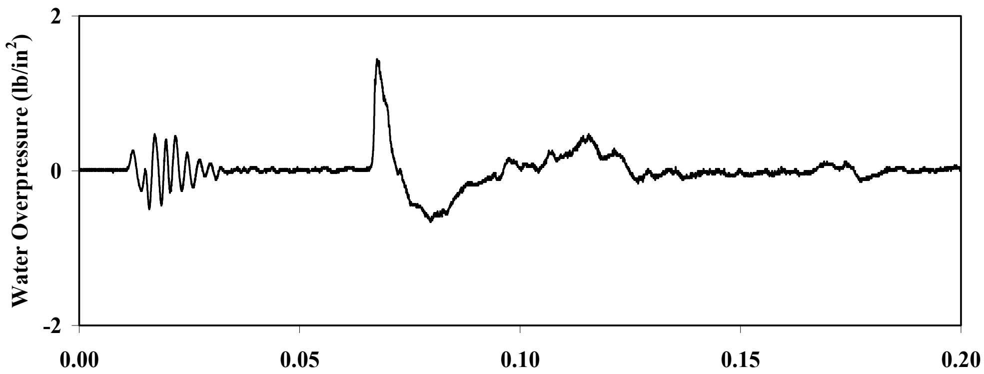

(39.7 SD)

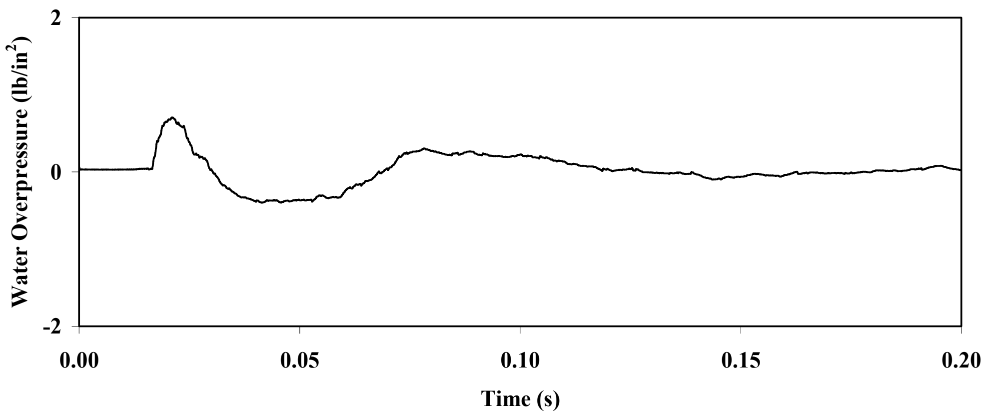

Stream pressures recorded during shot D2-1

Stream Distance (ft)	Scaled Distance ($ft/lbs^{1/3}$)	Positive Peak (lb/in^2)	Negative Peak (lb/in^2)	FFT Freq. (Hz)
78	13.5	1.45	-0.66	18.5
230	39.7	0.71	-0.40	10.5

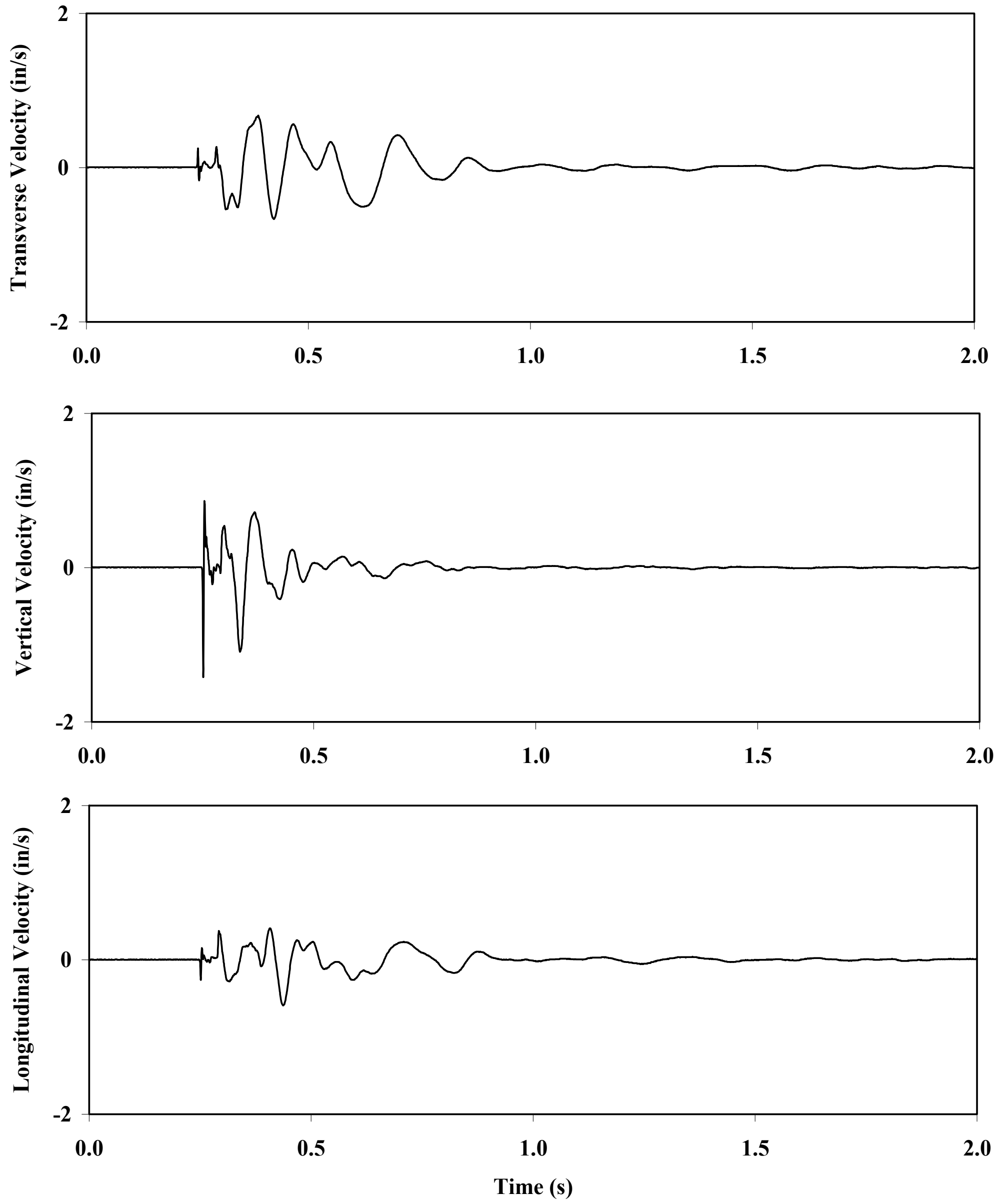

Streambed vibrations recorded during shot D2-1

Straight Distance (ft)	Scaled Distance (ft/lbs$^{1/2}$)	Transverse PPV (in/s)	FFT Freq. (Hz)	Vertical PPV (in/s)	FFT Freq. (Hz)	Long. PPV (in/s)	FFT Freq. (Hz)
58	4.2	0.68	6.5	1.41	12.8	0.59	4.8

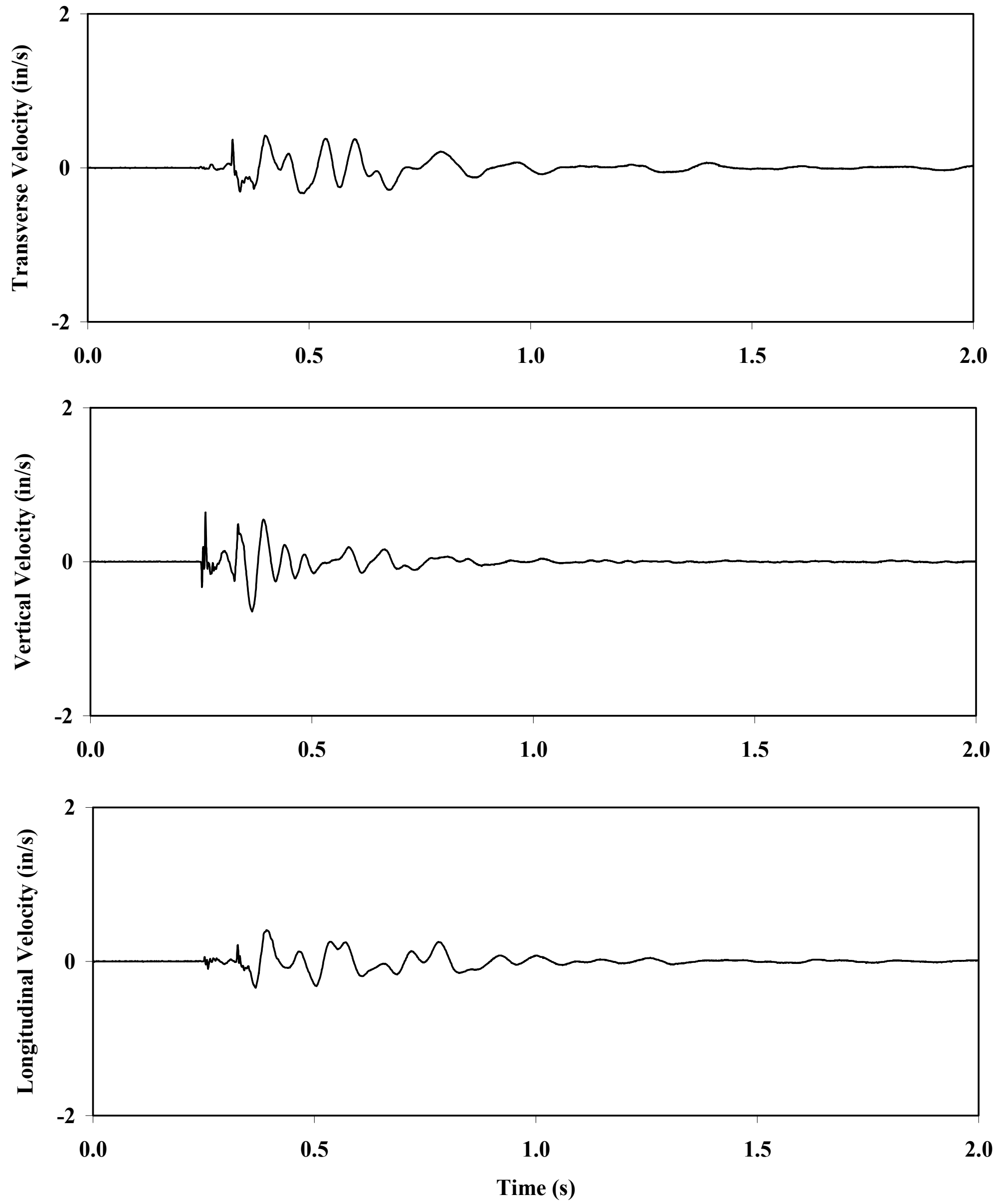

Streambed vibrations recorded during shot D2-1

Straight Distance (ft)	Scaled Distance ($ft/lbs^{1/2}$)	Transverse PPV (in/s)	FFT Freq. (Hz)	Vertical PPV (in/s)	FFT Freq. (Hz)	Long. PPV (in/s)	FFT Freq. (Hz)
65	4.7	0.16	4.8	0.72	10.0	0.55	6.0

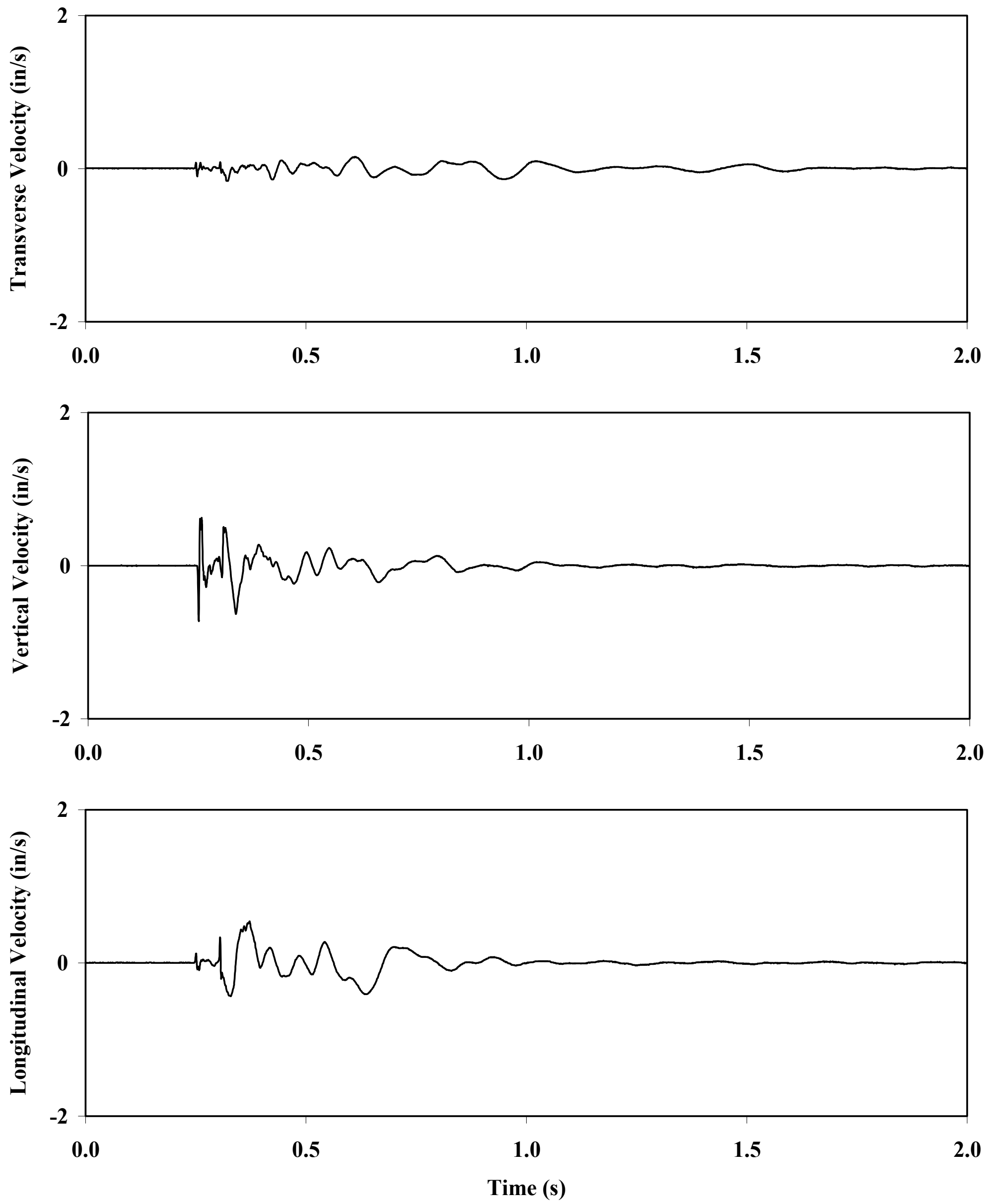

Streambed vibrations recorded during shot D2-1

Straight Distance (ft)	Scaled Distance (ft/lbs$^{1/2}$)	Transverse PPV (in/s)	FFT Freq. (Hz)	Vertical PPV (in/s)	FFT Freq. (Hz)	Long. PPV (in/s)	FFT Freq. (Hz)
80	5.7	0.42	5.3	0.65	21.8	0.41	5.8

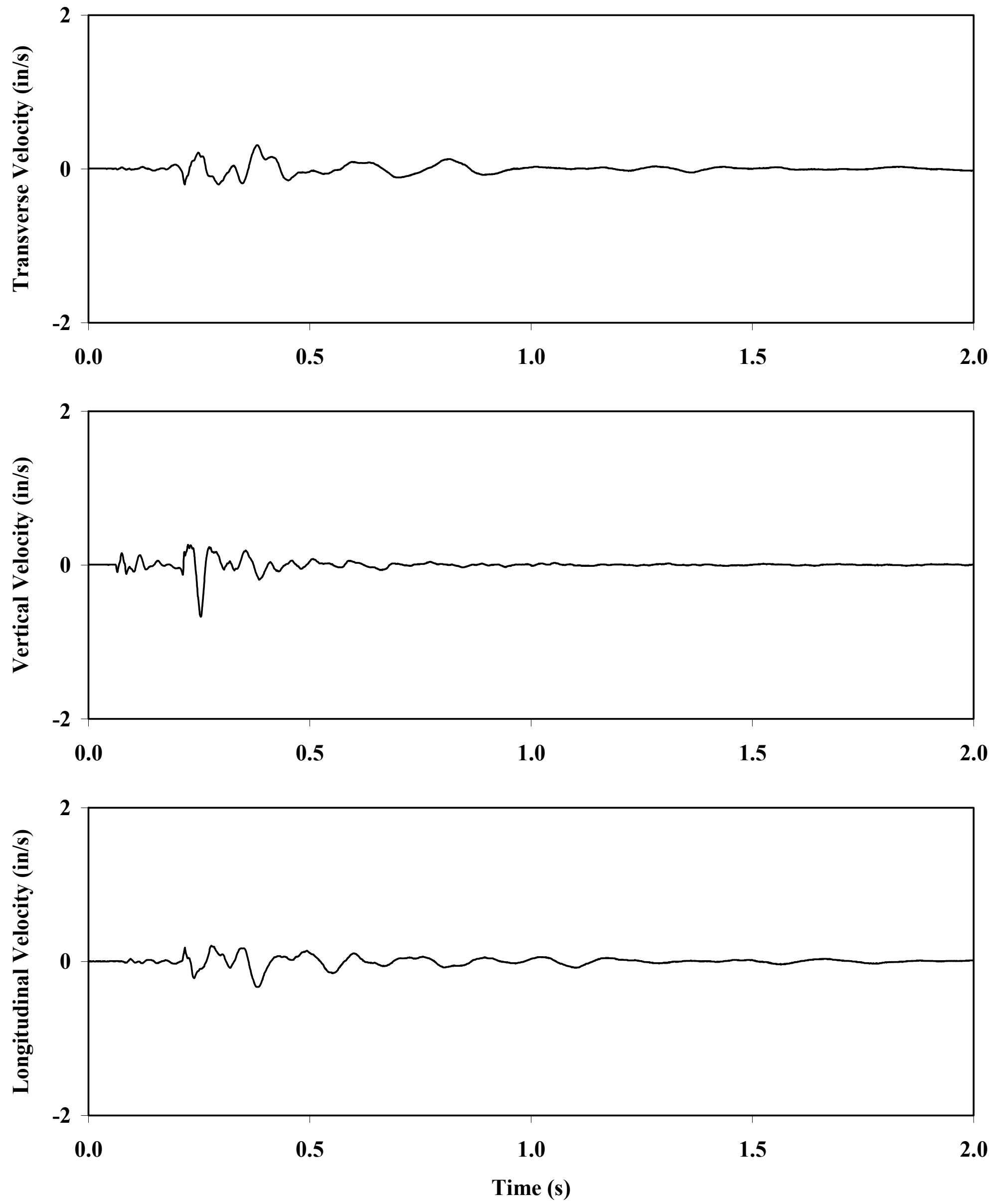

Streambed vibrations recorded during shot D2-1

Straight Distance (ft)	Scaled Distance (ft/lbs$^{1/2}$)	Transverse PPV (in/s)	FFT Freq. (Hz)	Vertical PPV (in/s)	FFT Freq. (Hz)	Long. PPV (in/s)	FFT Freq. (Hz)
150	10.7	0.31	5.0	0.67	17.3	0.33	7.0

APPENDIX 3 SITE D2-2 LOG CULVERT. Site diagram and setup information, hydrophone and geophone time histories

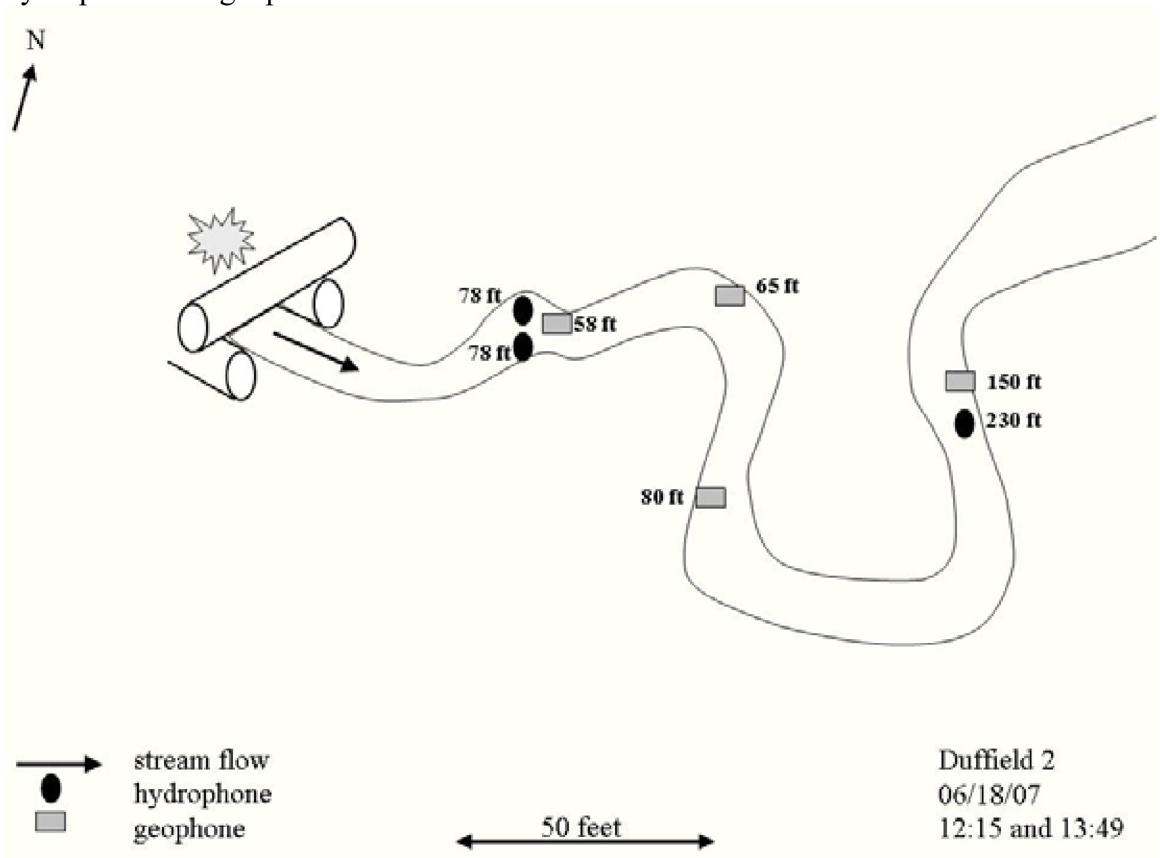

Structure, site, and shot information recorded during shot D2-2

Span / Length (ft)	Stringer Diameter (ft)	Between Sill Logs (ft)	Sill Log Diameter (ft)	Road Width (ft)	Fill Depth (ft)	Stream Grade (%)	Substrate Type
4	1.2	4.0	2.8	25	2.5	4-5	gravel

detcord (150 gr.) (ft)	ANFO (lbs)	Emulsion (lbs)	Total # / Delay (lbs)	TNT Equivalen t (lbs)	Coupling level
0	55	3	58	47	coupled

(21.6 SD)

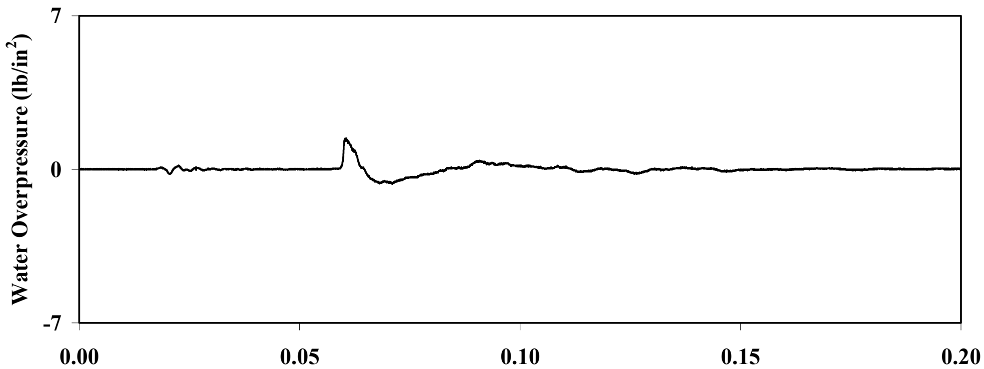

(21.6 SD)

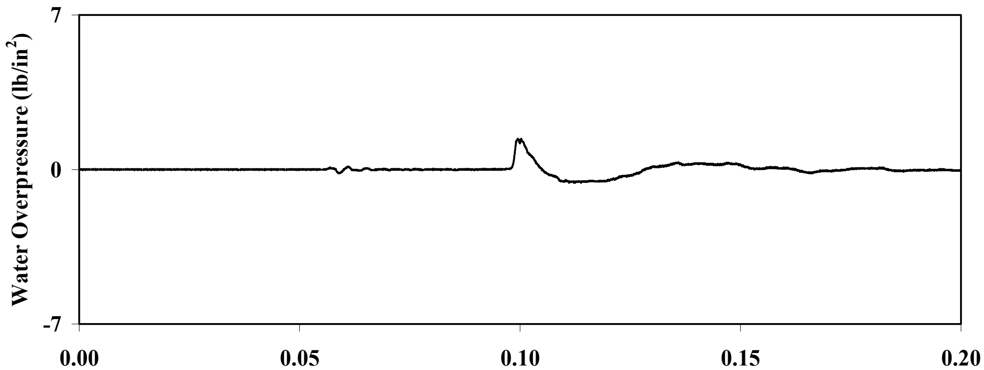

(63.7 SD)

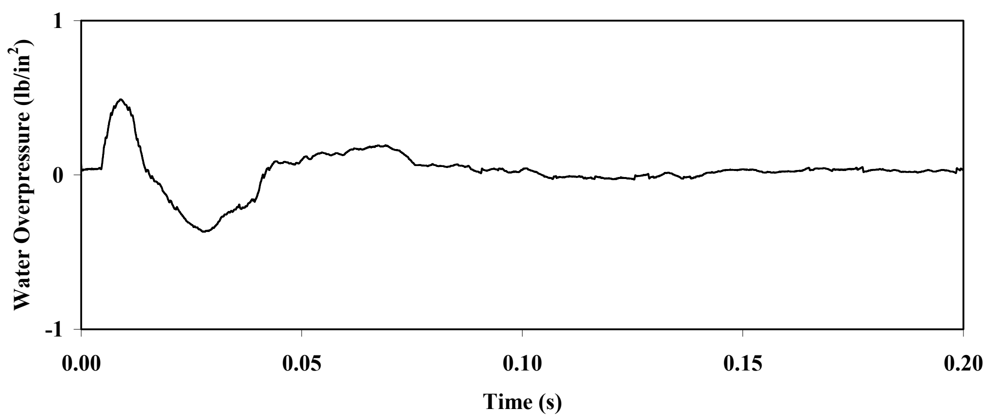

Stream pressures recorded during shot D2-2

Stream Distance (ft)	Scaled Distance (ft/lbs$^{1/3}$)	Positive Peak (lb/in^2)	Negative Peak (lb/in^2)	FFT Freq. (Hz)
78	21.6	1.40	-0.59	23.5
78	21.6	1.42	-0.66	23.5
230	63.7	0.49	-0.37	14.0

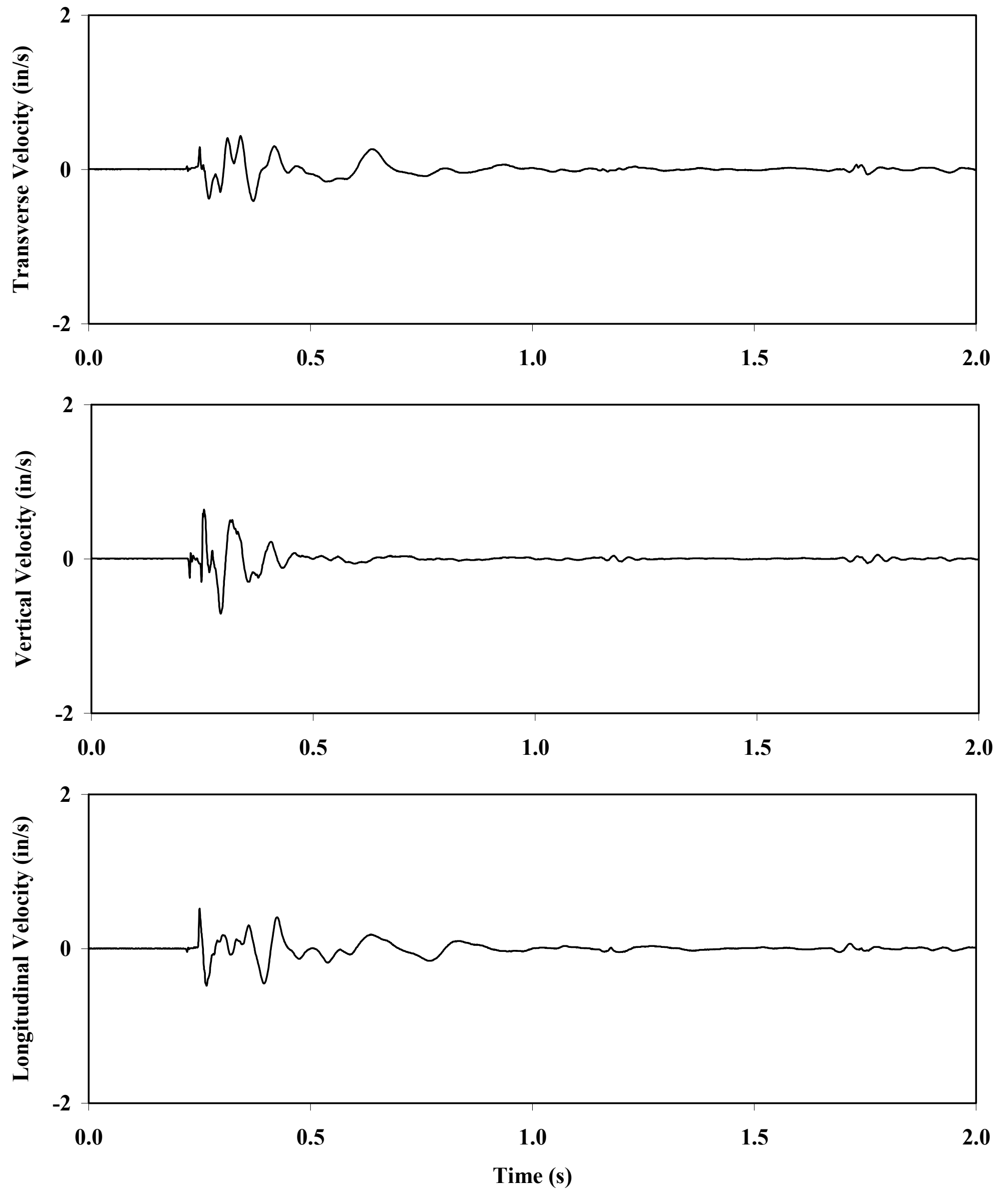

Streambed vibrations recorded during shot D2-2

Straight Distance (ft)	Scaled Distance (ft/lbs$^{1/2}$)	Transverse PPV (in/s)	FFT Freq. (Hz)	Vertical PPV (in/s)	FFT Freq. (Hz)	Long. PPV (in/s)	FFT Freq. (Hz)
58	8	0.44	10.5	0.71	13.5	0.52	15.8

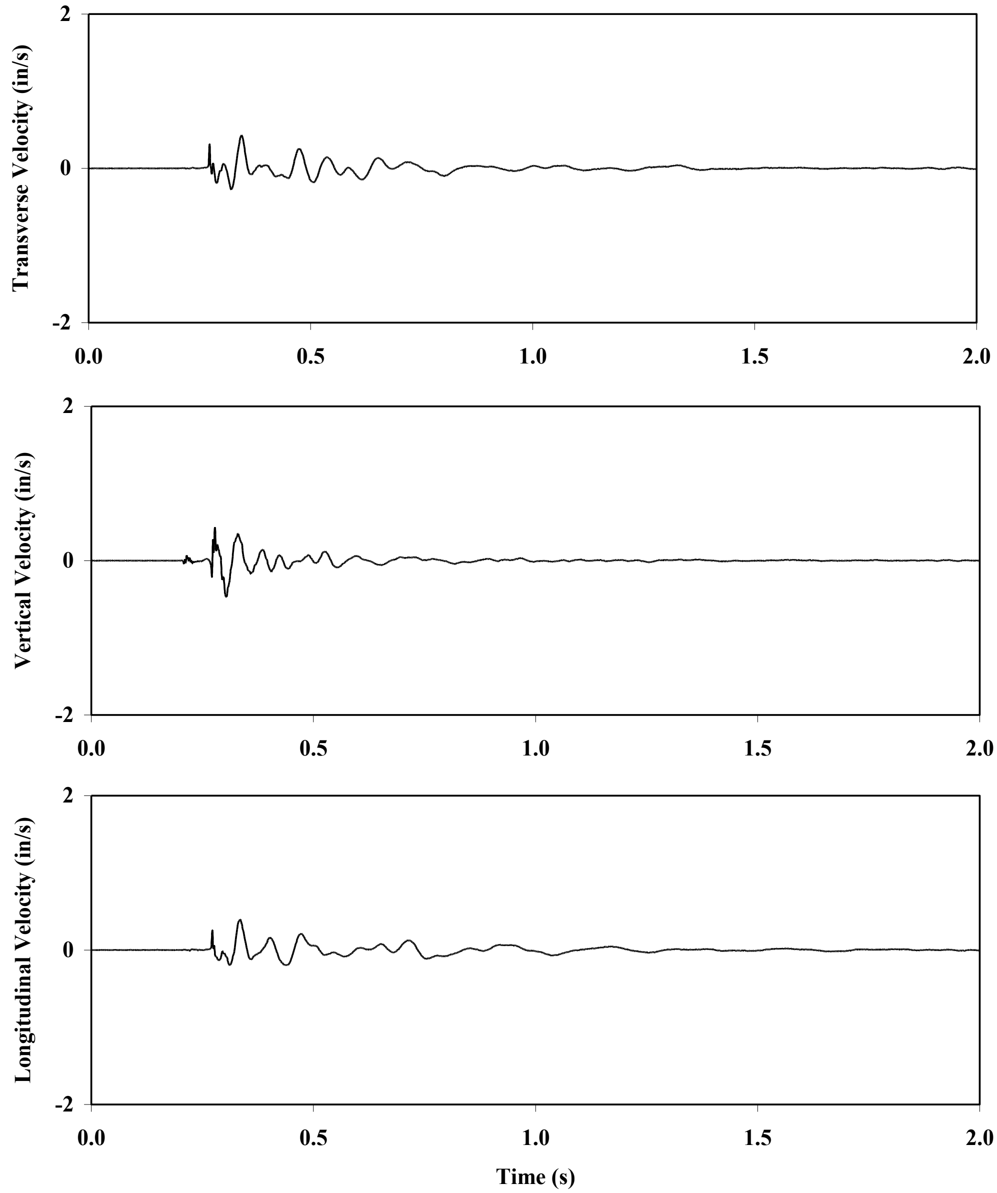

Streambed vibrations recorded during shot D2-2

Straight Distance (ft)	Scaled Distance (ft/lbs$^{1/2}$)	Transverse PPV (in/s)	FFT Freq. (Hz)	Vertical PPV (in/s)	FFT Freq. (Hz)	Long. PPV (in/s)	FFT Freq. (Hz)
65	9	0.15	5.0	0.56	22.0	0.44	16.5

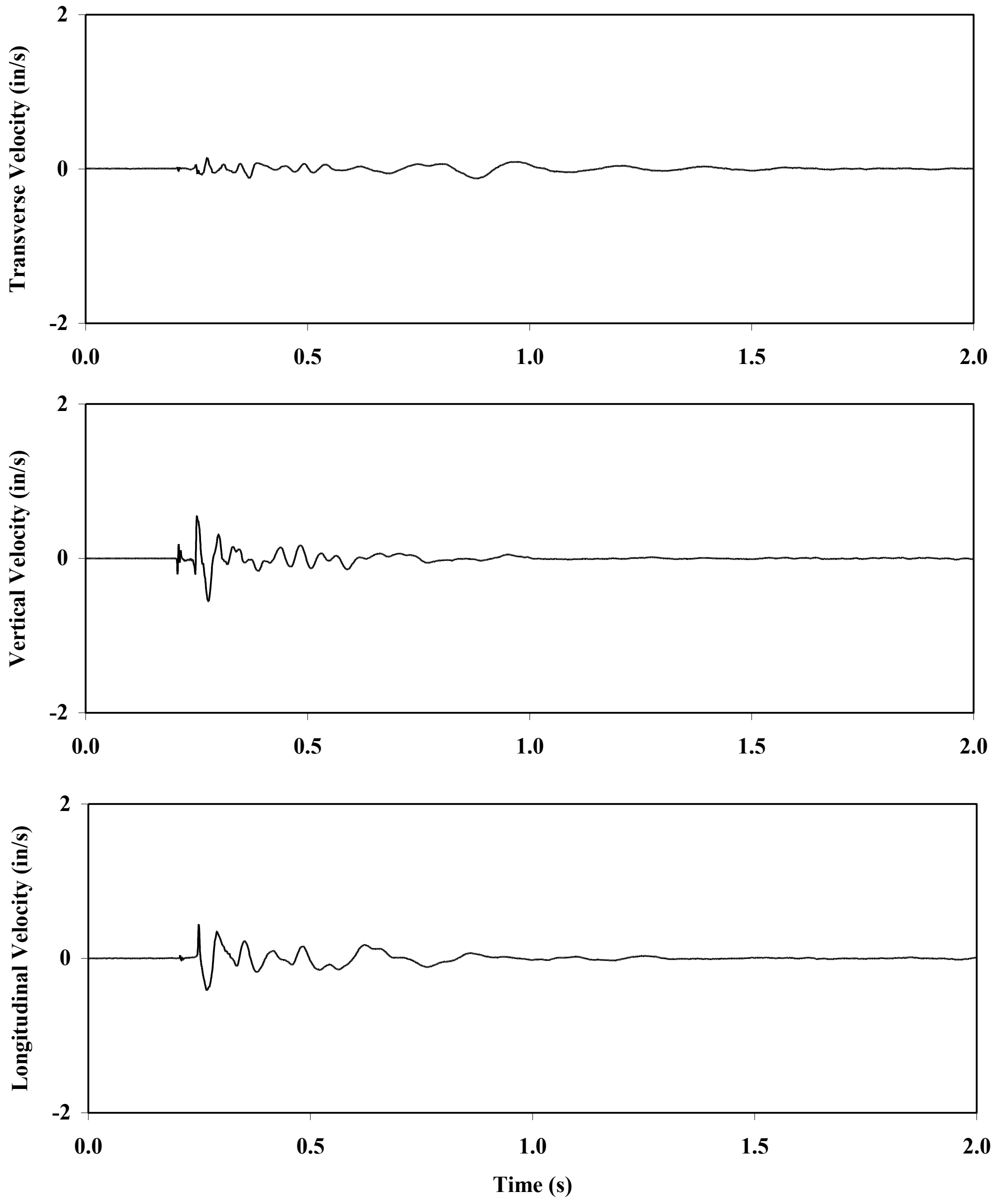

Streambed vibrations recorded during shot D2-2

Straight Distance (ft)	Scaled Distance (ft/lbs$^{1/2}$)	Transverse PPV (in/s)	FFT Freq. (Hz)	Vertical PPV (in/s)	FFT Freq. (Hz)	Long. PPV (in/s)	FFT Freq. (Hz)
80	12	0.43	16.8	0.47	20.3	0.40	13.5

APPENDIX 4 SITE D4 WATER BAR. Site diagram and setup information, hydrophone and geophone time histories

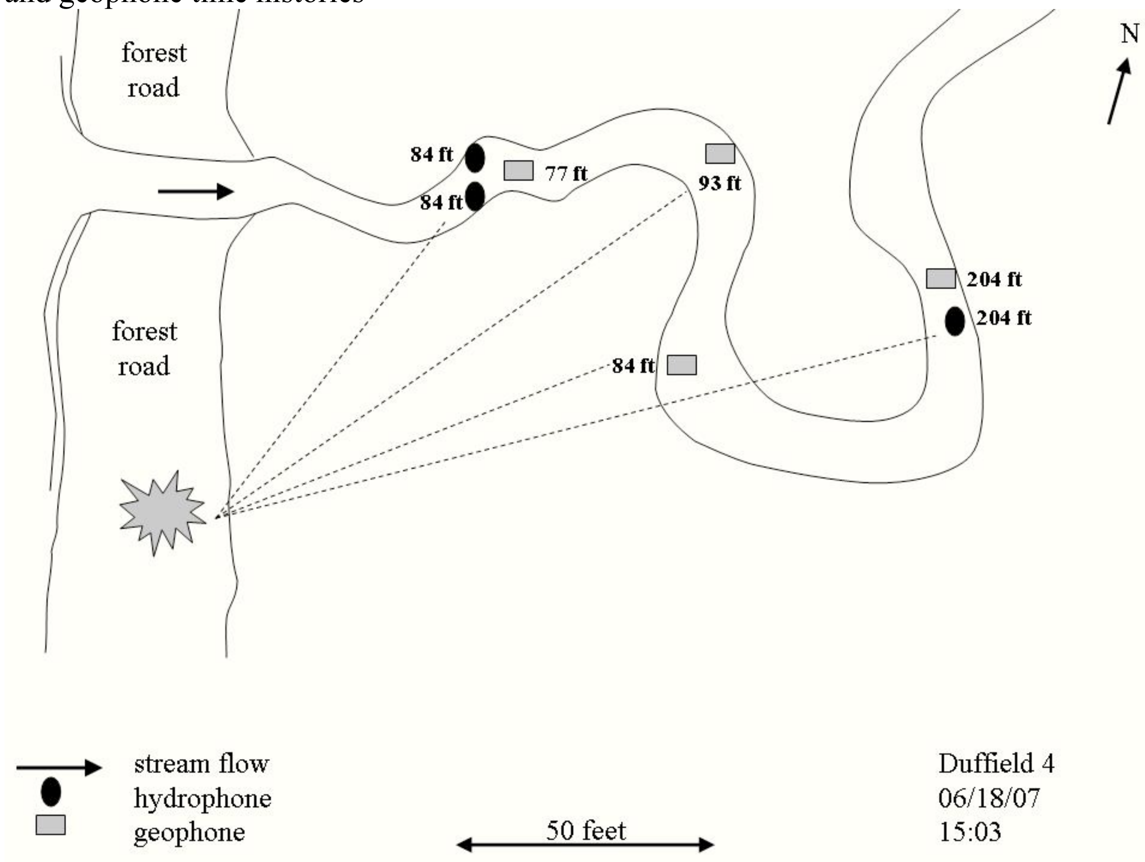

Structure, site, and shot information recorded during shot D4

Span / Length (ft)	Stringer Diameter (ft)	Between Sill Logs (ft)	Sill Log Diameter (ft)	Road Width (ft)	Fill Depth (ft)	Stream Grade (%)	Substrate Type
na	na	na	na	24	na	3-4	gravel

detcord (150 gr.) (ft)	ANFO (lbs)	Emulsion (lbs)	Total # / Delay (lbs)	TNT Equivalent (lbs)	Coupling level
300	605	40	651	529	well coupled

(84 ft)

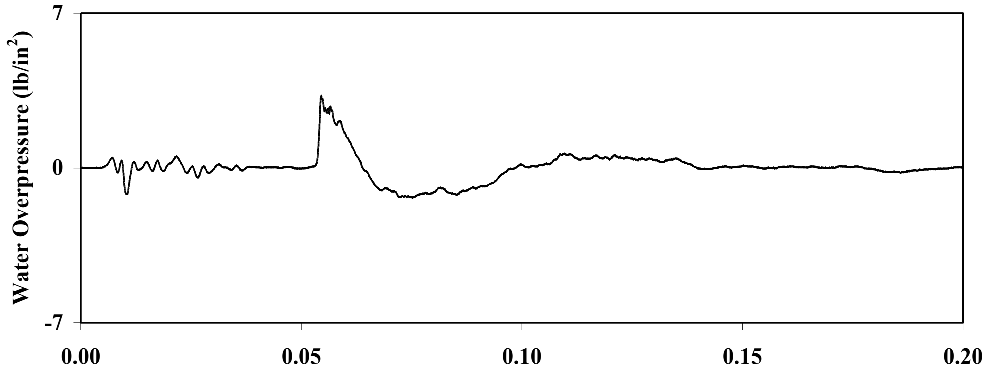

(84 ft)

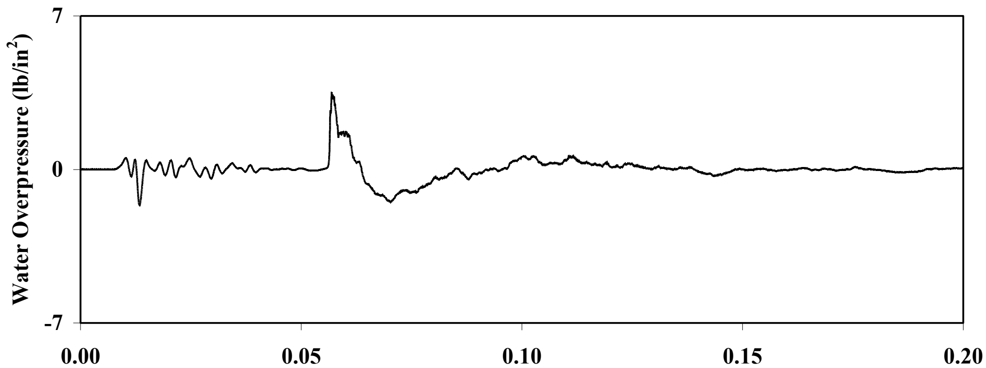

(204 ft)

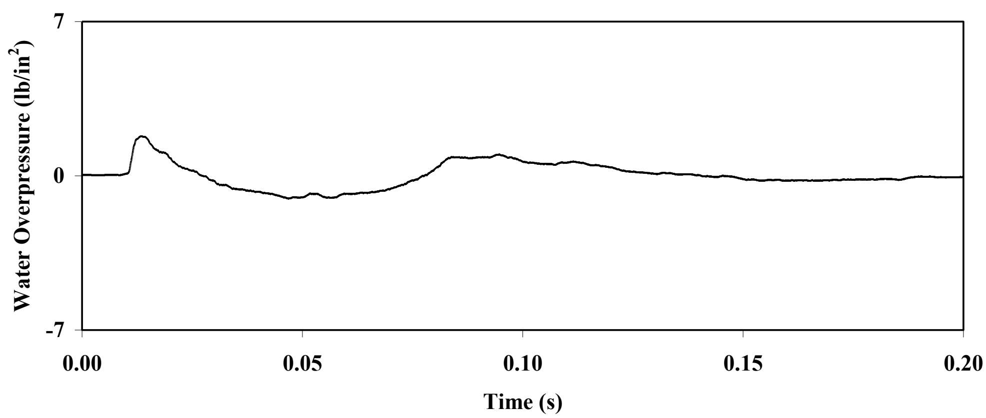

Stream pressures recorded during shot D4

Straight Distance (ft)	Scaled Distance (ft/lbs$^{1/3}$)	Positive Peak (lb/in^2)	Negative Peak (lb/in^2)	FFT Freq. (Hz)
84	na	1.79	-1.03	9.5
84	na	3.27	-1.35	16.5
204	na	3.53	-1.64	17.0

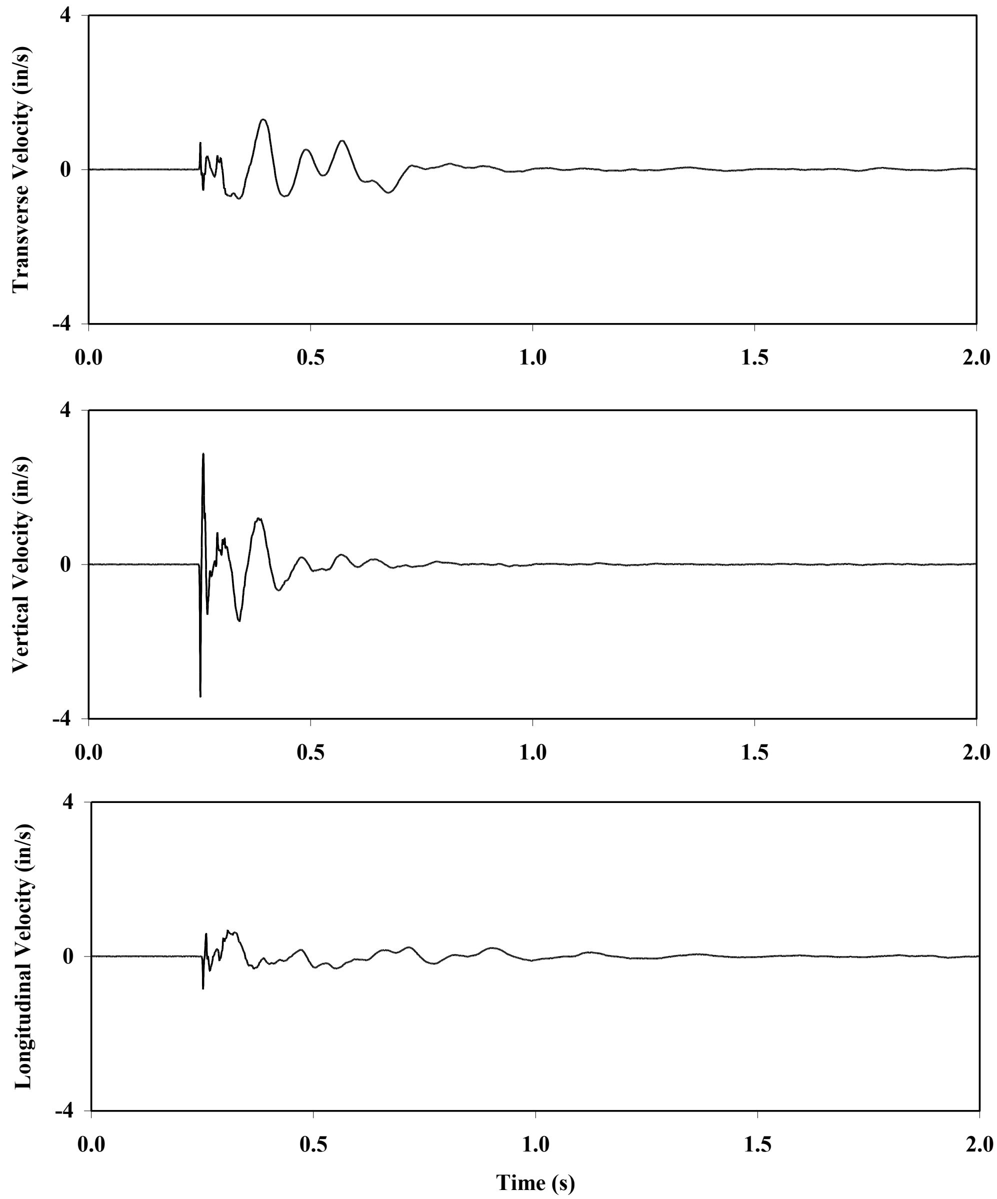

Streambed vibrations recorded during shot D4

Straight Distance (ft)	Scaled Distance (ft/lbs$^{1/2}$)	Transverse PPV (in/s)	FFT Freq. (Hz)	Vertical PPV (in/s)	FFT Freq. (Hz)	Long. PPV (in/s)	FFT Freq. (Hz)
77	3.3	1.31	9.5	3.40	11.0	0.86	5.0

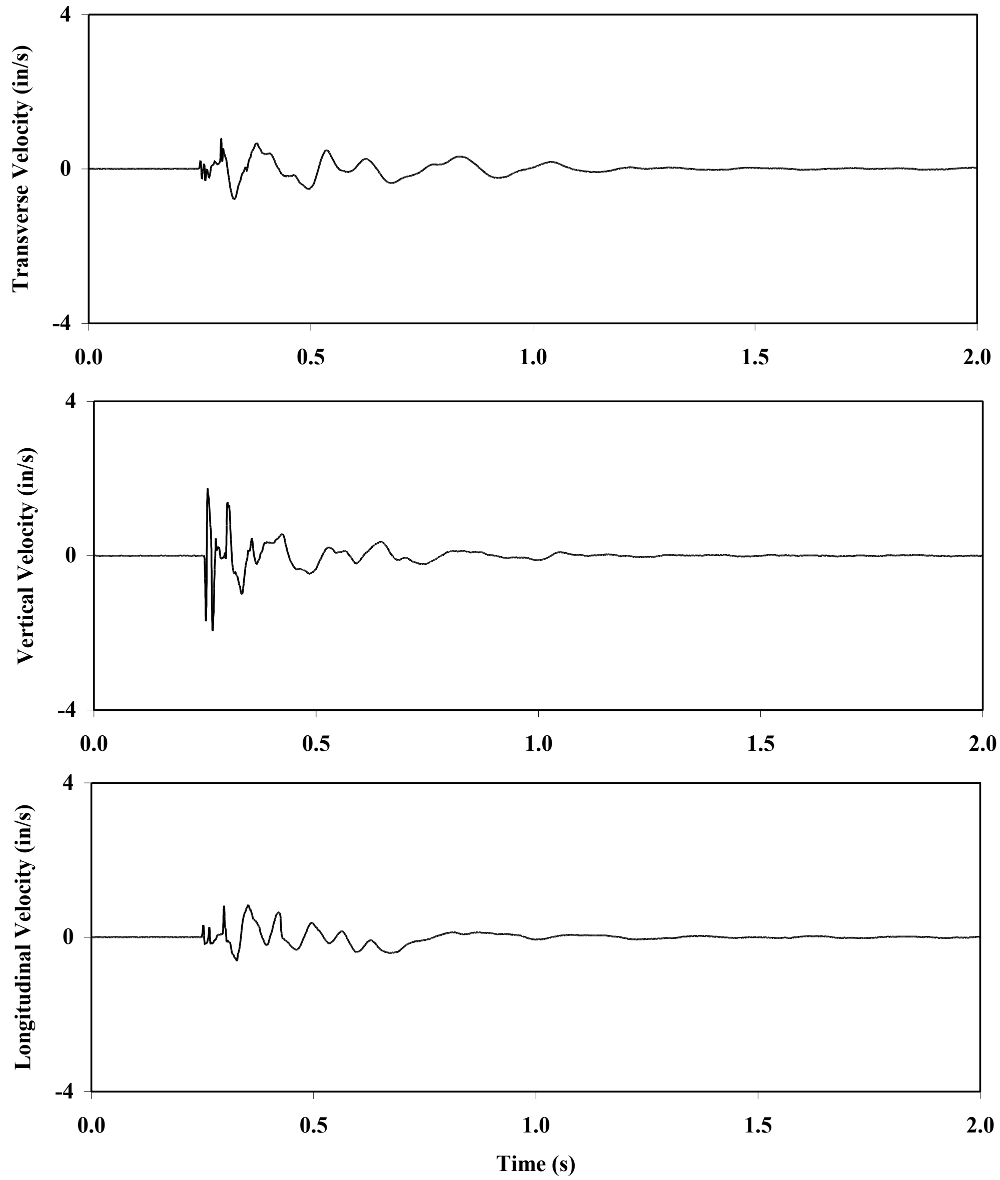

Streambed vibrations recorded during shot D4

Straight Distance (ft)	Scaled Distance (ft/lbs$^{1/2}$)	Transverse PPV (in/s)	FFT Freq. (Hz)	Vertical PPV (in/s)	FFT Freq. (Hz)	Long. PPV (in/s)	FFT Freq. (Hz)
84	3.7	0.79	4.8	1.95	7.8	0.84	2.0

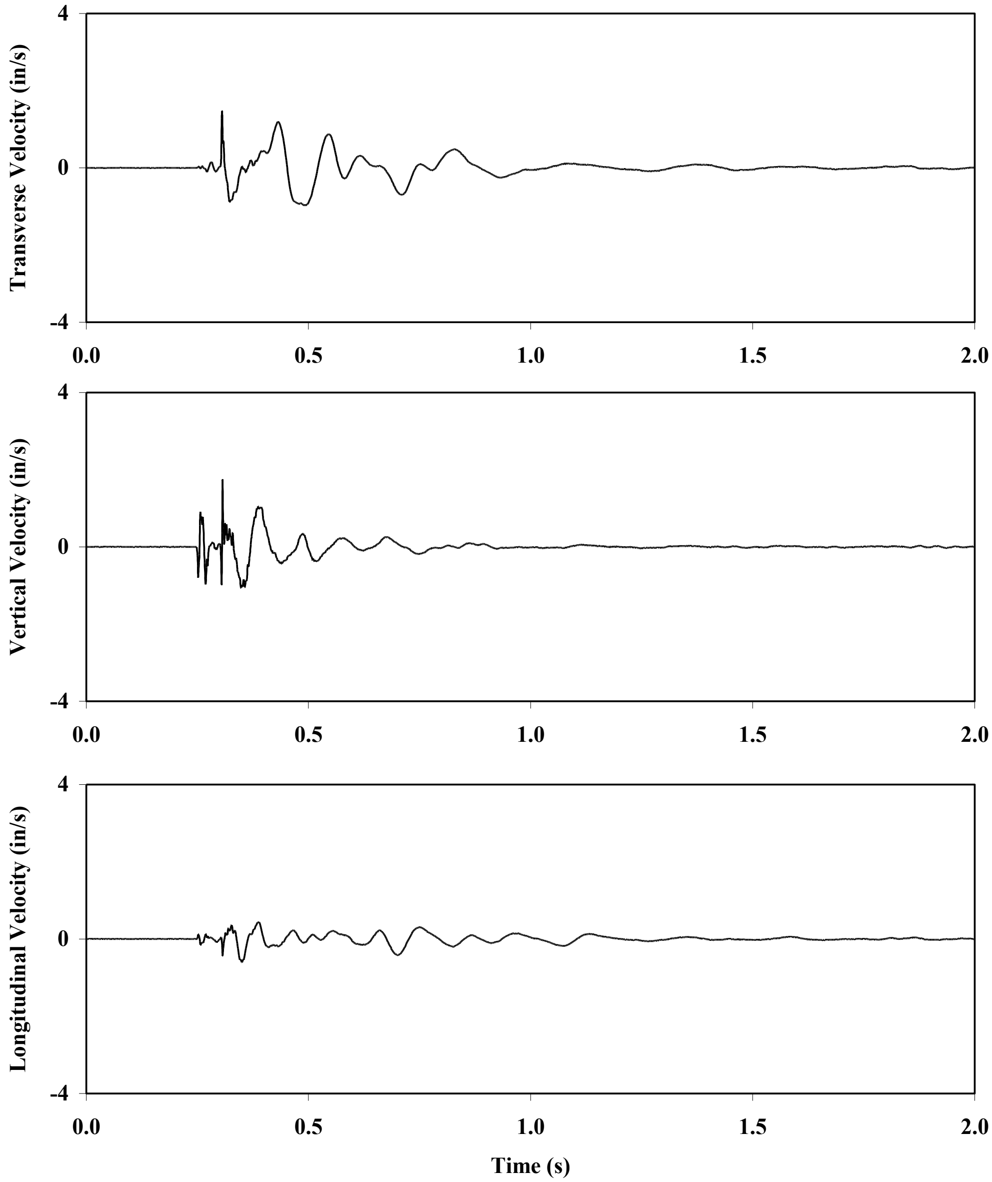

Streambed vibrations recorded during shot D4

Straight Distance (ft)	Scaled Distance (ft/lbs$^{1/2}$)	Transverse PPV (in/s)	FFT Freq. (Hz)	Vertical PPV (in/s)	FFT Freq. (Hz)	Long. PPV (in/s)	FFT Freq. (Hz)
93	4.0	1.46	5.3	1.72	10.8	0.60	10.8

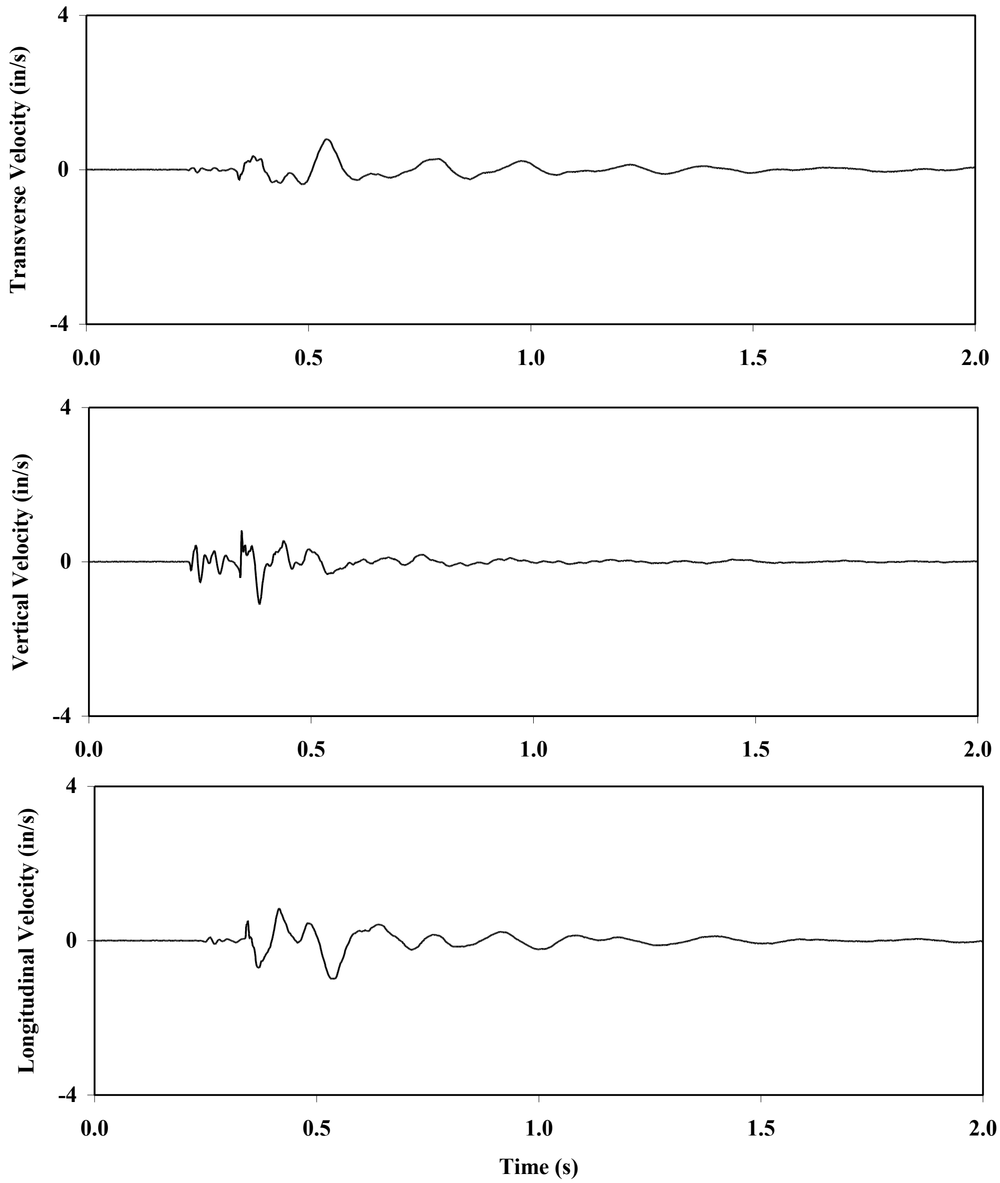

Streambed vibrations recorded during shot D4

Straight Distance (ft)	Scaled Distance (ft/lbs$^{1/2}$)	Transverse PPV (in/s)	FFT Freq. (Hz)	Vertical PPV (in/s)	FFT Freq. (Hz)	Long. PPV (in/s)	FFT Freq. (Hz)
204	8.9	0.80	5.0	1.10	12.5	0.99	4.5

APPENDIX 5 SITE D8 LOG BRIDGE. Site diagram and setup information, hydrophone and geophone time histories

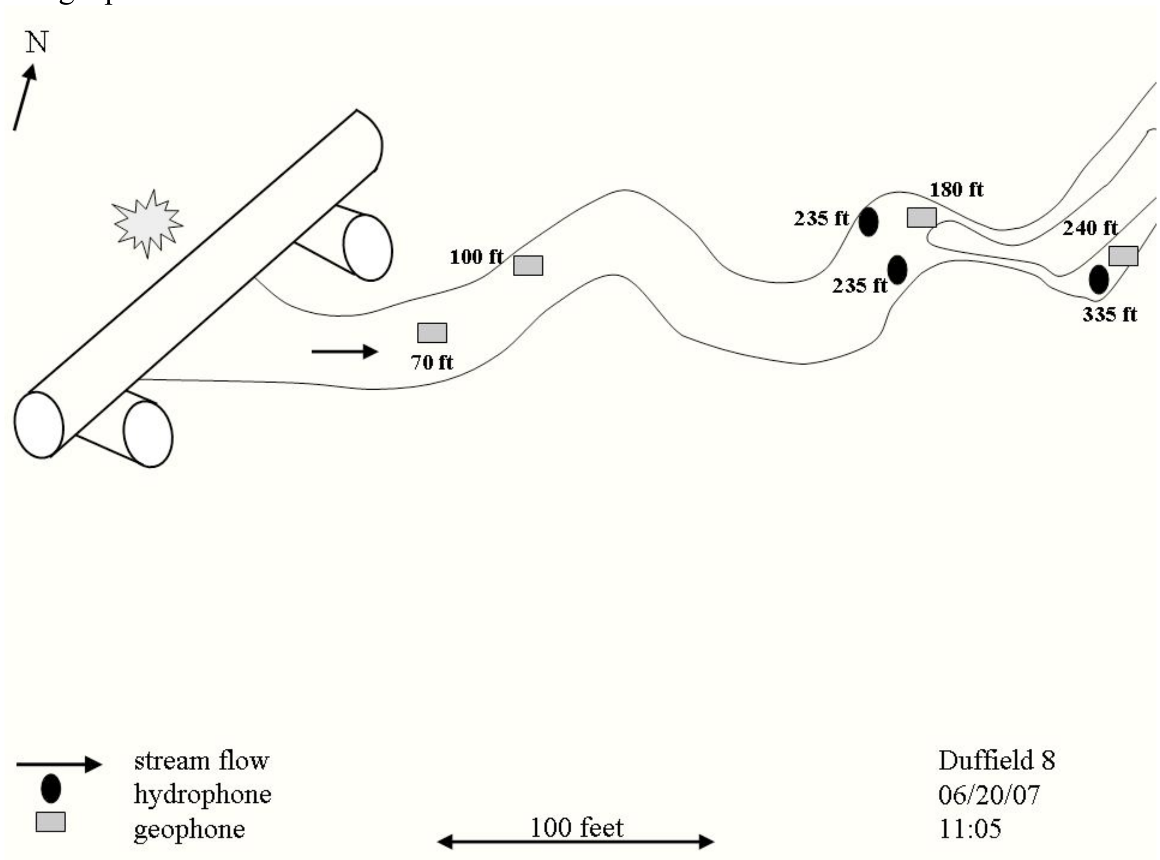

Structure, site, and shot information recorded during shot D8

Span / Length (ft)	Stringer Diameter (ft)	Between Sill Logs (ft)	Sill Log Diameter (ft)	Road Width (ft)	Fill Depth (ft)	Stream Grade (%)	Substrate Type
28	2.0	16.8	2.8	23	1.5	3-4	gravel

detcord (150 gr.) (ft)	ANFO (lbs)	Emulsion (lbs)	Total # / Delay (lbs)	TNT Equivalent (lbs)	Coupling level
150	825	45	873	708	coupled

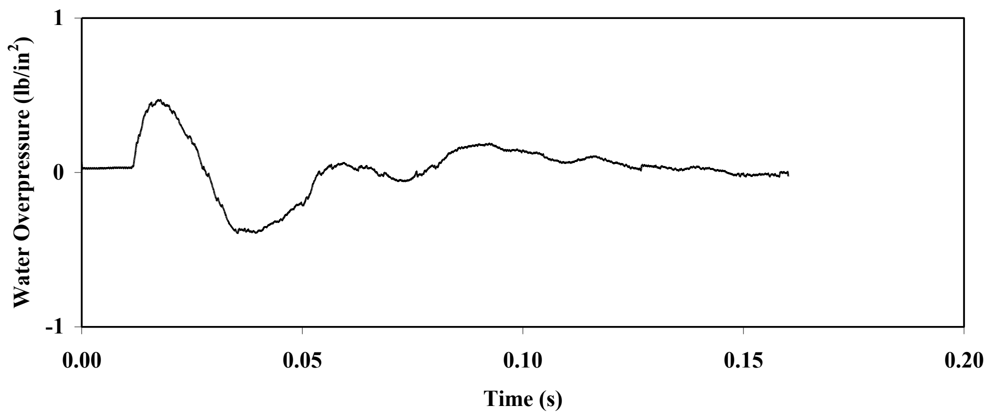

Stream pressures recorded during shot D8

Straight Distance (ft)	Scaled Distance ($ft/lbs^{1/3}$)	Positive Peak (lb/in^2)	Negative Peak (lb/in^2)	FFT Freq. (Hz)
335	37.6	0.47	-0.39	10.0

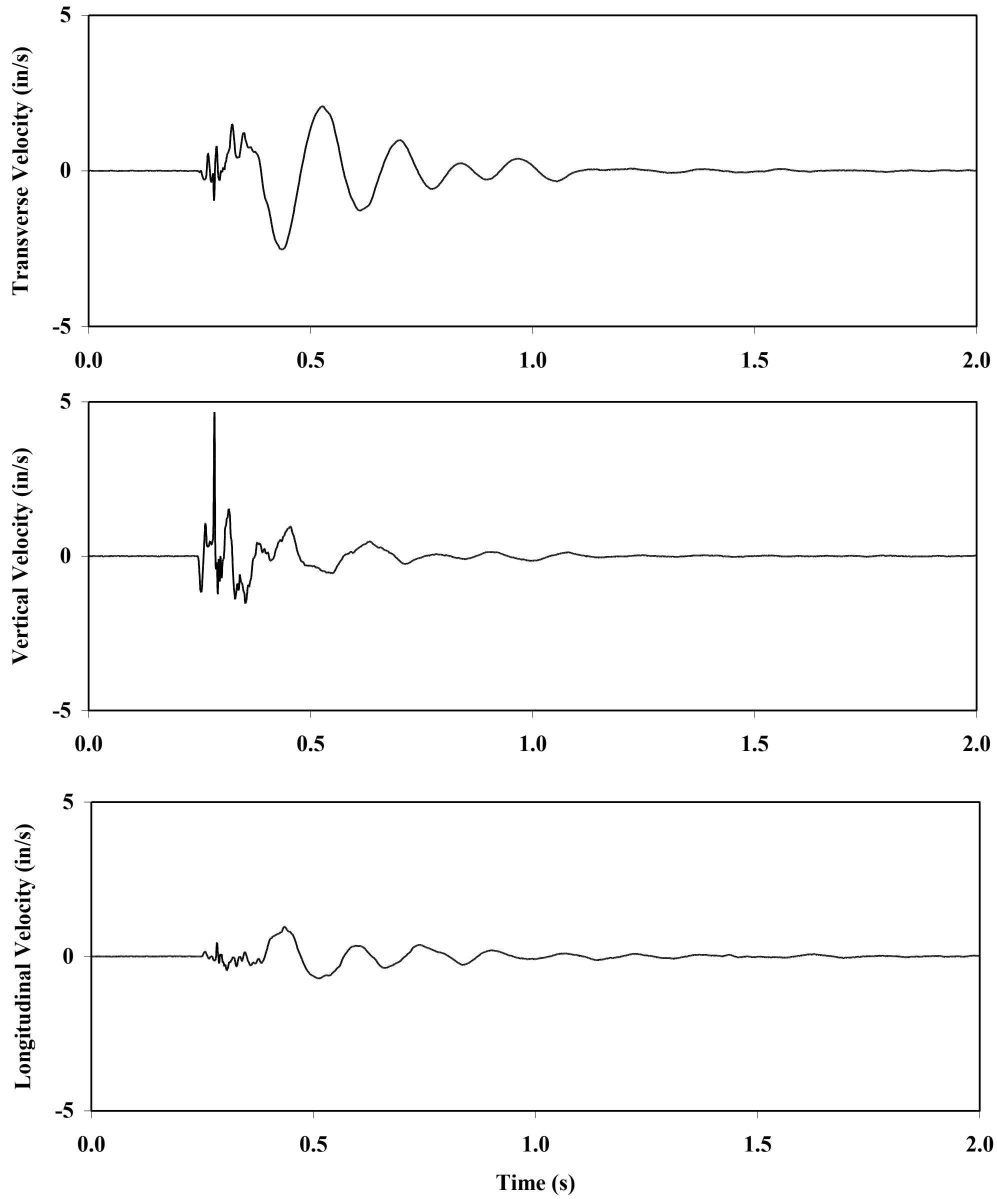

Streambed vibrations recorded during shot D8

Straight Distance (ft)	Scaled Distance (ft/lbs$^{1/2}$)	Transverse PPV (in/s)	FFT Freq. (Hz)	Vertical PPV (in/s)	FFT Freq. (Hz)	Long. PPV (in/s)	FFT Freq. (Hz)
70	2.6	2.52	6.0	4.67	6.5	0.97	6.3

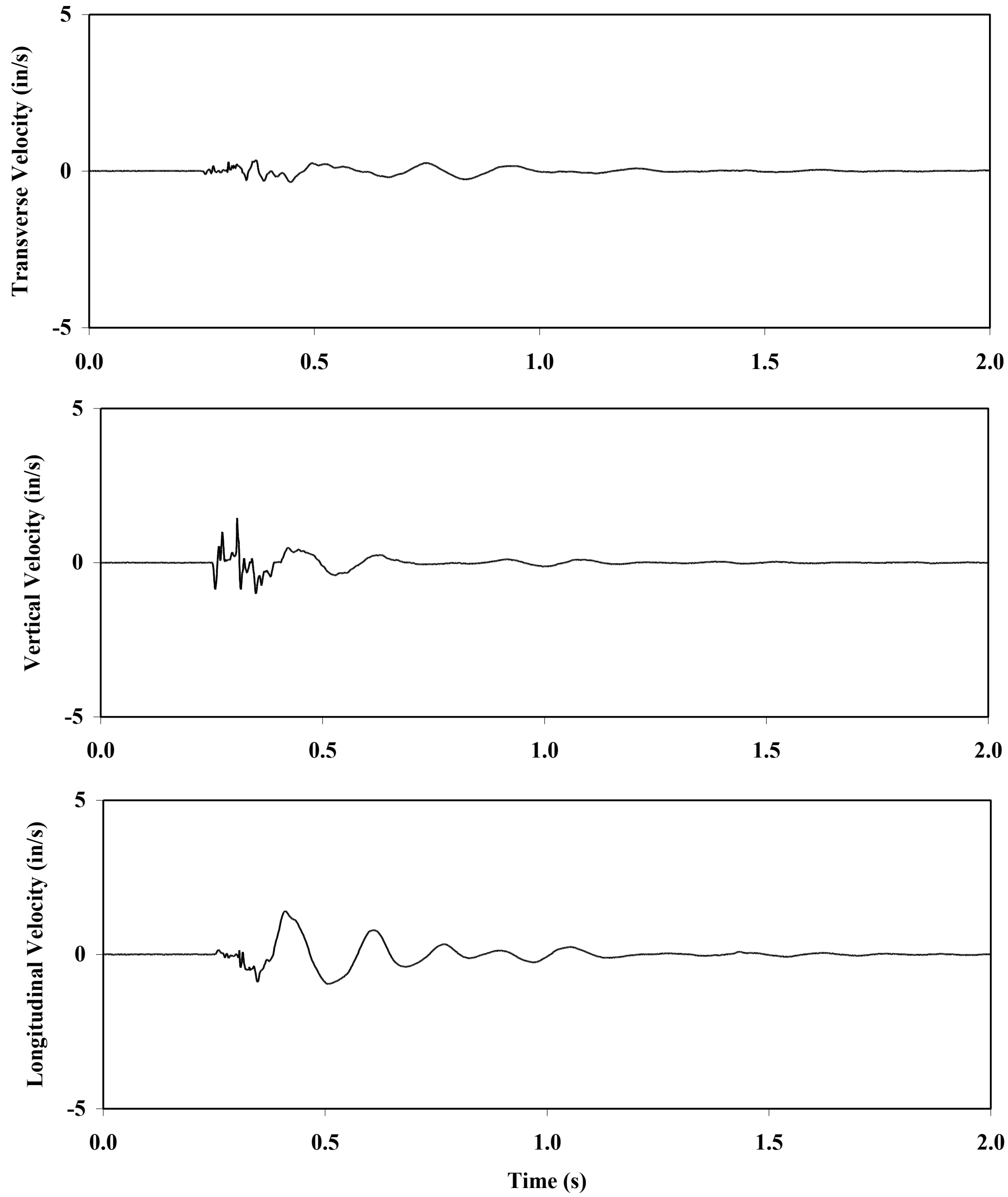

Streambed vibrations recorded during shot D8

Straight Distance (ft)	Scaled Distance (ft/lbs$^{1/2}$)	Transverse PPV (in/s)	FFT Freq. (Hz)	Vertical PPV (in/s)	FFT Freq. (Hz)	Long. PPV (in/s)	FFT Freq. (Hz)
100	3.8	0.36	4.8	1.42	6.5	1.41	6.3

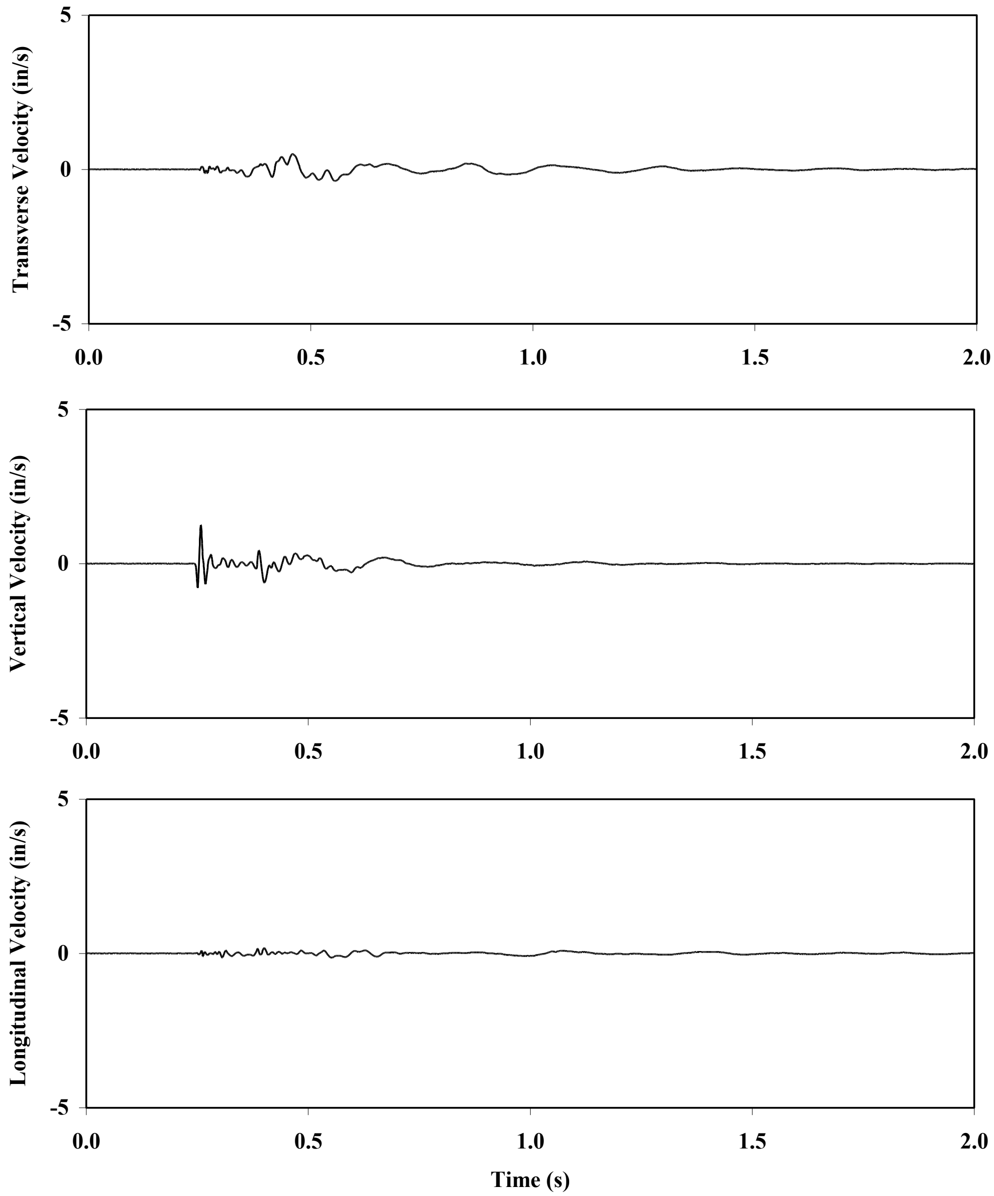

Streambed vibrations recorded during shot D8

Straight Distance (ft)	Scaled Distance (ft/lbs$^{1/2}$)	Transverse PPV (in/s)	FFT Freq. (Hz)	Vertical PPV (in/s)	FFT Freq. (Hz)	Long. PPV (in/s)	FFT Freq. (Hz)
180	6.8	0.50	5.0	1.26	5.0	0.17	3.3

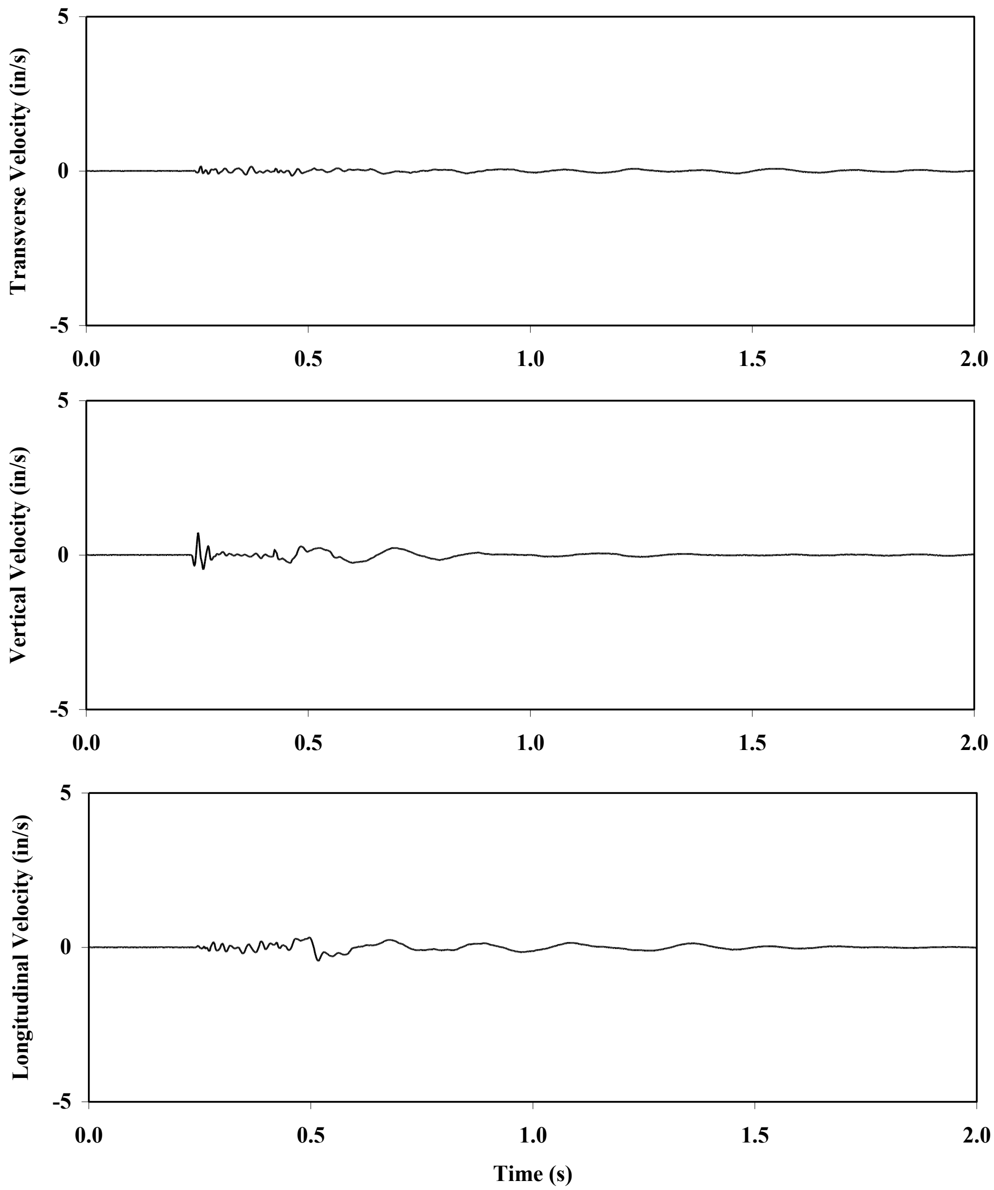

Streambed vibrations recorded during shot D8

Straight Distance (ft)	Scaled Distance (ft/lbs$^{1/2}$)	Transverse PPV (in/s)	FFT Freq. (Hz)	Vertical PPV (in/s)	FFT Freq. (Hz)	Long. PPV (in/s)	FFT Freq. (Hz)
240	9.0	0.16	6.5	0.73	5.0	0.44	4.8

APPENDIX 6 SITE D11 LOG CULVERT. Site diagram and setup information, hydrophone and geophone time histories

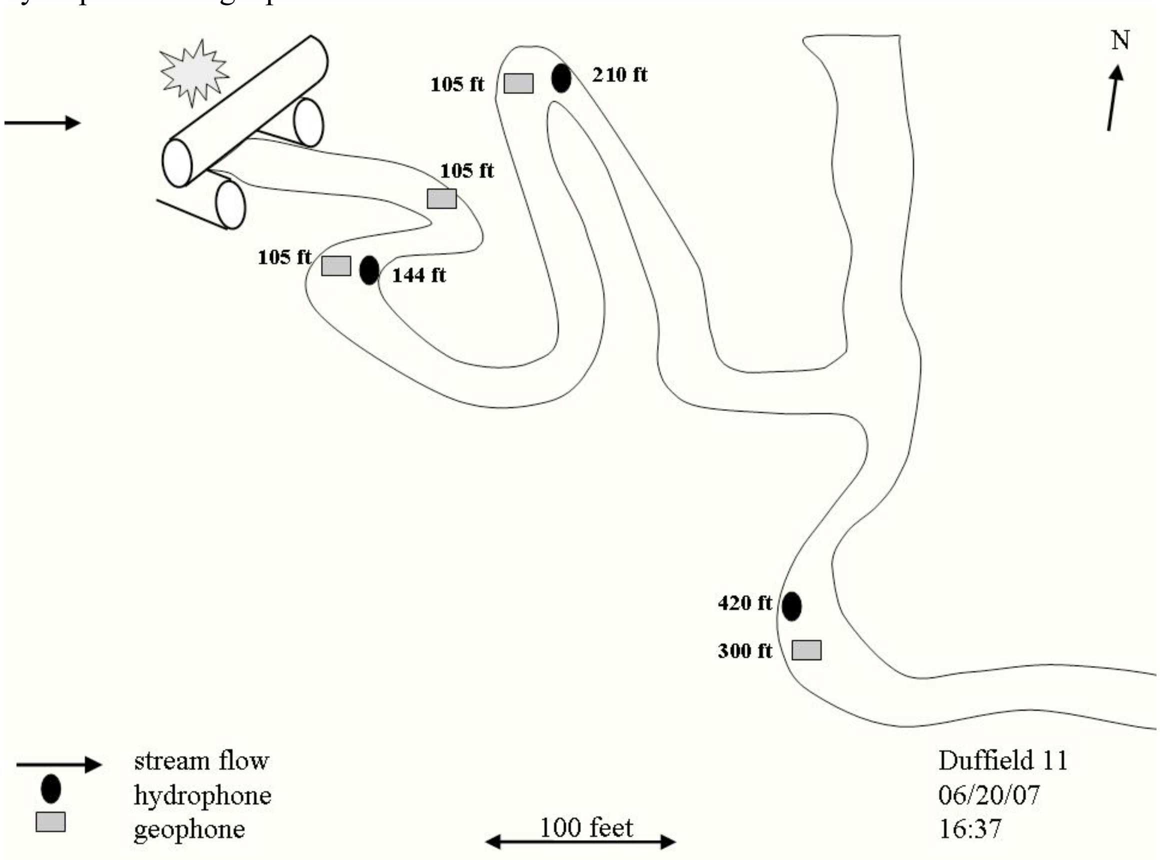

Structure, site, and shot information recorded during shot D11

Span / Length (ft)	Stringer Diameter (ft)	Between Sill Logs (ft)	Sill Log Diameter (ft)	Road Width (ft)	Fill Depth (ft)	Stream Grade (%)	Substrate Type
36	1.0	4.6	2.0	25	1.0	1-2	gravel

detcord (150 gr.) (ft)	ANFO (lbs)	Emulsion (lbs)	Total # / Delay (lbs)	TNT Equivalent (lbs)	Coupling level
75	220	15	237	192	coupled

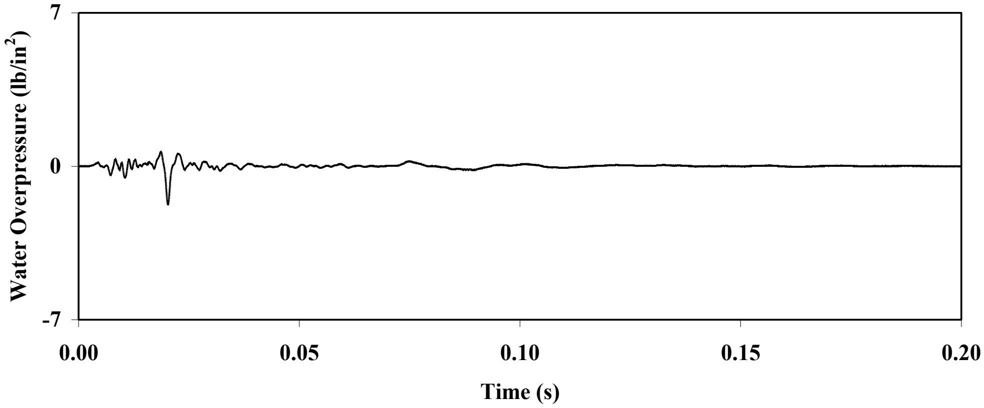

Stream pressures recorded during shot D11

Straight Distance (ft)	Scaled Distance (ft/lbs$^{1/3}$)	Positive Peak (lb/in^2)	Negative Peak (lb/in^2)	FFT Freq. (Hz)
144	25.0	0.66	-1.75	286.0

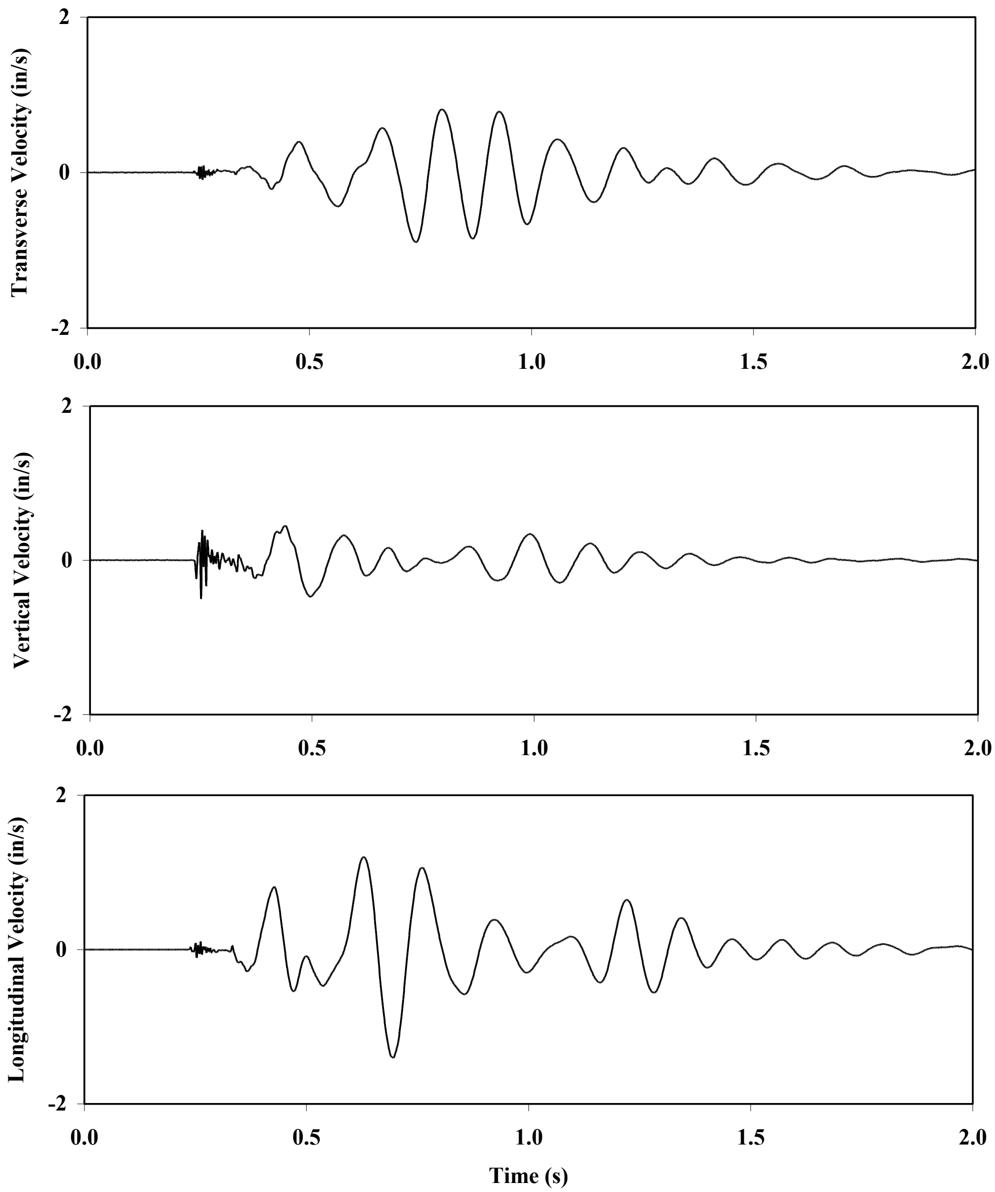

Streambed vibrations recorded during shot D11

Straight Distance (ft)	Scaled Distance (ft/lbs$^{1/2}$)	Transverse PPV (in/s)	FFT Freq. (Hz)	Vertical PPV (in/s)	FFT Freq. (Hz)	Long. PPV (in/s)	FFT Freq. (Hz)
120	8.7	0.90	7.0	0.50	7.5	1.40	6.8

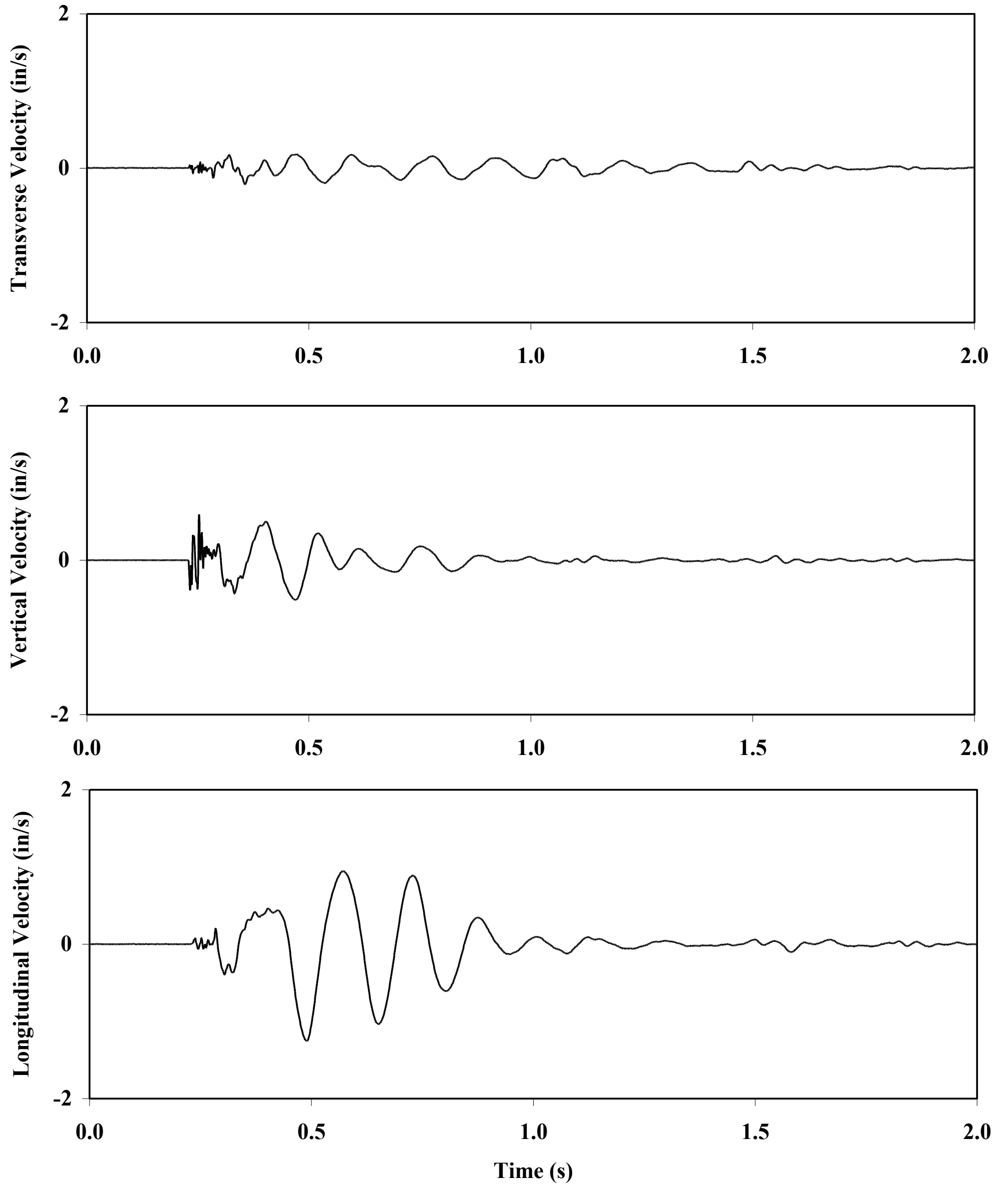

Streambed vibrations recorded during shot D11

Straight Distance (ft)	Scaled Distance ($ft/lbs^{1/2}$)	Transverse PPV (in/s)	FFT Freq. (Hz)	Vertical PPV (in/s)	FFT Freq. (Hz)	Long. PPV (in/s)	FFT Freq. (Hz)
160	11.5	0.21	7.0	0.60	8.5	1.25	6.5

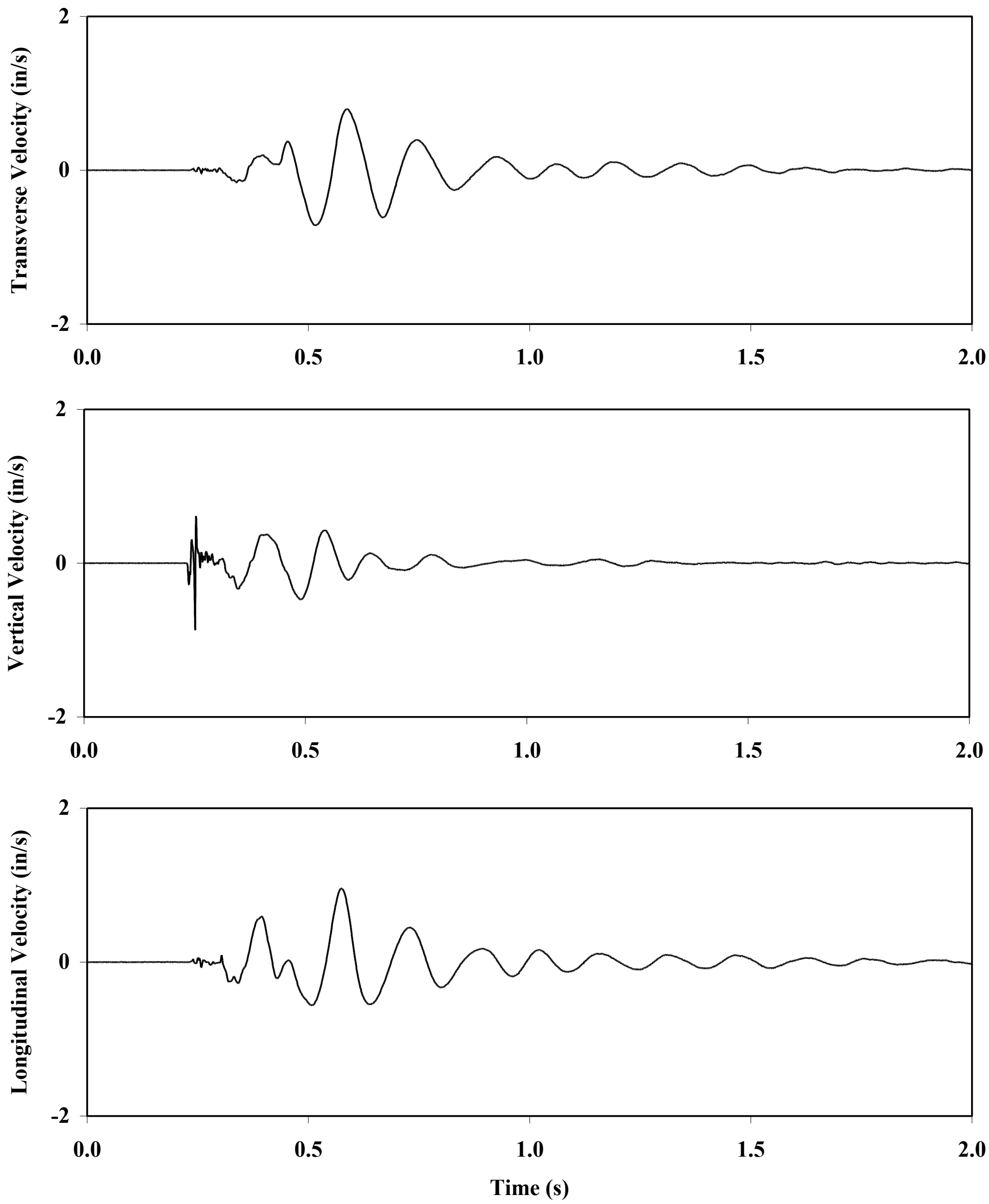

Streambed vibrations recorded during shot D11

Straight Distance (ft)	Scaled Distance ($ft/lbs^{1/2}$)	Transverse PPV (in/s)	FFT Freq. (Hz)	Vertical PPV (in/s)	FFT Freq. (Hz)	Long. PPV (in/s)	FFT Freq. (Hz)
180	11.5	0.80	6.8	0.84	8.3	0.96	6.8

APPENDIX 7 SITE D12 LOG CULVERT. Site diagram and setup information, hydrophone and geophone time histories

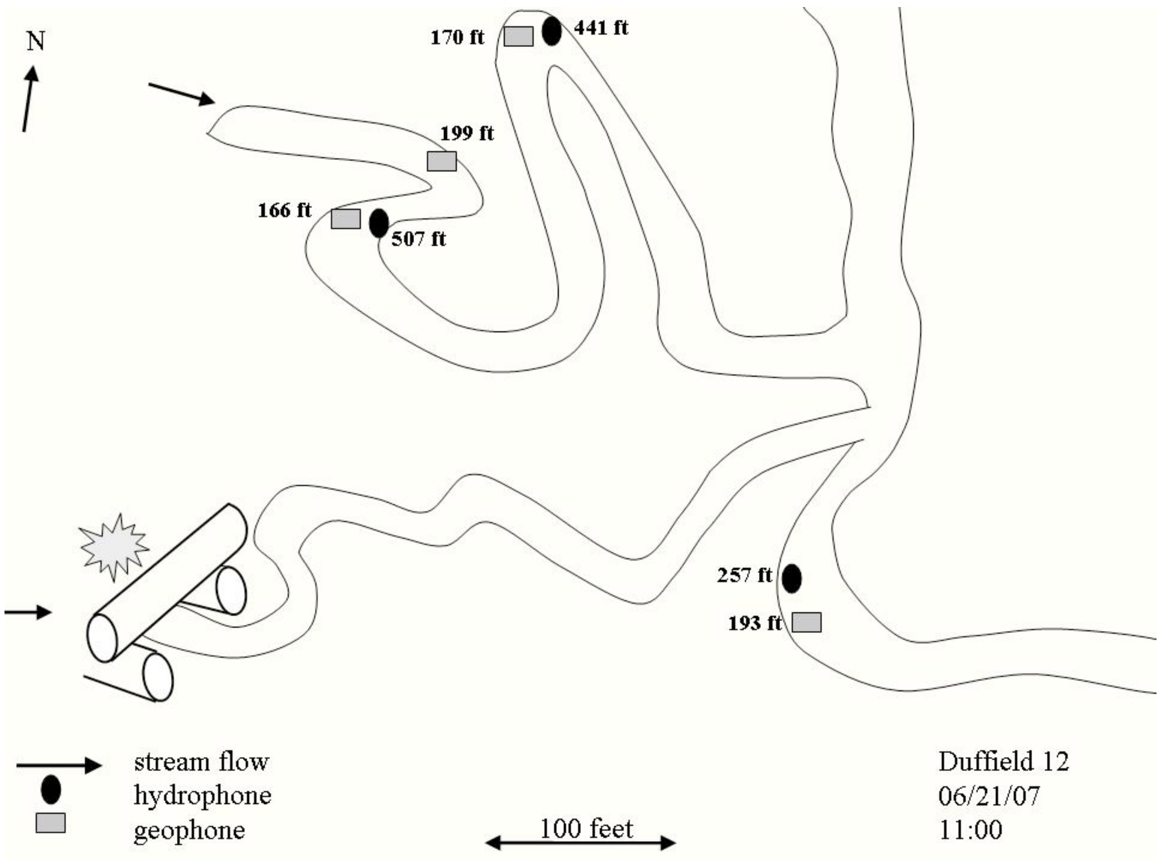

Structure, site, and shot information recorded during shot D12

Span / Length (ft)	Stringer Diameter (ft)	Between Sill Logs (ft)	Sill Log Diameter (ft)	Road Width (ft)	Fill Depth (ft)	Stream Grade (%)	Substrate Type
25	0.8	2.7	1.7	11	2.0	1-2	gravel

detcord (150 gr.) (ft)	ANFO (lbs)	Emulsion (lbs)	Total # / Delay (lbs)	TNT Equivalent (lbs)	Coupling level
125	275	15	293	238	de-coupled

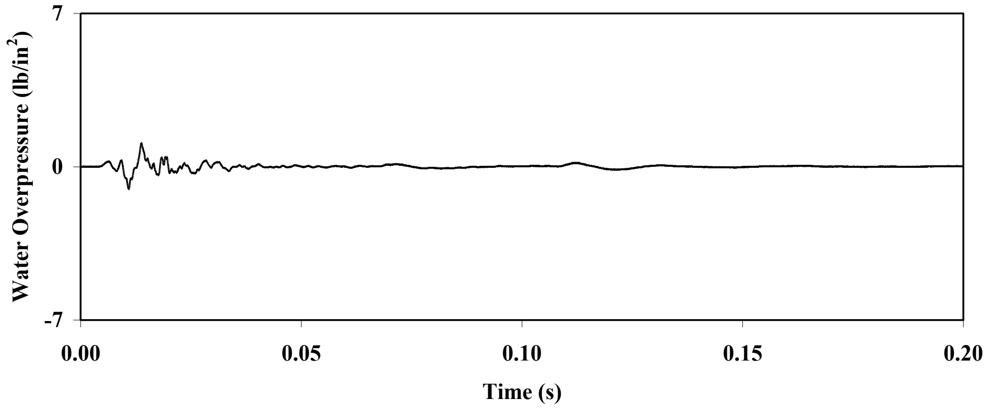

Stream pressures recorded during shot D12

Straight Distance (ft)	Scaled Distance (ft/lbs$^{1/3}$)	Positive Peak (lb/in^2)	Negative Peak (lb/in^2)	FFT Freq. (Hz)
507	81.8	1.09	-1.02	70.5

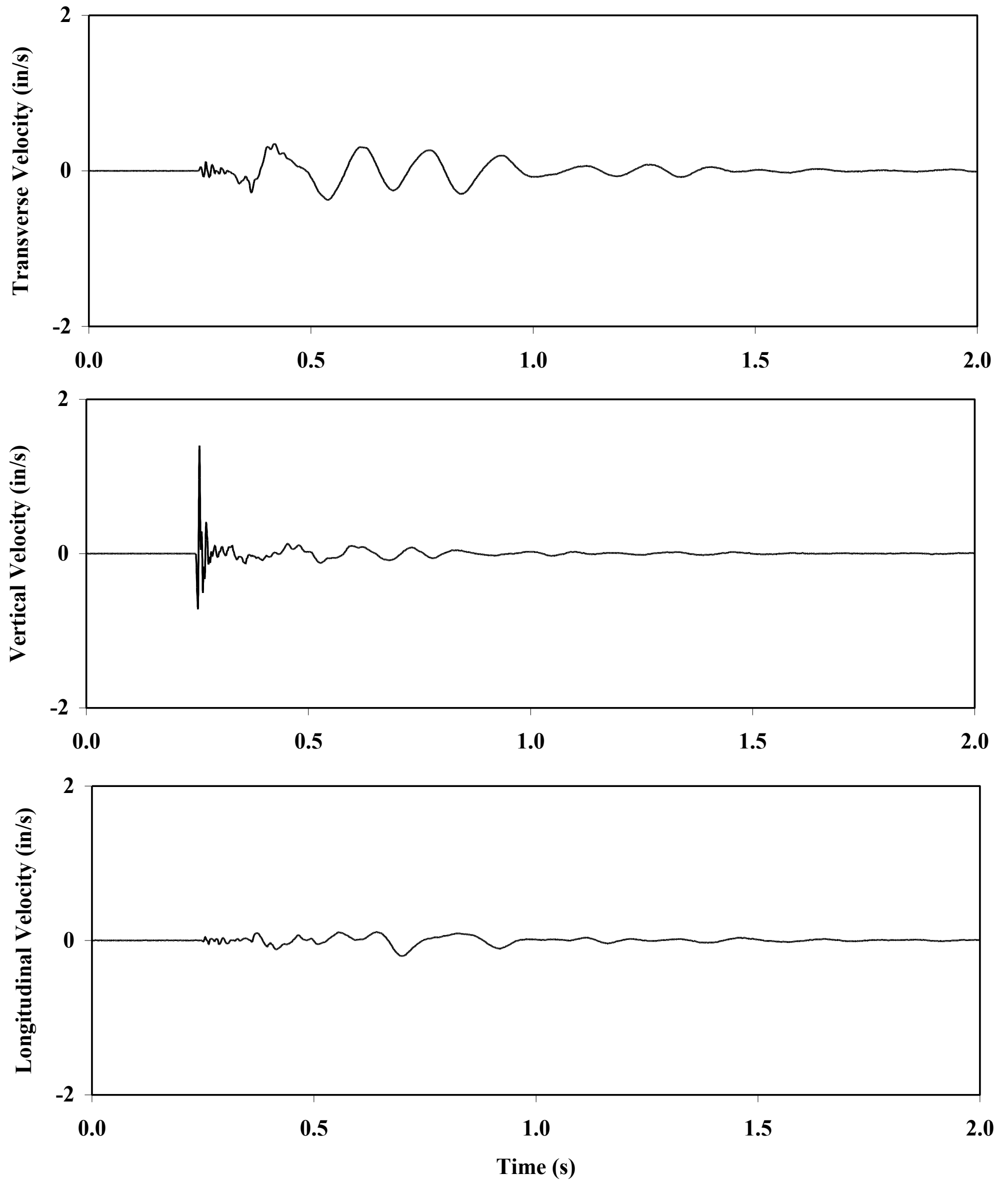

Streambed vibrations recorded during shot D12

Straight Distance (ft)	Scaled Distance ($ft/lbs^{1/2}$)	Transverse PPV (in/s)	FFT Freq. (Hz)	Vertical PPV (in/s)	FFT Freq. (Hz)	Long. PPV (in/s)	FFT Freq. (Hz)
166	10.8	0.38	6.3	1.40	7.5	0.20	4.8

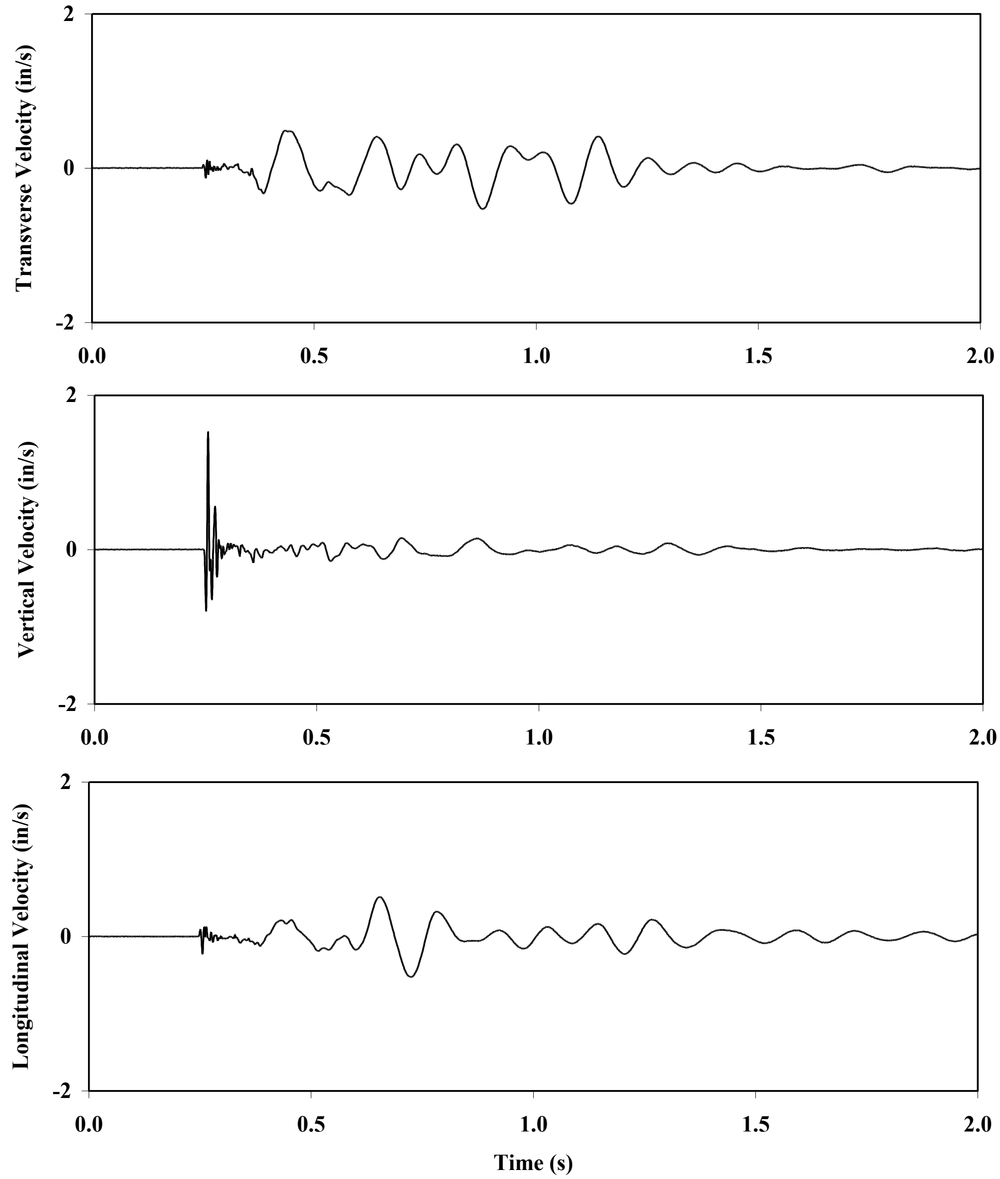

Streambed vibrations recorded during shot D12

Straight Distance (ft)	Scaled Distance (ft/lbs$^{1/2}$)	Transverse PPV (in/s)	FFT Freq. (Hz)	Vertical PPV (in/s)	FFT Freq. (Hz)	Long. PPV (in/s)	FFT Freq. (Hz)
170	11.0	0.53	6.0	1.52	7.3	0.53	8.5

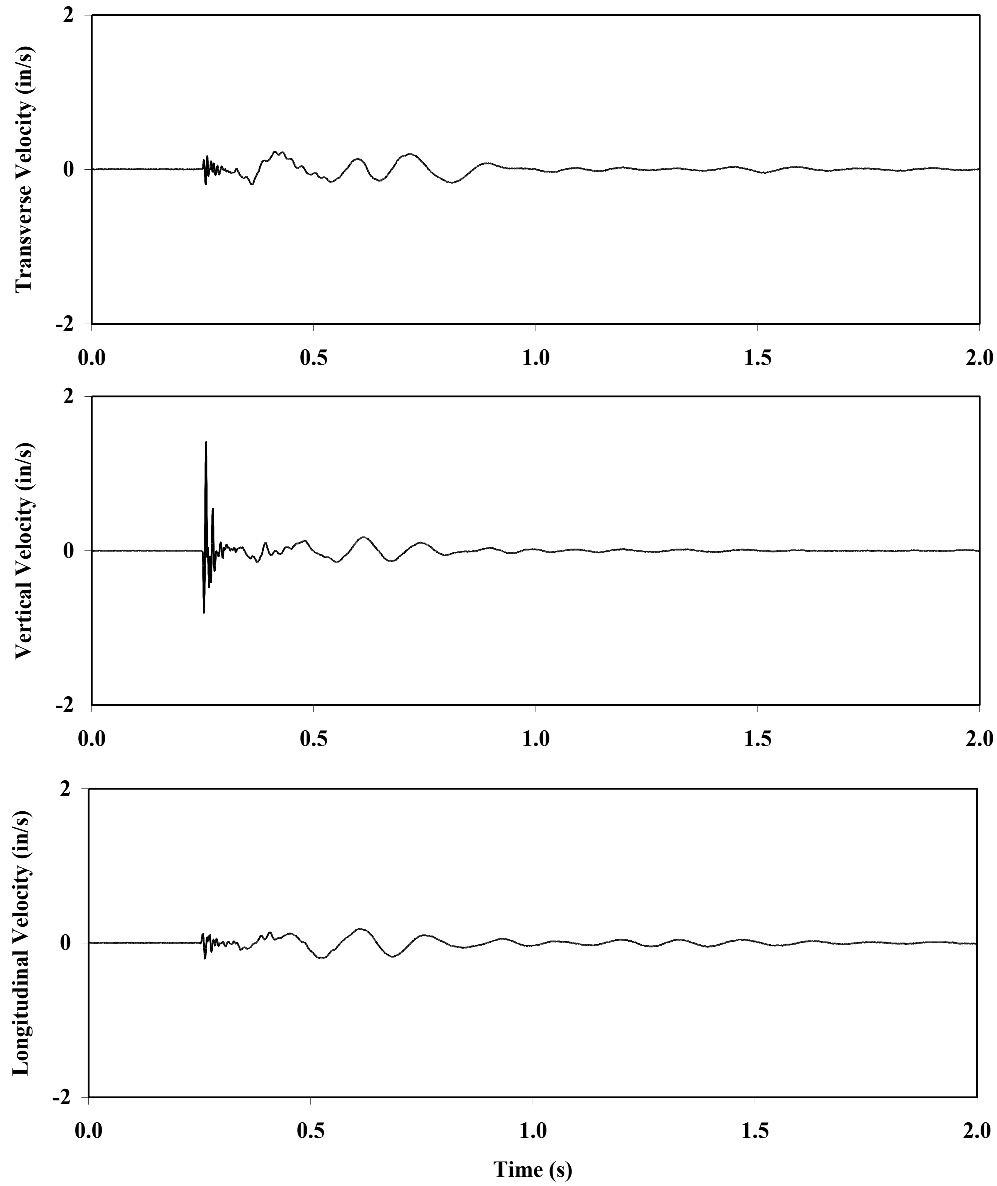

Streambed vibrations recorded during shot D12

Straight Distance (ft)	Scaled Distance (ft/lbs$^{1/2}$)	Transverse PPV (in/s)	FFT Freq. (Hz)	Vertical PPV (in/s)	FFT Freq. (Hz)	Long. PPV (in/s)	FFT Freq. (Hz)
193	12.5	0.34	6.0	0.85	5.8	0.24	5.8

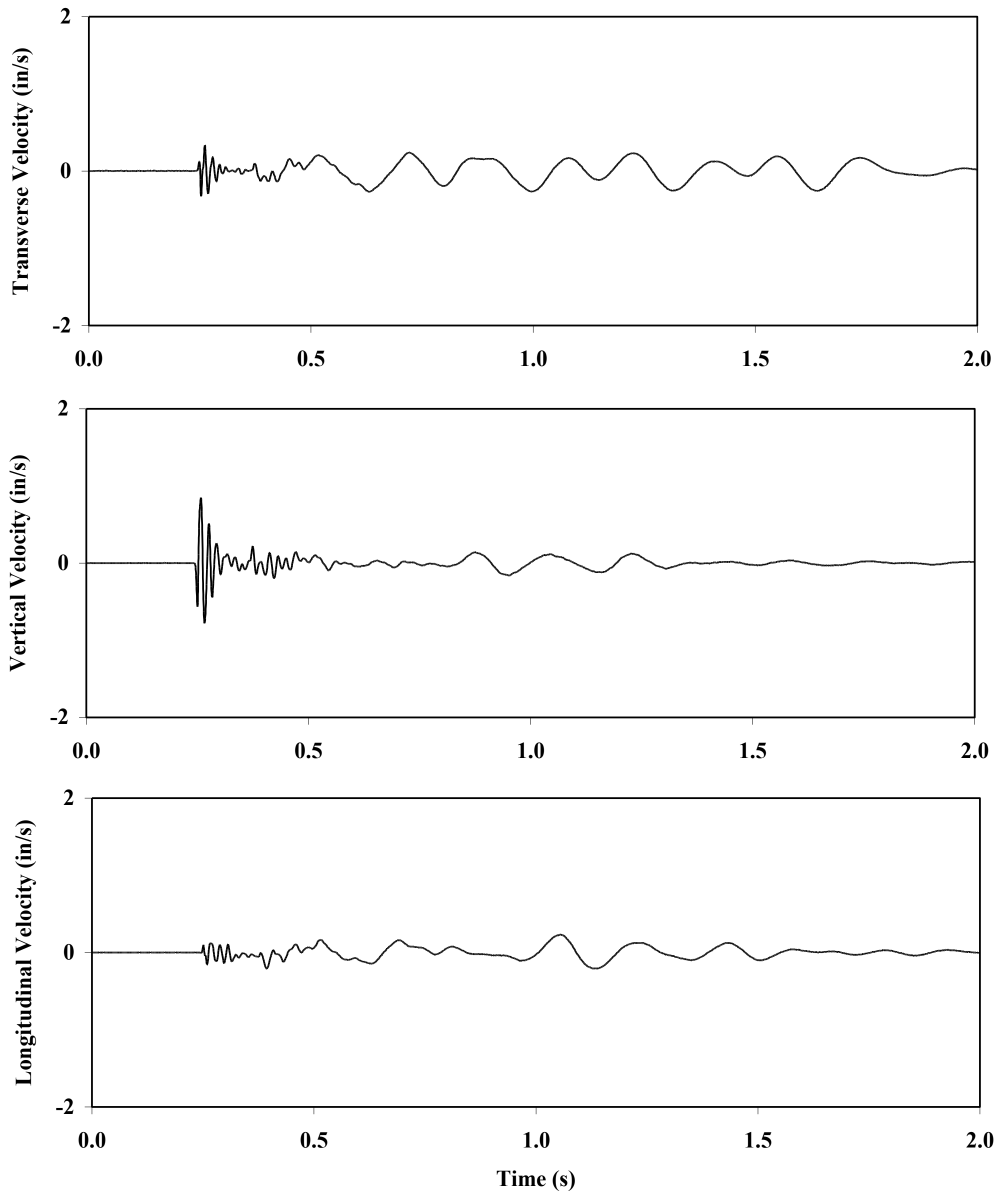

Streambed vibrations recorded during shot D12

Straight Distance (ft)	Scaled Distance (ft/lbs$^{1/2}$)	Transverse PPV (in/s)	FFT Freq. (Hz)	Vertical PPV (in/s)	FFT Freq. (Hz)	Long. PPV (in/s)	FFT Freq. (Hz)
199	12.9	0.24	7.0	1.40	7.0	0.21	7.0

APPENDIX 8 SITE D15 LOG CULVERT. Site diagram and setup information, hydrophone and geophone time histories

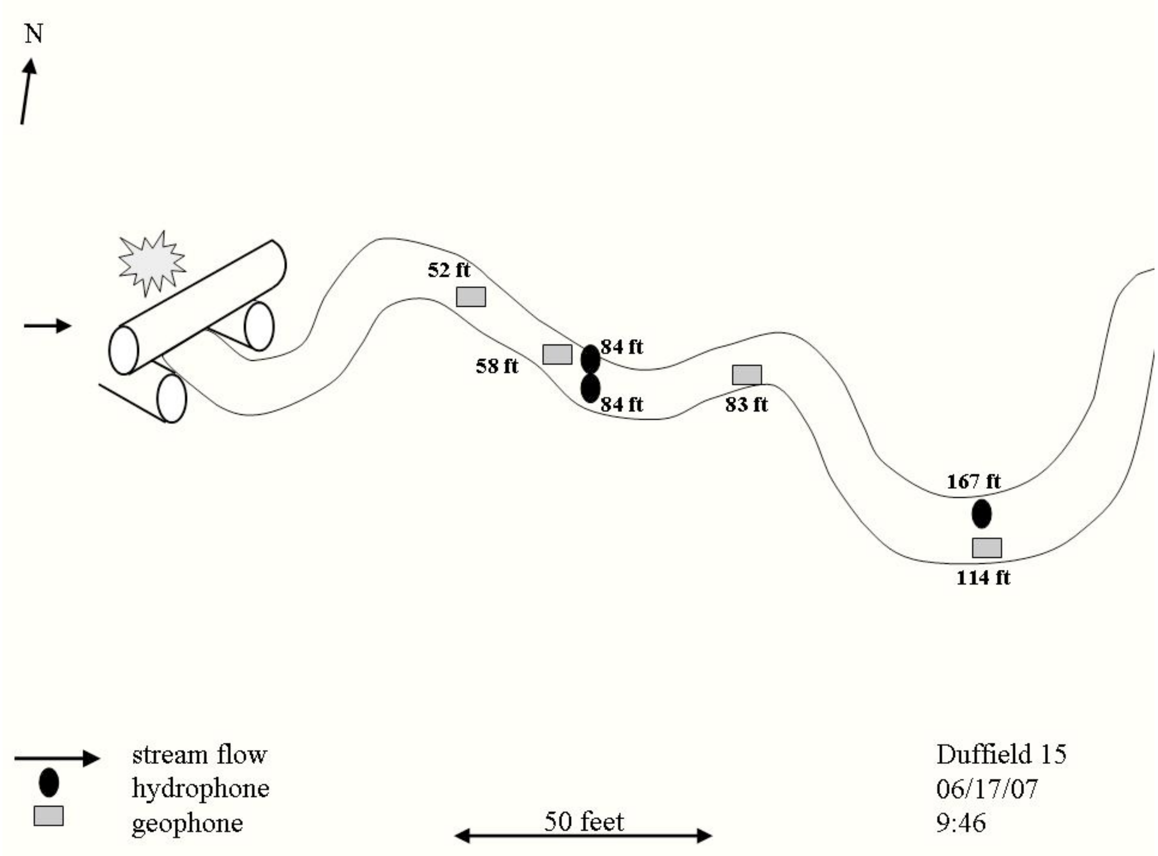

Structure, site, and shot information recorded during shot D15

Span / Length (ft)	Stringer Diameter (ft)	Between Sill Logs (ft)	Sill Log Diameter (ft)	Road Width (ft)	Fill Depth (ft)	Stream Grade (%)	Substrate Type
28	1.0	3.0	2.0	21	1.0	3	gravel

detcord (150 gr.) (ft)	ANFO (lbs)	Emulsion (lbs)	Total # / Delay (lbs)	TNT Equivalent (lbs)	Coupling level
200	275	15	294	240	coupled

(13.5 SD*)

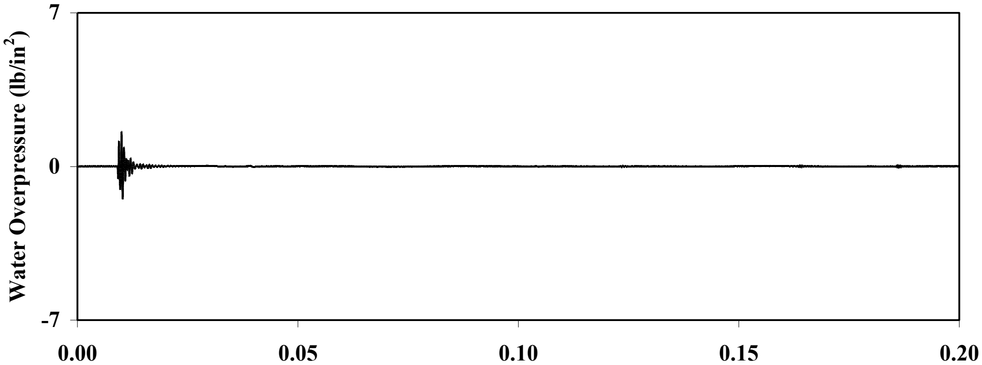

(26.9 SD*)

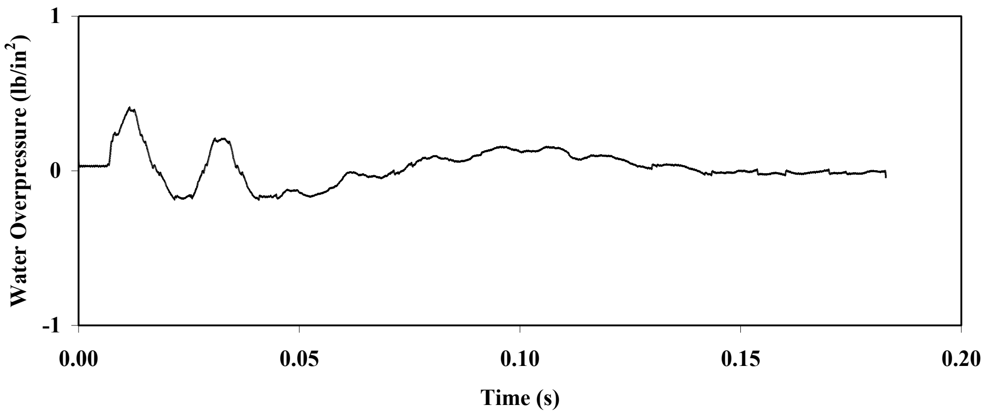

Stream pressures recorded during shot D15

Straight Distance (ft)	Scaled Distance ($ft/lbs^{1/3}$)	Positive Peak (lb/in^2)	Negative Peak (lb/in^2)	FFT Freq. (Hz)
84	13.5	1.59	-1.49	17.5
167	26.9	0.41	-0.19	9.5

*note the difference in scales

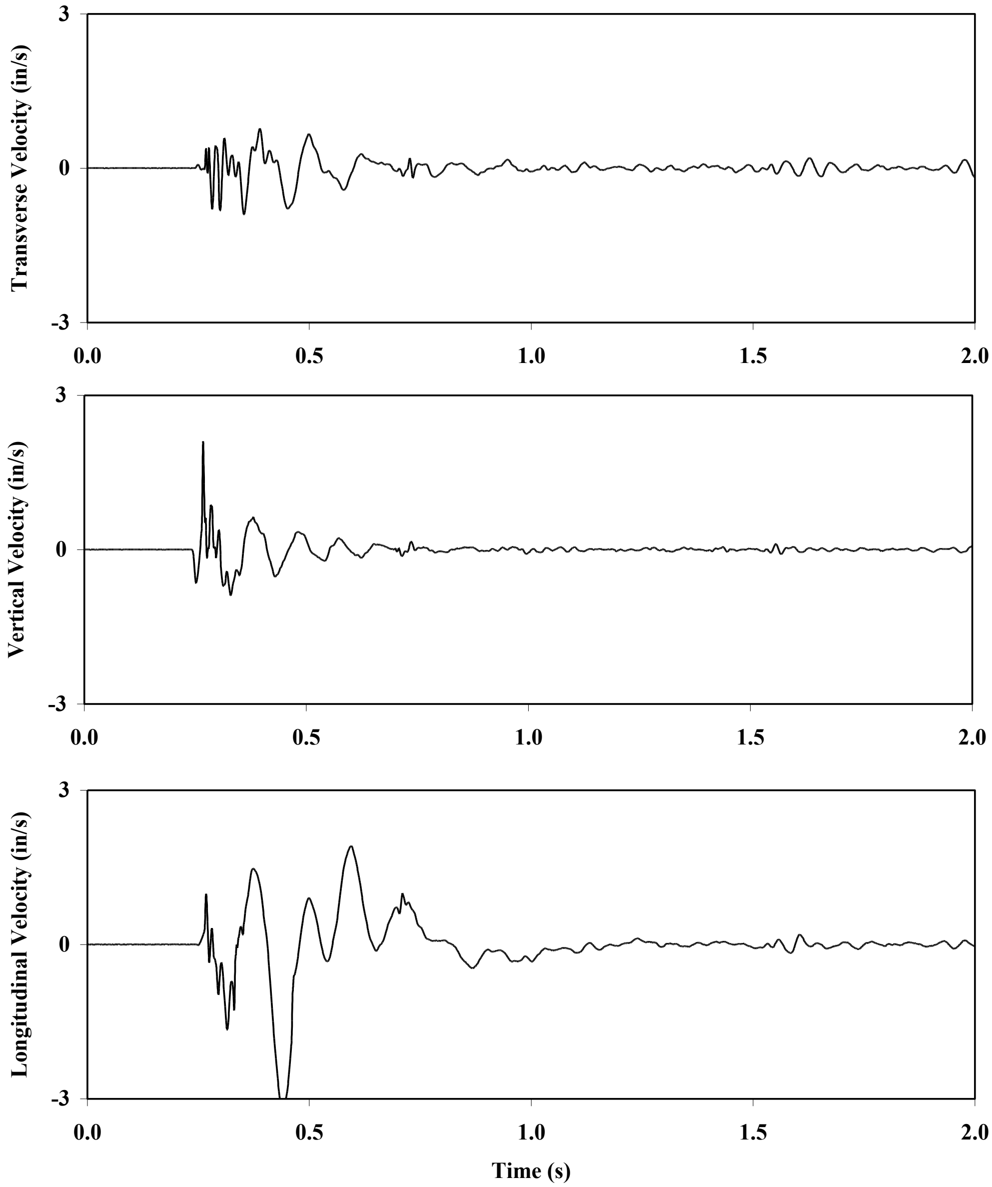

Streambed vibrations recorded during shot D15

Straight Distance (ft)	Scaled Distance ($ft/lbs^{1/2}$)	Transverse PPV (in/s)	FFT Freq. (Hz)	Vertical PPV (in/s)	FFT Freq. (Hz)	Long. PPV (in/s)	FFT Freq. (Hz)
52	3.4	0.89	9.3	2.11	10.3	3.19	9.3

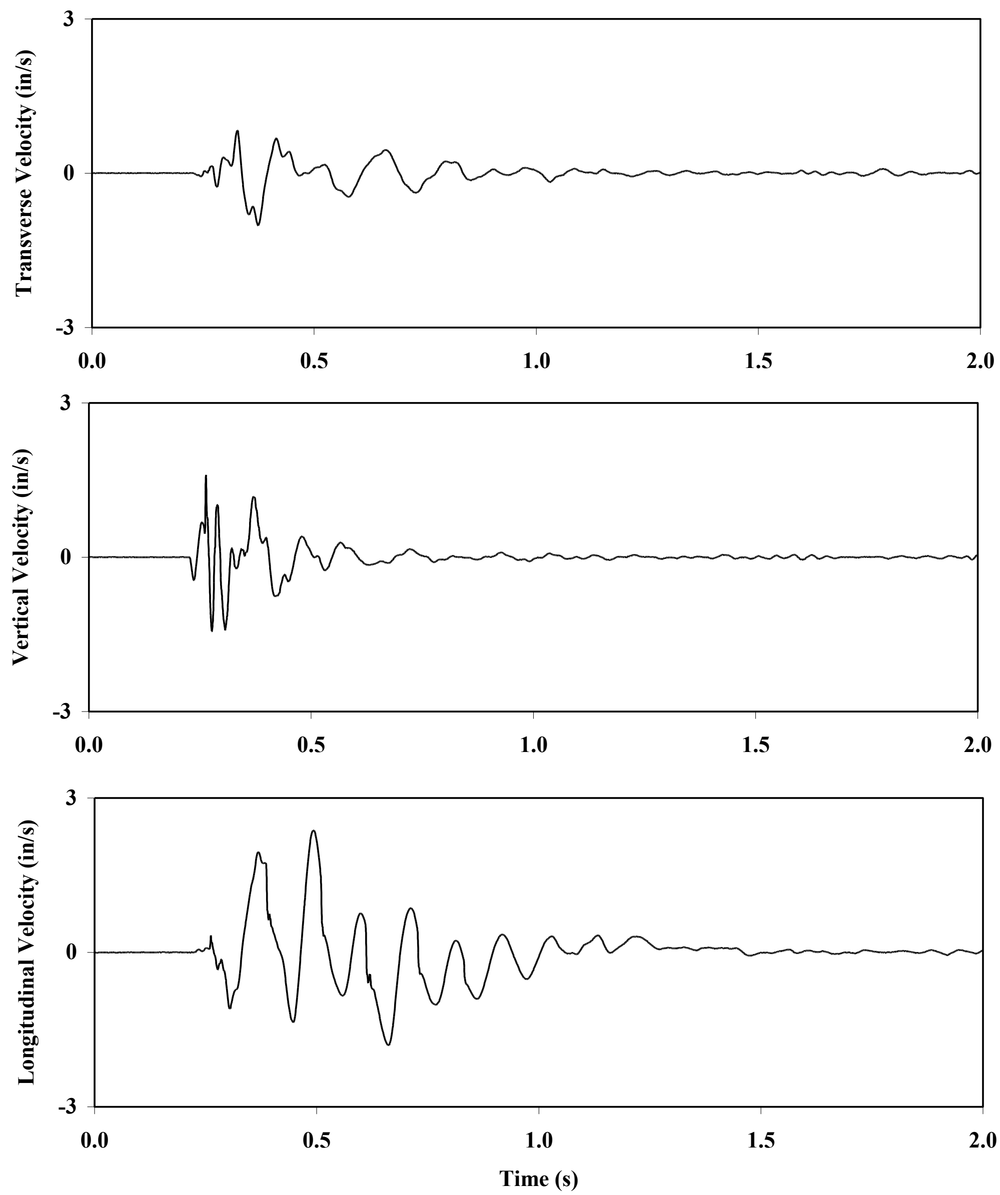

Streambed vibrations recorded during shot D15

Straight Distance (ft)	Scaled Distance (ft/lbs$^{1/2}$)	Transverse PPV (in/s)	FFT Freq. (Hz)	Vertical PPV (in/s)	FFT Freq. (Hz)	Long. PPV (in/s)	FFT Freq. (Hz)
58	3.7	1.02	6.3	1.60	9.3	2.37	9.5

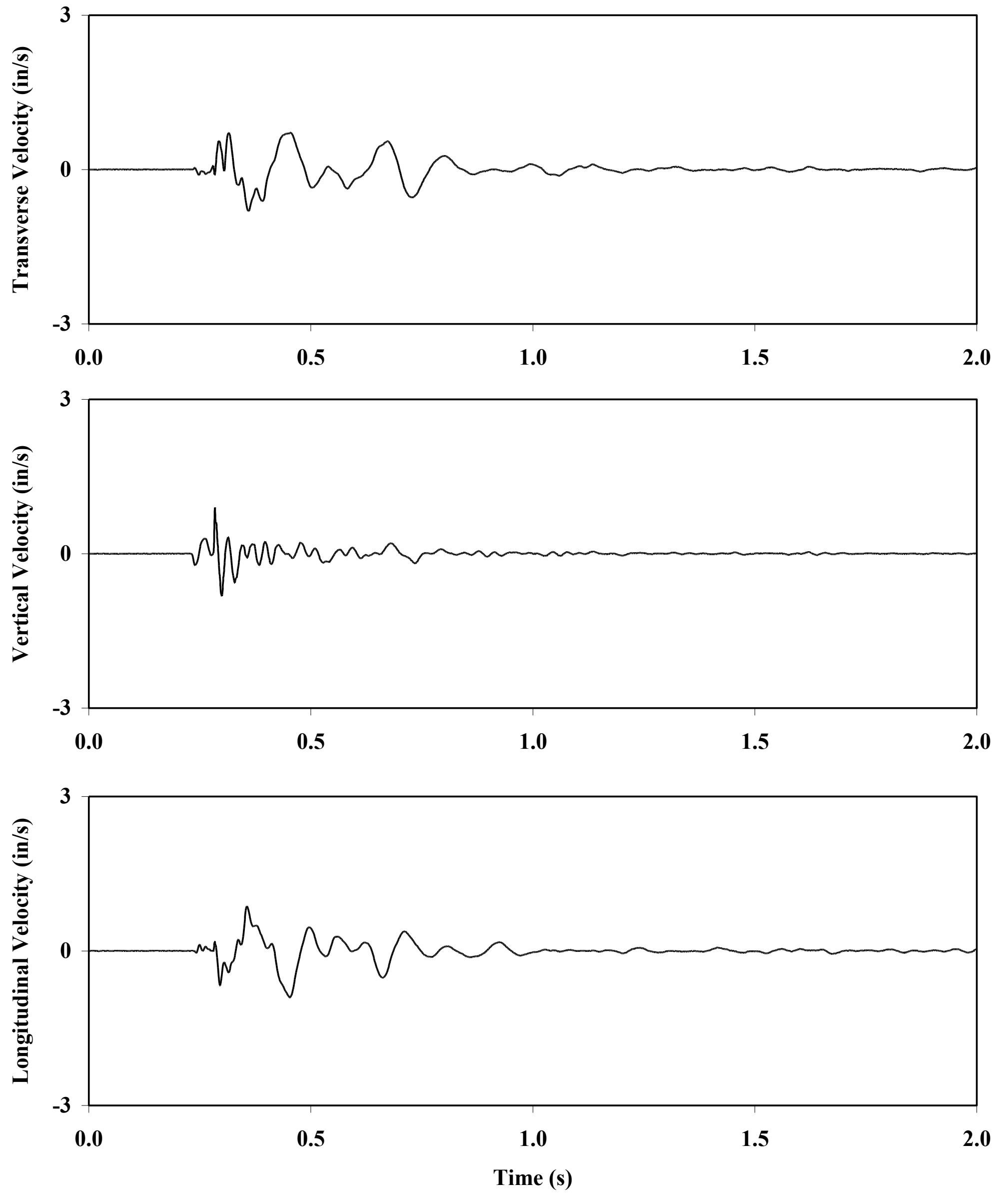

Streambed vibrations recorded during shot D15

Straight Distance (ft)	Scaled Distance (ft/lbs$^{1/2}$)	Transverse PPV (in/s)	FFT Freq. (Hz)	Vertical PPV (in/s)	FFT Freq. (Hz)	Long. PPV (in/s)	FFT Freq. (Hz)
83	5.4	0.81	6.0	0.90	9.8	0.90	6.0

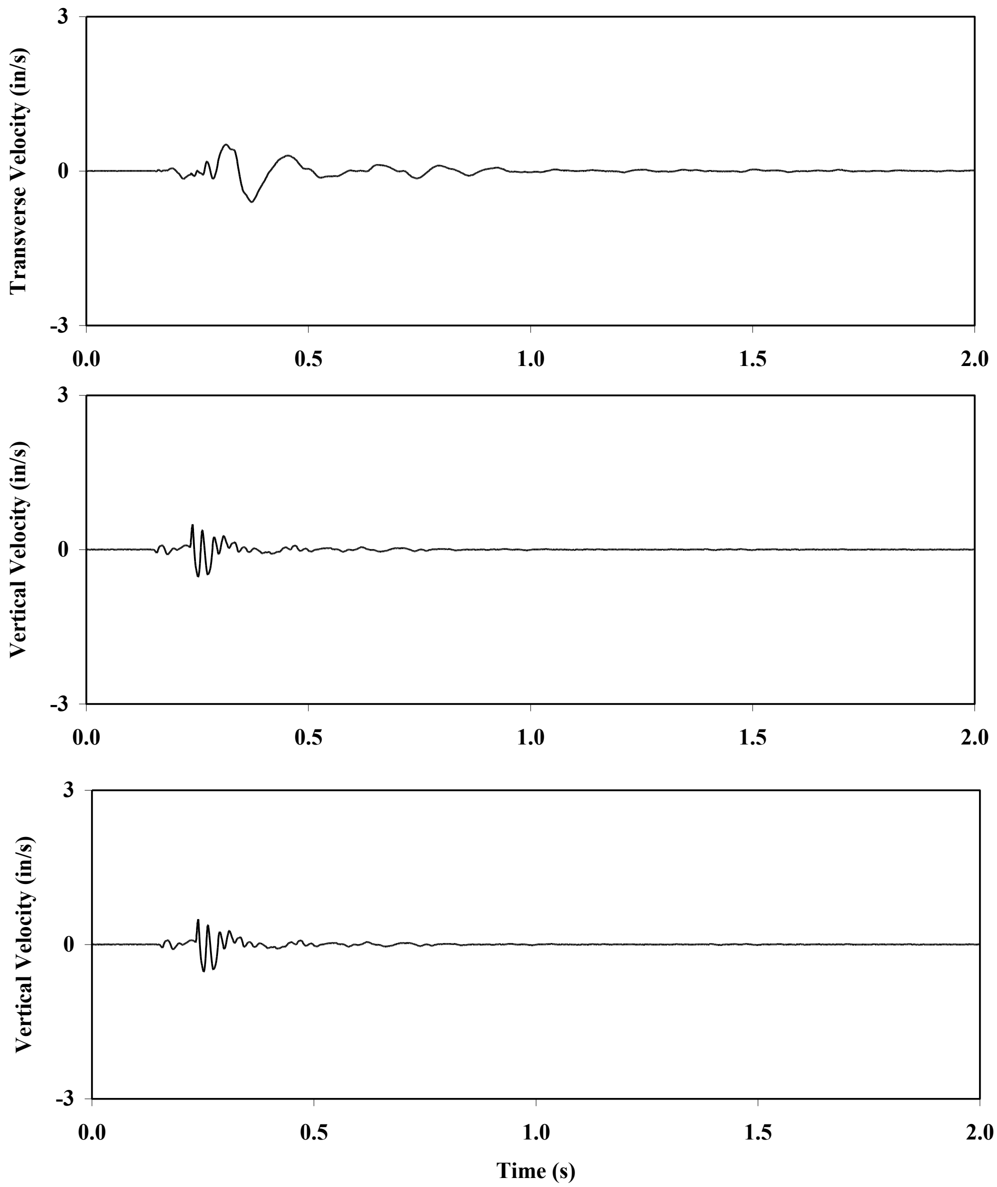

Streambed vibrations recorded during shot D15

Straight Distance (ft)	Scaled Distance (ft/lbs$^{1/2}$)	Transverse PPV (in/s)	FFT Freq. (Hz)	Vertical PPV (in/s)	FFT Freq. (Hz)	Long. PPV (in/s)	FFT Freq. (Hz)
114	7.4	0.61	6.5	0.56	43.0	0.46	6.3

APPENDIX 9 SITE D16 LOG CULVERT. Site diagram and setup information, hydrophone and geophone time histories

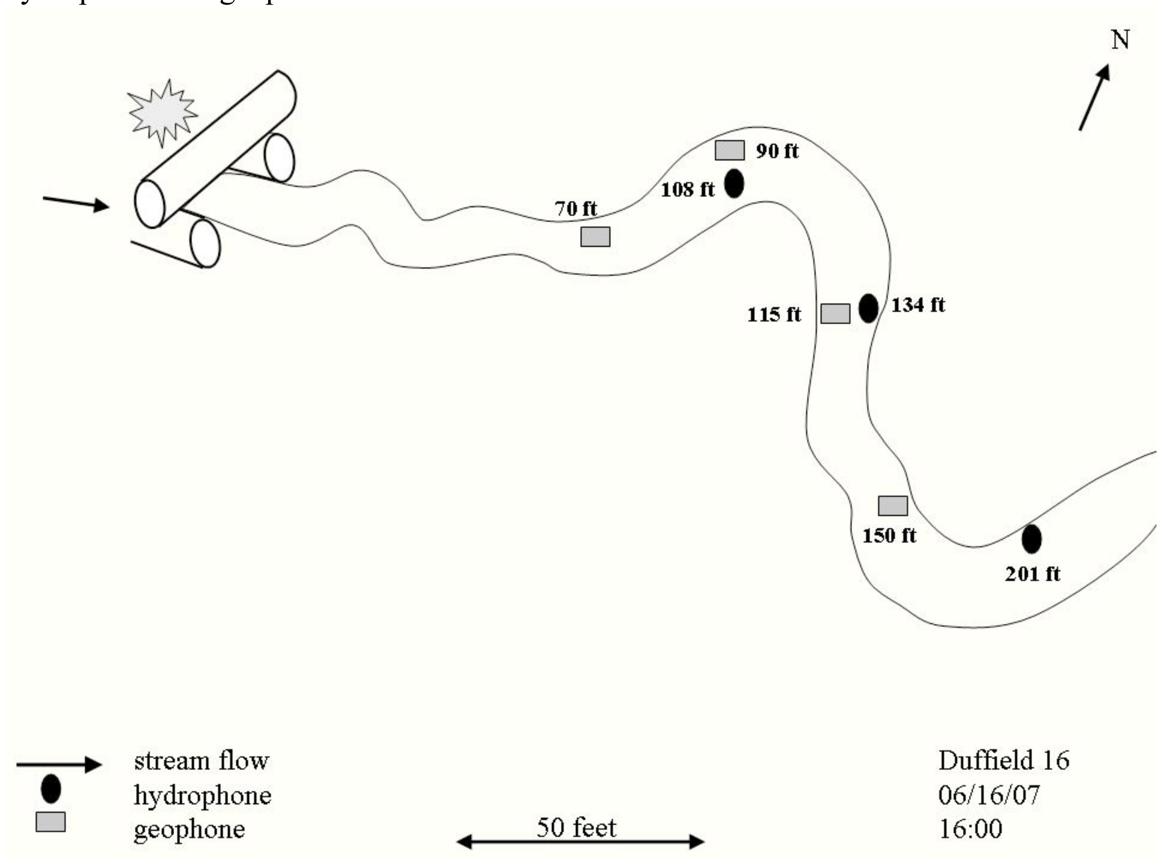

Structure, site, and shot information recorded during shot D16

Span / Length (ft)	Stringer Diameter (ft)	Between Sill Logs (ft)	Sill Log Diameter (ft)	Road Width (ft)	Fill Depth (ft)	Stream Grade (%)	Substrate Type
35	1.0	5.5	3.3	22	11.0	3-4	gravel

detcord (150 gr.) (ft)	ANFO (lbs)	Emulsion (lbs)	Total # / Delay (lbs)	TNT Equivalent (lbs)	Coupling level
170	275	25	304	246	coupled

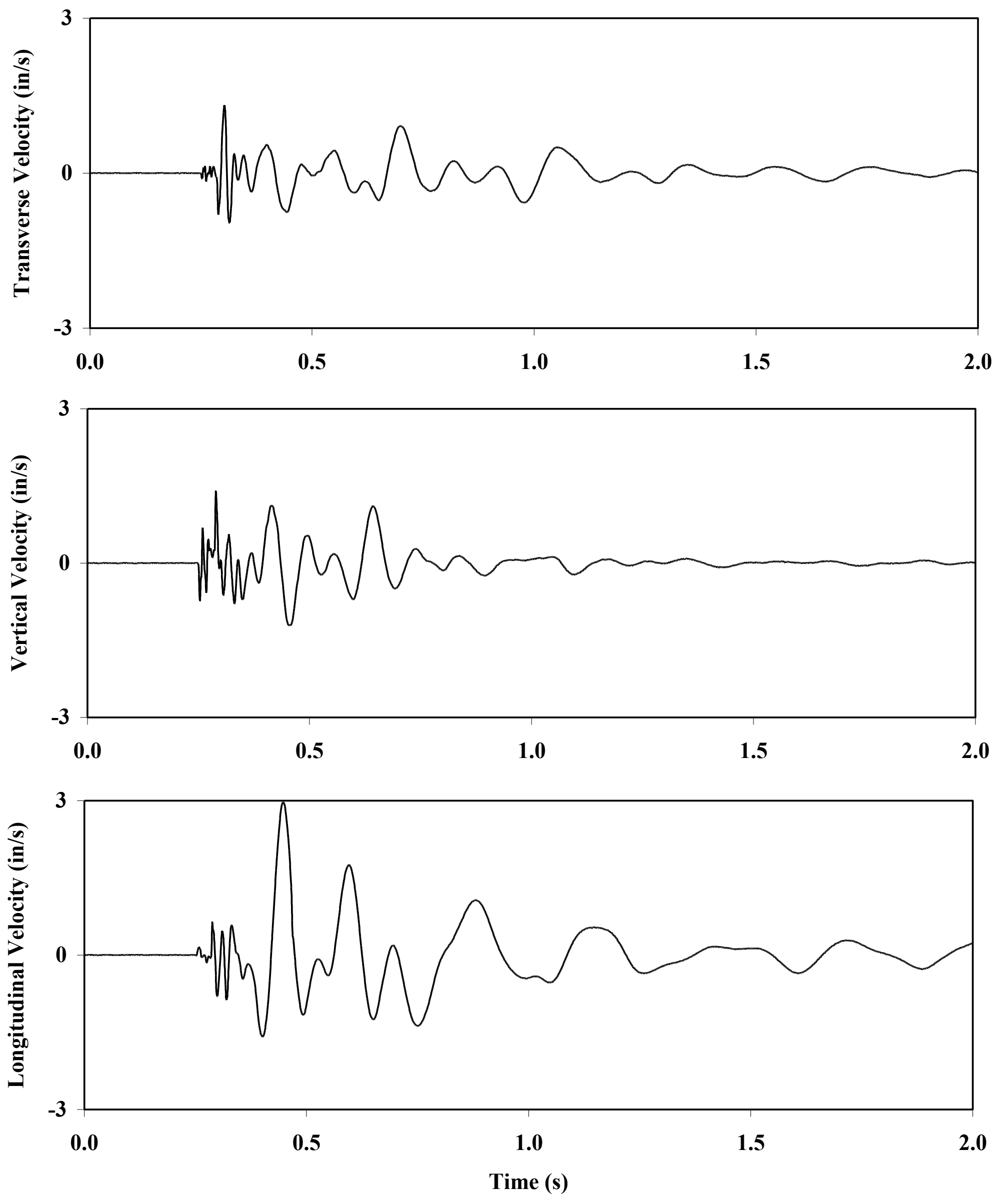

Streambed vibrations recorded during shot D16

Straight Distance (ft)	Scaled Distance (ft/lbs$^{1/2}$)	Transverse PPV (in/s)	FFT Freq. (Hz)	Vertical PPV (in/s)	FFT Freq. (Hz)	Long. PPV (in/s)	FFT Freq. (Hz)
70	4.5	1.32	6.0	1.39	9.3	2.97	3.8

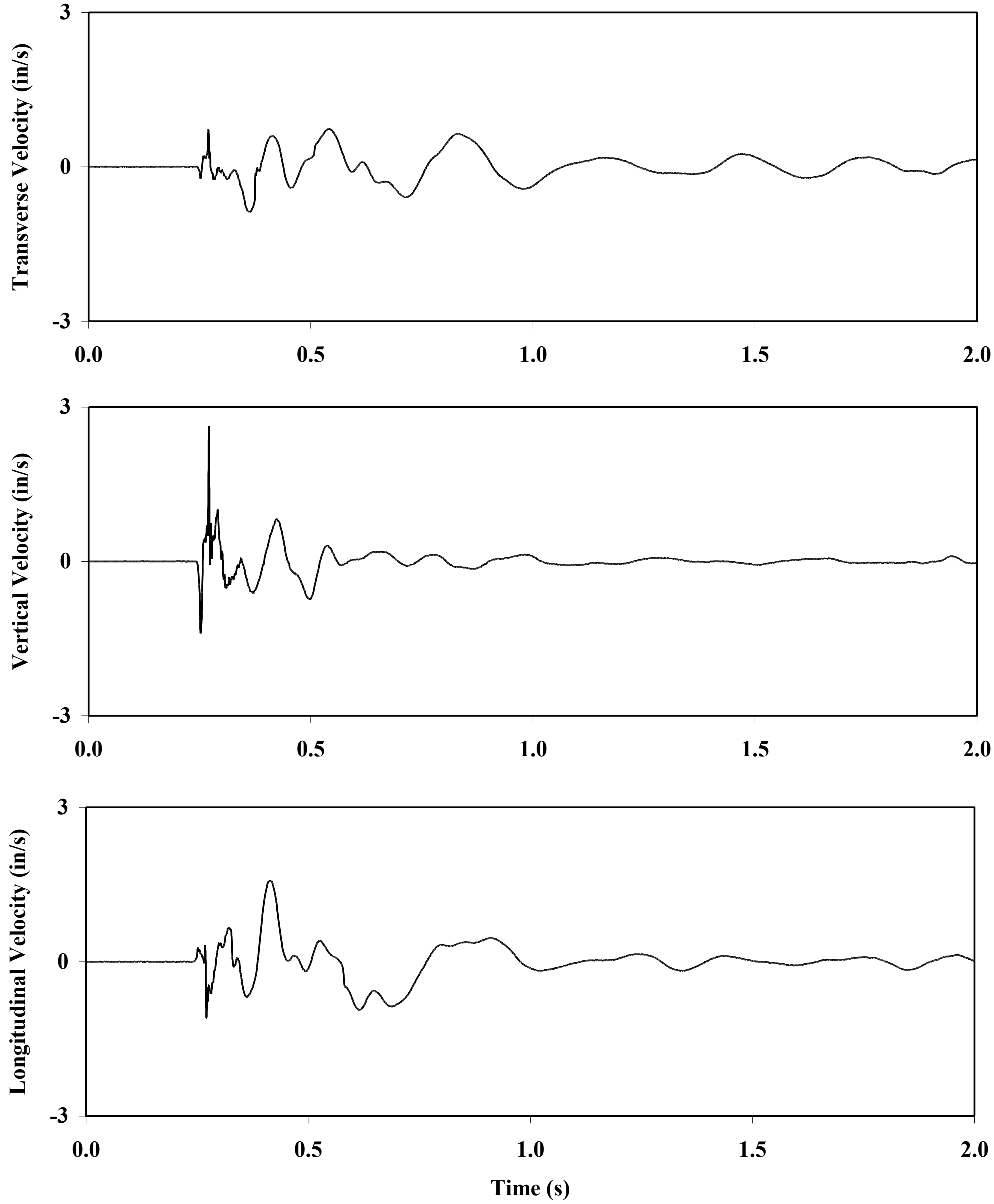

Streambed vibrations recorded during shot 16

Straight Distance (ft)	Scaled Distance (ft/lbs$^{1/2}$)	Transverse PPV (in/s)	FFT Freq. (Hz)	Vertical PPV (in/s)	FFT Freq. (Hz)	Long. PPV (in/s)	FFT Freq. (Hz)
90	5.7	0.88	3.5	2.61	8.3	1.58	2.5

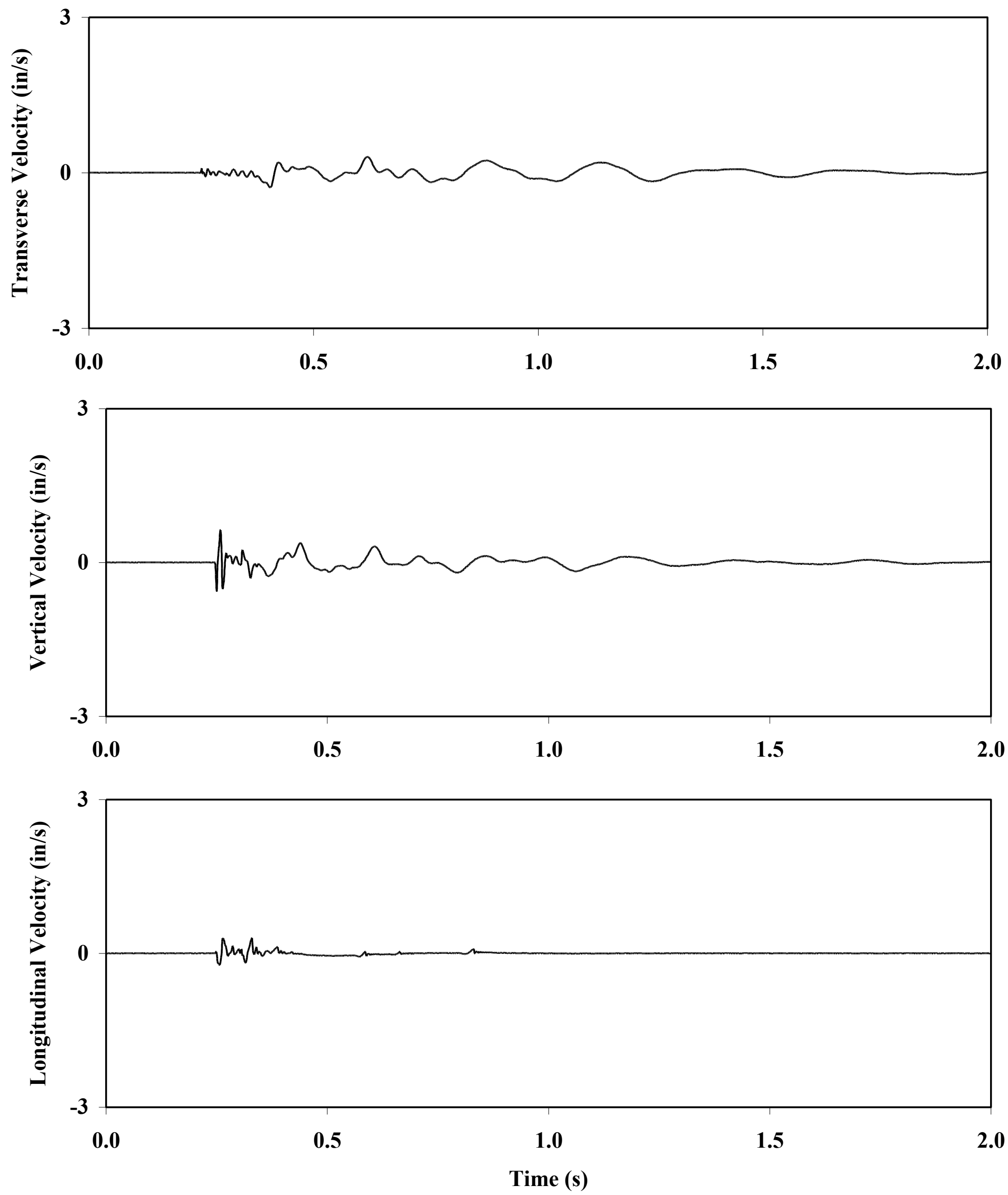

Streambed vibrations recorded during shot D16

Straight Distance (ft)	Scaled Distance (ft/lbs$^{1/2}$)	Transverse PPV (in/s)	FFT Freq. (Hz)	Vertical PPV (in/s)	FFT Freq. (Hz)	Long. PPV (in/s)	FFT Freq. (Hz)
115	7.3	0.31	4.5	0.64	4.0	0.31	1.8

APPENDIX 10 SITE D17 LOG CULVERT. Site diagram and setup information, hydrophone and geophone time histories

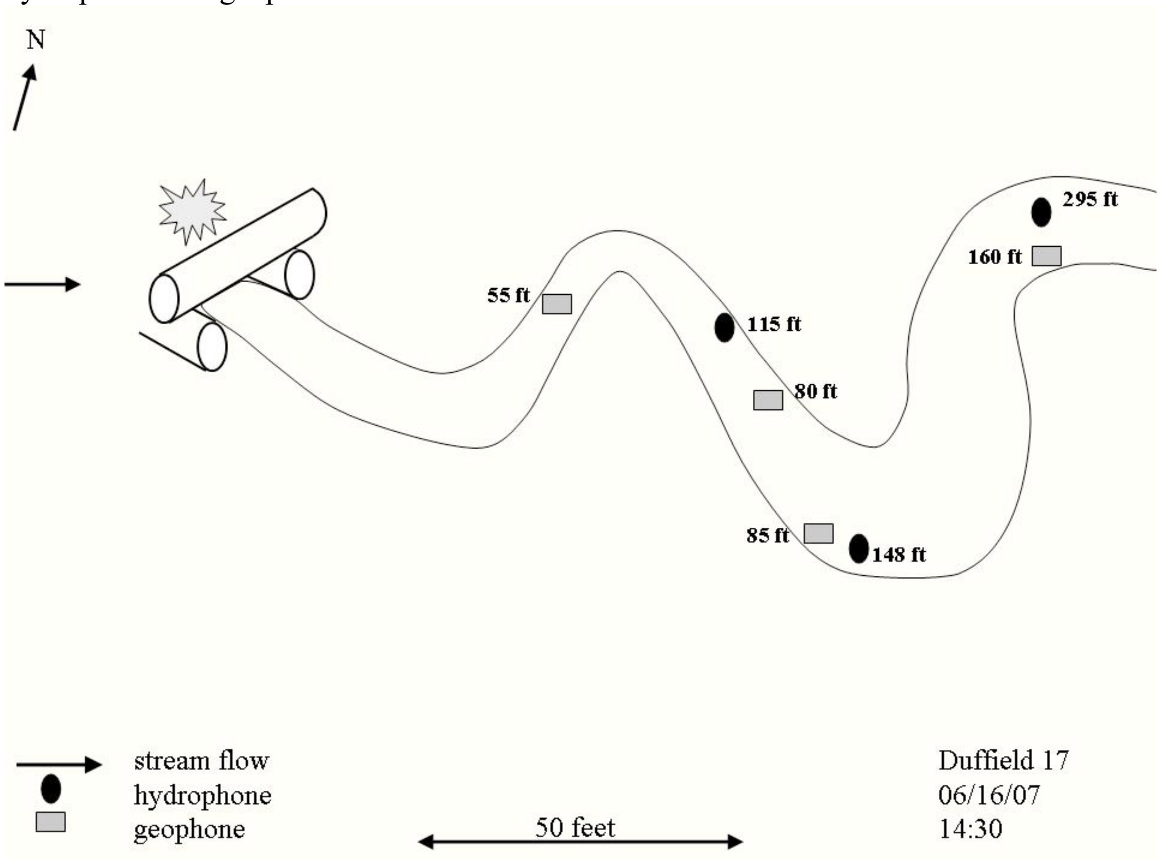

Structure, site, and shot information recorded during shot D17

Span / Length (ft)	Stringer Diameter (ft)	Between Sill Logs (ft)	Sill Log Diameter (ft)	Road Width (ft)	Fill Depth (ft)	Stream Grade (%)	Substrate Type
12	1.8	3.0	2.0	22	5.0	3-5	gravel

detcord (150 gr.) (ft)	ANFO (lbs)	Emulsion (lbs)	Total # / Delay (lbs)	TNT Equivalent (lbs)	Coupling level
0	165	55	220	169	de-coupled

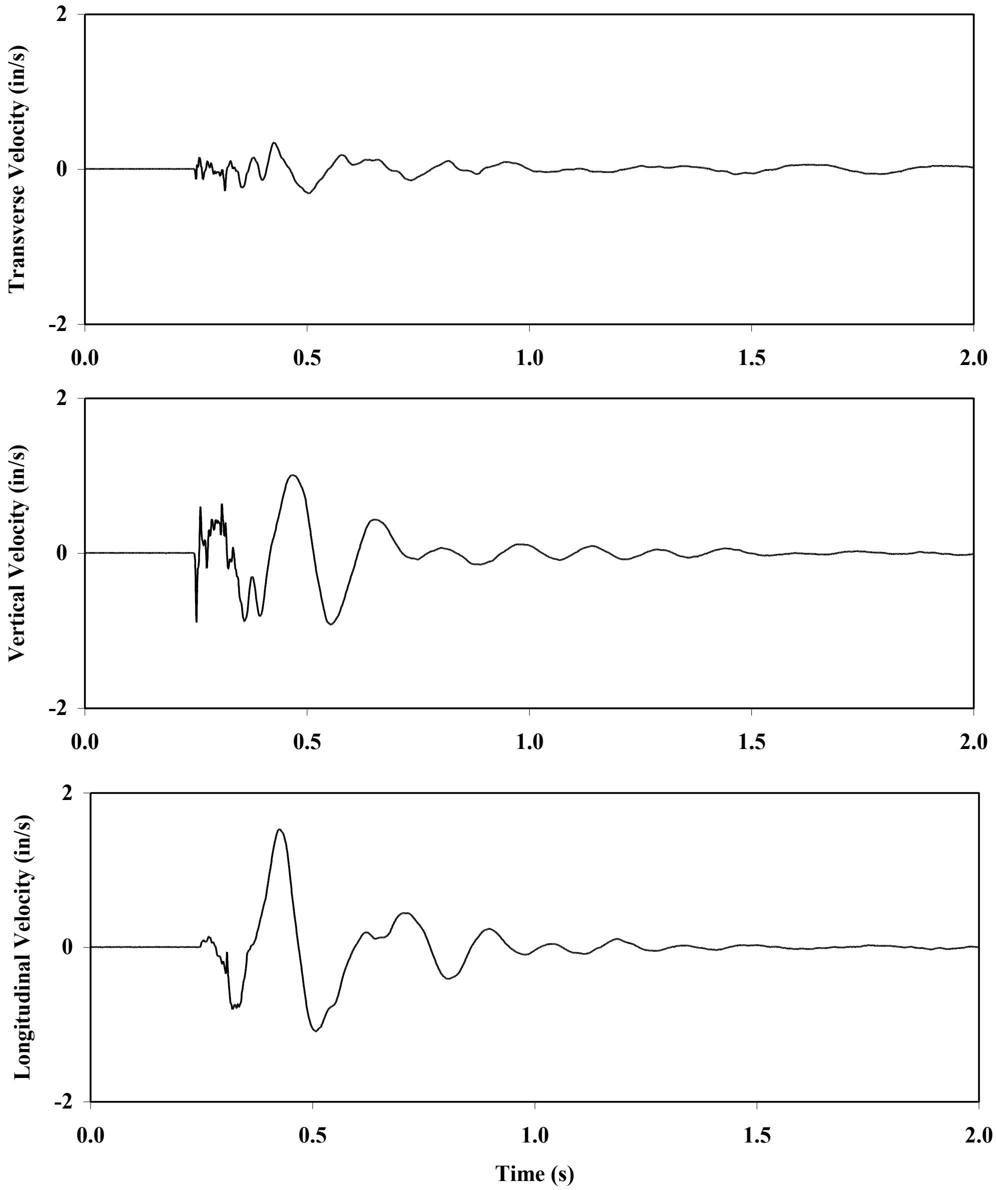

Streambed vibrations recorded during shot D17

Straight Distance (ft)	Scaled Distance (ft/lbs$^{1/2}$)	Transverse PPV (in/s)	FFT Freq. (Hz)	Vertical PPV (in/s)	FFT Freq. (Hz)	Long. PPV (in/s)	FFT Freq. (Hz)
55	4.2	1.60	24.8	1.05	2.3	1.84	2.3

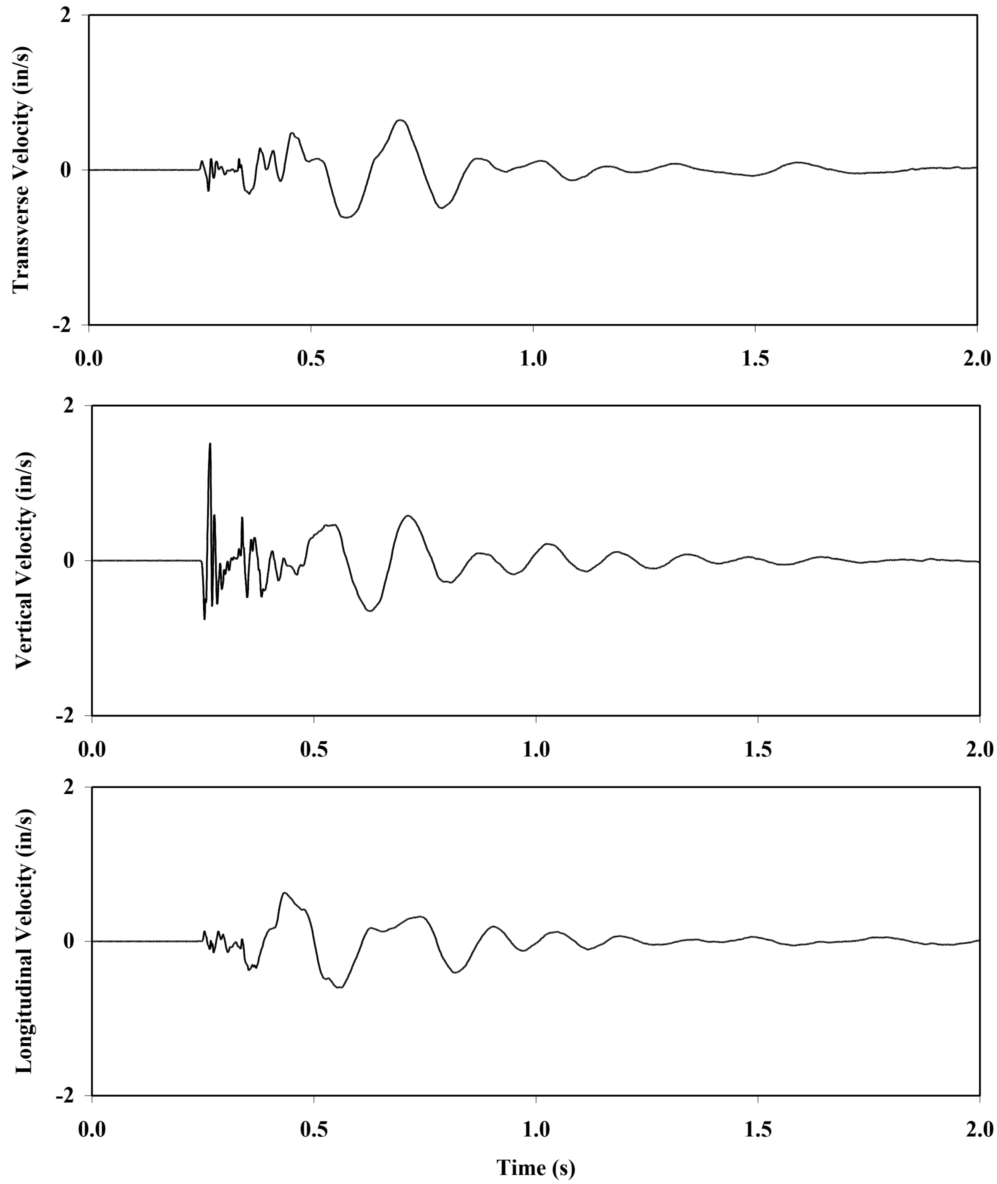

Streambed vibrations recorded during shot D17

Straight Distance (ft)	Scaled Distance (ft/lbs$^{1/2}$)	Transverse PPV (in/s)	FFT Freq. (Hz)	Vertical PPV (in/s)	FFT Freq. (Hz)	Long. PPV (in/s)	FFT Freq. (Hz)
80	6.2	0.65	4.8	1.51	6.3	0.64	4.0

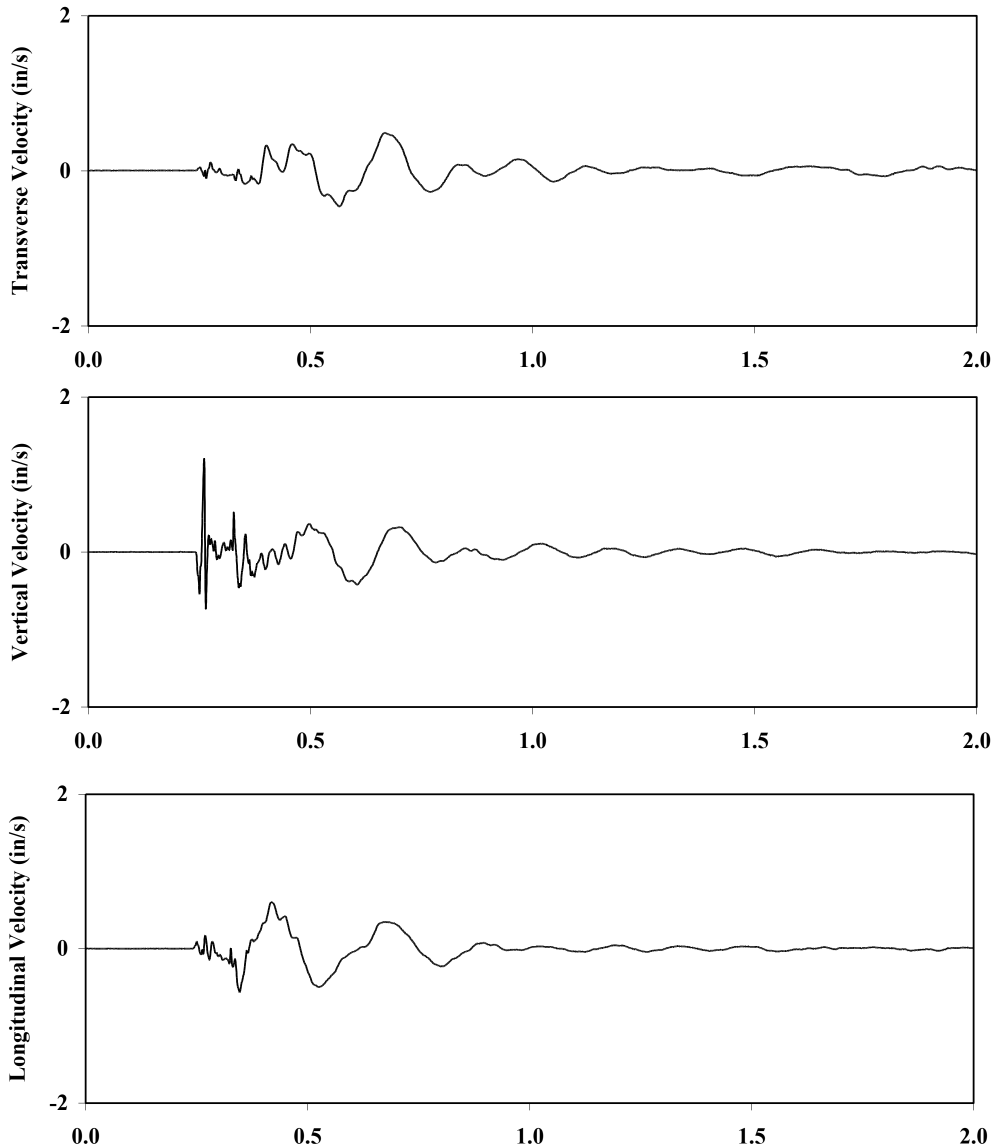

Streambed vibrations recorded during shot D17

Straight Distance (ft)	Scaled Distance ($ft/lbs^{1/2}$)	Transverse PPV (in/s)	FFT Freq. (Hz)	Vertical PPV (in/s)	FFT Freq. (Hz)	Long. PPV (in/s)	FFT Freq. (Hz)
85	6.5	0.49	4.3	1.20	4.3	0.61	4.0

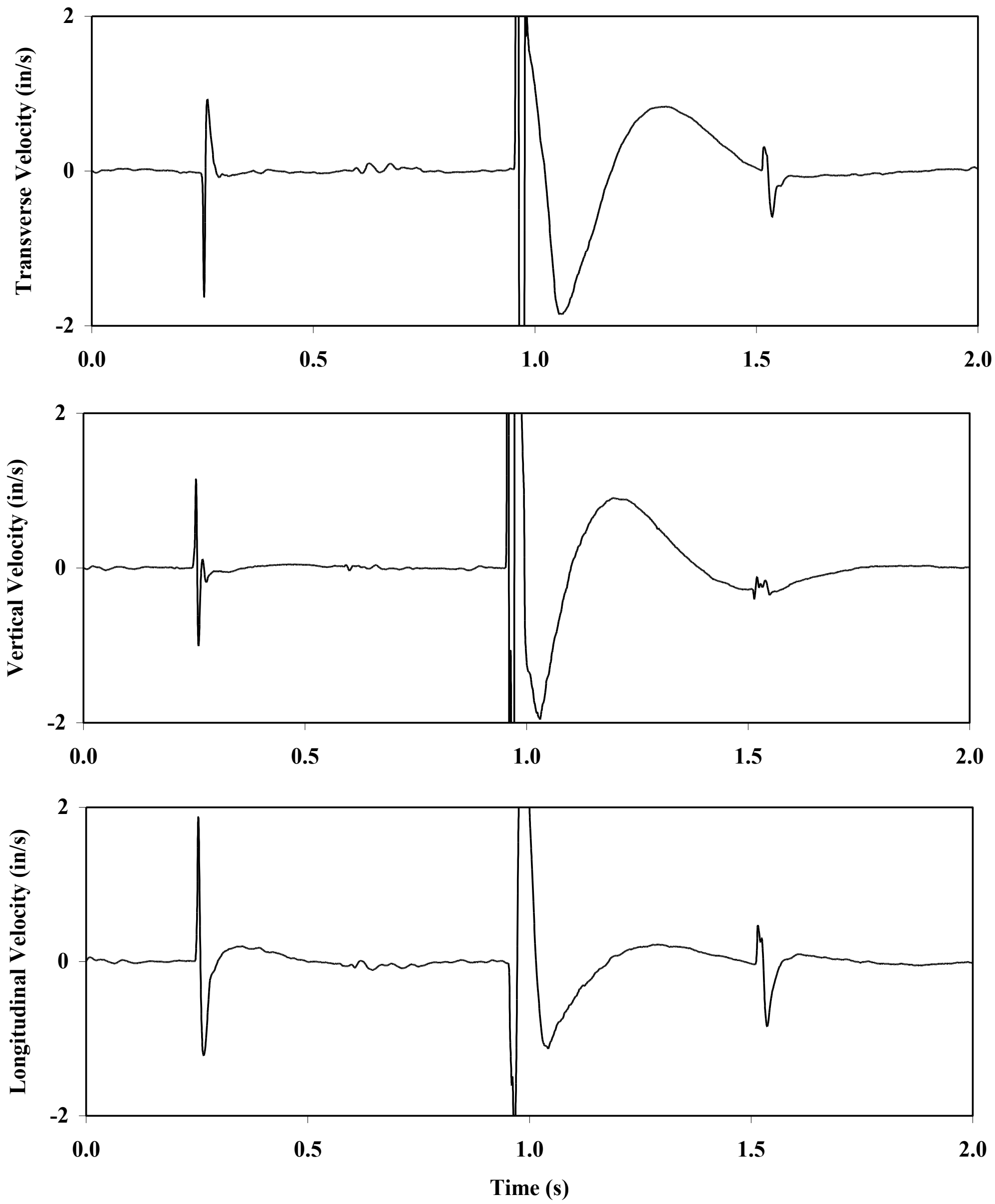

Streambed vibrations recorded during shot D17

Straight Distance (ft)	Scaled Distance (ft/lbs$^{1/2}$)	Transverse PPV (in/s)	FFT Freq. (Hz)	Vertical PPV (in/s)	FFT Freq. (Hz)	Long. PPV (in/s)	FFT Freq. (Hz)
160	12.3	0.35	3.3	1.01	6.3	1.53	4.0

APPENDIX 11 SITE D19 LOG CULVERT. Site diagram and setup information, hydrophone and geophone time histories

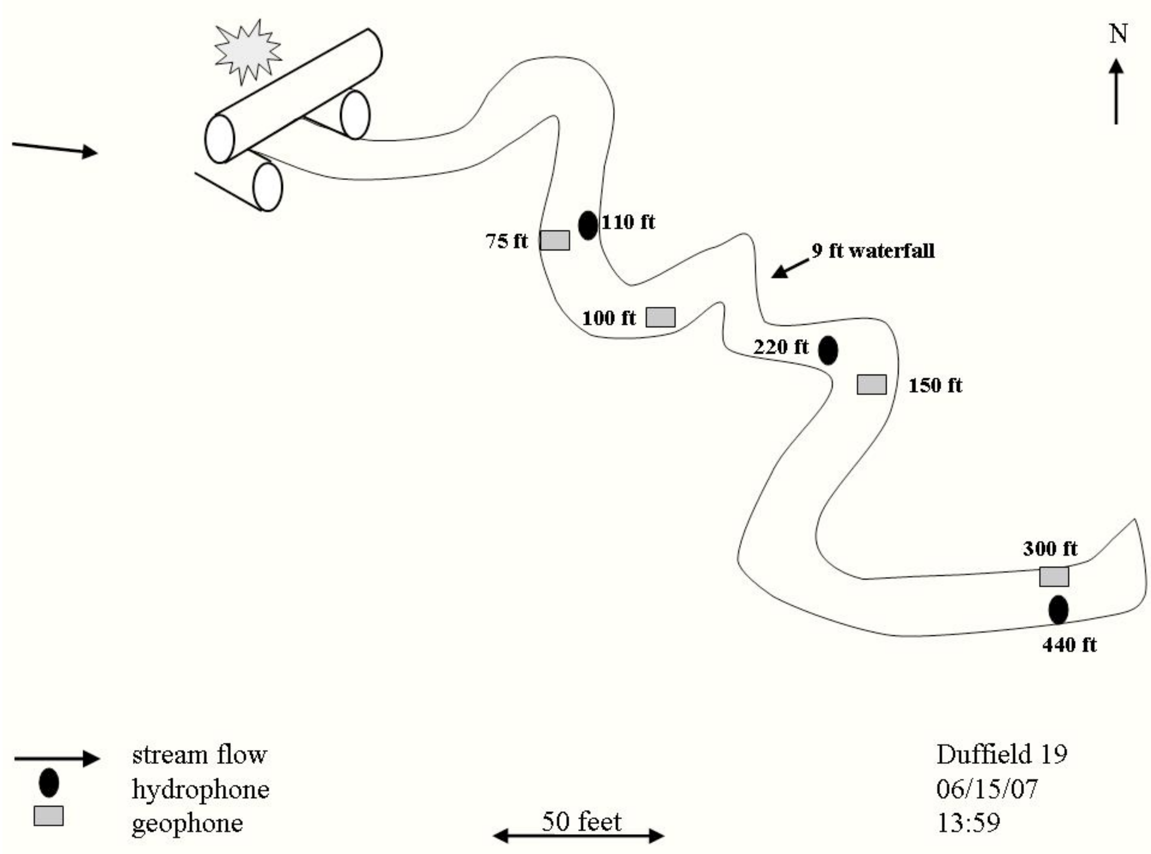

Structure, site, and shot information recorded during shot D19

Span / Length (ft)	Stringer Diameter (ft)	Between Sill Logs (ft)	Sill Log Diameter (ft)	Road Width (ft)	Fill Depth (ft)	Stream Grade (%)	Substrate Type
40	1.0	6.5	1.0	35	12.0	9-11	bedrock

detcord (150 gr.) (ft)	ANFO (lbs)	Emulsion (lbs)	Total # / Delay (lbs)	TNT Equivalent (lbs)	Coupling level
140	220	1140	853	530	well coupled / coupled

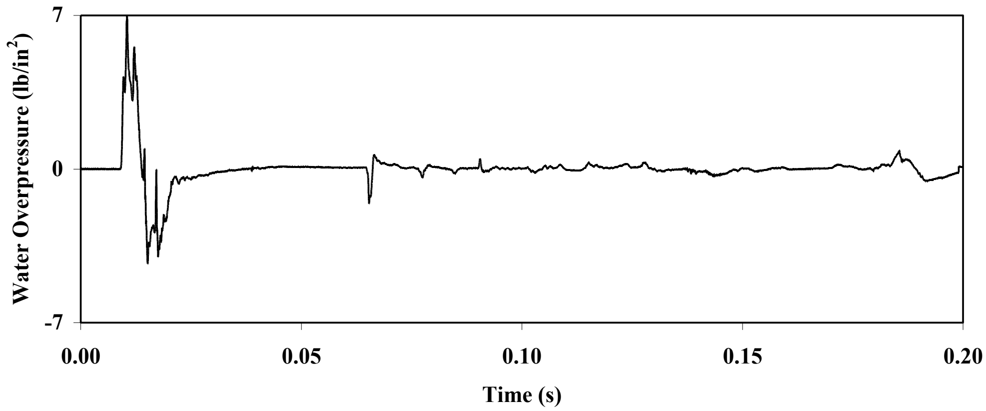

Stream pressures recorded during shot D19

Straight Distance (ft)	Scaled Distance (ft/lbs$^{1/3}$)	Positive Peak (lb/in^2)	Negative Peak (lb/in^2)	FFT Freq. (Hz)
110	13.6	6.99	-4.31	67.5

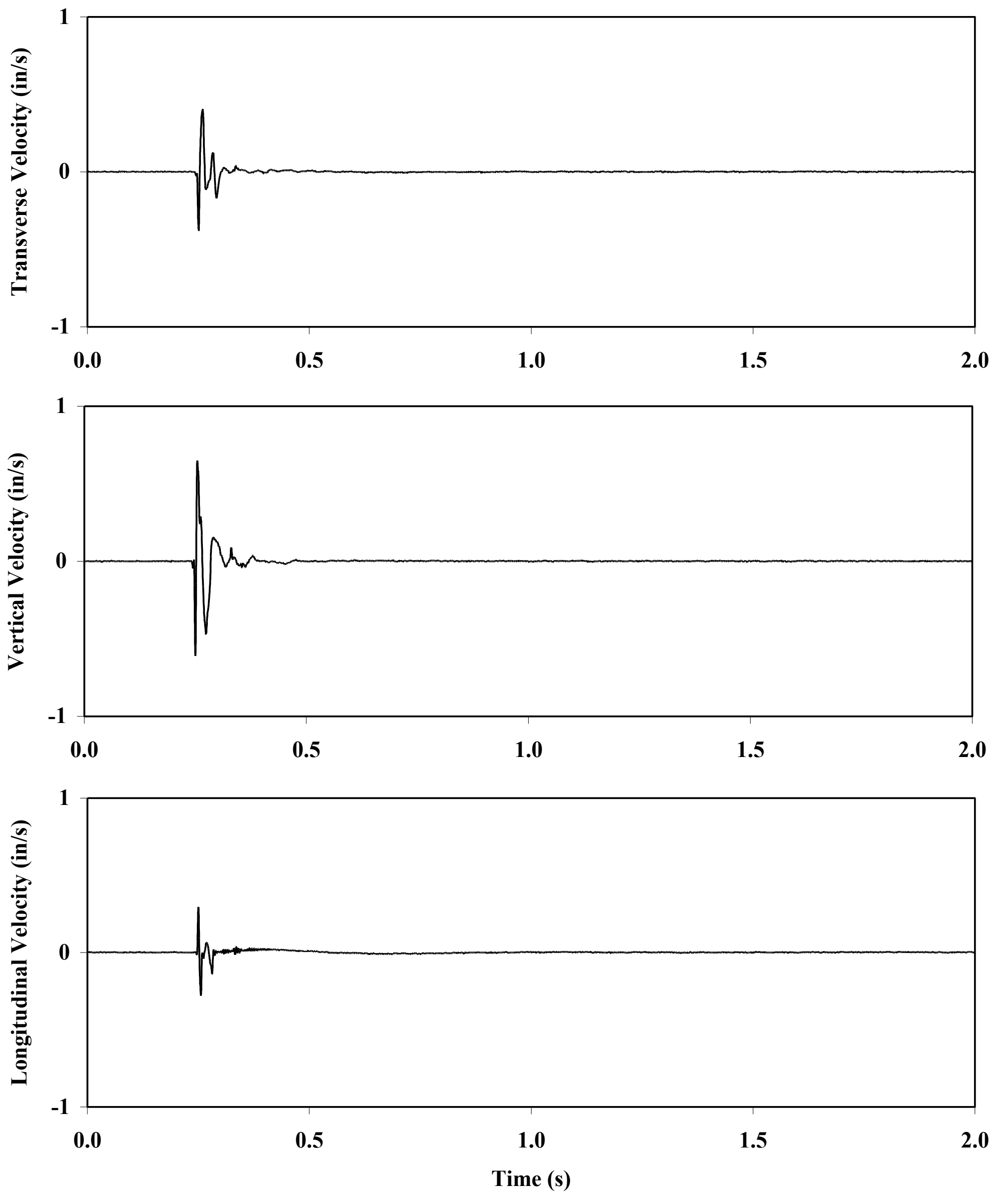

Streambed vibrations recorded during shot D19

Straight Distance (ft)	Scaled Distance ($ft/lbs^{1/2}$)	Transverse PPV (in/s)	FFT Freq. (Hz)	Vertical PPV (in/s)	FFT Freq. (Hz)	Long. PPV (in/s)	FFT Freq. (Hz)
75	3.3	0.40	45.5	0.65	27.0	0.30	1.8

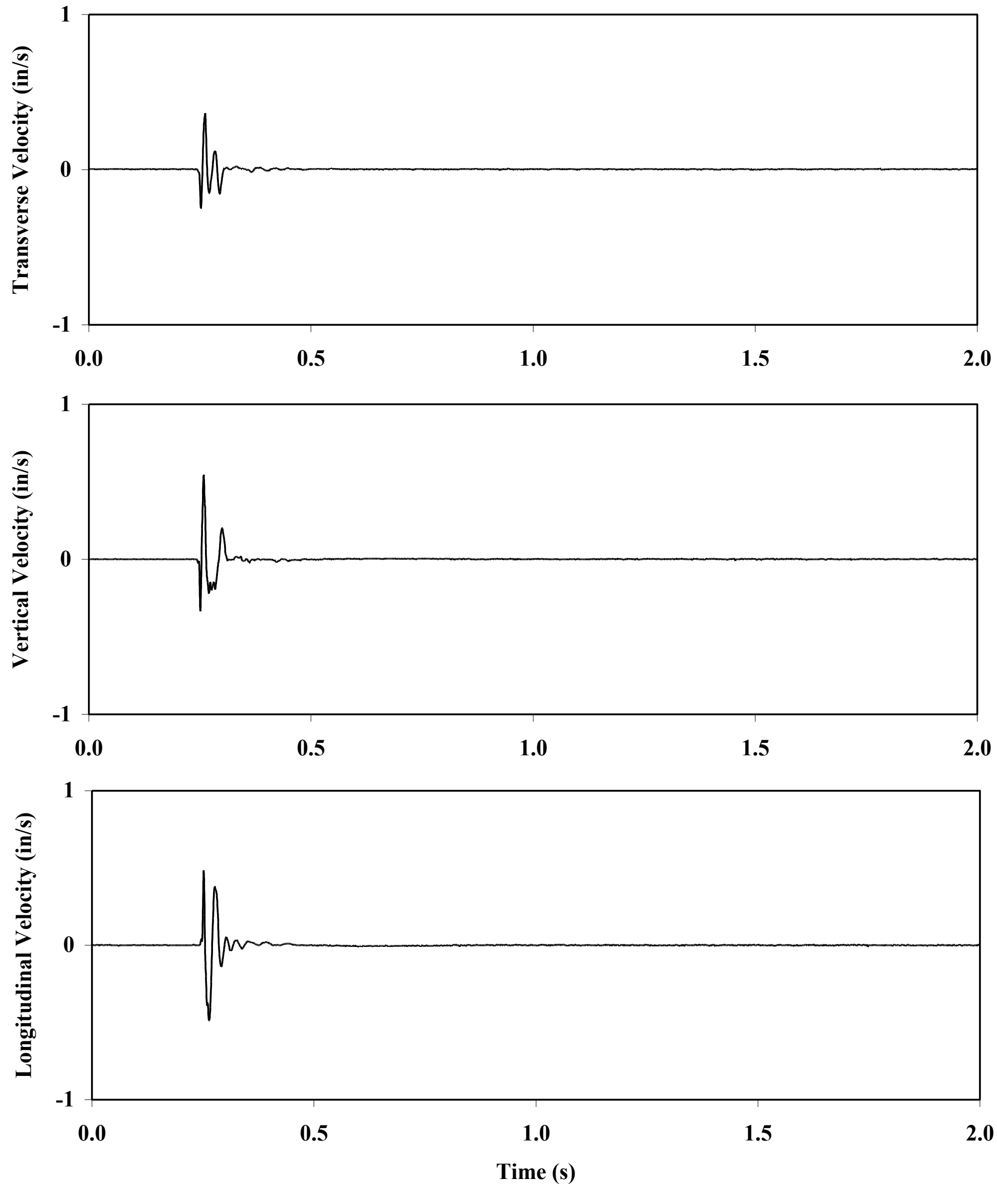

Streambed vibrations recorded during shot D19

Straight Distance (ft)	Scaled Distance (ft/lbs$^{1/2}$)	Transverse PPV (in/s)	FFT Freq. (Hz)	Vertical PPV (in/s)	FFT Freq. (Hz)	Long. PPV (in/s)	FFT Freq. (Hz)
100	4.3	0.37	43.0	0.54	25.3	0.49	37.3

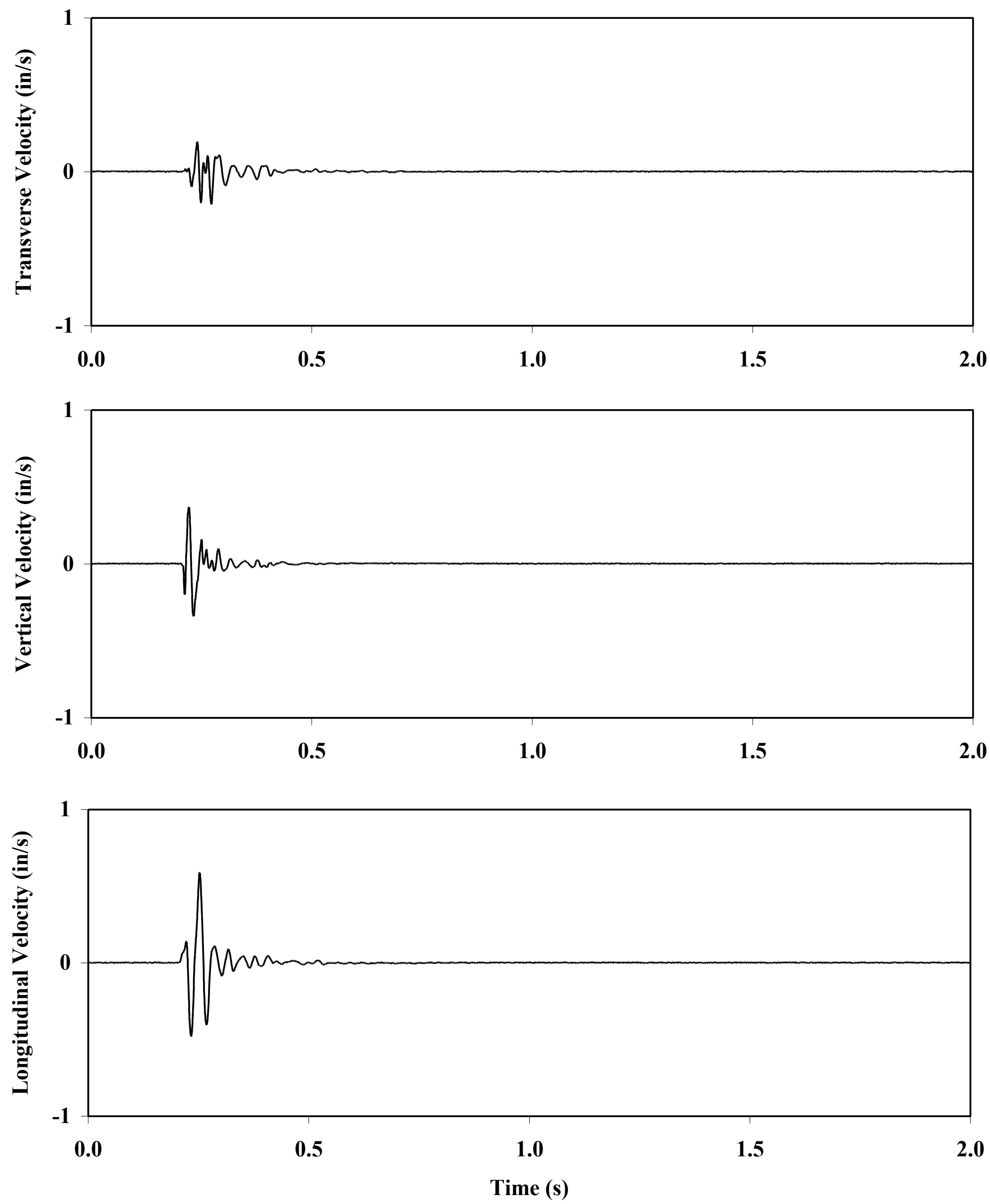

Streambed vibrations recorded during shot D19

Straight Distance (ft)	Scaled Distance (ft/lbs$^{1/2}$)	Transverse PPV (in/s)	FFT Freq. (Hz)	Vertical PPV (in/s)	FFT Freq. (Hz)	Long. PPV (in/s)	FFT Freq. (Hz)
150	6.5	0.21	39.8	0.37	31.5	0.59	30.0

APPENDIX 12 SITE D20 LOG CULVERT. Site diagram and setup information, hydrophone and geophone time histories

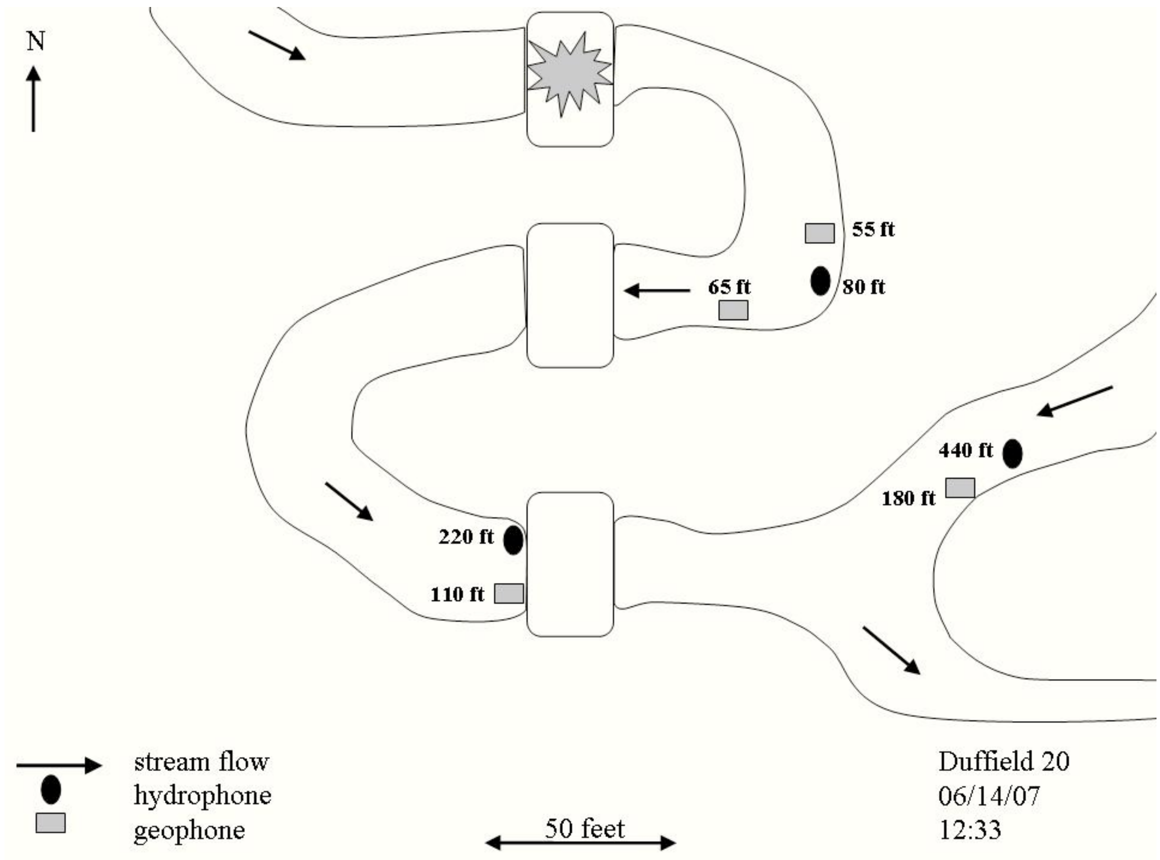

Structure, site, and shot information recorded during shot D20

Span / Length (ft)	Stringer Diameter (ft)	Between Sill Logs (ft)	Sill Log Diameter (ft)	Road Width (ft)	Fill Depth (ft)	Stream Grade (%)	Substrate Type
35	3.0	24.5	5.0	18	1.5	4-6	gravel

detcord (150 gr.) (ft)	ANFO (lbs)	Emulsion (lbs)	Total # / Delay (lbs)	TNT Equivalent (lbs)	Coupling level
250	0	1218.6	1224	762	coupled

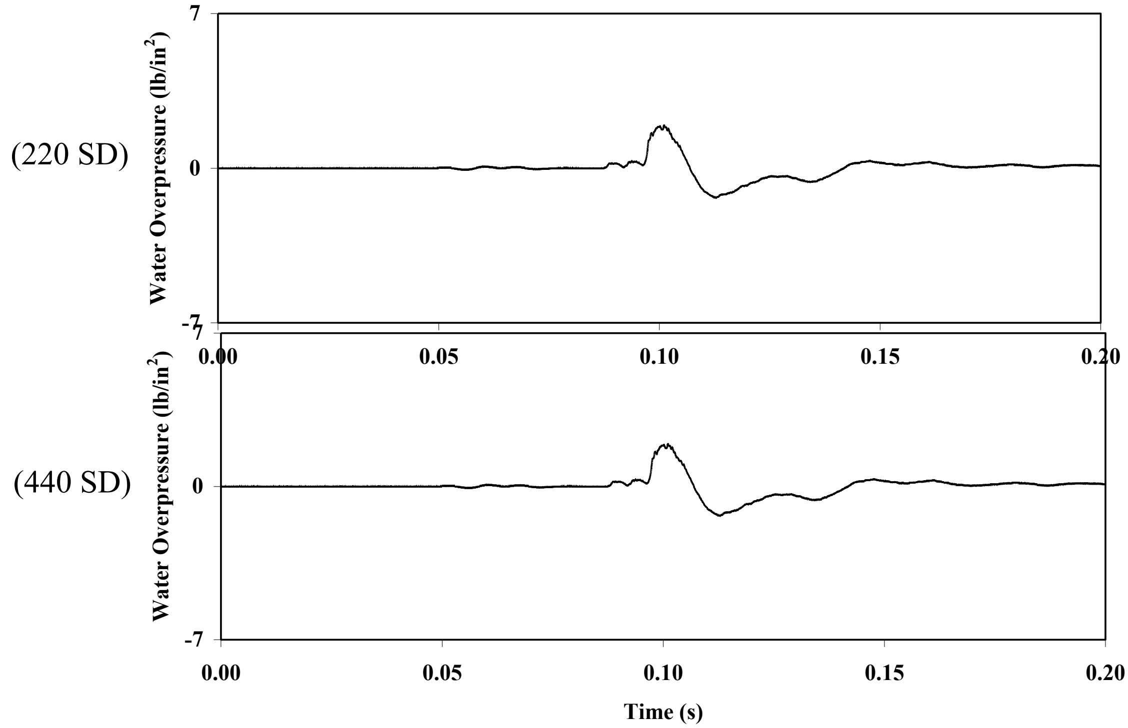

Stream pressures recorded during shot D20

Straight Distance (ft)	Scaled Distance ($ft/lbs^{1/3}$)	Positive Peak (lb/in^2)	Negative Peak (lb/in^2)	FFT Freq. (Hz)
80?	8.8	nt		
220	24.1	1.97	-1.35	18.0
440	48.2	0.24	0.22	8.5

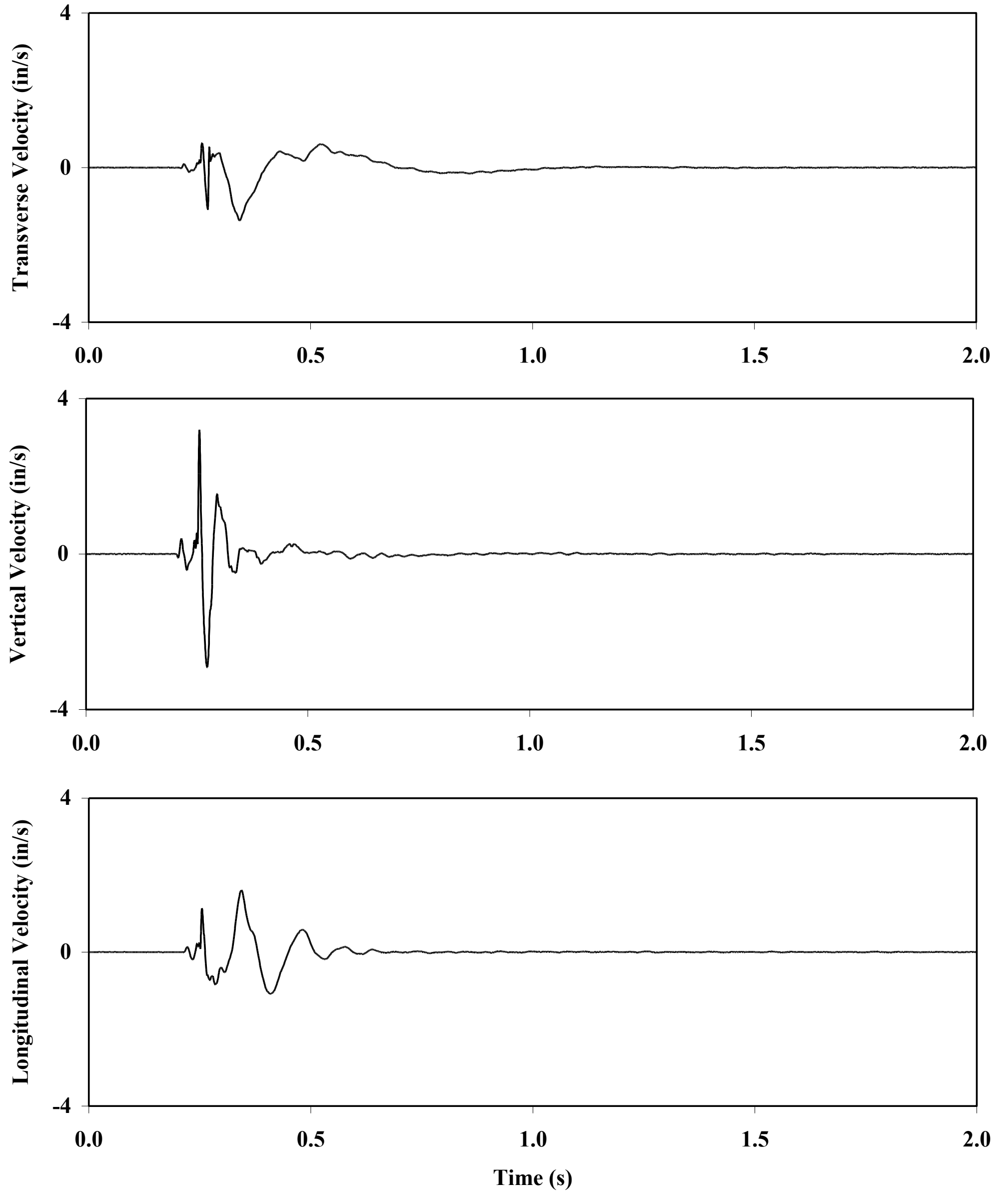

Streambed vibrations recorded during shot D20

Straight Distance (ft)	Scaled Distance (ft/lbs$^{1/2}$)	Transverse PPV (in/s)	FFT Freq. (Hz)	Vertical PPV (in/s)	FFT Freq. (Hz)	Long. PPV (in/s)	FFT Freq. (Hz)
55	2.0	1.37	2.0	3.20	18.8	1.61	8.0

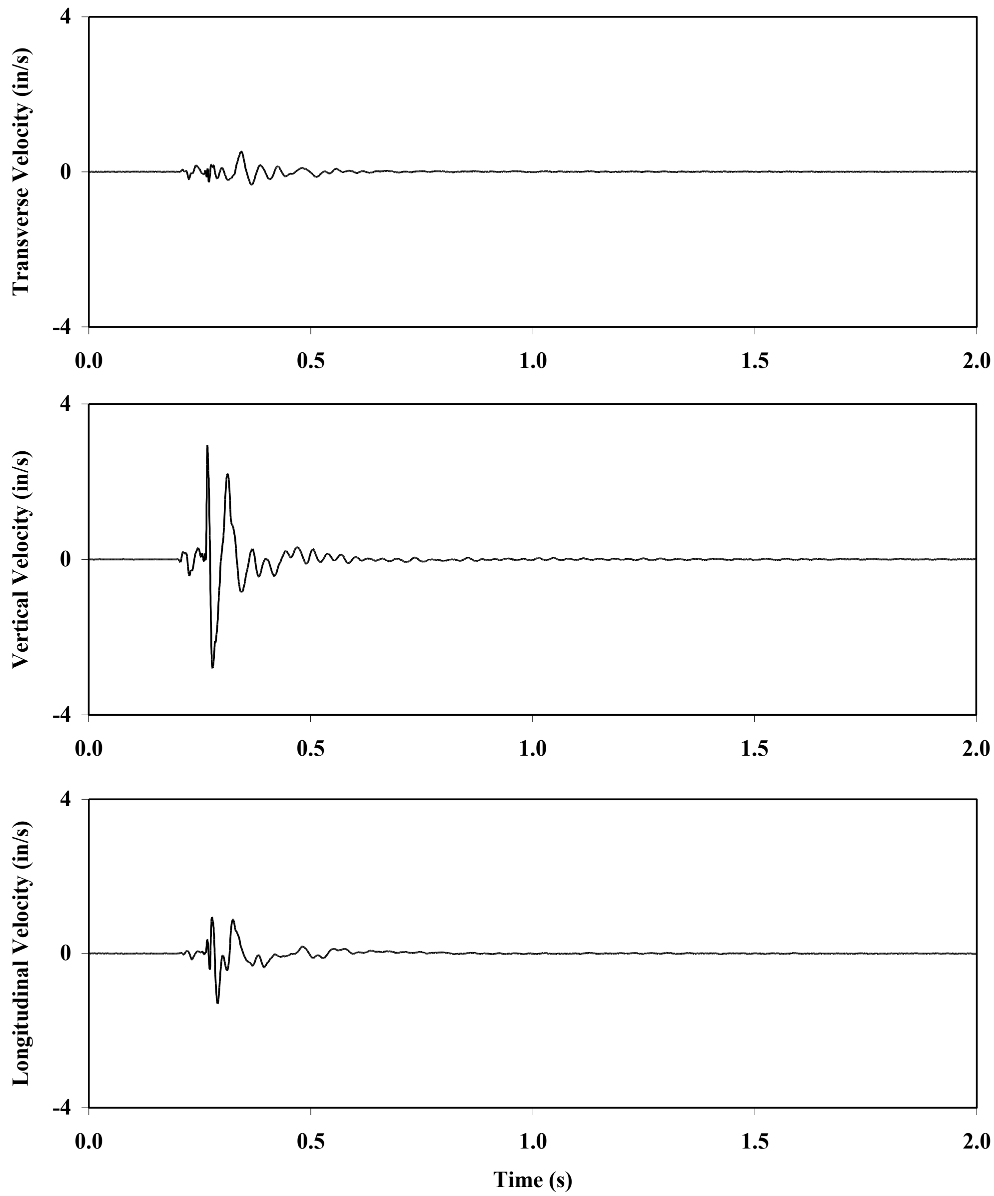

Streambed vibrations recorded during shot D20

Straight Distance (ft)	Scaled Distance (ft/lbs$^{1/2}$)	Transverse PPV (in/s)	FFT Freq. (Hz)	Vertical PPV (in/s)	FFT Freq. (Hz)	Long. PPV (in/s)	FFT Freq. (Hz)
65	2.4	0.53	22.0	2.94	16.5	1.30	13.3

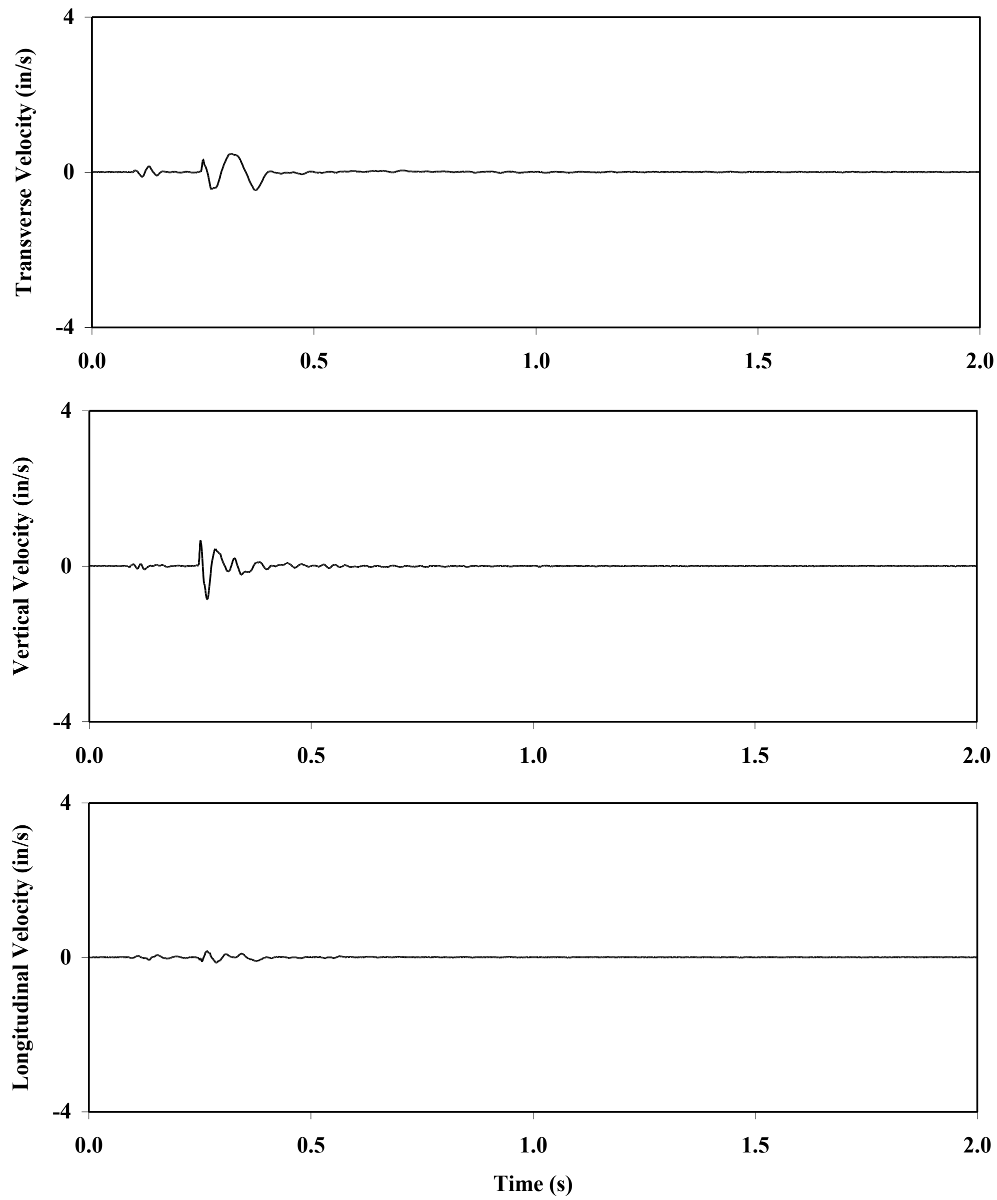

Streambed vibrations recorded during shot D20

Straight Distance (ft)	Scaled Distance (ft/lbs$^{1/2}$)	Transverse PPV (in/s)	FFT Freq. (Hz)	Vertical PPV (in/s)	FFT Freq. (Hz)	Long. PPV (in/s)	FFT Freq. (Hz)
110	4.0	0.47	10.5	0.85	22.0	0.17	25.5

APPENDIX 13 SITE D21 LOG CULVERT. Site diagram and setup information, hydrophone and geophone time histories

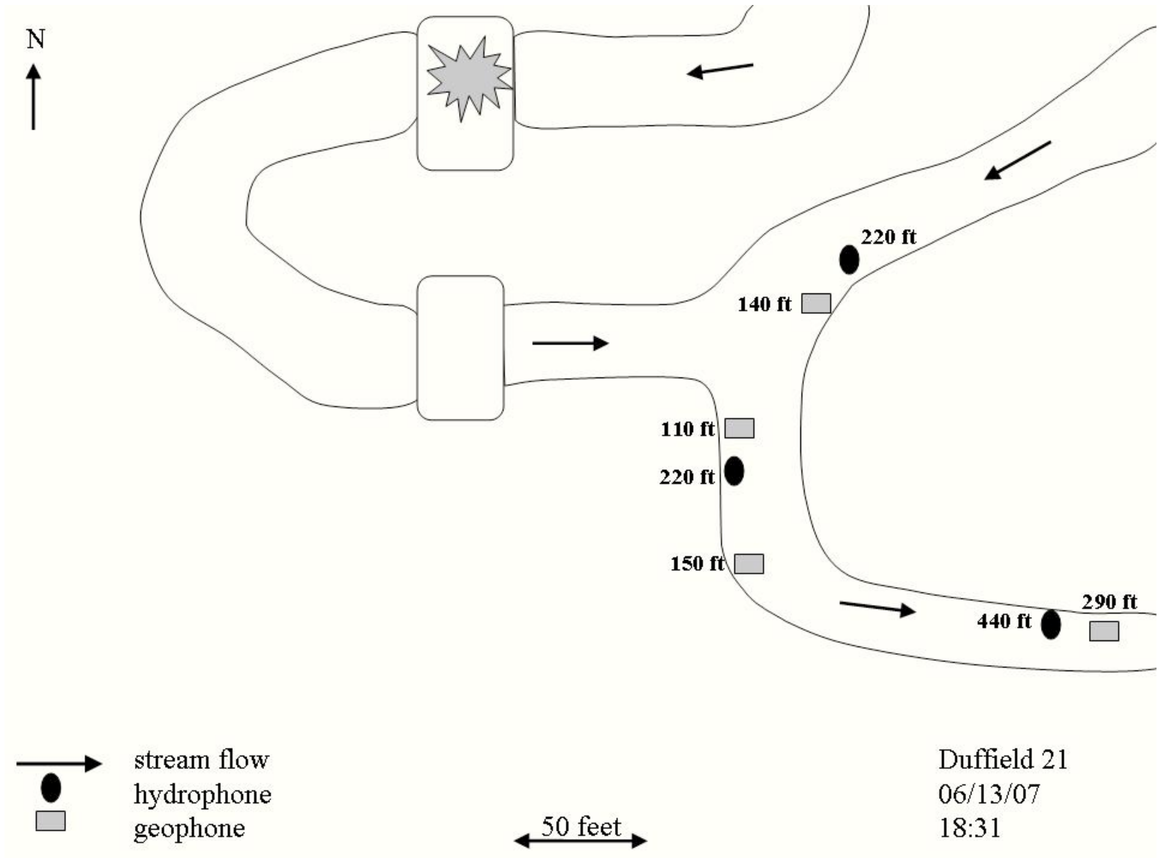

Structure, site, and shot information recorded during shot D21

Span / Length (ft)	Stringer Diameter (ft)	Between Sill Logs (ft)	Sill Log Diameter (ft)	Road Width (ft)	Fill Depth (ft)	Stream Grade (%)	Substrate Type
45	4.0	33.0	4.5	25	1.5	4-5	gravel

detcord (150 gr.) (ft)	ANFO (lbs)	Emulsion (lbs)	Total # / Delay (lbs)	TNT Equivalent (lbs)	Coupling level
290	0	1431	1437	895	coupled

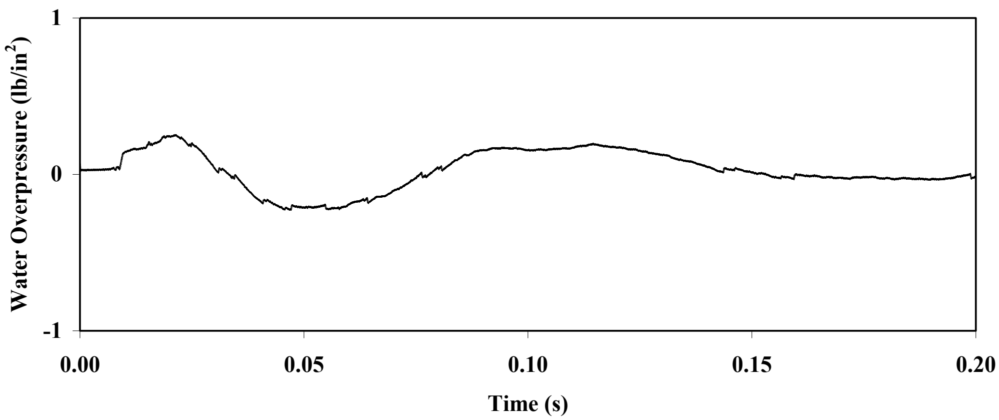

Stream pressures recorded during shot D21

Straight Distance (ft)	Scaled Distance ($ft/lbs^{1/3}$)	Positive Peak (lb/in^2)	Negative Peak (lb/in^2)	FFT Freq. (Hz)
440	45.7	0.25	-0.22	8.5

APPENDIX 14 SITE D22-1 LOG BRIDGE. Site diagram and setup information, hydrophone and geophone time histories

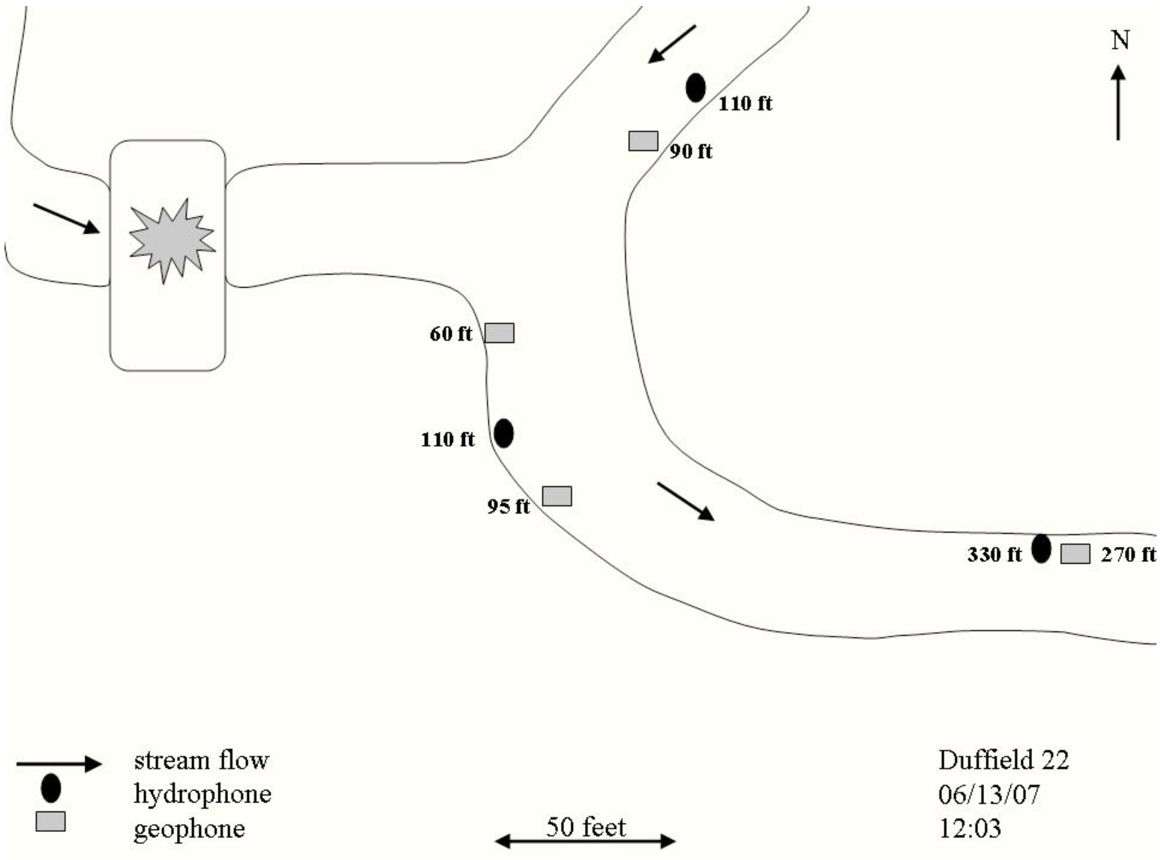

Structure, site, and shot information recorded during shot D22-1

Span / Length (ft)	Stringer Diameter (ft)	Between Sill Logs (ft)	Sill Log Diameter (ft)	Road Width (ft)	Fill Depth (ft)	Stream Grade (%)	Substrate Type
43	2.0	28.0	3.0	25	0.0	3-5	gravel

detcord (150 gr.) (ft)	ANFO (lbs)	Emulsion (lbs)	Total # / Delay (lbs)	TNT Equivalent (lbs)	Coupling level
0	0	218.6	219	136	de-coupled

(21.0 SD)

(63.1 SD)

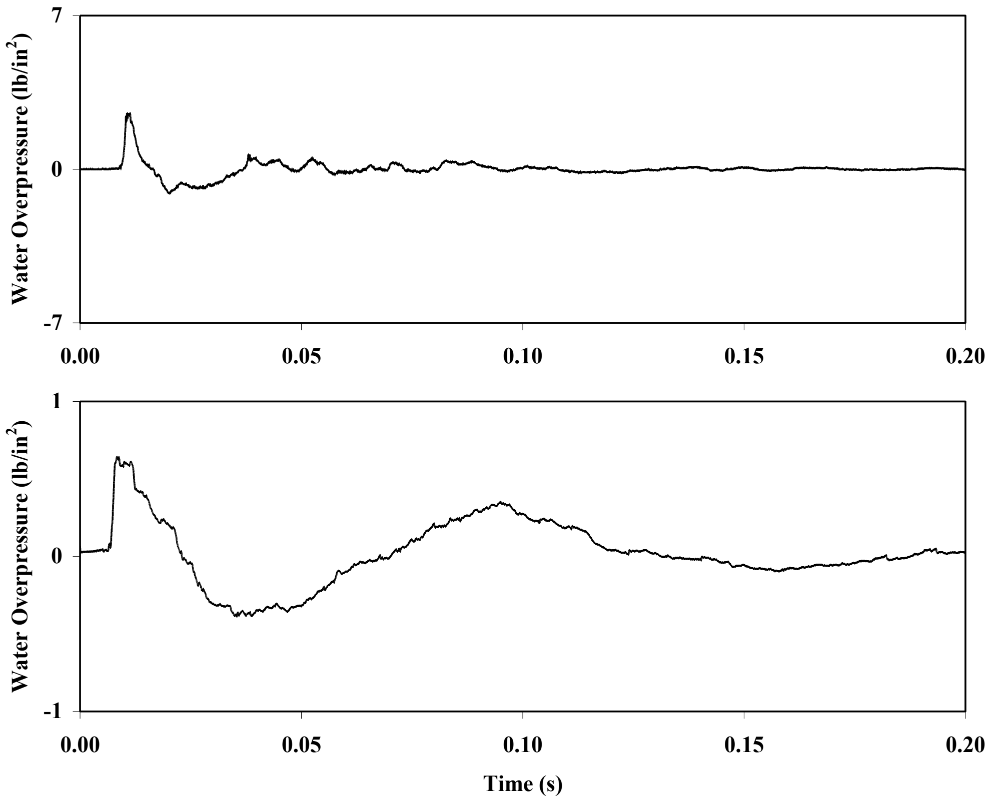

Stream pressures recorded during shot D22-1

Straight Distance (ft)	Scaled Distance ($ft/lbs^{1/3}$)	Positive Peak (lb/in^2)	Negative Peak (lb/in^2)	FFT Freq. (Hz)
110	21.0	2.56	-1.11	24.5
330	63.1	0.64	-0.39	10.5

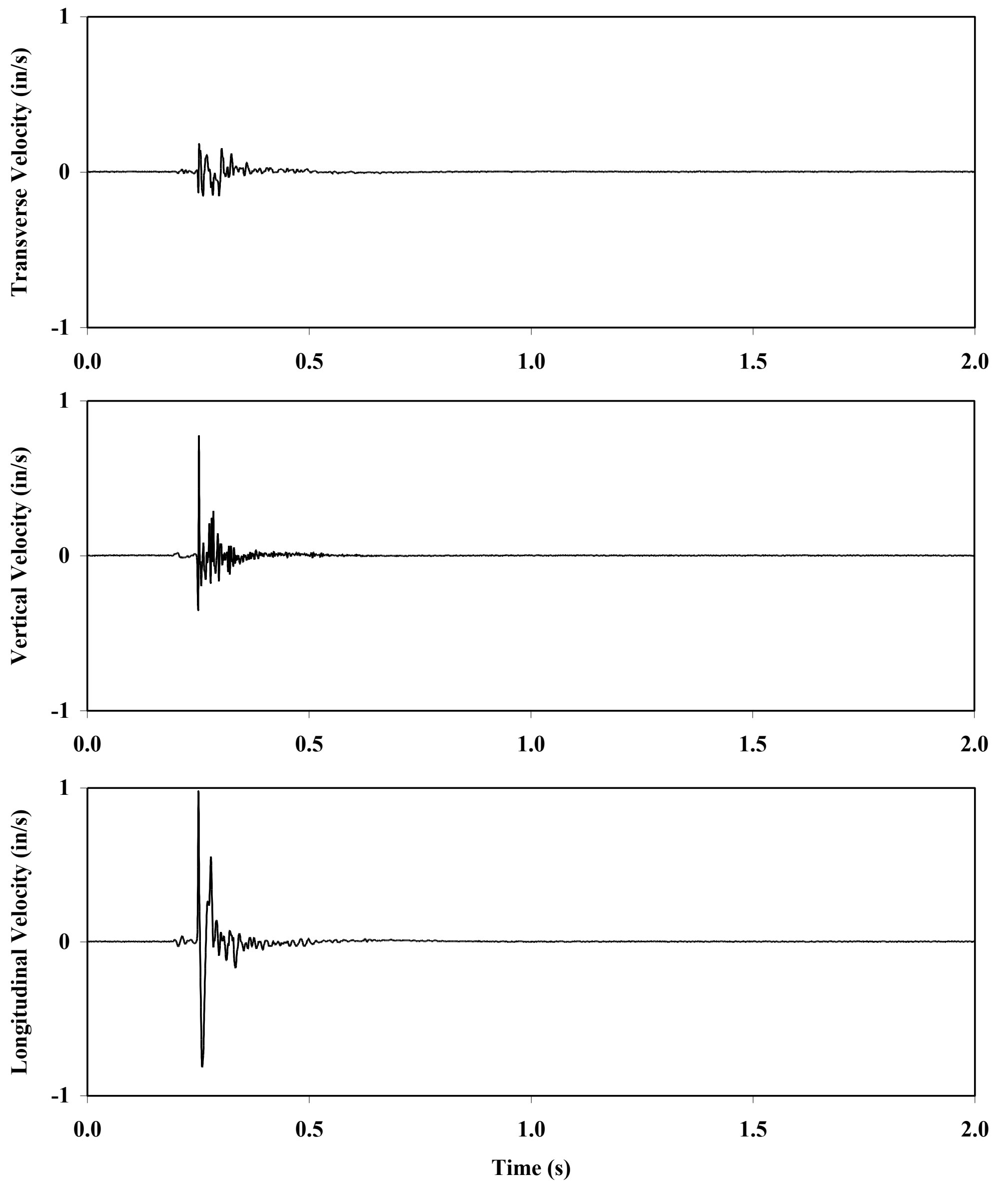

Streambed vibrations recorded during shot D22-1

Straight Distance (ft)	Scaled Distance (ft/lbs$^{1/2}$)	Transverse PPV (in/s)	FFT Freq. (Hz)	Vertical PPV (in/s)	FFT Freq. (Hz)	Long. PPV (in/s)	FFT Freq. (Hz)
90	7.5	0.18	55.5	0.77	99.8	0.97	40.0

APPENDIX 15 SITE D22-2 LOG BRIDGE. Site diagram and setup information, hydrophone and geophone time histories

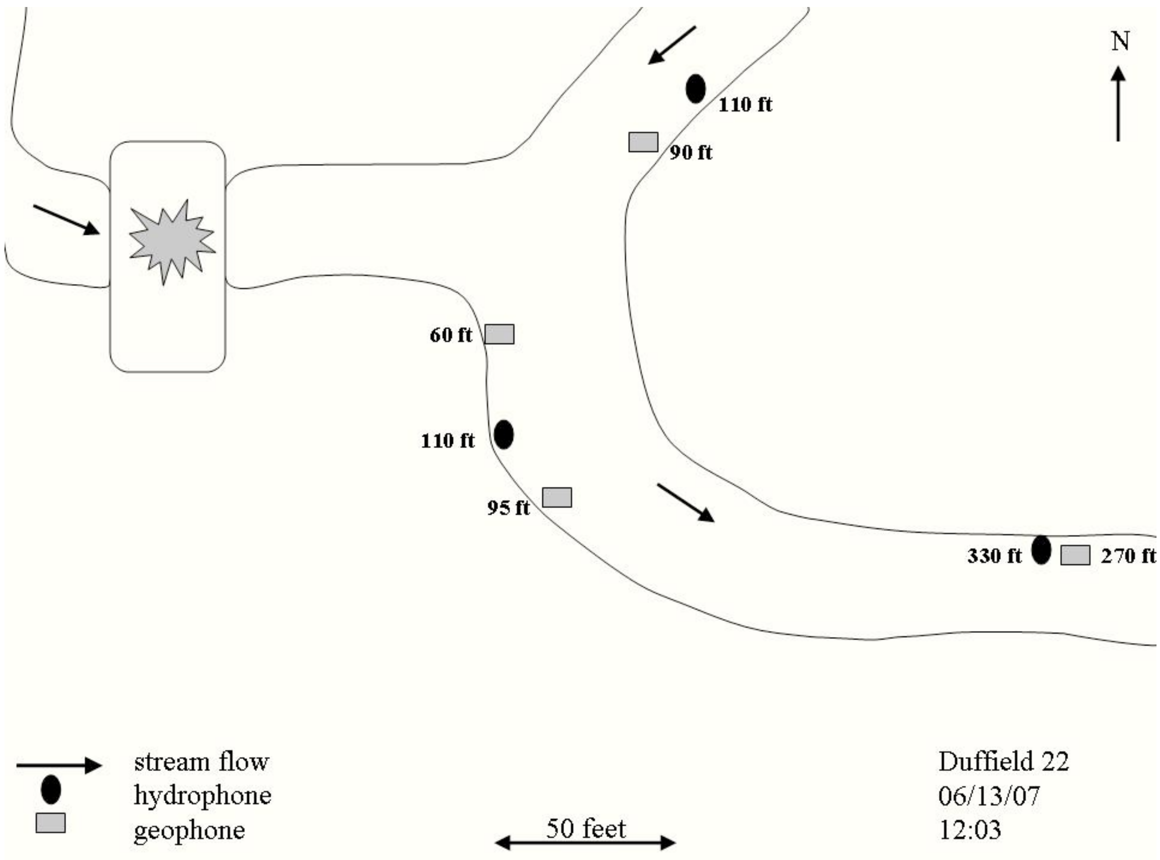

Structure, site, and shot information recorded during shot D22-2

Span / Length (ft)	Stringer Diameter (ft)	Between Sill Logs (ft)	Sill Log Diameter (ft)	Road Width (ft)	Fill Depth (ft)	Stream Grade (%)	Substrate Type
43	2.0	28.0	3.0	25	0.0	3-5	gravel

detcord (150 gr.) (ft)	ANFO (lbs)	Emulsion (lbs)	Total # / Delay (lbs)	TNT Equivalent (lbs)	Coupling level
0	0	231	231	143	de-coupled

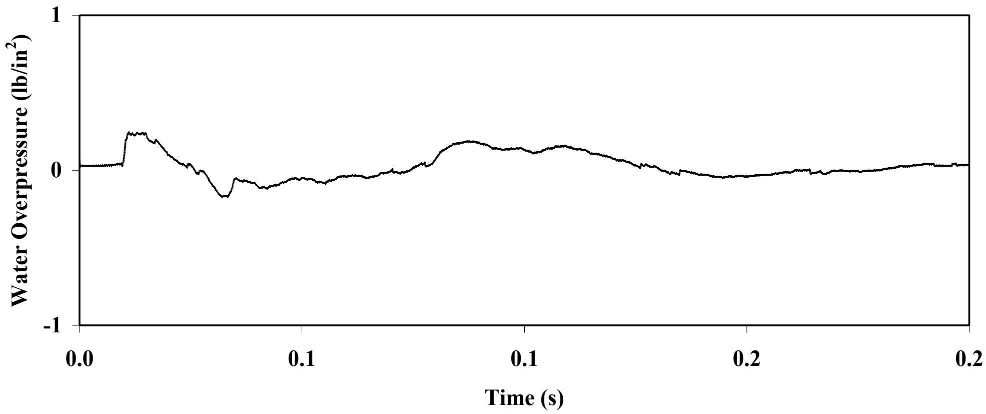

Stream pressures recorded during shot .D22-2

Straight Distance (ft)	Scaled Distance (ft/lbs$^{1/3}$)	Positive Peak (lb/in^2)	Negative Peak (lb/in^2)	FFT Freq. (Hz)
330.0	64.2	0.24	-0.17	10.0

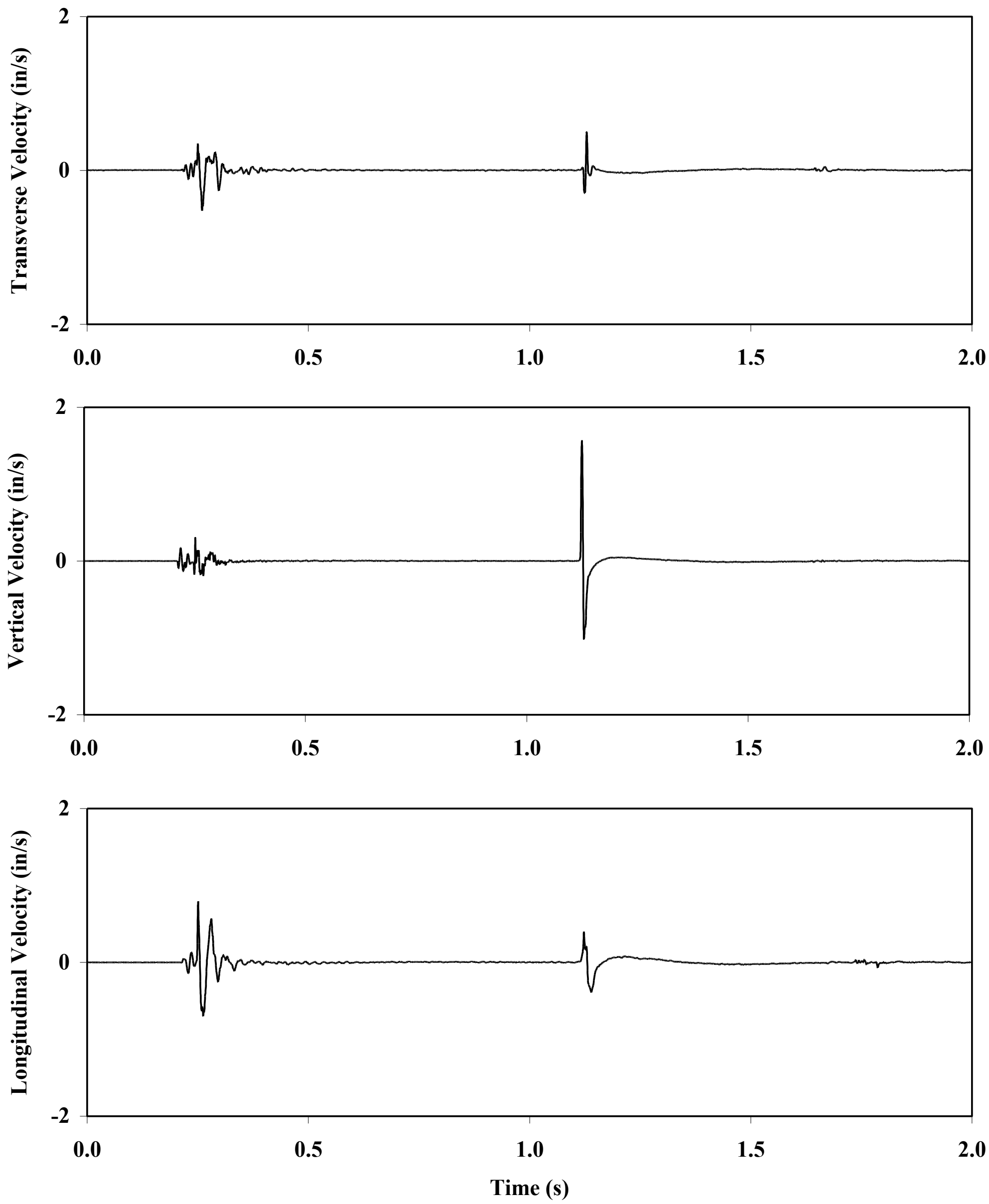

Streambed vibrations recorded during shot D22-2

Straight Distance (ft)	Scaled Distance (ft/lbs$^{1/2}$)	Transverse PPV (in/s)	FFT Freq. (Hz)	Vertical PPV (in/s)	FFT Freq. (Hz)	Long. PPV (in/s)	FFT Freq. (Hz)
60	5.1	0.53	56.0	1.56	53.3	0.80	31.0

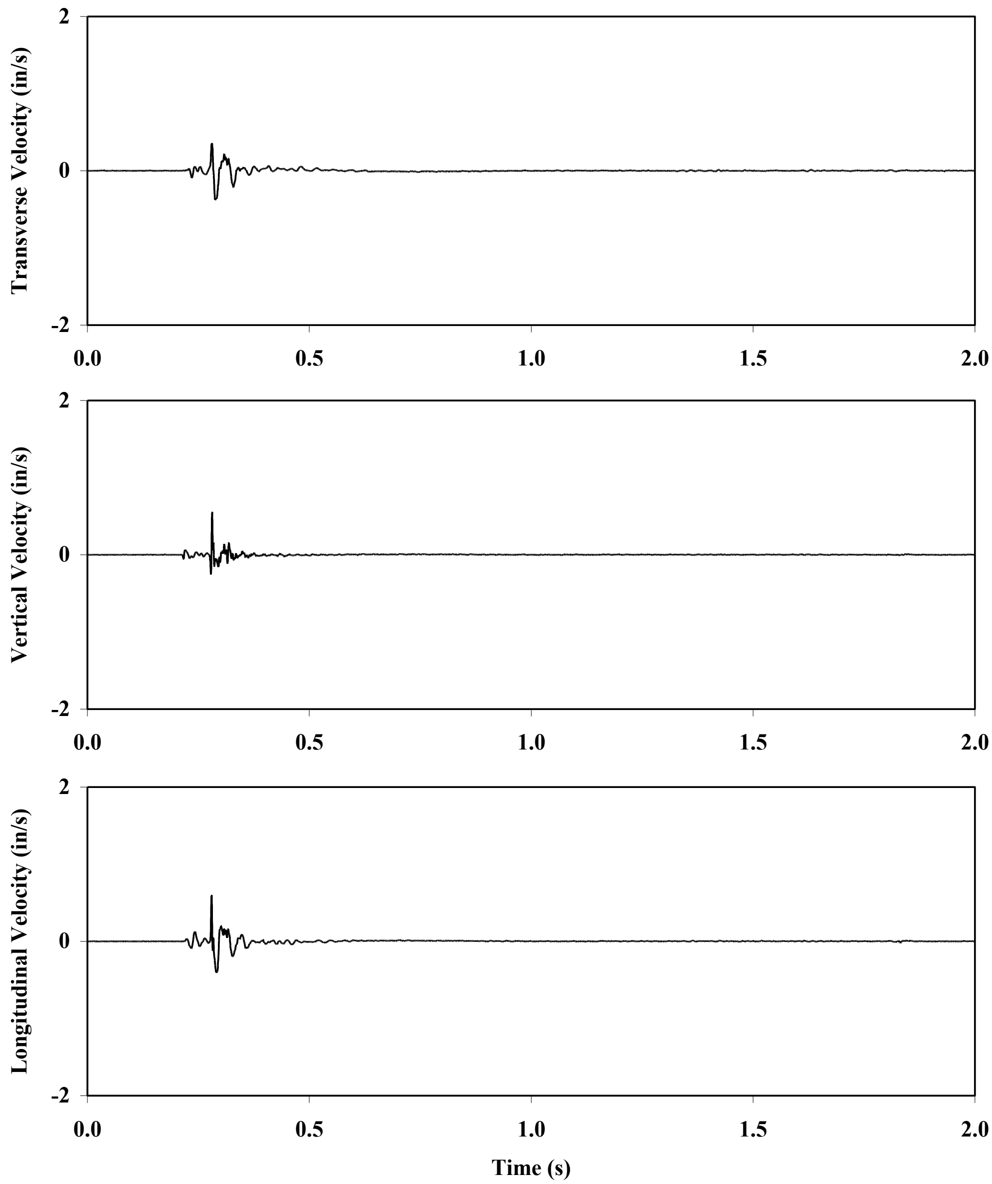

Streambed vibrations recorded during shot D22-2

Straight Distance (ft)	Scaled Distance (ft/lbs$^{1/2}$)	Transverse PPV (in/s)	FFT Freq. (Hz)	Vertical PPV (in/s)	FFT Freq. (Hz)	Long. PPV (in/s)	FFT Freq. (Hz)
95	8.1	0.38	29.0	0.55	32.3	0.59	29.3

APPENDIX 16 SITE F13 LOG BRIDGE. Site diagram and setup information, hydrophone and geophone time histories

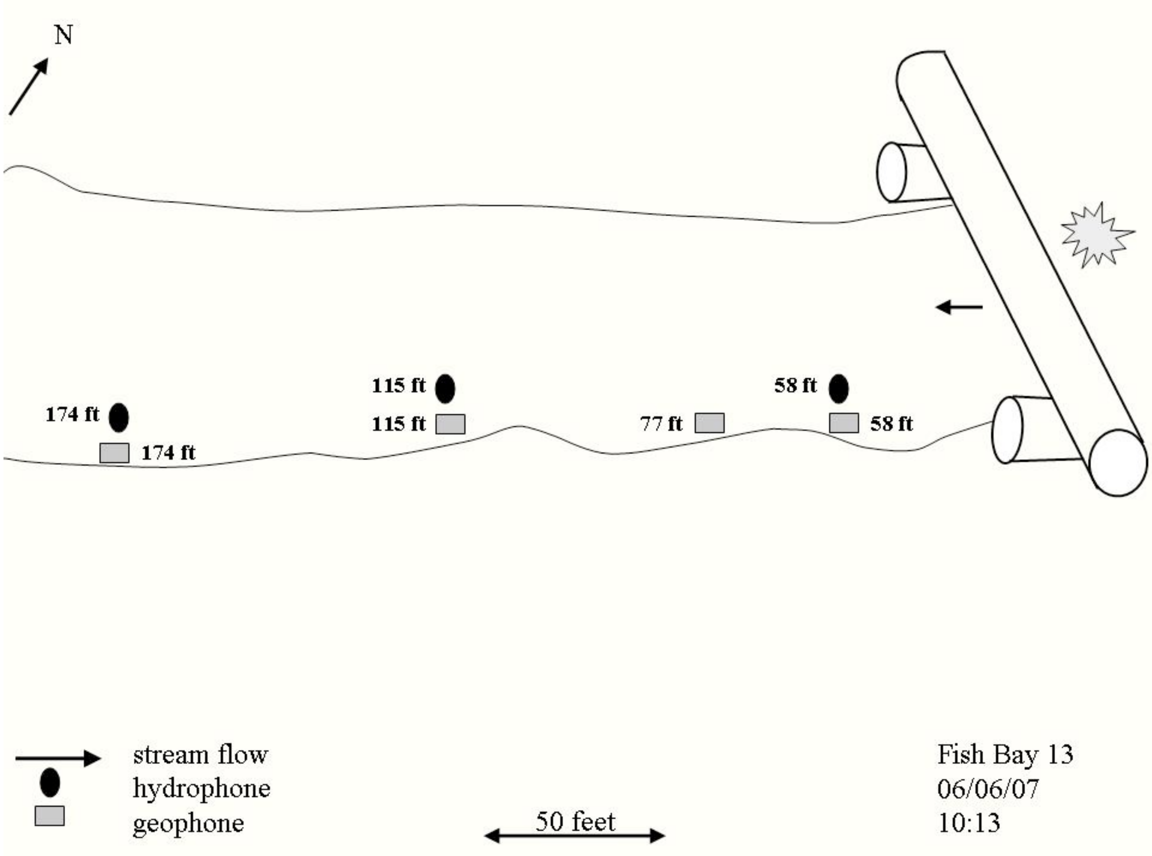

Structure, site, and shot information recorded during shot F13

Span / Length (ft)	Stringer Diameter (ft)	Between Sill Logs (ft)	Sill Log Diameter (ft)	Road Width (ft)	Fill Depth (ft)	Stream Grade (%)	Substrate Type
33	2.5	10.2	2.8	26	1.5	1	gravel

detcord (150 gr.) (ft)	ANFO (lbs)	Emulsion (lbs)	Total # / Delay (lbs)	TNT Equivalent (lbs)	Coupling level
380	495	190	693	534	coupled

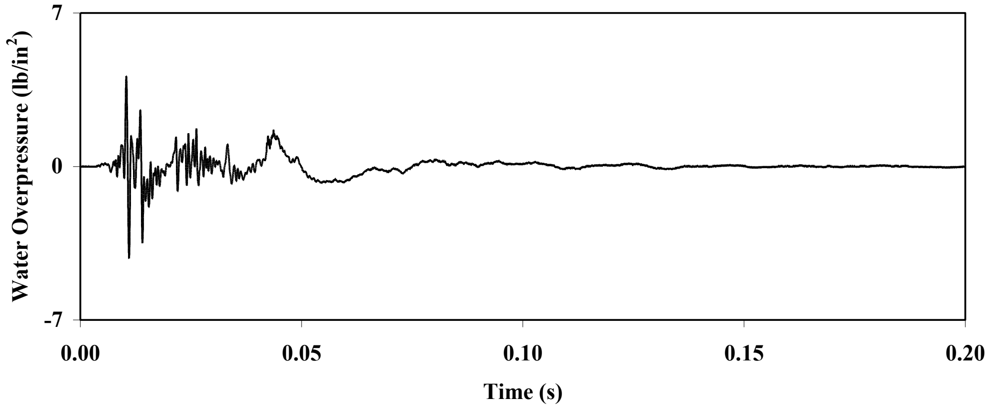

Stream pressures recorded during shot F13

Straight Distance (ft)	Scaled Distance (ft/lbs$^{1/3}$)	Positive Peak (lb/in^2)	Negative Peak (lb/in^2)	FFT Freq. (Hz)
58	7.1	4.12	-4.19	51.0

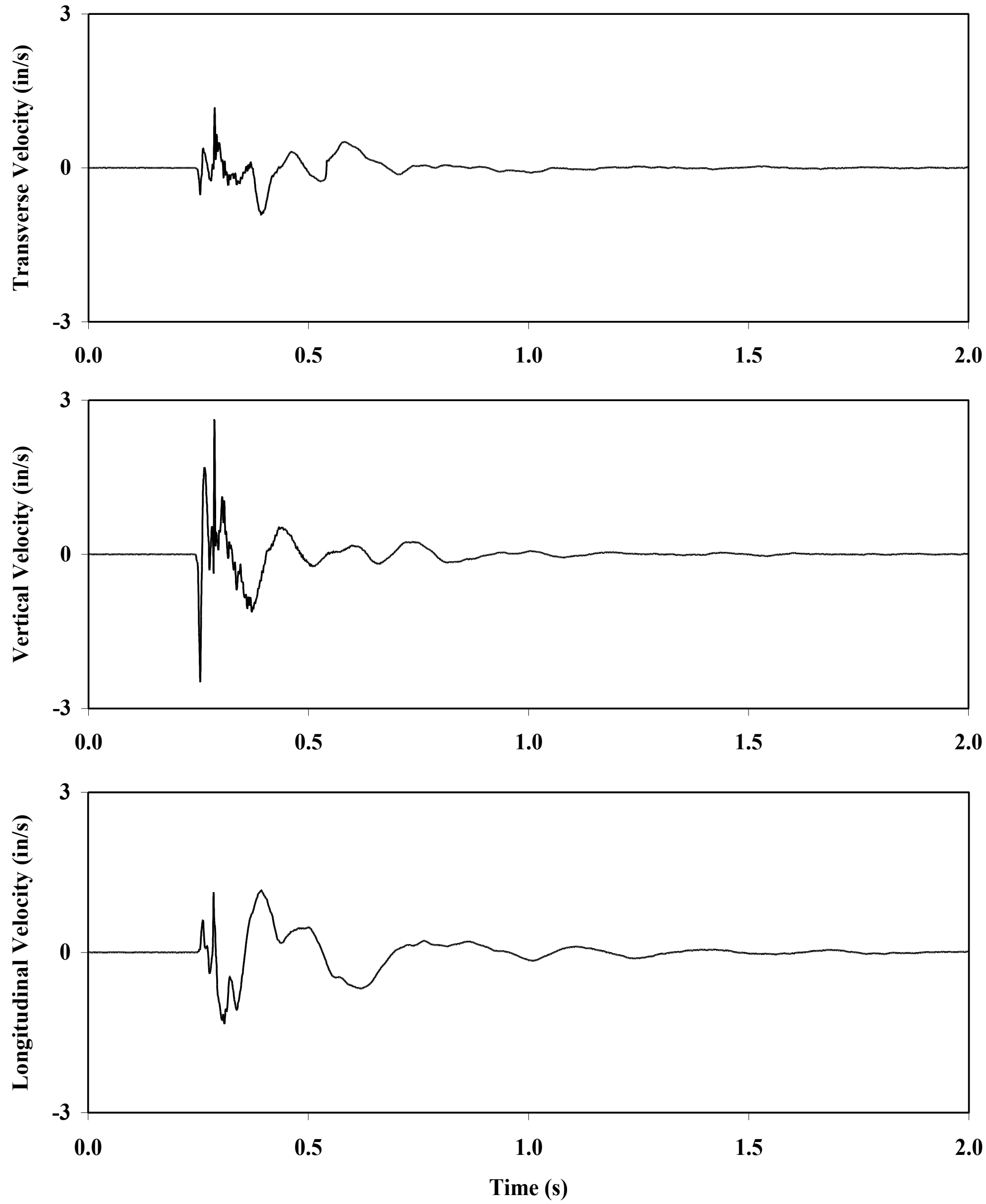

Streambed vibrations recorded during shot F13

Straight Distance (ft)	Scaled Distance (ft/lbs$^{1/2}$)	Transverse PPV (in/s)	FFT Freq. (Hz)	Vertical PPV (in/s)	FFT Freq. (Hz)	Long. PPV (in/s)	FFT Freq. (Hz)
58	2.5	1.16	6.8	2.58	7.0	1.34	3.3

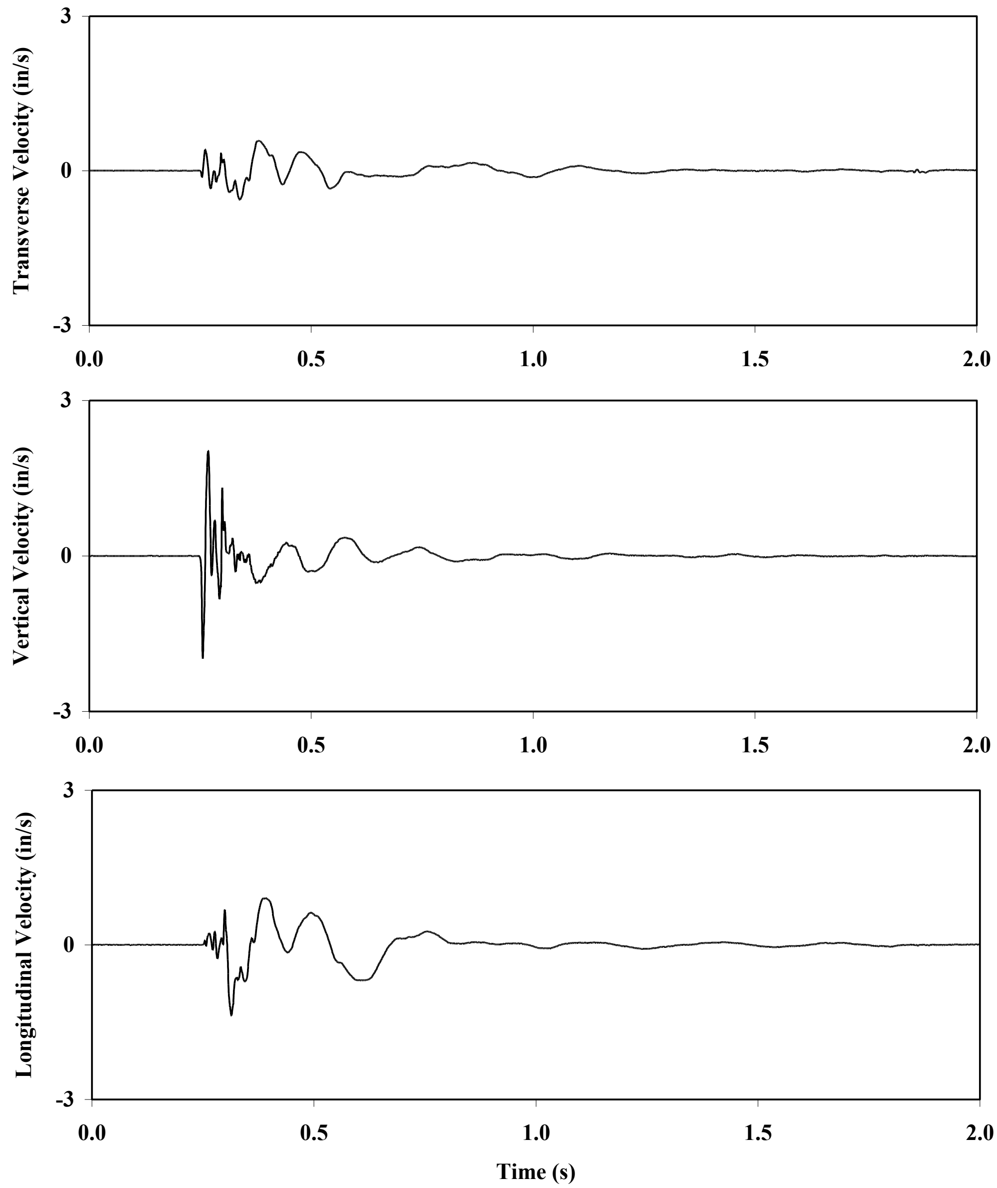

Streambed vibrations recorded during shot F13

Straight Distance (ft)	Scaled Distance (ft/lbs$^{1/2}$)	Transverse PPV (in/s)	FFT Freq. (Hz)	Vertical PPV (in/s)	FFT Freq. (Hz)	Long. PPV (in/s)	FFT Freq. (Hz)
77	3.3	0.59	3.0	2.03	7.0	1.37	3.5

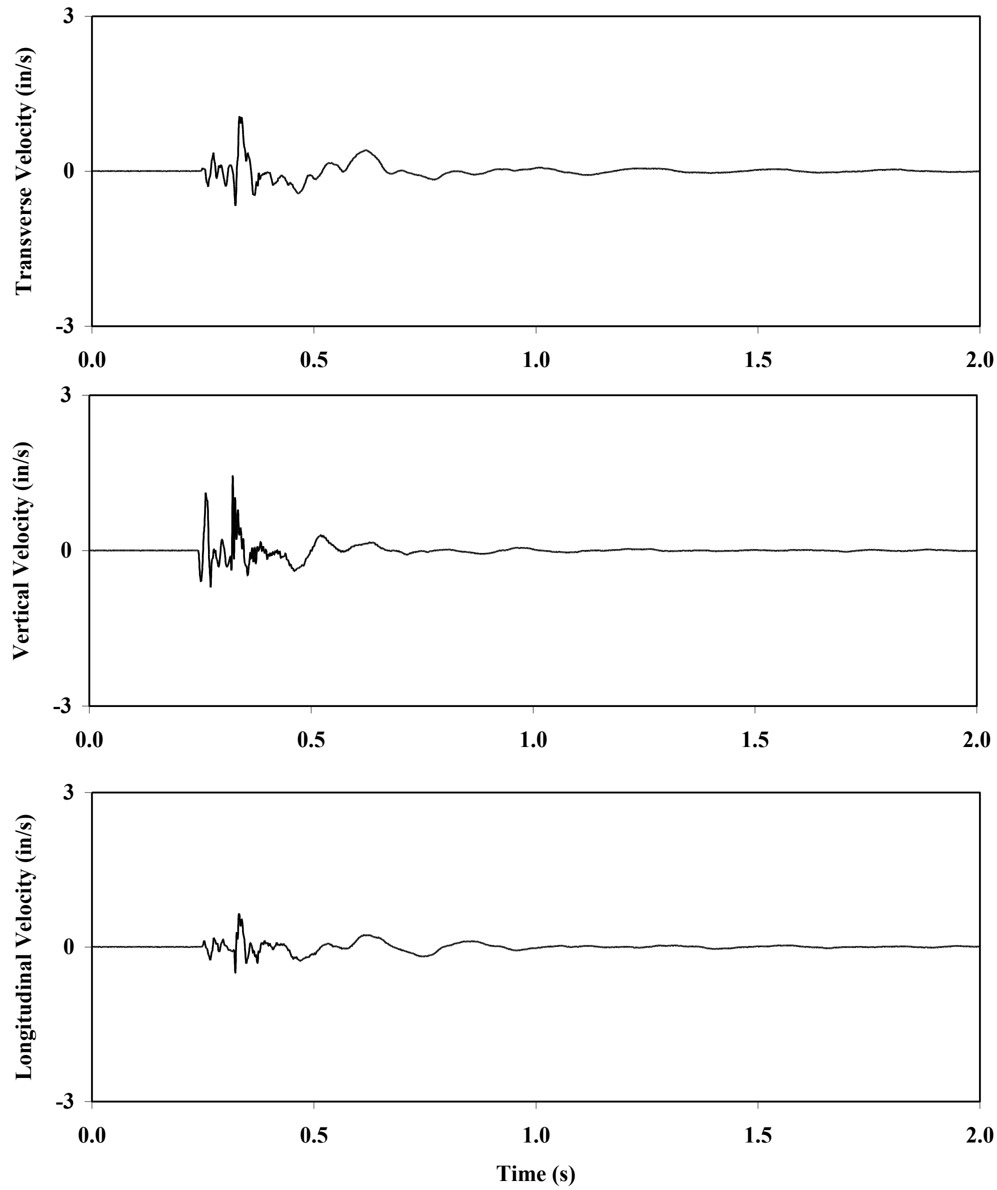

Streambed vibrations recorded during shot F13

Straight Distance (ft)	Scaled Distance ($ft/lbs^{1/2}$)	Transverse PPV (in/s)	FFT Freq. (Hz)	Vertical PPV (in/s)	FFT Freq. (Hz)	Long. PPV (in/s)	FFT Freq. (Hz)
115	5.0	1.05	3.5	1.43	3.5	0.66	4.5

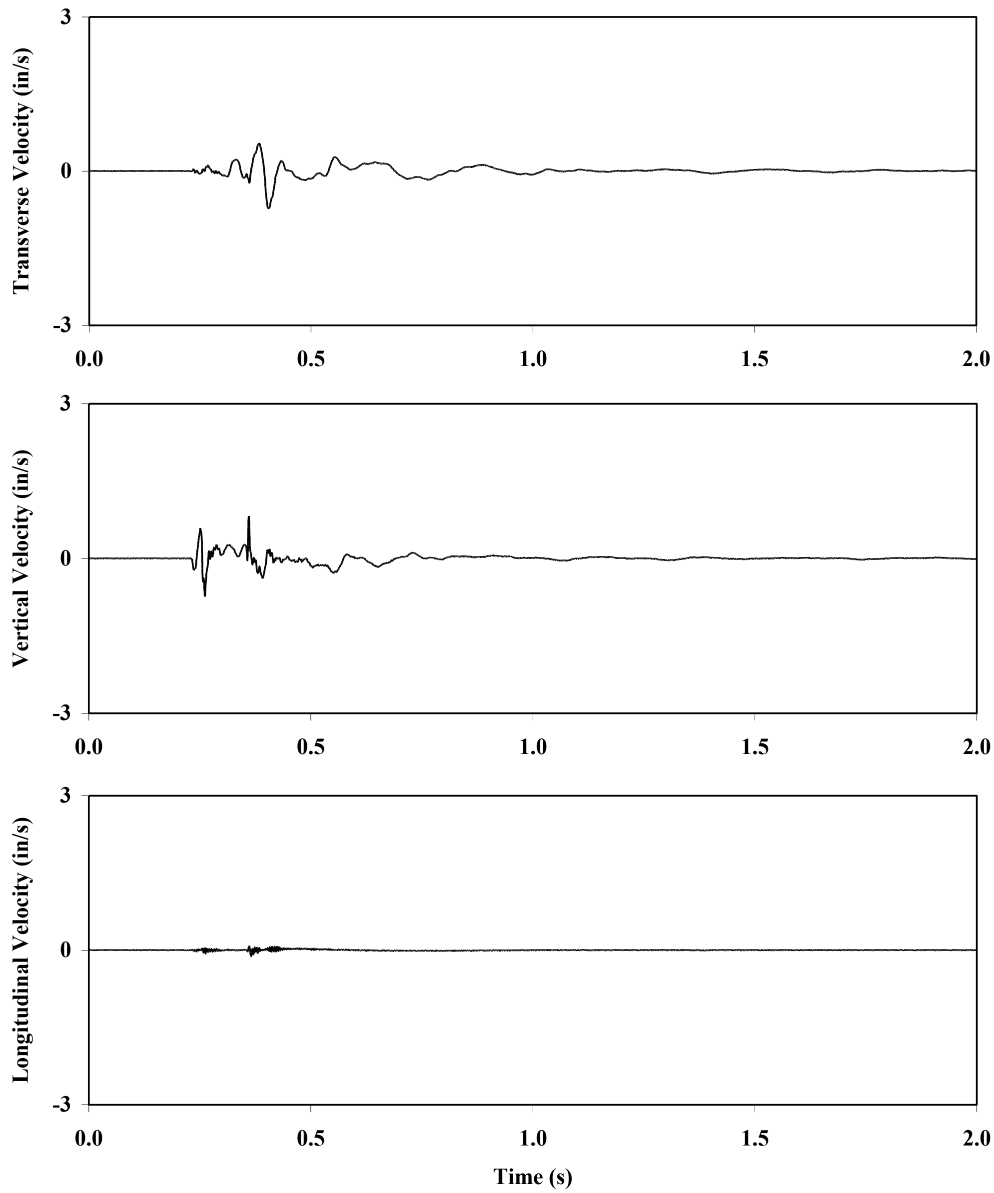

Streambed vibrations recorded during shot F13

Straight Distance (ft)	Scaled Distance (ft/lbs$^{1/2}$)	Transverse PPV (in/s)	FFT Freq. (Hz)	Vertical PPV (in/s)	FFT Freq. (Hz)	Long. PPV (in/s)	FFT Freq. (Hz)
174	7.5	0.73	3.5	0.83	7.5	0.12	1.5

APPENDIX 17 SITE F14 LOG BRIDGE. Site diagram and setup information, hydrophone and geophone time histories

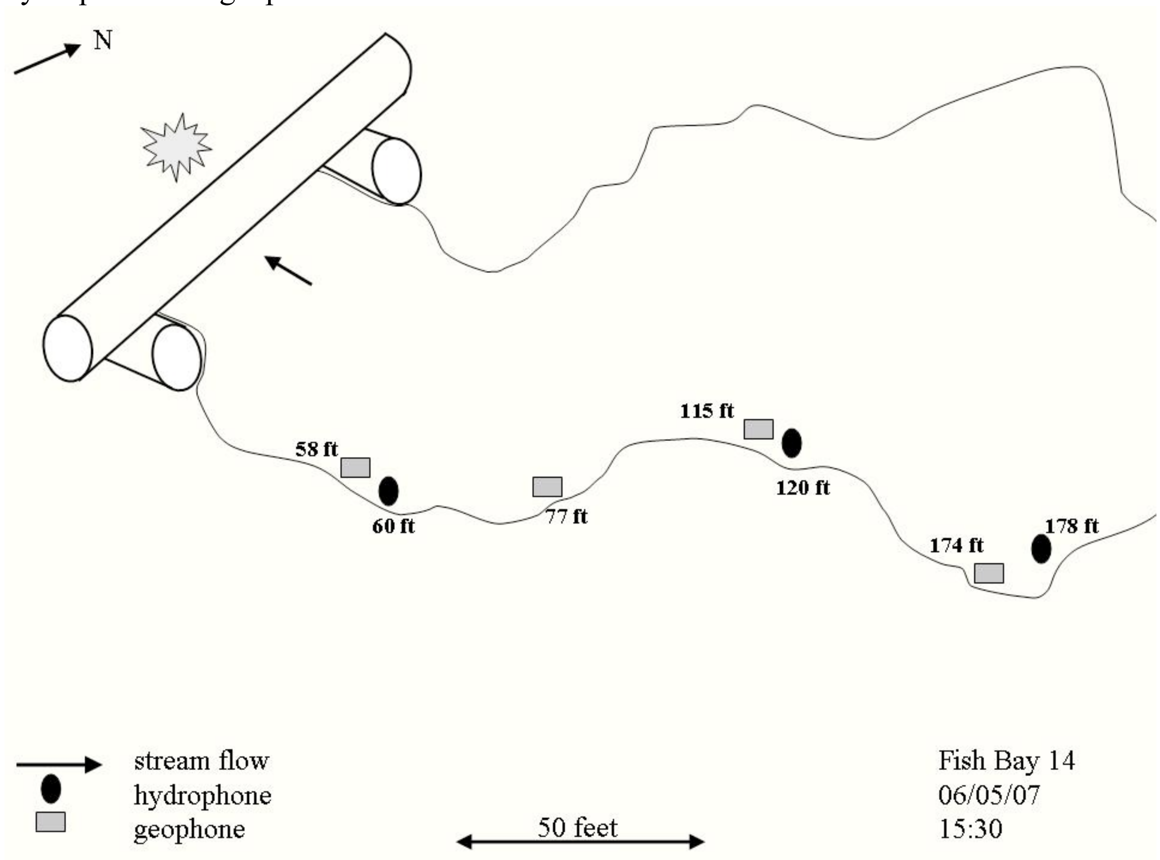

Structure, site, and shot information recorded during shot F14

Span / Length (ft)	Stringer Diameter (ft)	Between Sill Logs (ft)	Sill Log Diameter (ft)	Road Width (ft)	Fill Depth (ft)	Stream Grade (%)	Substrate Type
26	2.0	23.5	1.7	21	0.6	1	gravel

detcord (150 gr.) (ft)	ANFO (lbs)	Emulsion (lbs)	Total # / Delay (lbs)	TNT Equivalent (lbs)	Coupling level
250	495	200	700	537	coupled

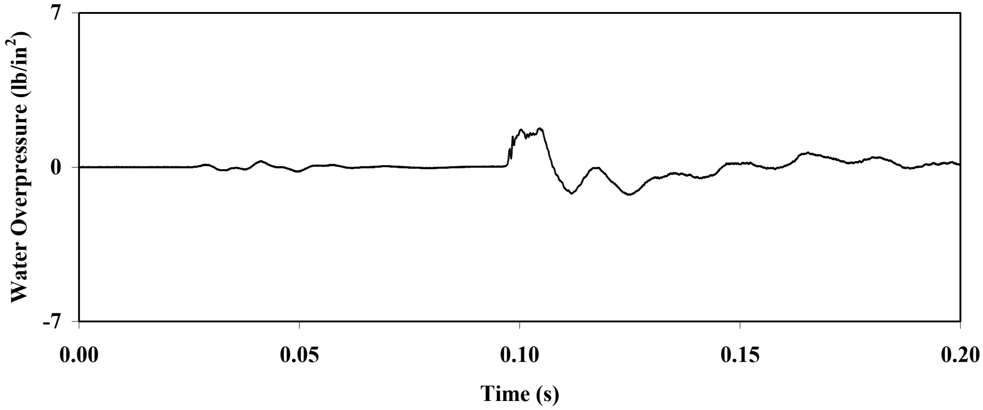

Stream pressures recorded during shot F14

Straight Distance (ft)	Scaled Distance (ft/lbs$^{1/3}$)	Positive Peak (lb/in^2)	Negative Peak (lb/in^2)	FFT Freq. (Hz)
120	14.8	1.78	-1.28	13.0

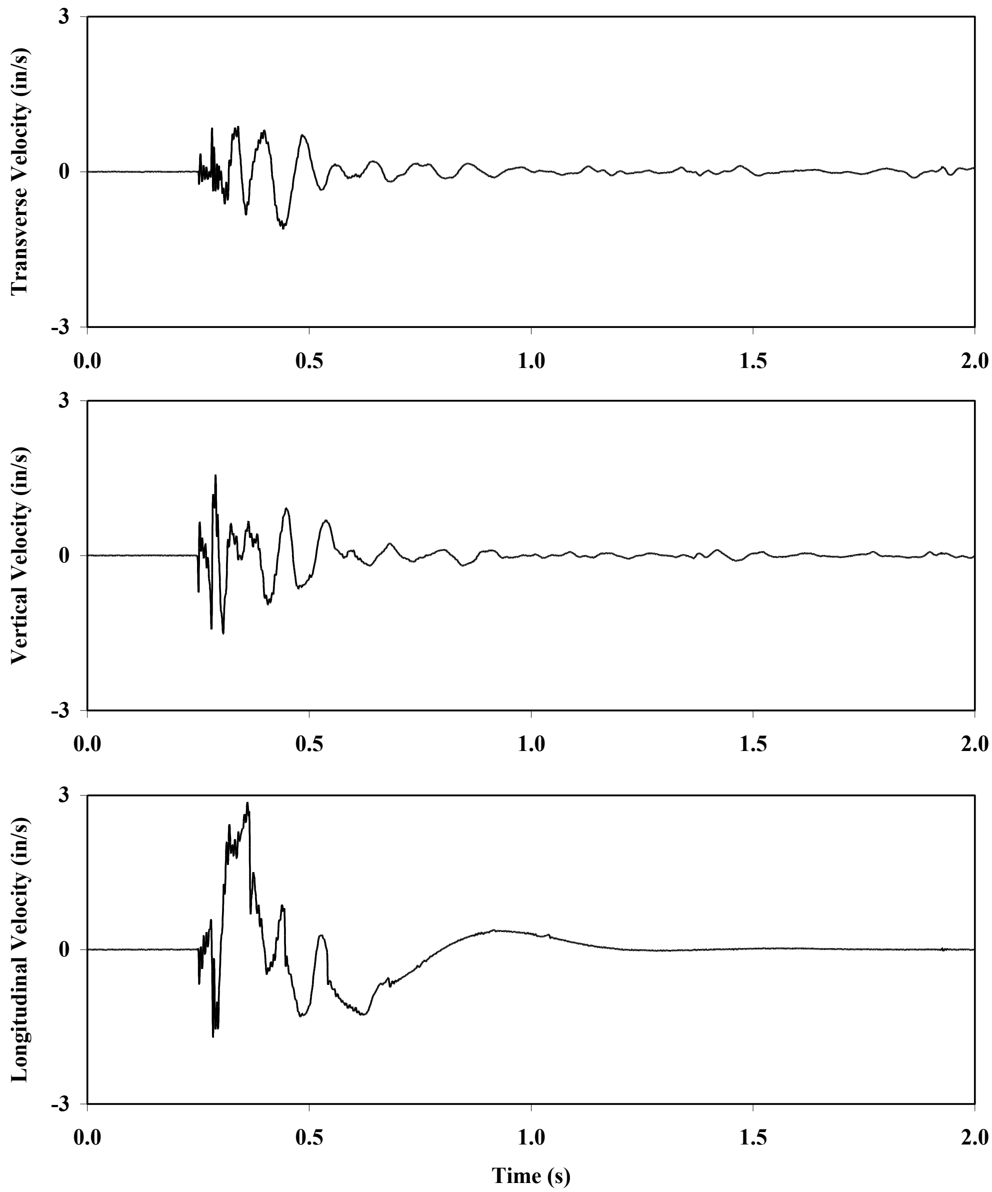

Streambed vibrations recorded during shot F14

Straight Distance (ft)	Scaled Distance (ft/lbs$^{1/2}$)	Transverse PPV (in/s)	FFT Freq. (Hz)	Vertical PPV (in/s)	FFT Freq. (Hz)	Long. PPV (in/s)	FFT Freq. (Hz)
58	2.5	1.11	13.0	1.57	11.5	2.87	1.8

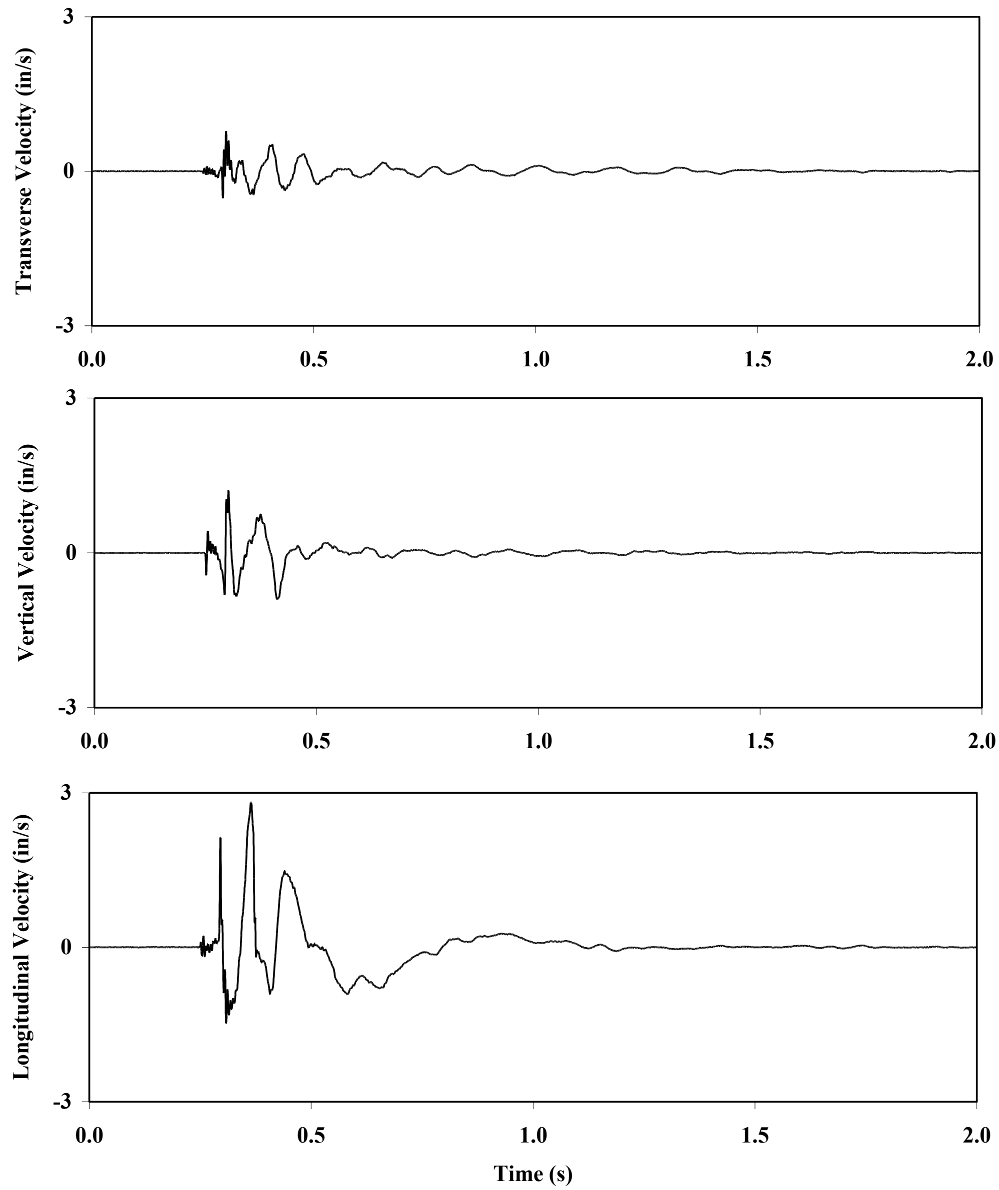

Streambed vibrations recorded during shot F14

Straight Distance (ft)	Scaled Distance ($ft/lbs^{1/2}$)	Transverse PPV (in/s)	FFT Freq. (Hz)	Vertical PPV (in/s)	FFT Freq. (Hz)	Long. PPV (in/s)	FFT Freq. (Hz)
77	3.3	0.78	13.3	1.20	11.8	2.81	2.0

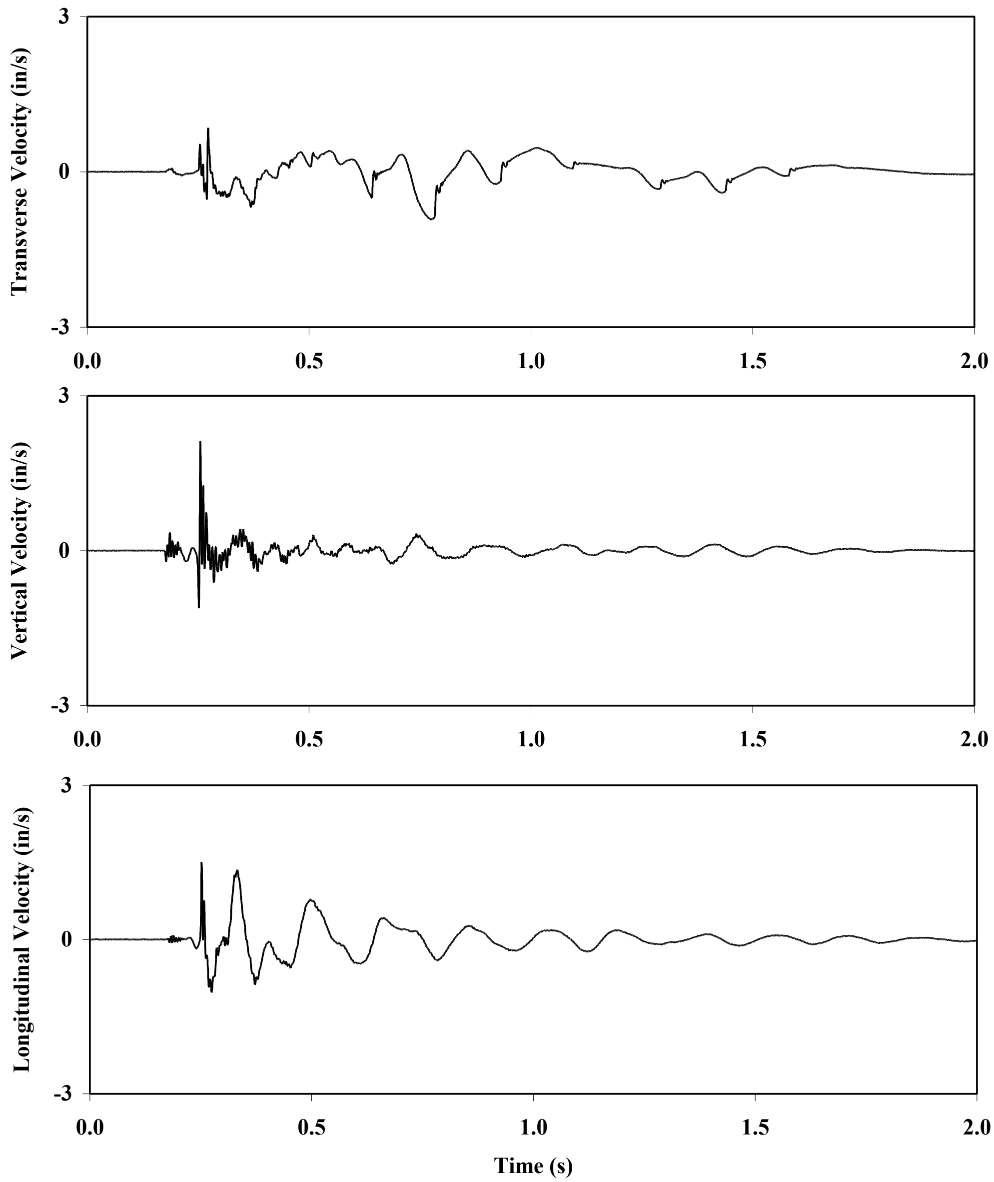

Streambed vibrations recorded during shot F14

Straight Distance (ft)	Scaled Distance (ft/lbs$^{1/2}$)	Transverse PPV (in/s)	FFT Freq. (Hz)	Vertical PPV (in/s)	FFT Freq. (Hz)	Long. PPV (in/s)	FFT Freq. (Hz)
115	5.0	0.93	2.0	2.10	6.3	1.49	6.0

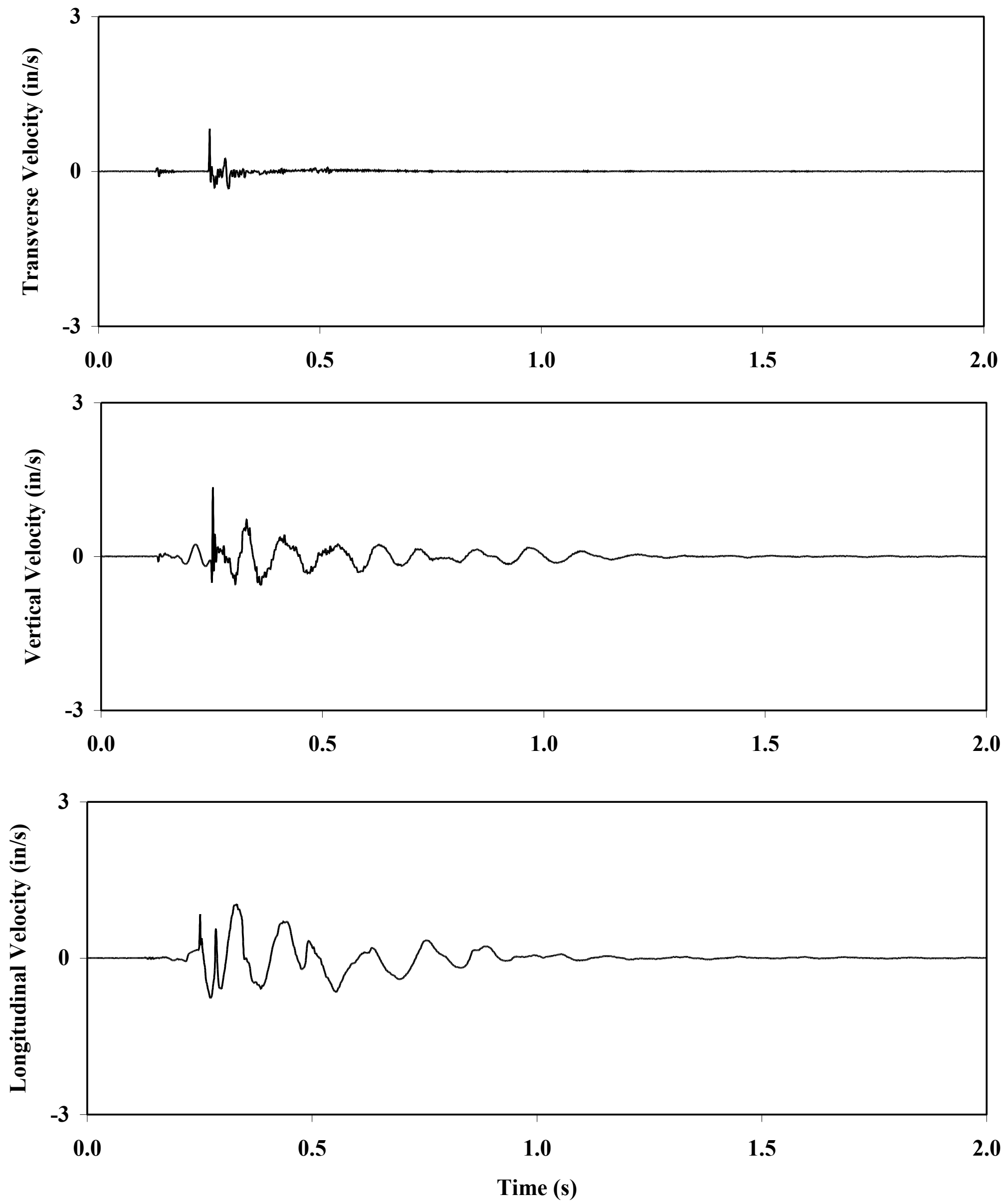

Streambed vibrations recorded during shot F14

Straight Distance (ft)	Scaled Distance ($ft/lbs^{1/2}$)	Transverse PPV (in/s)	FFT Freq. (Hz)	Vertical PPV (in/s)	FFT Freq. (Hz)	Long. PPV (in/s)	FFT Freq. (Hz)
174	7.5	0.83	2.0	1.33	9.3	1.04	7.3

APPENDIX 18 SITE F16 CORRUGATED METAL PIPE. Site diagram and setup information, hydrophone and geophone time histories

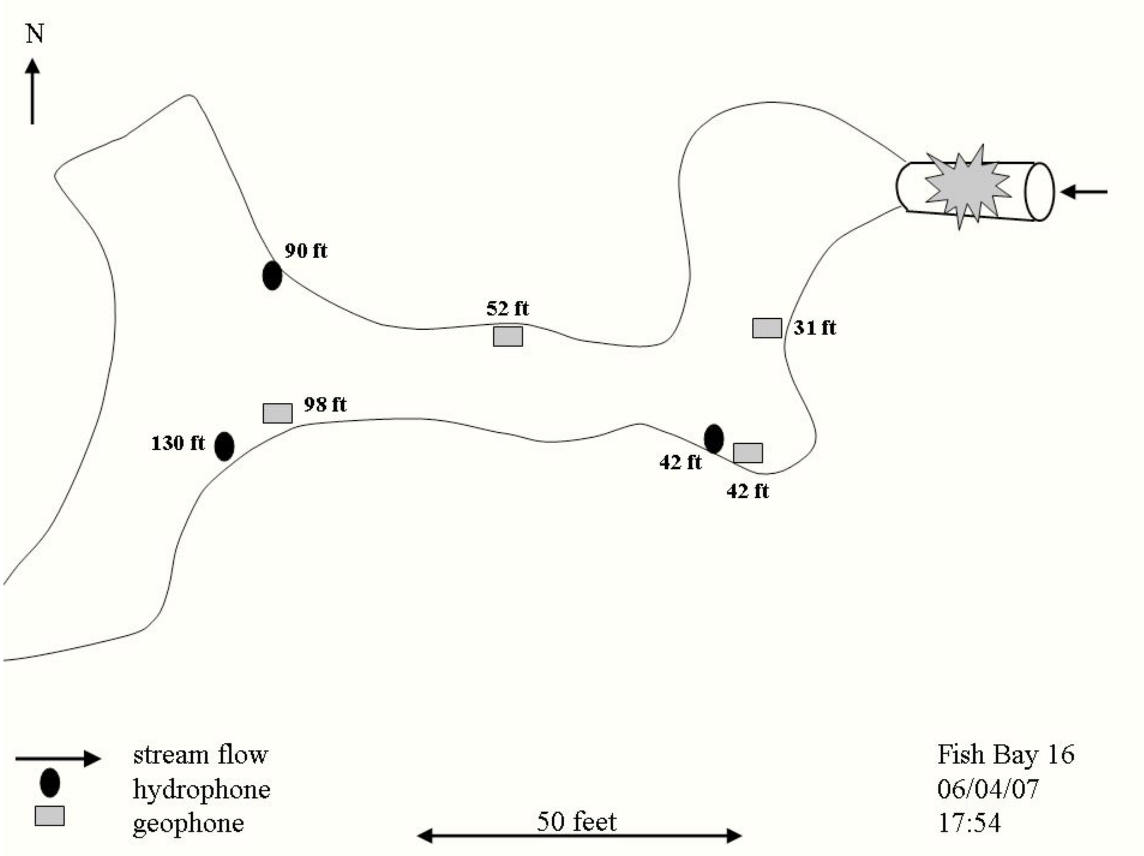

Structure, site, and shot information recorded during shot F16

Culvert Diameter	Culvert Length	Road Width	Fill Depth	Stream Grade	Substrate Type
(ft)	(ft)	(ft)	(ft)	(%)	
2.0	24	22	0.0	1	gravel

detcord (150 gr.)	ANFO	Emulsion	Total # / Delay	TNT Equivalent	Coupling level
(ft)	(lbs)	(lbs)	(lbs)	(lbs)	
240	0	250	255	162	coupled

(7.7 SD)

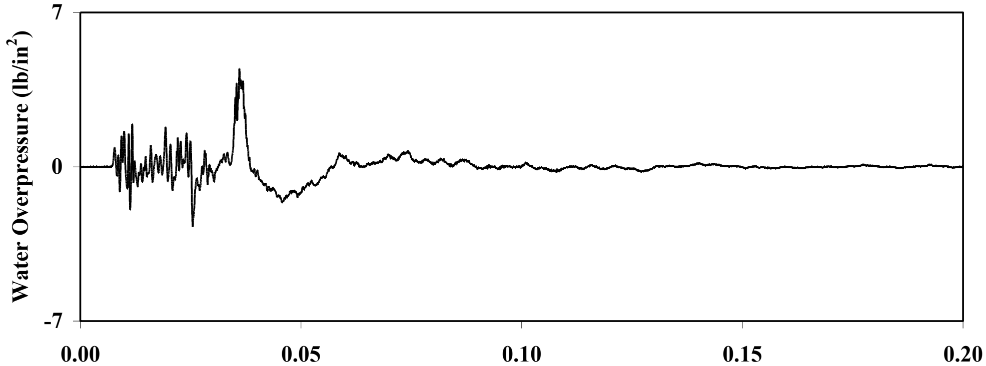

(16.5 SD)

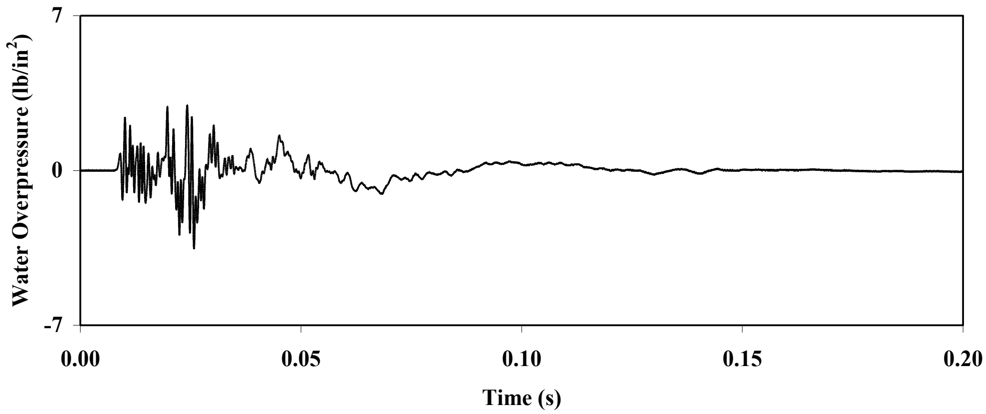

Stream pressures recorded during shot F16

Straight Distance (ft)	Scaled Distance ($ft/lbs^{1/3}$)	Positive Peak (lb/in^2)	Negative Peak (lb/in^2)	FFT Freq. (Hz)
42	7.7	4.45	-2.73	27.5
90	16.5	2.96	-3.55	16.5

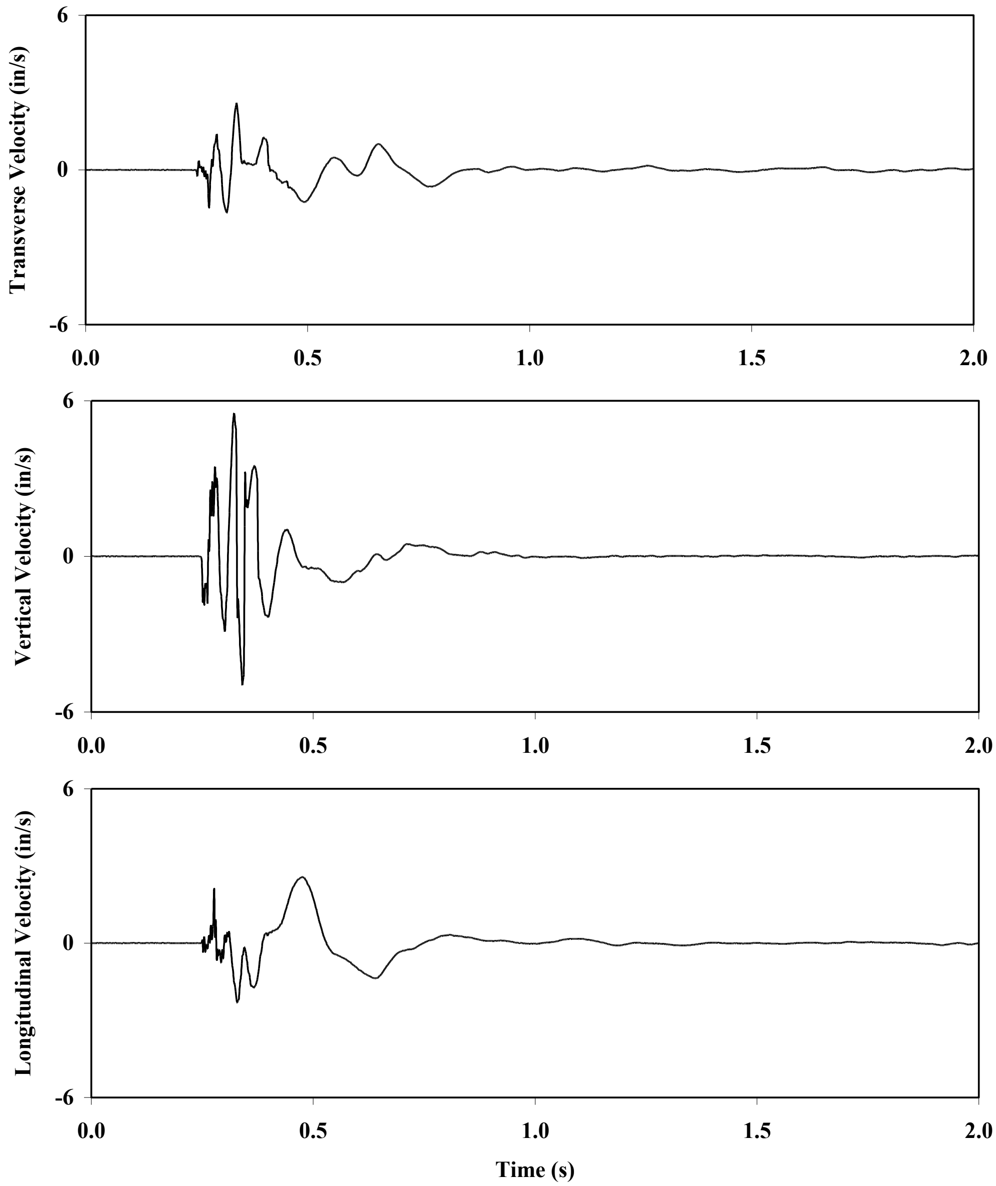

Streambed vibrations recorded during shot F16

Straight Distance (ft)	Scaled Distance (ft/lbs$^{1/2}$)	Transverse PPV (in/s)	FFT Freq. (Hz)	Vertical PPV (in/s)	FFT Freq. (Hz)	Long. PPV (in/s)	FFT Freq. (Hz)
31	2.4	2.60	3.3	5.52	22.0	2.58	3.3

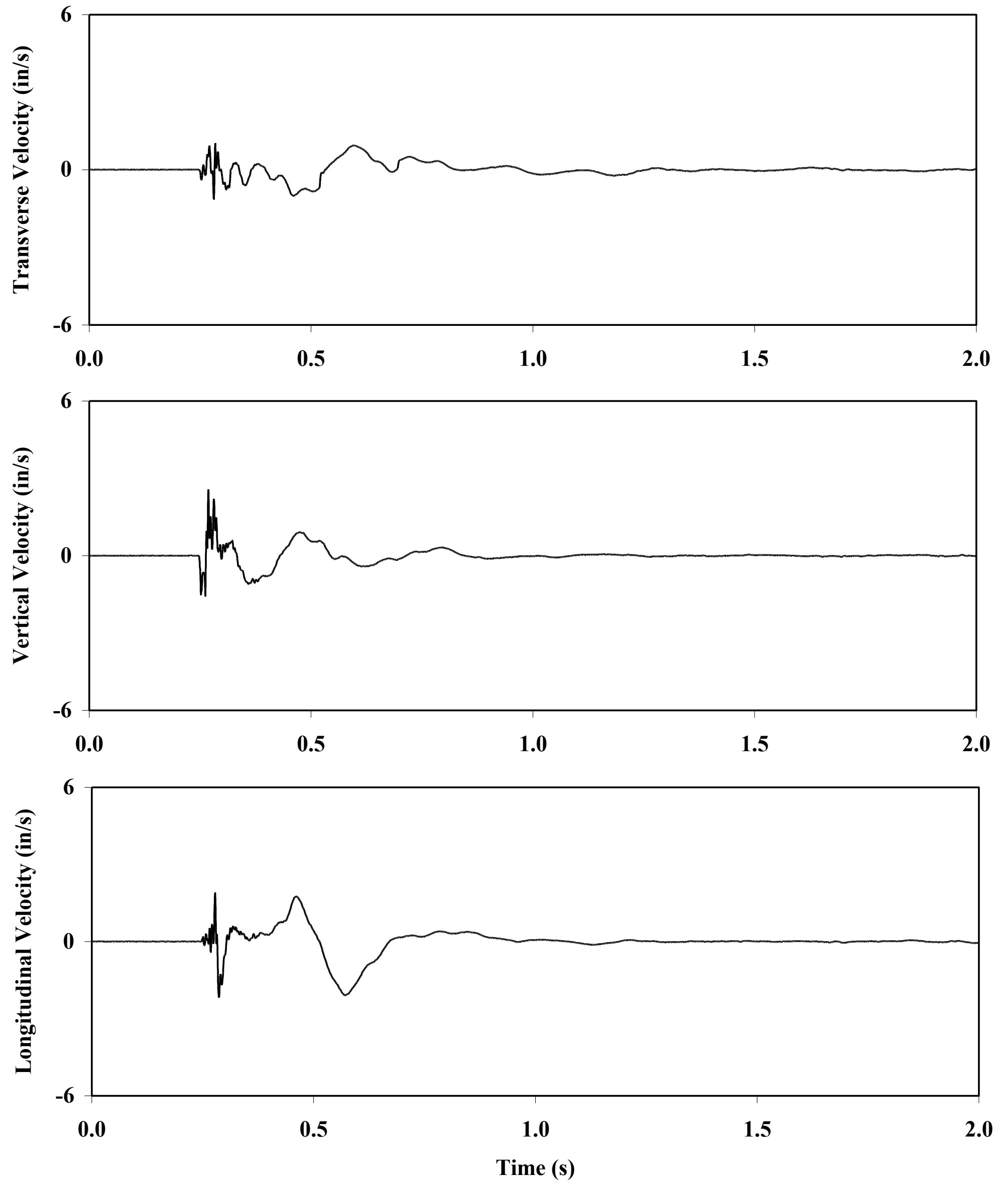

Streambed vibrations recorded during shot F16

Straight Distance (ft)	Scaled Distance (ft/lbs$^{1/2}$)	Transverse PPV (in/s)	FFT Freq. (Hz)	Vertical PPV (in/s)	FFT Freq. (Hz)	Long. PPV (in/s)	FFT Freq. (Hz)
42	3.3	1.12	1.5	2.58	4.3	2.18	2.8

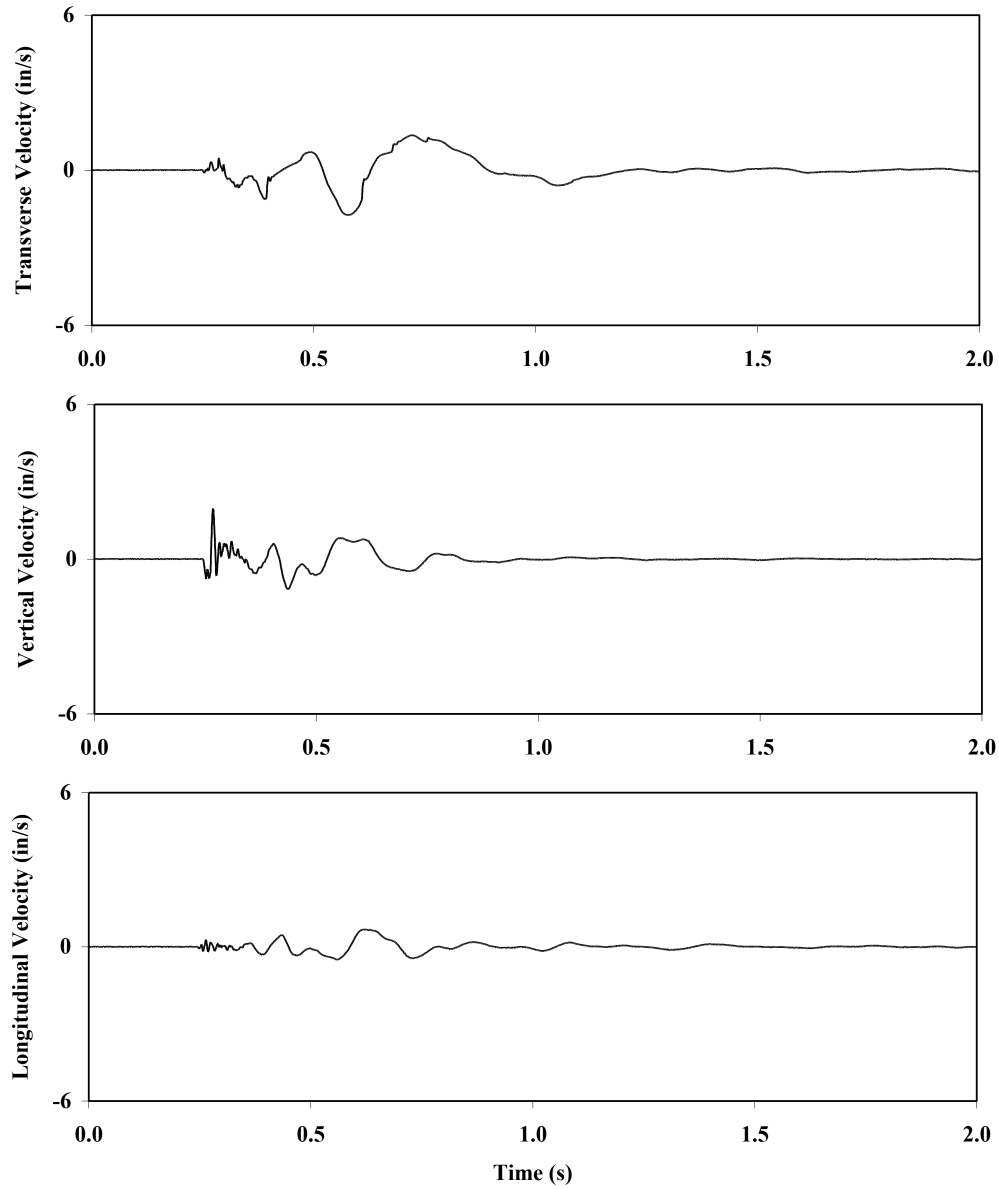

Streambed vibrations recorded during shot F16

Straight Distance (ft)	Scaled Distance ($ft/lbs^{1/2}$)	Transverse PPV (in/s)	FFT Freq. (Hz)	Vertical PPV (in/s)	FFT Freq. (Hz)	Long. PPV (in/s)	FFT Freq. (Hz)
52	4.1	1.73	1.8	1.97	4.0	0.68	4.0

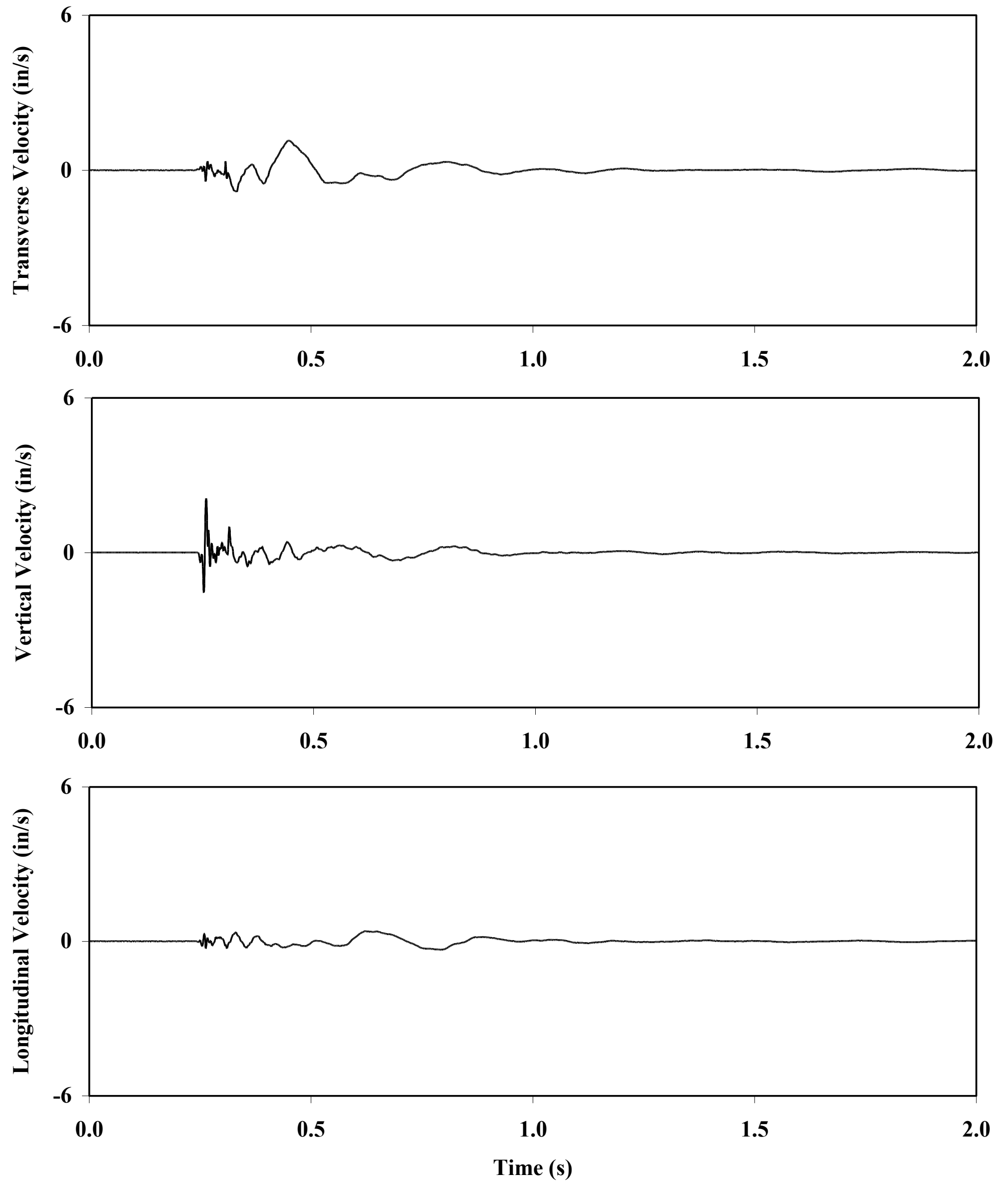

Streambed vibrations recorded during shot F16

Straight Distance (ft)	Scaled Distance (ft/lbs$^{1/2}$)	Transverse PPV (in/s)	FFT Freq. (Hz)	Vertical PPV (in/s)	FFT Freq. (Hz)	Long. PPV (in/s)	FFT Freq. (Hz)
98	7.7	1.15	3.0	2.11	4.0	0.40	3.0

APPENDIX 19 SITE F19 CORRUGATED METAL PIPE. Site diagram and setup information, hydrophone and geophone time histories

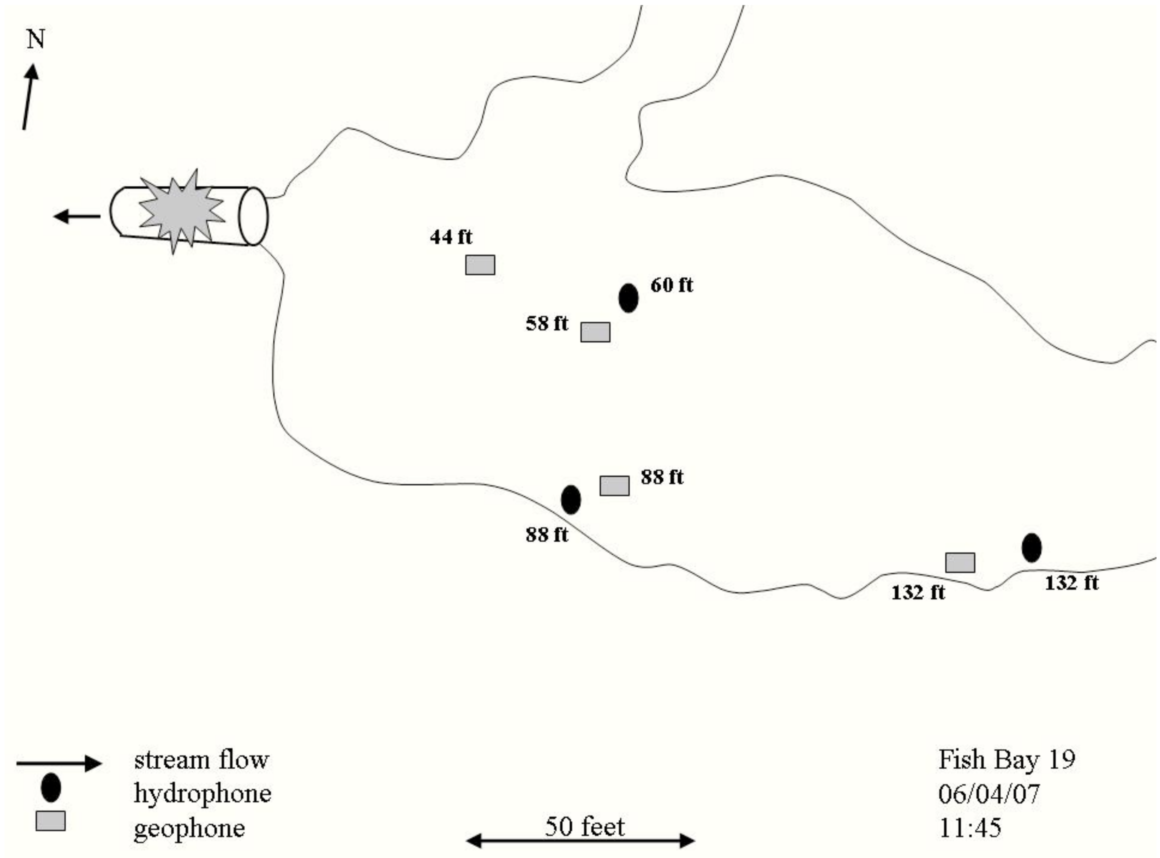

Structure, site, and shot information recorded during shot F19

Culvert Diameter	Culvert Length	Road Width	Fill Depth	Stream Grade	Substrate Type
(ft)	(ft)	(ft)	(ft)	(%)	
1.3	24	23	2.0	0	gravel

detcord (150 gr.)	ANFO	Emulsion	Total # / Delay	TNT Equivalent	Coupling level
(ft)	(lbs)	(lbs)	(lbs)	(lbs)	
60	0	200	201	126	coupled

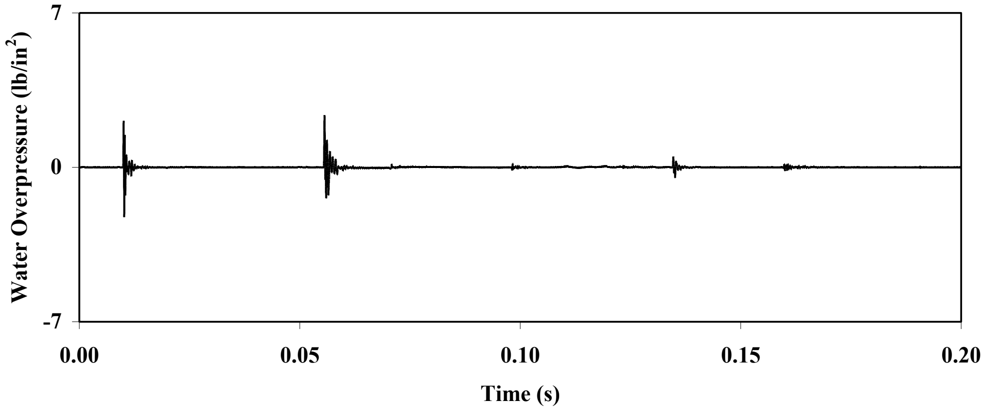

Stream pressures recorded during shot F19

Straight Distance (ft)	Scaled Distance (ft/lbs$^{1/3}$)	Positive Peak (lb/in^2)	Negative Peak (lb/in^2)	FFT Freq. (Hz)
60	12.0	2.37	-2.25	1490.0

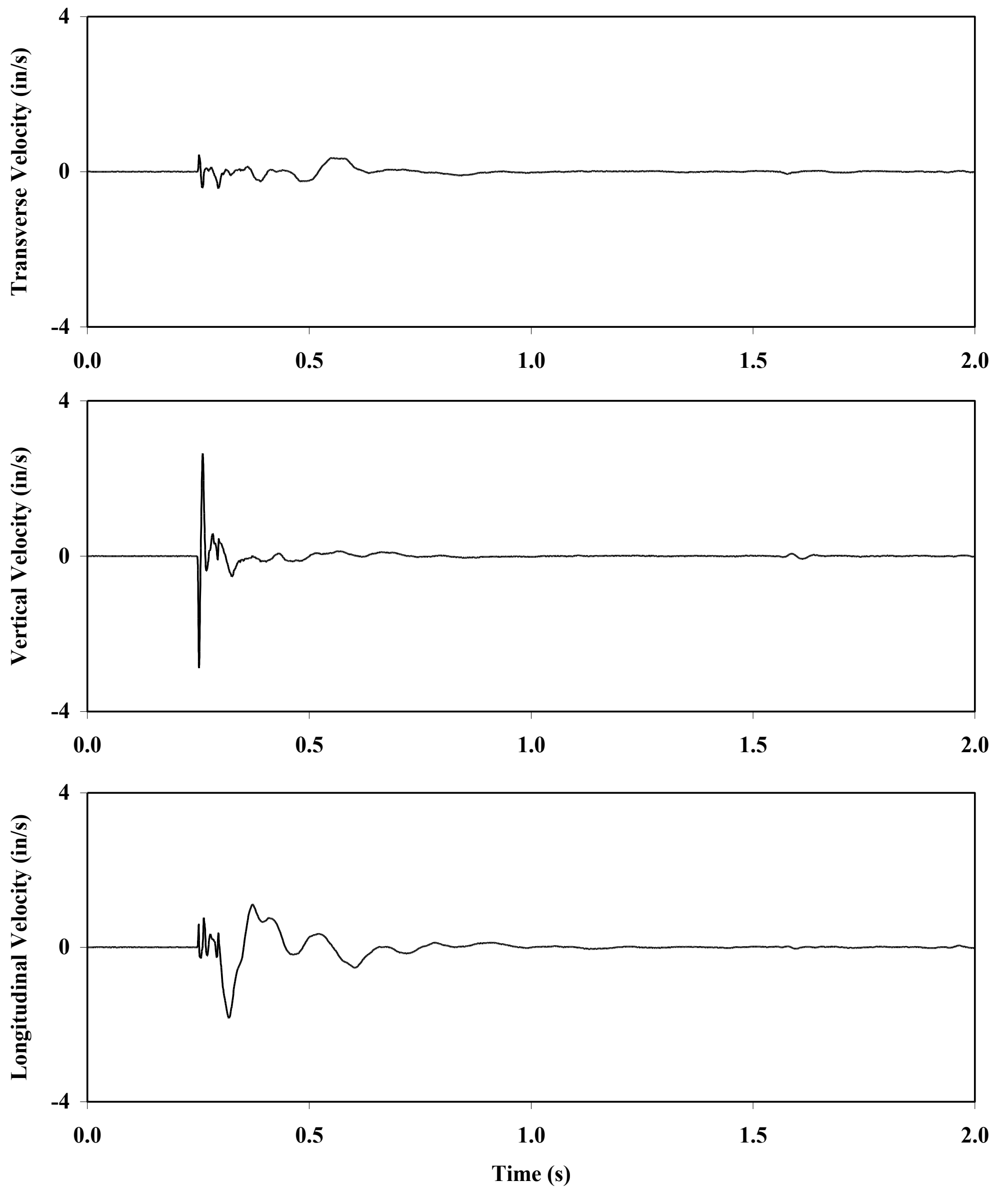

Streambed vibrations recorded during shot F19

Straight Distance (ft)	Scaled Distance (ft/lbs$^{1/2}$)	Transverse PPV (in/s)	FFT Freq. (Hz)	Vertical PPV (in/s)	FFT Freq. (Hz)	Long. PPV (in/s)	FFT Freq. (Hz)
44	3.9	0.69	2.5	3.42	2.5	1.88	2.5

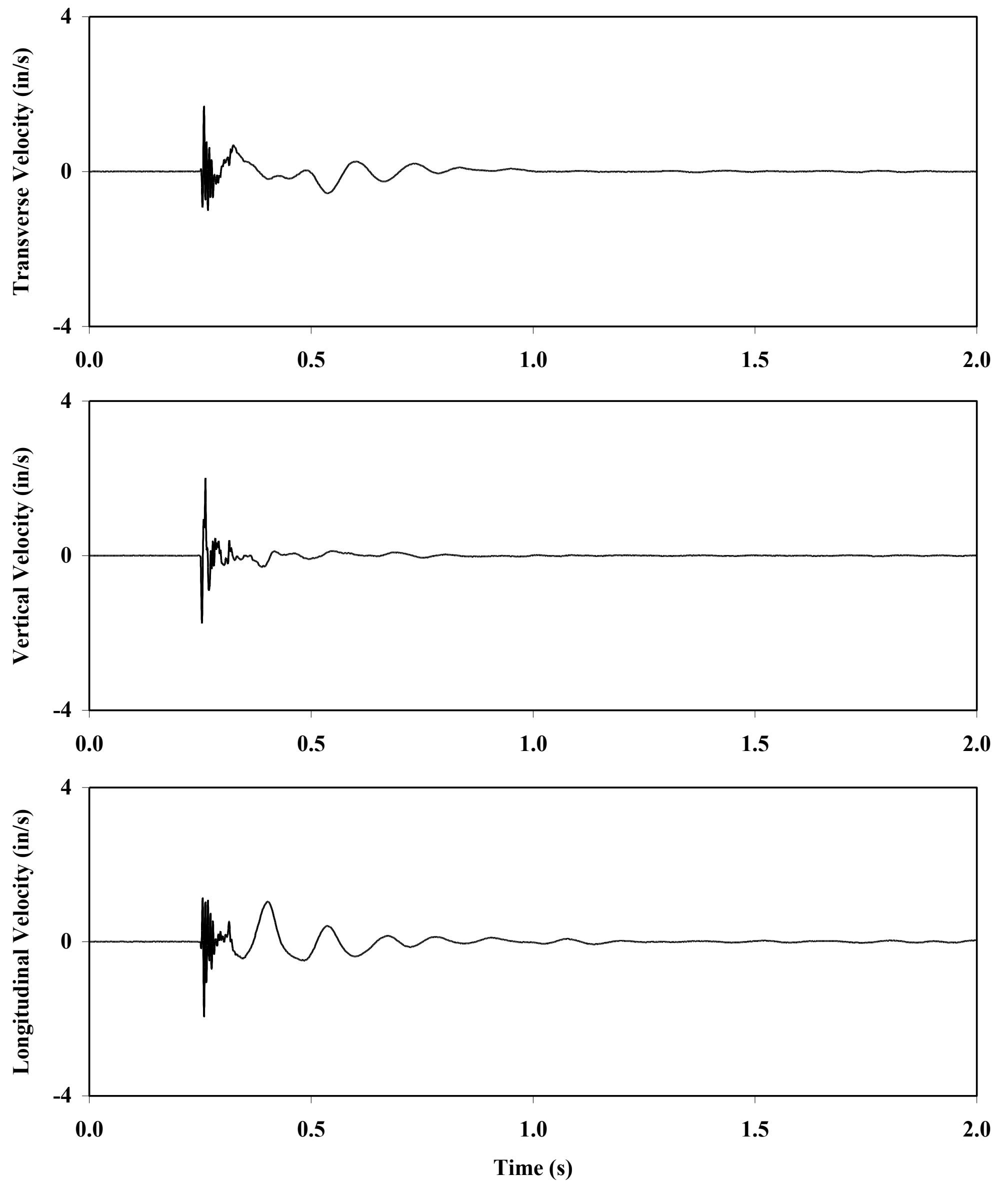

Streambed vibrations recorded during shot F19

Straight Distance (ft)	Scaled Distance (ft/lbs$^{1/2}$)	Transverse PPV (in/s)	FFT Freq. (Hz)	Vertical PPV (in/s)	FFT Freq. (Hz)	Long. PPV (in/s)	FFT Freq. (Hz)
58	5.2	0.44	5.5	2.88	7.8	1.83	7.5

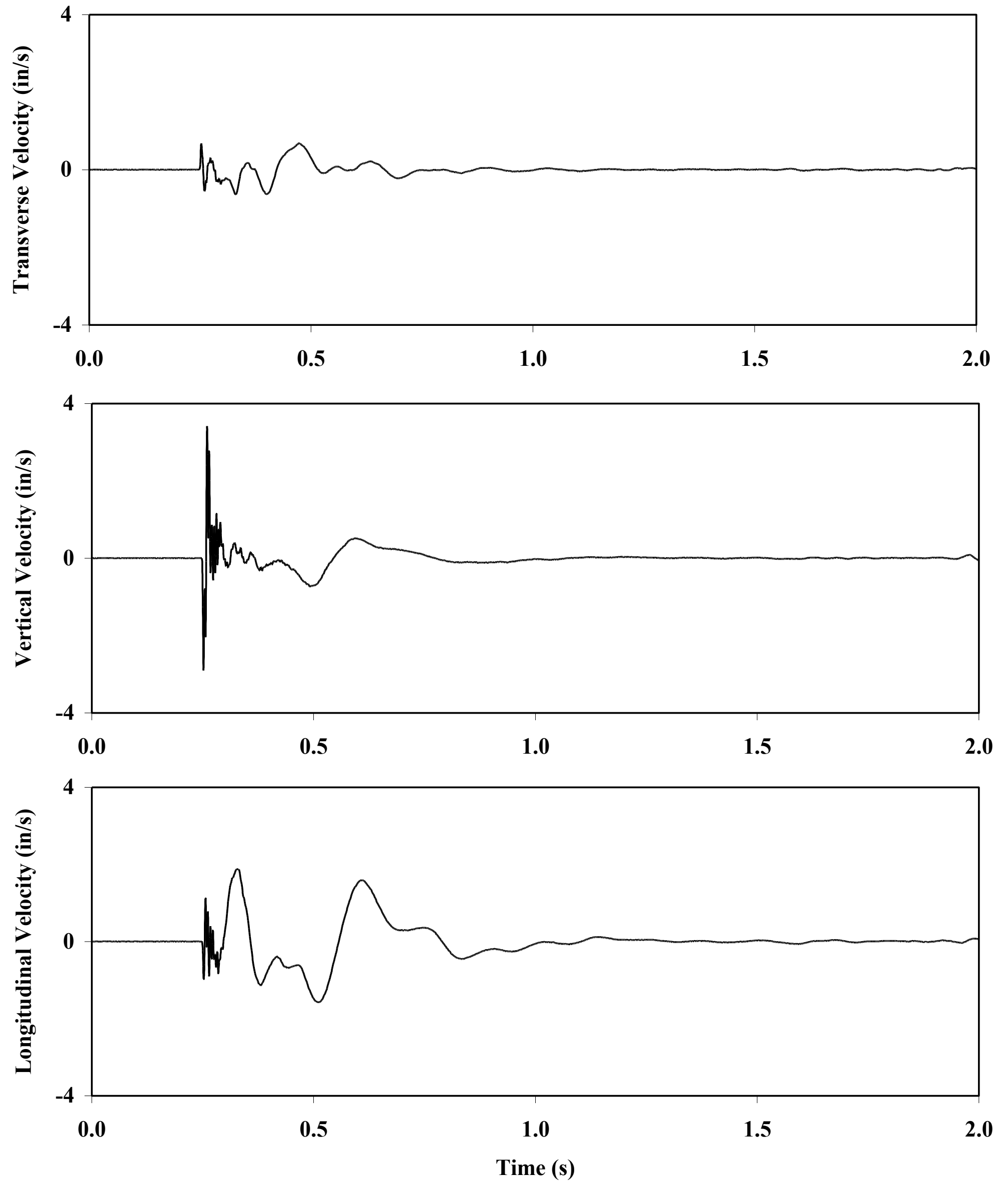

Streambed vibrations recorded during shot F19

Straight Distance (ft)	Scaled Distance ($ft/lbs^{1/2}$)	Transverse PPV (in/s)	FFT Freq. (Hz)	Vertical PPV (in/s)	FFT Freq. (Hz)	Long. PPV (in/s)	FFT Freq. (Hz)
88	7.8	1.67	7.8	2.01	7.8	1.92	7.8

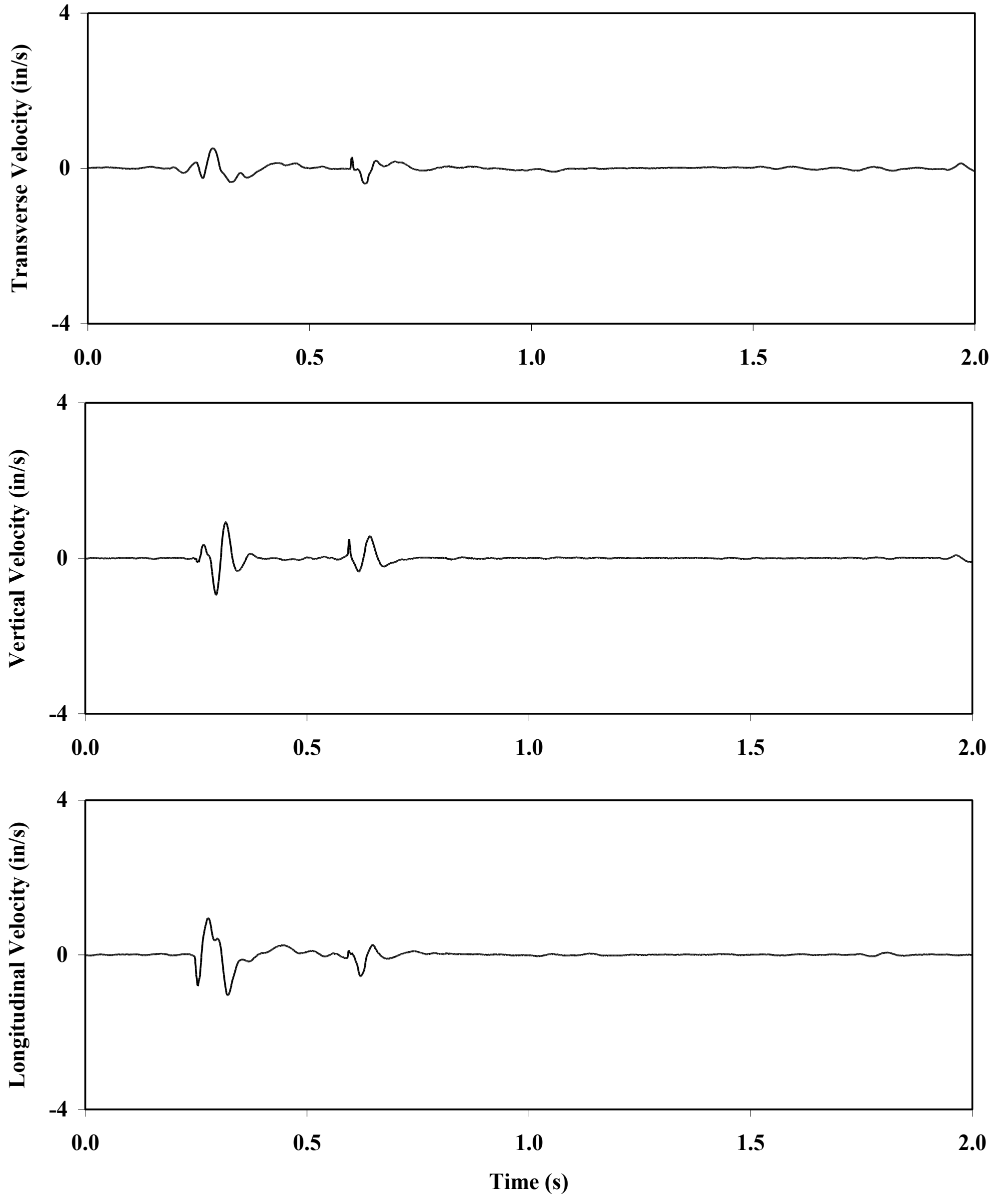

Streambed vibrations recorded during shot F19

Straight Distance (ft)	Scaled Distance (ft/lbs$^{1/2}$)	Transverse PPV (in/s)	FFT Freq. (Hz)	Vertical PPV (in/s)	FFT Freq. (Hz)	Long. PPV (in/s)	FFT Freq. (Hz)
132	11.8	0.52	7.5	0.94	18.5	1.04	14.0

APPENDIX 20 SITE F21 CORRUGATED METAL PIPE. Site diagram and setup information, hydrophone and geophone time histories

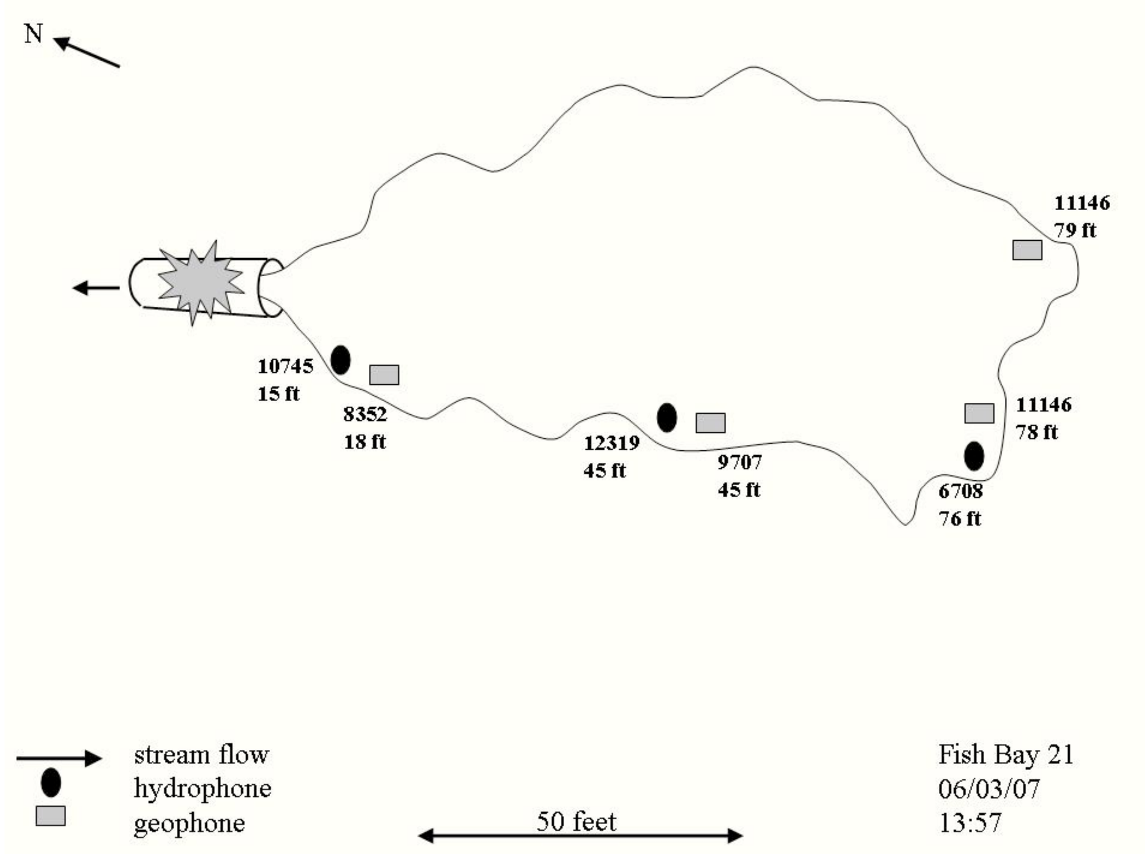

Structure, site, and shot information recorded during shot F21

Culvert Diameter (ft)	Culvert Length (ft)	Road Width (ft)	Fill Depth (ft)	Stream Grade (%)	Substrate Type
2.0	30	24	1.9	0-2	fines

detcord (150 gr.) (ft)	ANFO (lbs)	Emulsion (lbs)	Total # / Delay (lbs)	TNT Equivalent (lbs)	Coupling level
80	0	350	352	219	coupled

(2.5 SD)

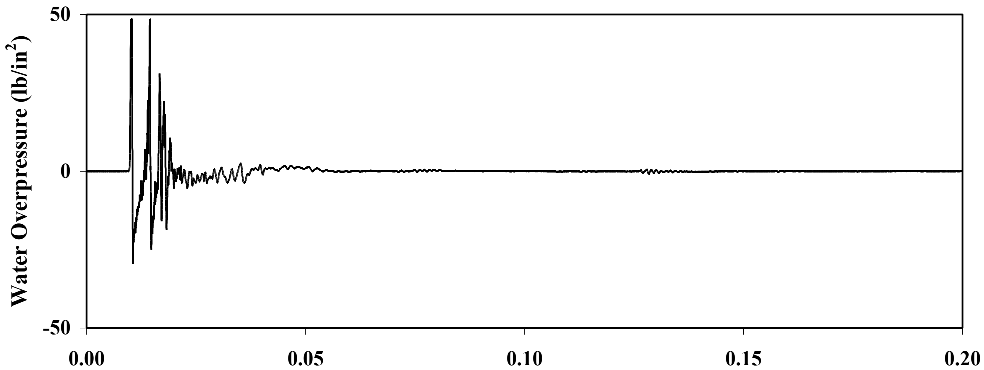

(7.5 SD)

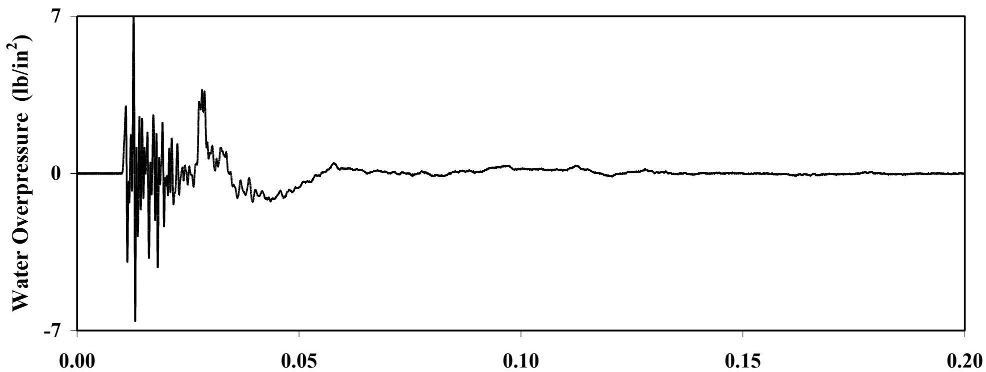

(12.6 SD)

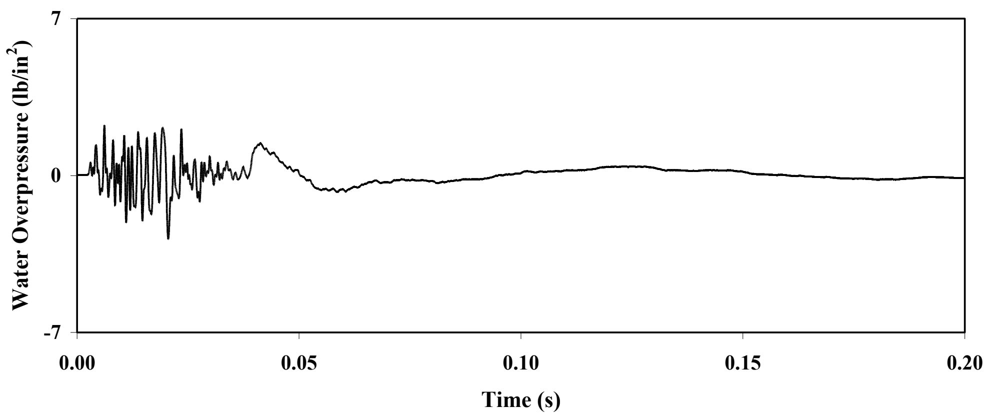

Stream pressures recorded during shot F21

Straight Distance (ft)	Scaled Distance (ft/lbs$^{1/3}$)	Positive Peak (lb/in^2)	Negative Peak (lb/in^2)	FFT Freq. (Hz)
15	2.5	88.5*	*	*
45	7.5	7.01	-6.61	26.5
76	12.6	2.24	-2.84	9.0

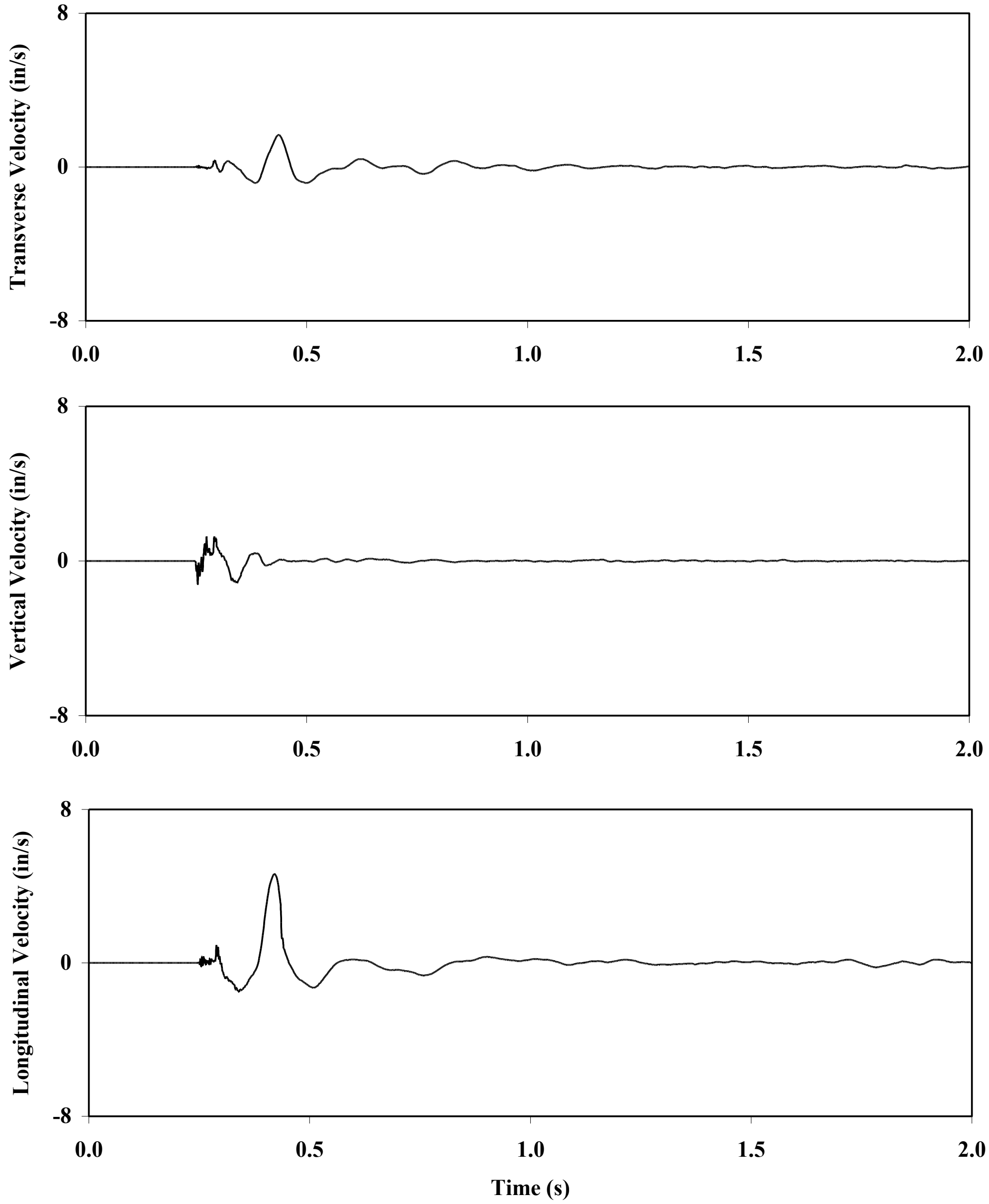

Streambed vibrations recorded during shot F21

Straight Distance (ft)	Scaled Distance (ft/lbs$^{1/2}$)	Transverse PPV (in/s)	FFT Freq. (Hz)	Vertical PPV (in/s)	FFT Freq. (Hz)	Long. PPV (in/s)	FFT Freq. (Hz)
45	3.0	4.79	4.0	7.41	0.7	5.76	3.3

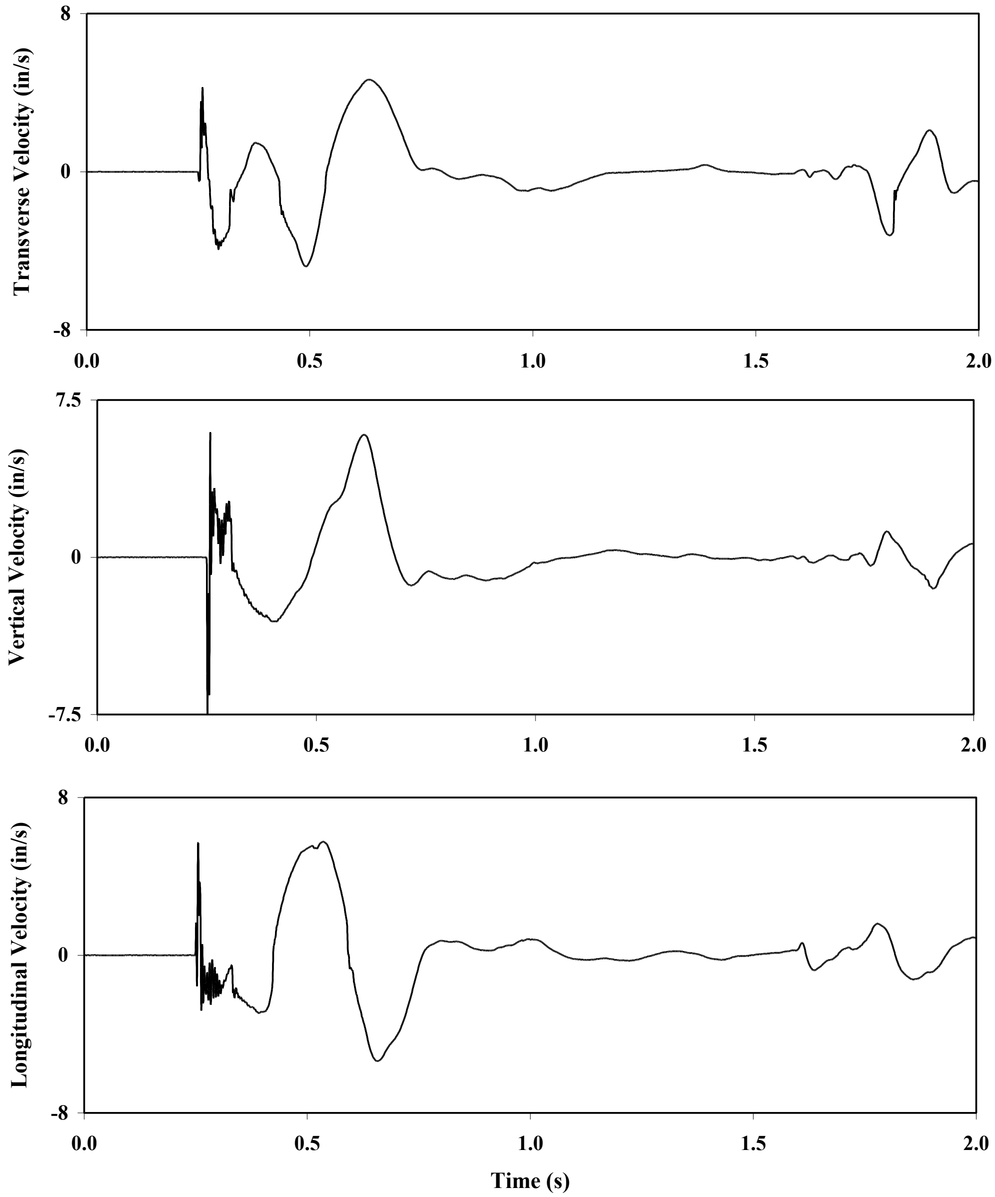

Streambed vibrations recorded during shot F21

Straight Distance (ft)	Scaled Distance (ft/lbs$^{1/2}$)	Transverse PPV (in/s)	FFT Freq. (Hz)	Vertical PPV (in/s)	FFT Freq. (Hz)	Long. PPV (in/s)	FFT Freq. (Hz)
78	5.3	4.77	4.3	3.59	7.8	1.99	3.0

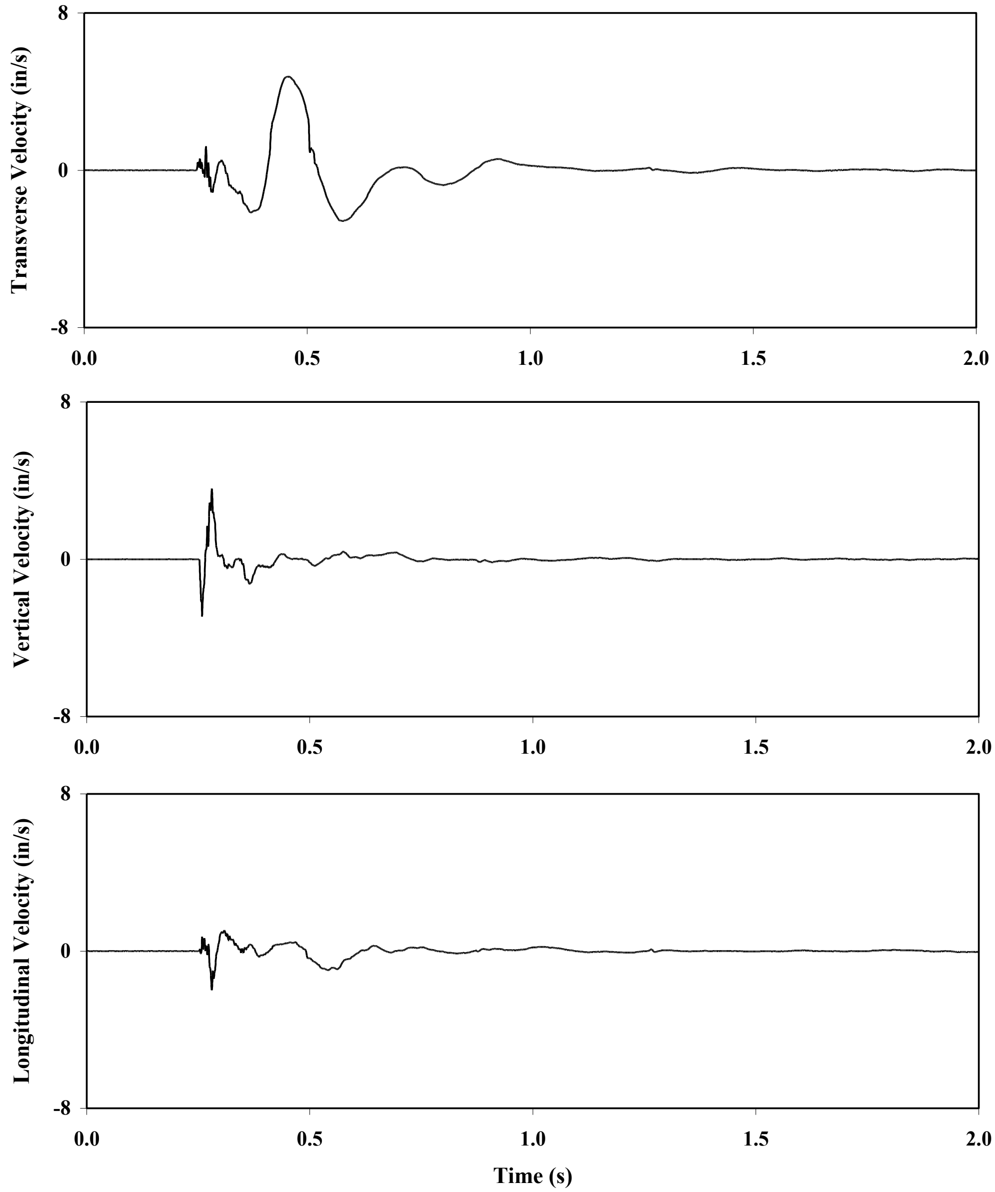

Streambed vibrations recorded during shot F21

Straight Distance (ft)	Scaled Distance ($ft/lbs^{1/2}$)	Transverse PPV (in/s)	FFT Freq. (Hz)	Vertical PPV (in/s)	FFT Freq. (Hz)	Long. PPV (in/s)	FFT Freq. (Hz)
79	5.3	1.67	7.8	1.27	10.3	4.63	4.8